VNIVERSITAT DE VALÈNCIA

Facultat de Farmàcia
Departament de Medicina Preventiva i Salut Pública, Ciències de L'Alimentació, Toxicologia i Medicina Legal

Programa de Doctorado en Ciencias de la Alimentación

APROXIMACIÓN METABOLÓMICA A LOS ZUMOS DE FRUTA MEDIANTE LA CROMATOGRAFÍA DE LÍQUIDOS Y DE GASES ACOPLADA A LA ESPECTROMETRÍA DE MASAS

TESIS DOCTORAL

Presentada por:

Manuela Cerdán Calero

Dirigida por:

Dr. Enrique Sentandreu Vicente

Dr. José Luis Navarro Fabra

Valencia, 2014

D. Enrique Sentandreu Vicente, Dr. en Farmacia y D. José Luis Navarro Fabra, Dr. en Ciencias Químicas y Profesor de Investigación, pertenecientes al Consejo Superior de Investigaciones Científicas con destino en el Instituto de Agroquímica y Tecnología de Alimentos.

CERTIFICAN QUE:

La licenciada en Ciencia y Tecnología de los Alimentos **D.ª Manuela Cerdán Calero** ha realizado bajo su dirección y en el Instituto de Agroquímica y Tecnología de los Alimentos (IATA-CSIC), el trabajo que tiene el titulo "*Aproximación metabolómica a los zumos de fruta mediante la cromatografía de líquidos y de gases acoplada a la espectrometría de masas*". Este trabajo ha sido plasmado en 7 artículos, publicados o que se publicarán en las siguientes revistas:

- *Gas chromatography coupled to mass spectrometry analysis of volatiles, sugars, organic acids and aminoacids in Valencia Late orange juice and reliability of the Automated Mass Spectral Deconvolution and Identification System for their automatic identification and quantification*. (2012). Journal of Chromatography A, 1241, 84-95. Impact Factor: 4.258

- *Valencia Late orange juice preserved by pulp reduction and high pressure homogenization: Sensory quality and gas chromatography-mass spectrometry analysis of volatiles*. (2013). LWT - Food Science and Technology, 51(2), 476-483. Impact Factor: 2.468

- *Evaluation of minimal processing of orange juice by automated data analysis of volatiles and non volatile polar compounds determined by GAS chromatography coupled to mass spectrometry*. (2014). International Journal of Food Science and Technology, 49(6), 1432-1440. Impact Factor: 1.354

- *Phenolic profile characterization of pomegranate (Punica granatum) juice by high-performance liquid chromatography with diode array detection coupled to an electrospray ion trap mass analyzer*. (2013). Journal of Food Composition and Analysis, 30(1), 32-40. Impact Factor: 2.259

- *Determination of the antiradical activity and kinetics of pomegranate juice using 2,2-diphenylpicyrl-1-hydrazyl as the antiradical probe*. (2014). Food Science and Technology International. (En prensa). Impact Factor: 0.981

- *Metabolite profiling of pigments from acid-hydrolyzed persimmon (Diospyros kaki) extracts by HPLC-DAD/ESI-MS^n analysis*. (2014). Journal of Food Composition and Analysis. (Aceptado para su publicación). Impact Factor: 2.259

- *Rapid screening of low molecular weight phenols from persimmon (Diospyros. kaki) pulp using liquid chromatography-UV/Vis-electrospray mass spectrometry analysis.* (2014). Journal of the Science of Food and Agriculture. (En prensa). Impact Factor: 1.879

Por la cual, autorizan su presentación para optar al Grado de Doctor en el programa de doctorado de Ciencias de la Alimentación por la Universidad de Valencia. Y para que así conste, expiden y firman el presente certificado en Burjassot, 01 de Septiembre de 2014.

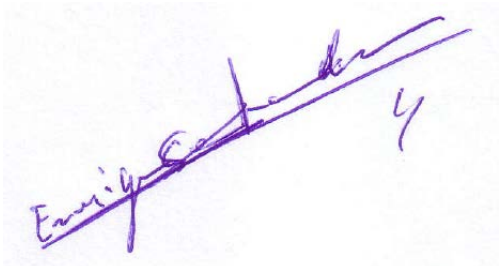

Fdo. Dr. Enrique Sentandreu Vicente

Fdo. Dr. José Luis Navarro Fabra

VNIVERSITAT DE VALÈNCIA
Facultat de Farmàcia

DEPARTAMENT DE MEDICINA PREVENTIVA I SALUT PÚBLICA,
CIÈNCIES DE L'ALIMENTACIÓ, TOXICOLOGIA I MEDICINA LEGAL
Av. Vicent Andrés Estellés, s/n.
46100 Burjassot - València - Spain

Tel. 96 354 49 59
Fax 96 354 49 54
E-mail: dep.medicina.preventiva@uv.es

D.ª Mª José Ocio Zapata, Catedrática de la Universidad de Valencia.

CERTIFICA QUE:

La licenciada en Ciencia y Tecnología de los Alimentos **D.ª Manuela Cerdán Calero,** ha realizado bajo su tutela y la dirección del Dr. Enrique Sentandreu Vicente y del Dr. José Luis Navarro Fabra, y en el Instituto de Agroquímica y Tecnología de los Alimentos (IATA-CSIC), el trabajo con titulo "*Aproximación metabolómica a los zumos de fruta mediante la cromatografía de líquidos y de gases acoplada a la espectrometría de masas*", que presenta como Tesis Doctoral para optar al Grado de Doctor por la Universidad de Valencia.

Y para que así conste a todos los efectos oportunos, expide y firma el presente certificado en Burjassot, 01 de Septiembre de 2014.

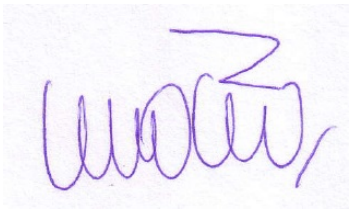

Fdo. Dra. Mª José Ocio Zapata

Manuela Cerdán Calero ha disfrutado de una beca para el desarrollo de tesis doctorales en el marco del Programa *"Junta de Ampliación de Estudios" (JAE Predoc)* otorgada por la Agencia Estatal Consejo Superior de Investigaciones Científicas (2010-2014).

Este trabajo ha sido financiado por:

- Proyecto de investigación: **"***Obtención de zumos cítricos de alta calidad sensorial por reducción de su contenido en pulpa y homogeneización a alta presión"*. Plan Nacional de I+D+i. Dirección General de Investigación, MICINN (AGL 2009-11805/ALI).

La presente Tesis Doctoral forma parte del Programa de Doctorado *"Ciencias de la Alimentación"* (Real Decreto 1393/2007) de la Universidad de Valencia.

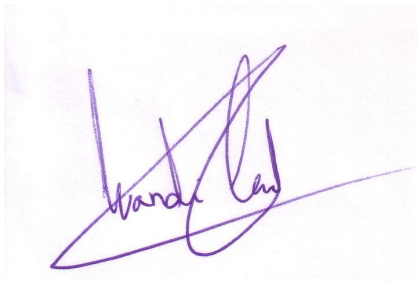

Fdo. Manuela Cerdán Calero

A mis padres, por su sacrificio

A mi hermano Jose

AGRADECIMIENTOS

Por fin llegó el momento más esperado durante el proceso de escritura de una tesis, ahora toca escribir sus últimas líneas. Después de tantos meses deseando llegar a este apartado es inevitable sentir emoción al no saber por dónde empezar, pues han pasado casi cuatro años que empecé esta aventura en el IATA, y mi etapa de formación predoctoral ha finalizado y con ella mi estancia en el centro. Han sido muchas las personas que han contribuido a hacer posible este trabajo, espero no dejarme a nadie.

En primer lugar me gustaría agradecer a mis directores de tesis, Quique y José Luis, y al resto del grupo de zumos, Luis, Pepe Carbonell y Pepe Sendra, por estos años de formación. Gracias por darme la oportunidad de ser vuestra doctoranda, de formarme científicamente, de transmitirme esos valores y esa pasión por la ciencia. De todo corazón, Quique, te doy las gracias por darme esta gran oportunidad, sin apenas conocerme. Y sobre todo, gracias por la paciencia que has tenido conmigo. Siempre serás mi mentor, mi maestro. Gracias a todos por vuestro tiempo y apoyo, sabéis que sin vosotros todo este trabajo no hubiera sido posible. También doy las gracias a Mª Carmen e Imma, por el tiempo, aunque poco, que coincidimos en el laboratorio, por hacerme más amenas las horas muertas.

A todas esas personas con las que he coincidido por algún motivo fuera del laboratorio, pero dentro del IATA, aunque yo haya preferido pasar desapercibida, entre ellos mis compañeros de máster Ana, Jesús y Joana. A Arancha, reciente Doctora, por todo su apoyo desde el principio, por los momentos "confesionario", y por intentar integrarme en Valencia. A Miguel Ángel por preocuparse siempre de como me iba todo.

Gracias a los evaluadores externos y miembros del tribunal de mi tesis (Jordi Mañes, Noelia Betoret, Pepe Carbonell, Mª Jesús Lagarda, Pedro Fito, Mª Jesús Rodrigo) por la aceptación de evaluar tanto mi tesis como mi capacidad investigadora.

Toda nueva etapa tiene una anterior, gracias a todos los que me acompañasteis durante la carrera, sobre todo a Ester, Fernando, Aurora y Mª Ángeles, por cada momento vivido con vosotros, nuestras andanzas por la EPSO y por Elche. Gracias al Dr. Vicente Micol, por darme la oportunidad de pertenecer a su grupo de investigación e iniciarme en el mundo de la ciencia, y a todos las personas que allí conocí (Lorena, María, Angela, Maite,…).

Continúo estos agradecimientos fuera del IATA y del ámbito profesional. En primer lugar agradecer a mi familia, especialmente a mis padres, Manola y Salva, por su apoyo, su comprensión, su amor, por aguantar mi mala leche y rabietas, que solo saco en casa, y por enseñarme los valores de la vida: gracias por ser maravillosos, porque sin vosotros no hubiera sido posible este largo camino. Gracias mama, por tranquilizarme en cada momento de agobio a través del teléfono. A ti papa, por ser un ejemplo de superación. Os quiero.

A mi hermano Jose, por ponerme en mi lugar en cada momento con su bordería y sobre todo gracias por ser tan buena persona y apoyarme a tu manera. A mi iaia Estebana, mi segunda madre, por su gran frase: "*el que te riñe y te hace llorar, es el que te quiere*", espero que sigas muchos años con nosotros a pesar de tus casi 94 años. Y a mis tíos y a mis primos, por esta unión tan especial que tenemos.

A Carlos, por acompañarme en esta aventura desde hace 3 años y aguantar mis momentos de histeria, debidos a mi facilidad por ahogarme

en un vaso de agua, gracias por quitarle importancia a mis problemas tontos. Espero que estés orgulloso. Te quiero.

A mis amig@s de Bonete, los de siempre, a los cuales veo poco pero hacen que disfrute al máximo cada momento y sacan lo mejor de mí, y en especial a Bea y Marisa mis incondicionales, por ser más que amigas, por nuestras conversaciones y discusiones en la esquina (aunque ahora son más por WhatsApp), gracias por vuestro apoyo, por estar siempre ahí, a pesar de la distancia. A Mari y Marijose, por ser tan buenas amigas y muy especiales para mí. Y a Nico (Topo), por interesarse siempre por todo lo que hago.

A mis amig@s de Valencia, por acogerme en vuestro grupo, y poder tener una vida fuera del laboratorio en esta ciudad, donde llegue sola, y sin ganas de conocerla. Ahora la odio menos.

En fin, gracias a todos y a cada uno de vosotros (y muchos más a los que no he nombrado) por ser como sois, por vuestro tiempo y apoyo. Habéis sido unos compañeros de viaje increíbles.

"*La ciencia será siempre una búsqueda, jamás un descubrimiento real. Es un viaje, nunca una llegada*" (Karl Popper).

ÍNDICE

ÍNDICE

ABREVIATURAS

ABREVIATURAS

AMDIS: Sistema automático de deconvolución e identificación de espectros de masas (Automated Mass Spectral Deconvolution and Identification System).

APCI: Ionización química a presión atmosférica (Atmospheric Pressure Chemical Ionization).

API: Ionización a presión atmosférica (Atmospheric Pressure Ionization).

CID: Disociación inducida por colisión (Collision-Induced Dissociation).

DAD: Detector de diodos en filas (Diode-Array Detector).

DPPH$^{\bullet}$: 2,2-difenil-1-picrilhidrazil.

EE. UU.: Estados Unidos.

EI: Ionización por impacto electrónico (Electron Impact).

ESI: Ionización por electroespray (Electrospray Ionization).

ETD: Disociación por transferencia de electrones (Electron Transfer Dissociation).

eV: Electronvoltio.

FAB: Bombardeo con átomos rápidos (Fast Atom Bombardment).

FAO: Organización de las Naciones Unidas para la alimentación y la agricultura (Food and Agriculture Organization of the United Nations).

GC: Cromatografía de gases (Gas Chromatography).

ha: Hectáreas.

HPH: Homogenización a Altas presiones (High Pressure Homogenization).

HPLC: Cromatografía líquida de alta resolución (High Performance Liquid Chromatography).

HS/SPME: Microextracción en fase sólida de espacio de cabeza (HeadSpace/Solid-Phase MicroExtraction).

ICR: Resonancia ciclotrónica de iones (Ion Cyclotron Resonance).

LC: Cromatografía líquida (Liquid Chromatography).

MAGRAMA: Ministerio de Agricultura, Alimentación y Medio Ambiente de España.

MALDI: Ionización/desorción por láser (Matrix-Assisted Laser Desorption/Ionization).

MPa: Megapascal.

MS: Espectrometría de masas (Mass spectrometry).

MS^n: Espectrometría de masas en tándem (Multiple stage mass spectrometry).

m/z: Relación masa/carga (mass-to-charge ratio).

M^-/M^+: Iones moleculares (Ionización negativa/positiva).

NIST: Instituto nacional de estándares y tecnología (National Institute of Standards and Technology).

PEF: Pulsos eléctricos de alta intensidad (Pulsed Electric Field).

RAE: Real Academia Española.

s: Segundos.

SIM: Monitoreo del ión seleccionado (Single Ion Monitoring).

SPME: Microextracción en fase sólida (Solid-Phase MicroExtraction).

TIC: Cromatograma de iones totales (Total Ion Current).

TMS-derivados: Trimetilsilil-derivados.

TOF: Tiempo de vuelo (Time-Of-Flight).

Torr: Torricelli.

UV-Vis: Espectroscopia ultravioleta-visible.

INTRODUCCIÓN

1. INTRODUCCIÓN

1.1. FRUTAS Y SUS DERIVADOS. ZUMOS

Según la Real Academia Española (RAE), las frutas son frutos comestibles de ciertas plantas cultivadas, como la pera, guinda, fresa, etc. El Código Alimentario Español las define como: "Frutos, infrutescencias o partes carnosas de órganos florales que han alcanzado un grado adecuado de madurez y son propias para el consumo humano". Es decir, se denominan frutas a los frutos comestibles de naturaleza carnosa, que se pueden comer sin preparación.

Desde la antigüedad, las frutas han estado presentes en la alimentación humana como fuente de energía y de nutrientes necesarios para sobrevivir, siendo probablemente la base de la alimentación de los primeros homínidos; además, constituyen, junto a otros grupos de alimentos, la esencia de lo que entendemos por dieta mediterránea.

En los últimos años, se ha tomado conciencia de la importancia de su valor nutricional para la salud; su riqueza en vitaminas, elementos minerales, fibra, etc., hacen que su consumo sea imprescindible para conseguir una alimentación sana y equilibrada. Además, son una excelente fuente de otros compuestos bioactivos, denominados "fitoquímicos", cuya biodisponibilidad y actividad biológica han sido objeto de muchas investigaciones (Acosta-Estrada *et al.*, 2014; Benzie y Choi, 2014; Chen *et al*., 2007; Dillard y German, 2000; Thilakarathna y Rupasinghe, 2013).

El consumo de frutas y verduras tiene una evolución moderada en España, siendo uno de los países con mayor consumo en Europa, pero dicho consumo está por debajo de las recomendaciones de las guías alimentarias. *Dietary Guidelines for Americans 2010* (U.S. Department of Agriculture and U.S. Departamente of Health and Human Services, 2010) recomienda tomar cada día, al menos 5 raciones de frutas y verduras. En España, este consejo está siendo fuertemente impulsado por el movimiento internacional "5 al día" que promociona el consumo de frutas y hortalizas en el mundo y

que está presente en más de 40 países (Cullum, 2003). Según el Ministerio de Agricultura, Alimentación y Medio Ambiente (MAGRAMA) durante el año 2013 el consumo de frutas frescas en España descendió un 2,2% con respecto al año anterior (Figura 1), observándose un estancamiento en la tendencia de consumo.

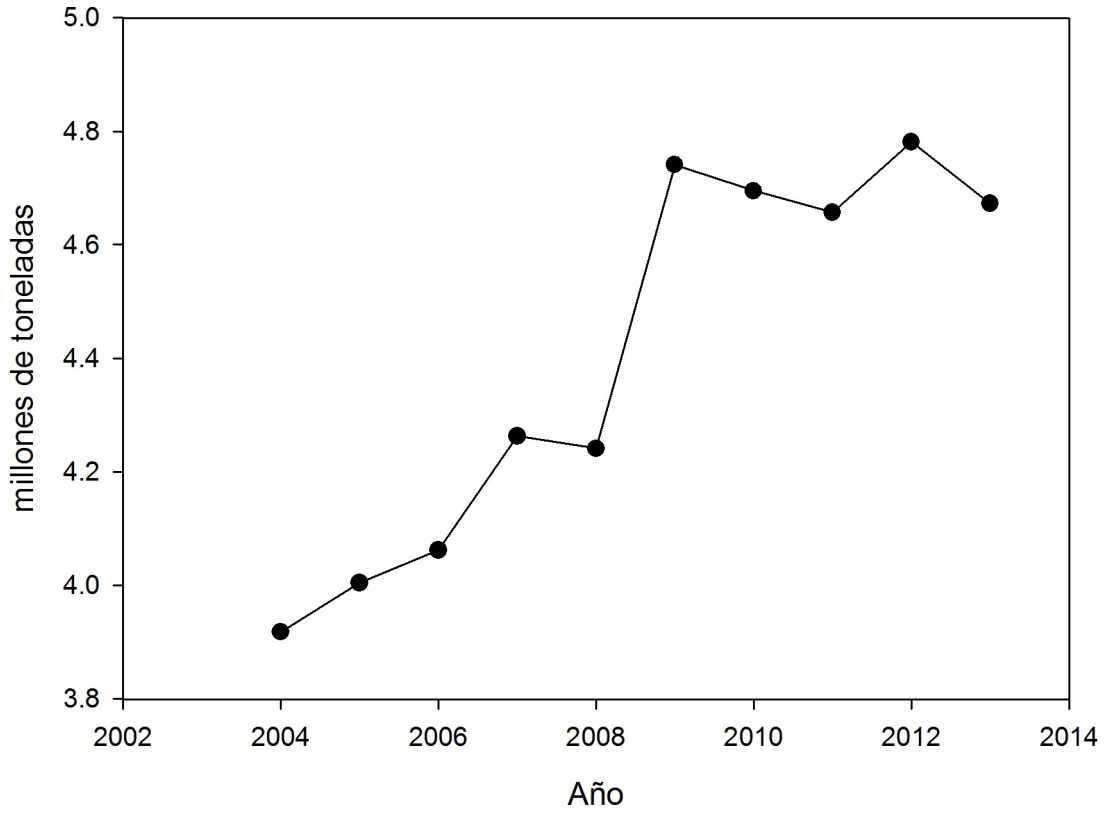

Figura 1. Evolución del consumo de frutas en España durante los últimos 10 años. Datos MAGRAMA

A lo largo de los años, los hábitos alimentarios han evolucionado, pasando de las necesidades basadas en la supervivencia del hombre primitivo a las demandas que en las sociedades desarrolladas los consumidores plantean en lo relacionado con los alimentos, como son la calidad nutricional, sensorial y la seguridad de los mismos, además de aumentar la demanda de alimentos procesados y cuya preparación ocupe el menor

tiempo posible. Esta situación ha llevado a la industria alimentaria a aumentar la producción de este tipo de alimentos, así como a los investigadores y tecnólogos de alimentos a realizar un gran esfuerzo para que la calidad de los productos procesados se vea mínimamente afectada durante su procesado y el almacenamiento, desarrollando nuevas tecnologías en lo referente a la manipulación de los alimentos.

Por su parte, los zumos de frutas son un claro ejemplo de esta nueva tendencia en la obtención de alimentos procesados de alta calidad, ajustándose a los gustos de los consumidores y resultando ser una fuente de salud fácil de adquirir y consumir. Actualmente, se dispone en el mercado de una amplia oferta de zumos con infinidad de sabores, propiedades y beneficios para el organismo.

1.1.1. Naranja

La naranja se originó hace unos 20 millones de años en la región tropical y subtropical de Asia; fue introducida en Europa por los árabes a través del sur de España, en el siglo X, aunque el naranjo dulce no comenzó a cultivarse hasta los siglos XV-XVI. Desde entonces hasta ahora ha sufrido numerosas modificaciones debido a la selección natural e hibridaciones tanto naturales como inducidas por el hombre.

El naranjo es uno de los frutales más extendidos por todo el mundo; siendo los principales productores mundiales por orden decreciente: Brasil, EE. UU., China, México, India, España (Valencia, Murcia, Sevilla y Huelva), Egipto, Italia, Indonesia, Turquía, Sudáfrica, Pakistán e Irán. Según la FAO, en el año 2012, a nivel mundial se destinó una superficie total de 3.816.962 ha para el cultivo de la naranja, con una producción de 68.223.759 toneladas, de las cuales aproximadamente 2.940.000 toneladas las produce España (sexto productor mundial); siendo el principal productor la Comunidad Valenciana con 1.422.679 toneladas, seguido por Andalucía con 1.291.507 toneladas. Se trata de una producción orientada hacia el mercado en fresco, solo un pequeño porcentaje se destina a la industia de zumos, que habitualmente se

corresponde con destríos o segundas calidades retiradas del circuito en fresco (FAOSTAT, 2012; MAGRAMA, 2012).

Existen dos grupos principales de naranjas, las cuales son fácilmente distinguibles por el sabor: las naranjas amargas (*Citrus aurantium*), son ácidas y amargas, por lo que no se consumen en fresco y se reservan para la elaboración de mermeladas y aceites esenciales; y las naranjas dulces (*Citrus sinensis*), también conocidas como naranjas de mesa, donde encontramos 4 subgrupos:

- Navel: presentan un ombligo característico y no tienen semillas. No son adecuadas para hacer zumos, por su sabor amargo (liberación de limonina), aparte de proporcionar una menor cantidad de jugo que otras variedades. Dentro de este grupo encontramos: Lane Late (menor cantidad de limonina), Navel, Navelate, Newhall, Washington o Naranja Bahía.
- Naranjas blancas: forma esférica achatada y sin ombligo, posee una acidez inferior a la de otros grupos de variedades y ausencia de sabor amargo en su zumo, con lo que las hace muy interesantes para la industria. En este subgrupo encontramos: Ambersweet, Hamlin, Pera, Salustiana, Jaffa o Shamouti, Valencia Late (la variedad más ampliamente cultivada del mundo).
- Naranjas pigmentadas (sanguina o roja): muy similares a las del grupo de las naranjas blancas, aunque se diferencian en que sintetizan pigmentos rojos (antocianinas) en la pulpa, y a veces en la piel, que necesitan del frío para activarse. El zumo obtiene un sabor especial parecido al de las cerezas o las frambuesas. El grupo de naranjas sanguinas solamente se cultivan en la región mediterránea, y encontramos variedades como: Doble fina, Maltaise, Moro, Sanguinelli (variedad española muy cultivada antiguamente), Sanguinello.
- Naranjas sucreñas: variedades ligeramente insípidas y con menor acidez, por esto actualmente son poco cultivadas. Las variedades más importantes de este grupo son: Succari, Sucreña, Lima, Vaniglia.

Entre los zumos de frutas, el de naranja es el de mayor producción y consumo (principalmente a partir de concentrado), representando el 50% del consumo total de zumos a nivel mundial; siendo Brasil y EE. UU. los principales productores, suministrando un 85% del zumo total. En España, la cantidad de naranja que se destina a la obtención de zumos depende fundamentalmente de la demanda del mercado en fresco (exportación y consumo nacional). Tradicionalmente, el elevado precio de la naranja como fruta de mesa había impedido el interés hacia la obtención de zumos en países como España. Sin embargo, la generación de beneficios comerciales a partir de destríos y de excesos en la producción, ha promovido durante los últimos años el desarrollo de nuevas metodologías destinadas a la obtención industrial de zumos de alta calidad. Así pues, el zumo de naranja ha sido objeto de numerosos estudios científicos y técnicos, que han cubierto prácticamente todos los aspectos de importancia.

1.1.2. Granada

La granada (*Punica granatum*), originaria del medio oriente, ha sido tradicionalmente un fruto valorado y admirado en numerosas civilizaciones, cuyo cultivo se conoce desde la antigüedad. Se trata de uno de los frutales bíblicos, como la vid, el olivo o la palmera, cuya característica principal es su adaptación a tierras pobres y su resistencia a la sequía. Existen diferentes variedades de granada, en España las más conocidas y comerciales son las siguientes: Mollar de Elche, Mollar valenciana y Wonderful, se trata de una fruta más grande de lo normal con un sabor más agradable.

Actualmente su cultivo se extiende por países como España, EE. UU., Irán, Turquía, India, Israel, China y países de la costa norte de África, entre otros. España se sitúa como el productor más importante y el mayor exportador de Europa, cuya producción se centra en la Comunidad Valenciana, Andalucía y Región de Murcia. La superficie actual de granado en España supera las 2.500 ha, con una producción próxima a las 37.000 toneladas (MAGRAMA, 2012).

La granada, se consume generalmente en fresco. Sin embargo, existe una gran parte de la cosecha que no posee suficiente calidad visual como para ser destinada al consumo en fresco, ya que su aceptación por parte del consumidor es muy baja, la cual se destina a la producción de otros productos industrializados como: zumos de granada (ampliamente comercializados en EE. UU. y con un gran potencial en España); arilos en IV gama; mermeladas; vinos, vinagres y licores; productos nutracéuticos elaborados a partir de extracto de corteza, etc. (Calín-Sánchez y Carbonell-Barrachina, 2012).

La composición del zumo de granada varía dependiendo de la variedad de la granada utilizada, las condiciones de crecimiento y maduración del fruto, así como de las técnicas de extracción del zumo y los tratamientos de estabilización del mismo para alargar su vida útil. Para la extracción del zumo, la fruta puede procesarse de distintas maneras, influyendo en la concentración final de compuestos bioactivos (Miguel *et al*., 2004).

1.1.3. Caqui

El caqui (*Diopyros kaki*) es un frutal que comprende más de 2.000 especies y tiene una gran importancia en algunos países asiáticos, especialmente en China, de donde es originario y donde su cultivo empezó algunos siglos antes de Cristo. En España, el caqui fue introducido a finales del siglo XIX, siendo un cultivo, especialmente de la costa Mediterránea, de árboles aislados, mezclados con otros frutales en los jardines, huertos familiares o en pequeñas plantaciones destinadas al consumo local. Se consumía totalmente blando, en su forma clásica, pues era la única forma en la que el fruto perdía su astringencia y era comestible. A mitad de los 70, se detectó una mutación de la variedad histórica "Picudo", en la zona de la Ribera del Xúquer (Carlet, L'Alcudia), que mejoraba notablemente el producto, y que se identificó con el nombre "Rojo Brillante" (Llácer y Badenes, 2002).

En los últimos 15 años, el cultivo de caqui en España ha experimentado un importante incremento, centralizado principalmente en la variedad "Rojo Brillante"; cuya producción en la Ribera del Júcar representa el 96% de la producción total en la Comunidad Valenciana y el 83% de la producción española, habiendo superado ya a la producción italiana que durante muchos años ha sido la más importante de Europa (Bellini *et al.*, 2008).

Según la FAO, en el año 2012 se cultivaron 813.536 ha a nivel mundial, de las cuales solo 2.257 ha, pertenecían a la Unión Europea, donde se obtuvo una producción de 47.681 toneladas de las 4.468.955 toneladas totales producidas a nivel mundial. Algunos países como España, Portugal, Turquía y otros, no figuran en las estadísticas de la FAO sobre el caqui, aunque actualmente sobrepasan largamente las cifras anteriores, probablemente porque este frutal se incluye en las estadísticas de esos países junto con otras especies frutales menores (FAOSTAT, 2012).

Los frutos de caqui se clasifican en cultivares "no astringentes" y "astringentes", dependiendo de si pierden o no la astringencia en el árbol o durante su postrecolección (Yamada *et al.*, 2012). Los primeros son aquellos que pueden ser consumidos inmediatamente tras la recolección; los segundos por el contrario, deben ser sometidos a procesos de sobremaduración o eliminación de la astringencia antes de ser consumidos. El caqui "Rojo Brillante" pertenece al grupo de los cultivares astringentes en el momento de la recolección, proporciona frutos muy grandes y atractivos por su forma y color con buen sabor y aroma, sin presentar dificultad para la eliminación de la astringencia (Arnal y del Rio, 2003; Besada *et al.*, 2008).

Habitualmente, el caqui se comercializa en fresco, cuando su textura es firme y el producto puede resistir adecuadamente el estrés mecánico. Además, es un fruto muy perecedero, de consumo estacional, y su comercialización se restringe a zonas próximas a las de producción, pues no soporta una conservación frigorífica prolongada y aún no se han desarrollado casi productos derivados de él, debido a que es un producto difícil de industrializar pues cuando se transforma en puré tiende a gelificar y pardear. Por otra

parte, si se aplica un tratamiento térmico intenso de conservación y en condiciones ácidas las formas no astringentes de tanino se hidrolizan y dan lugar a taninos solubles, con lo que el producto se vuelve astringente.

1.2. PROCESADO DE FRUTAS. TRATAMIENTOS INDUSTRIALES

La estacionalidad y el carácter perecedero de las frutas explican la necesidad de aplicar tratamientos industriales y tecnologías de conservación. La demanda de alimentos mínimamente procesados ha aumentado en los últimos años y además, el consumidor prefiere alimentos de alta calidad semejantes a los productos frescos (aroma, sabor, color y valor nutritivo). El interés del consumidor por los productos frescos puede satisfacerse con productos refrigerados. Sin embargo, en estas condiciones la vida útil de estos es limitada, lo cual representa una oportunidad comercial para la industria de los alimentos tratados por alta presión que consiguen incrementarla (Torres y Velázquez, 2005). Adaptarse a las nuevas corrientes y exigencias del consumidor ha sido uno de los objetivos prioritarios de la industria alimentaria, por lo que desde hace algunos años se están elaborando zumos más parecidos a los naturales, con una ligera pasteurización, que se comercializan bajo refrigeración con un tiempo de vida útil limitado. El objetivo es combinar el aumento de la vida media con el mantenimiento de las características nutritivas y sensoriales del alimento (Giannakourou y Taoukis, 2003).

Tradicionalmente, el tratamiento térmico ha sido el método más utilizado para la conservación de los alimentos. Aunque esta tecnología sea económica, efectiva para la inactivación de microorganismos, en muchos casos su aplicación induce modificaciones fisicoquímicas que producen pérdidas importantes en la calidad de los alimentos, destruyendo constituyentes deseables a nivel nutricional, color, aroma y textura, sobre todo cuando se utilizan temperaturas elevadas durante largo tiempo (Nagy *et al*., 1989).

Las tendencias actuales en la producción de alimentos tratan de desarrollar nuevas tecnologías no térmicas para la conservación de los mismos con el mínimo

tratamiento, y así obtener alimentos con una mayor calidad nutritiva y sensorial; el procesado por altas presiones dinámicas (HPH) o por pulsos eléctricos de alta intensidad (PEF) permiten la inactivación de microorganismos patógenos y enzimas, con cambios mínimos en su textura, color y sabor (Sentandreu *et al.*, 2006; Torres y Velazquez, 2005; Vervoort *et al*., 2011).

En este estudio se han empleado los siguientes tratamientos de conservación en los zumos de naranja:

- Pasteurización: tratamiento por calor que reduce la carga microbiana e inactiva las enzimas del alimento, propiciando en función de la temperatura alcanzada diferentes pérdidas de aroma, sabor, textura y calidad nutritiva, además de inducir una destrucción selectiva de la población microbiana patógena. El producto resultante tiene una vida media acorde con la intensidad del tratamiento aplicado y necesita de otro método de conservación (como la refrigeración o la congelación) en los tratamientos suaves. Actualmente, los zumos de alta calidad se someten a temperaturas entre los 70-95 ºC durante 15-30 segundos, obteniendo así una vida útil en refrigeración de entre dos y cuatro semanas. En el zumo de naranja, y como se ha mencionado anteriormente, los efectos no deseables de este tratamiento varían en función del vigor del tratamiento aplicado, variando entre unas pérdidas apreciables de aroma, sabor y valor nutritivo (Marcotte *et al.*, 1998) hasta cambios poco significativos de los mismos (Sentandreu *et al*., 2005).
- Altas Presiones dinámicas: tratamiento de conservación que emplea presiones elevadas (hasta 870 MPa), con o sin aplicación de calor, inactivando microorganismos perjudiciales y produciendo perdidas mínimas en la calidad del alimento. Los cambios químicos y microbiológicos que se producen en los alimentos dependen de la temperatura alcanzada y del tiempo de tratamiento. Estudios realizados han demostrado que los productos tratados por HPH mantienen casi en su totalidad las características originales de los productos

frescos (Oey *et al*., 2008). Actualmente, los tratamientos por HPH están siendo aplicados en una amplia gama de alimentos para garantizar su seguridad y aumentar su vida útil, entre los que se encuentran productos lácteos, zumos y bebidas.

1.3. IMPORTANCIA DEL CONSUMO DE FRUTAS Y ZUMOS COMO FUENTE DE SALUD

Las frutas y sus derivados, en forma de zumos principalmente, se han convertido actualmente en alimentos imprescindibles para cualquier dieta sana y equilibrada ya que contienen elevadas cantidades de minerales, vitaminas, provitaminas, fenoles y carotenoides (Figura 2). Dichos componentes, además de tener un papel bioquímico y fisiológico importante en las plantas, tienen un gran interés a nivel farmacológico y nutricional (Chen *et al.,* 2007) derivado principalmente de su carácter como antioxidantes.

A lo largo de este último siglo, el papel de la nutrición en relación con la salud ha pasado por distintas etapas, desde la prevención de las llamadas enfermedades carenciales, hasta más recientemente, su papel potencial en la consecución de una salud óptima. Uno de los objetivos clave de la investigación en nutrición se centra en establecer relaciones evidentes entre los componentes de la dieta y las enfermedades crónicas, considerando que determinados nutrientes podrían proporcionar resultados beneficiosos para la salud, en este sentido, el consumo de frutas y verduras tiene un gran efecto protector frente al riesgo de determinadas enfermedades degenerativas y otras disfunciones relacionadas con el estrés oxidativo como el cáncer, enfermedades cardiovasculares, cataratas, disfunciones del cerebro entre otras (Dillard y German, 2000; Grassi *et al*., 2009; Kaur y Kapoor, 2001; Krajcovicova-Kudlackova, 2005; Scalbert *et al*., 2005), aunque no se conocen con exactitud todos los mecanismos bioquímicos por los cuales los componentes de un alimento afectan a las funciones fisiológicas del individuo.

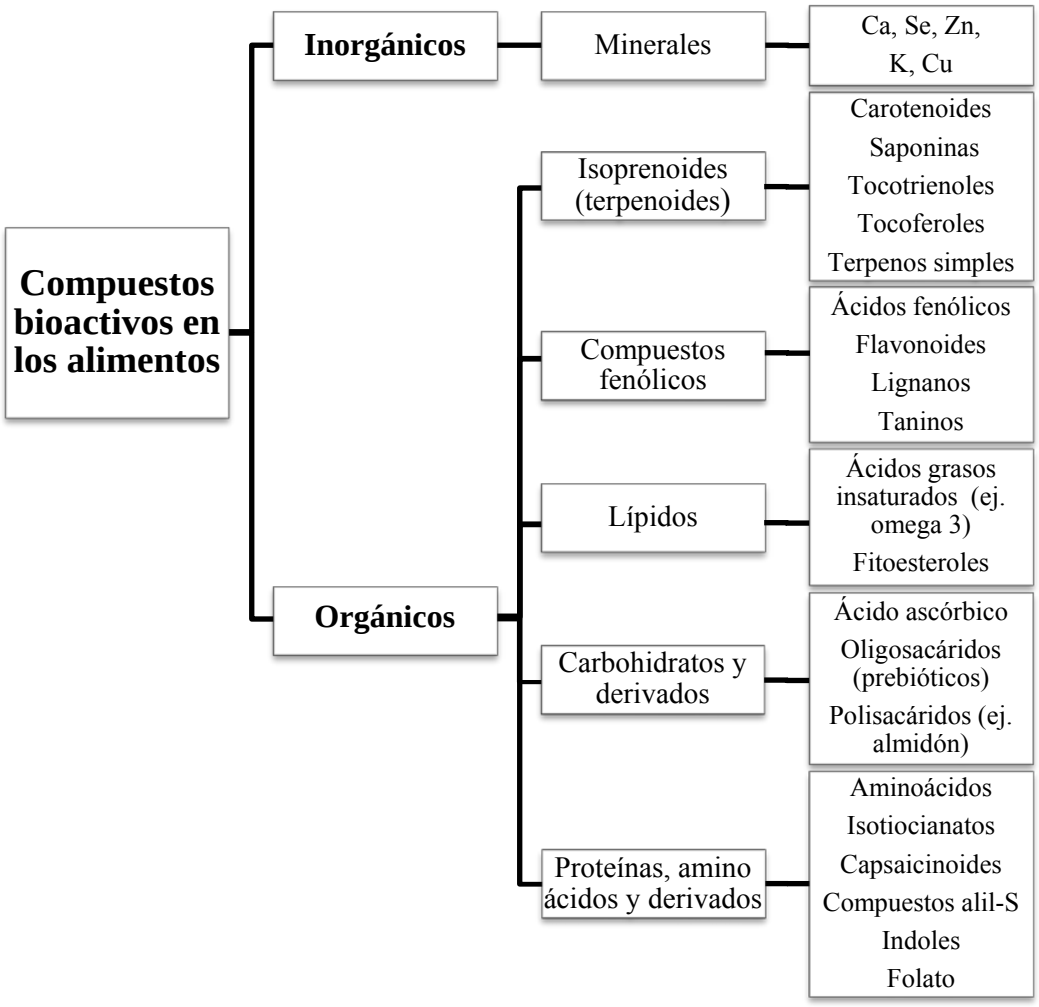

Figura 2. Algunos de los compuestos bioactivos que se pueden encontrar en los alimentos, clasificados según su naturaleza química (Martínez-Hernández y Martí del Moral, 2005).

Según Lampe (1999), los efectos potencialmente beneficiosos del consumo de frutas y hortalizas son:

- Actividad antioxidante.
- Modulación de enzimas detoxificantes.
- Estimulación del sistema inmune.

- Disminución de la agregación plaquetaria.
- Alteración del metabolismo del colesterol.
- Modulación de la concentración de hormonas esteroideas y del metabolismo hormonal.
- Disminución de la presión sanguínea.
- Actividad antiviral y antibacteriana.

El efecto beneficioso de los compuestos bioactivos y otros nutrientes presentes en los alimentos depende de la cantidad que dicho compuesto consigue alcanzar determinados lugares del organismo en la forma químicamente activa. Hay que tener en cuenta que algunos de los compuestos bioactivos incorporados por la dieta no llegan en cantidades óptimas a los tejidos, bien porque no están presentes en cantidades suficientes o porque su biodisponibilidad, cantidad de un nutriente que se absorbe y puede ser utilizado por el organismo, es baja debido a otros factores asociados al alimento como por ejemplo, la acción de estructuras celulares que dificultan su liberación e interacción con otros nutrientes que puede potenciar o inhibir su absorción y/o captación por los tejidos (Granado *et al.*, 2003). Durante el procesado de los alimentos se favorece la reacción de las enzimas con sus correspondientes sustratos y la salida de nutrientes y compuestos bioactivos desde los orgánulos y otros compartimentos celulares. Este hecho da lugar a modificaciones relacionadas con la calidad sensorial (color, textura, aroma) y nutricional de los alimentos. De esta manera y de manera adicional, la biodisponibilidad de los nutrientes es afectada por las modificaciones de la microestructura como consecuencia del procesado (Parada y Aguilera, 2007).

Como ejemplo tenemos el estudio de los componentes bioactivos de la granada y sus efectos sobre la salud. Se ha comprobado que tanto la granada como sus productos derivados contienen componentes que pueden servir para la prevención de enfermedades y para el mantenimiento de la salud (Lansky y Newman, 2007). La granada posee numerosos compuestos químicos de alto valor biológico en sus diferentes partes: corteza, membranas carpelares, arilos y granos (semilla y vesícula). Los

compuestos fitoquímicos de mayor relevancia presentes en la granada son una gama de diferentes compuestos fenólicos tales como los antocianos, taninos condensados (proantocianidinas) y taninos hidrolizables (elagitaninos y galotaninos) (Aguilar *et al*., 2008; Jaiswal *et al*., 2010).

Los antocianos son los compuestos considerados responsables del color rojo de las granadas, los cuales presentan una potente acción antioxidante y antirradical que protege frente a los radicales libres, retrasando el proceso de envejecimiento celular (El Kar *et al.*, 2011; Gil *et al*., 2000). Los elagitaninos y antocianos son los principales compuestos fenólicos de la granada, teniendo a la punicalagina y punicalina como específicos de este fruto, confiriéndole una potente actividad antirradical (Lu, J. *et al.*, 2008; Machado *et al*., 2002). Los diferentes compuestos fenólicos son extraídos en niveles significantes en el zumo durante el proceso hidrostático industrial, confiriéndole al zumo comercial de granada una potente actividad antioxidante (Aguilar *et al*., 2008).

Por su parte, el caqui ha desempeñado un papel importante en la medicina tradicional china desde hace más de 2.000 años, principalmente por sus propiedades diuréticas, antihipertensivas, antioxidantes, antiinfecciosas y anticancerígenas (Giordani *et al.*, 2011). Algunas investigaciones (Daood *et al*., 1992; Gorinstein *et al*., 1998; Wright y Kader, 1996) han demostrado que el caqui es una fuente abundante de polifenoles (taninos y ácidos fenólicos principalmente), vitamina C, minerales y carotenoides (principalmente localizados en la piel), lo que contribuye en gran medida al color naranja intenso de la fruta madura (Giordani *et al*., 2011). En esta línea y de gran interés organoléptico, el caqui contiene una importante cantidad de taninos condensados (proantocianidinas del grupo B), que tienen la propiedad de formar complejos estables con metales y proteínas siendo los responsables de la astringencia característica de estos frutos (Nakatsubo *et al.*, 2002; Santos-Buelga y Scalbert, 2000), los cuales se convierten a taninos insolubles (no astrigentes) durante la maduración (Arnal y Del Río, 2003). Como curiosidad indicar que los cultivos no astringentes tienen muchos menos polifenoles, catequinas y taninos que los cultivos astringentes (Chen *et al.,* 2008; Giordani *et al*., 2011).

1.4. CARACTERIZACIÓN DE FRUTAS Y SUS ZUMOS

La caracterización de frutas y sus zumos presenta numerosos motivos de interés, entre los que encontramos:

- En primer lugar y como se ha mencionado anteriormente, son muchos los efectos beneficiosos del consumo de frutas y sus derivados sobre la prevención de múltiples enfermedades, y las recomendaciones nutricionales tienden a un mayor consumo de este tipo de alimentos; así pues el conocimiento concreto de la composición de cada fruta tendría muchas aplicaciones prácticas en el campo de la nutrición.
- En segundo lugar, es muy conocido el fenómeno de fraude por adulteración en la fabricación de zumos, mermeladas y otros productos derivados de las frutas, a los que en algunas ocasiones se les añade agua, azúcares, colorantes o se utilizan frutas de menor valor económico. Algunos compuestos como los azúcares y los compuestos polifenólicos pueden ser utilizados como marcadores específicos para la evaluación del proceso de elaboración y vida útil, así como la autenticidad, de los productos derivados (Elkins *et al.*, 1988). En este sentido, es muy útil el conocimiento de la composición química de las distintas especies de fruta a considerar ya que al realizar los pertinentes análisis composicionales podrían detectarse adulteraciones no percibidas sensorialmente. En concreto, es de gran ayuda en la determinación de la autenticidad de los productos derivados de las frutas el conocimiento de la composición de compuestos polifenólicos, ya que cada especie tiene unos constituyentes concretos y en una proporción determinada, aún variando en función de múltiples factores como el grado de madurez, variedad y origen geográfico.
- Por último, el estudio de los cambios producidos en la composición/proporción de compuestos volátiles, azúcares, ácidos orgánicos y compuestos fenólicos durante el procesamiento y almacenamiento de frutas y sus derivados, ayuda a

conocer los efectos producidos sobre su calidad organoléptica y nutricional. Esto facilita la toma de decisiones encaminadas a la mejora del producto final.

Por todo esto, es de gran interés científico la obtención de cualquier información acerca del perfil composicional característico de las frutas y de sus derivados. En el presente trabajo, dicha caracterización se ha llevado a cabo mediante diferentes métodos de preparación de muestra y su posterior estudio por técnicas de cromatografía de gases (GC) y cromatografía líquida de alta resolución (en inglés High performance liquid chromatography, HPLC) acopladas a la espectrometría de masas (MS).

1.4.1. Determinación de compuestos volátiles en zumo de naranja por GC-MS

El "flavor", aroma y sabor, de los zumos de cítricos es un atributo muy complejo ya que está determinado por el equilibrio entre sus ácidos, azúcares y componentes volátiles principalmente. Su estudio constituye un criterio básico para la evaluación de la calidad de los productos frescos y procesados, y es uno de los factores determinantes de la aceptación del producto final por el consumidor (Pérez-Cacho y Rouseff, 2008).

El perfil aromático de los zumos cítricos se debe a un grupo de sustancias tales como alcoholes, aldehídos, cetonas, ésteres y compuestos hidrocarbonados (monoterpenos y sesquiterpenos), constituyendo una fracción complicada cuyo análisis requiere de una técnica instrumental de gran poder analítico como la GC-MS.

Estos compuestos se encuentran dentro de una matriz no volátil compleja formada principalmente por agua y carbohidratos, por lo que es necesaria su extracción previa al análisis por GC-MS. Así pues, en los años 90, Pawliszyn y colaboradores desarrollaron la técnica de Microextracción en fase sólida (Solid Phase Microextraction, SPME) (Arthur *et al*., 1992) como solución práctica para su extracción eficaz. Esta técnica se basa en la extracción y concentración de los analitos de una matriz compleja mediante una fibra de sílice fundida, de muy pequeñas dimensiones, recubierta con una

fase estacionaria polar o no. Es un método sencillo, fácil, rápido, barato y de gran versatilidad debido al amplio número de fibras comerciales existentes.

Una variación de la técnica SPME, es la extracción de espacio de cabeza o headspace (HS/SPME) donde la fibra se expone en el espacio de cabeza del recipiente que contiene la muestra produciéndose un proceso de equilibrio entre tres fases del sistema: el espacio de cabeza, la fase estacionaria de la fibra y la solución acuosa (Zhang y Pawlinszyn, 1993). Una de las principales ventajas de este modo de extracción es que se alarga la vida útil de la fibra ya que se evitan interferencias con otros componentes de la muestra, sobre todo aquellos de elevado peso molecular. Por esta razón, es el tipo de extracción más utilizado en el análisis de volátiles y semivolátiles en alimentos (Kataoka *et al.*, 2000; Stashenko y Martínez, 2007). Los volátiles en zumos de naranja, por lo general, han sido determinados por HS/SPME combinado con GC-MS, identificándose entre 50-90 volátiles en total (Barboni *et al.*, 2009; González-Mas *et al.*, 2011; Högnadóttir y Rouseff, 2003; Riu-Aumatell *et al*., 2004).

El procedimiento de HS/SPME (Figura 3) aplicado a los zumos de naranja consta de las siguientes fases:

- Acondicionamiento de la fibra: Consiste en la desorción térmica de los compuestos volátiles retenidos en la fase procedentes del ambiente o de anteriores determinaciones. Normalmente se trata de una desorción térmica que se lleva a cabo exponiendo la fibra a temperaturas que dependen de cada fase polimérica, por lo general superiores a 250 ºC.
- Equilibrio: La muestra líquida se coloca durante cierto tiempo en un vial sellado, bien a temperatura ambiente o calentada a una temperatura moderada, hasta alcanzar en el espacio de cabeza el equilibrio termodinámico de los compuestos entre la fase de la muestra y la fase gaseosa que la rodea.
- Extracción: Cuando los analitos volátiles de la muestra están en equilibrio con la fase gaseosa que los rodea, la fibra se introduce en el espacio de cabeza del vial.

En esta etapa se produce la migración de los analitos desde el espacio de cabeza hacia la fibra hasta alcanzar una nueva situación de equilibrio.

- Desorción: En esta etapa se liberan los analitos retenidos por la fibra. La más común es la desorción térmica, que se lleva a cabo cuando la fibra se acopla al inyector del cromatógrafo de gases, que se encuentra a una temperatura suficientemente elevada para que de forma instantánea se desorban los analitos entrando en la columna cromatográfica.

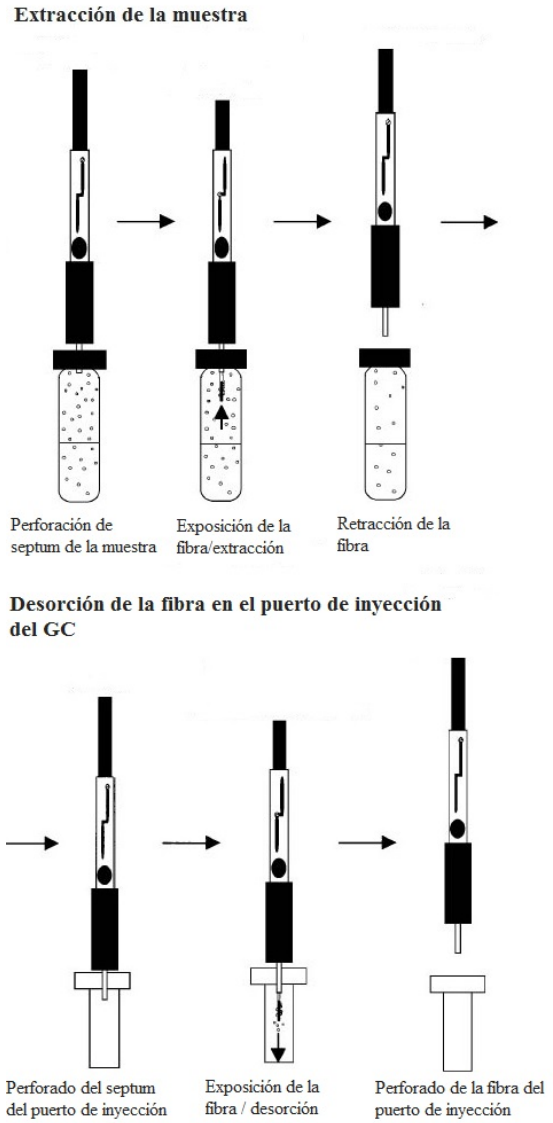

Figura 3. HS/SPME
La fila superior muestra el proceso para la recogida de una muestra con una fibra de SPME.
Y la fila inferior muestra el procedimiento para la transferencia de la muestra al instrumento.

1.4.2. Determinación de compuestos polares no volátiles en zumo de naranja por GC-MS

Para esta determinación es necesaria la derivatización previa de los azúcares, aminoácidos y ácidos orgánicos contenidos en la muestra, inicialmente no volátiles, para convertirlos en compuestos de mayor volatilidad, y por tanto analizables por esta técnica. De este modo, podremos llevar a cabo la determinación simultánea de todos ellos. Entre las distintas derivatizaciones utilizadas para la determinación de estos compuestos por GC-MS se encuentran los acetatos, metil éteres, trifluoroacetatos y trimetilsilil (TMS) derivados.

En el caso particular de los TMS-derivados, el proceso consiste en la sustitución de los grupos hidroxilo de los analitos por el radical $Si(CH_3)_3$, tal y como ilustra la Figura 4. Los derivados obtenidos presentan unas características de volatilidad y estabilidad muy adecuadas, por lo que han sido ampliamente utilizados en el análisis composicional de vegetales (Katona *et al*., 1999; Roessner-Tunali *et al.*, 2003; Sheperd *et al.*, 2007), aunque de escasa aplicación en el caso de los zumos cítricos (Füzfai y Molnár-Perl, 2007).

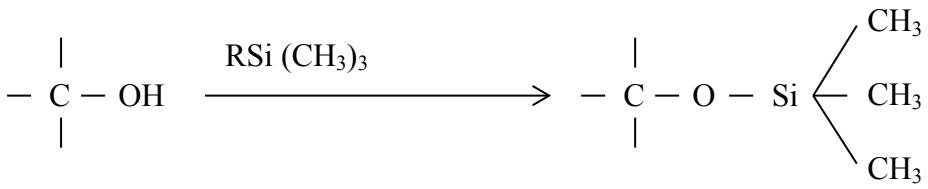

Figura 4. Formación de TMS-derivados

1.4.3. Determinación de compuestos fenólicos en zumo de granada y en pulpa de caqui por HPLC-DAD/ESI-MS^n

En la mayoría de las ocasiones, se trata de componentes minoritarios que se encuentran en concentraciones muy pequeñas por lo que son necesarias técnicas

analíticas sensibles, selectivas y con gran capacidad de resolución. En los últimos 20 años, la técnica analítica que ha predominado a la hora de llevar a cabo la separación y caracterización de los compuestos fenólicos ha sido mediante HPLC. Existe una amplia variedad de equipos y fases móviles disponibles para la determinación de flavonoides, proantocianidinas, ácidos benzoicos, etc.

La variación de polaridad de los diferentes compuestos fenólicos permite su extracción con disolventes, solos o en mezclas (agua, etanol, metanol, acetona, acetonitrilo etc.). Algunos métodos implican la extracción primaria con disolventes muy apolares para la eliminación de grasas y ceras principalmente para con posterioridad, utilizar mezclas acuosas con disolventes orgánicos menos agresivos de polaridad intermedios (Lock y Cabello, 2006).

En ocasiones, a los compuestos fenólicos conjugados se les somete a un proceso de hidrólisis, consiguiendo la liberación de la fracción no azucarada (aglicona) y su posterior identificación. Esta hidrólisis preliminar de las muestras se ha usado como herramienta para la elucidación estructural y caracterización de compuestos glicosilados, para eliminar interferencias en futuros análisis por técnicas separativas, así como para simplificar los datos obtenidos de los análisis sobre todo en aquellos casos en los que no existen estándares comerciales (Markham, 1982). No obstante, hay que tener en cuenta las posibles reorganizaciones de las agliconas liberadas durante el proceso de hidrólisis, dando lugar a complejos cuya identificación se ve dificultada.

1.4.4. Determinación *in vitro* de la actividad antirradical de zumo de granada. Método del DPPH$^{\bullet}$ (2,2-difenil-1-picrilhidrazil)

Debido al interés que suscita la relación entre la presencia de radicales libres y el riesgo de padecer ciertos tipos de enfermedades, se han desarrollado diferentes métodos *in vitro* para determinar la capacidad antirradical de los alimentos. Estos métodos se basan en comprobar cómo los agentes antioxidantes de los alimentos reducen un sustrato oxidado.

El fundamento del método DPPH$^{\bullet}$ consiste en determinar la capacidad de los antioxidantes de la muestra para captura del radical libre DPPH$^{\bullet}$. Este radical presenta en su estado oxidado un pico máximo de absorción a 515 nm. Tras la incorporación del antioxidante (o mezcla de varios) se produce una disminución de la absorbancia de la solución que contiene la sonda oxidada la cual es proporcional a la concentración y actividad de los antioxidantes adicionados tal y como muestra la Figura 5 (Brand-Williams *et al.*, 1995). La sonda antirradical, que muestra un intenso color púrpura, es estable y está disponible comercialmente, lo que reduce el tiempo de análisis al no tener que ser generado antes del ensayo. Además, este método es fácilmente comparable con otros métodos de medida basados en la captura de radicales libres.

Este método ha sido aplicado a diferentes alimentos y bebidas tales como vinos (Villaño *et al*., 2006), aceites (Gorinstein *et al.*, 2003), zumos de naranja (Sendra *et al.*, 2006). Hay que hacer constar que tan importante como la determinación de la capacidad antirradical *in vitro* de los extractos naturales es la medida de sus cinéticas de actividad (ultrarápida, rápida y lenta), las cuales pueden ser utilizadas como marcadores específicos (huella dactilar) de las muestras estudiadas (Sentandreu *et al*., 2008).

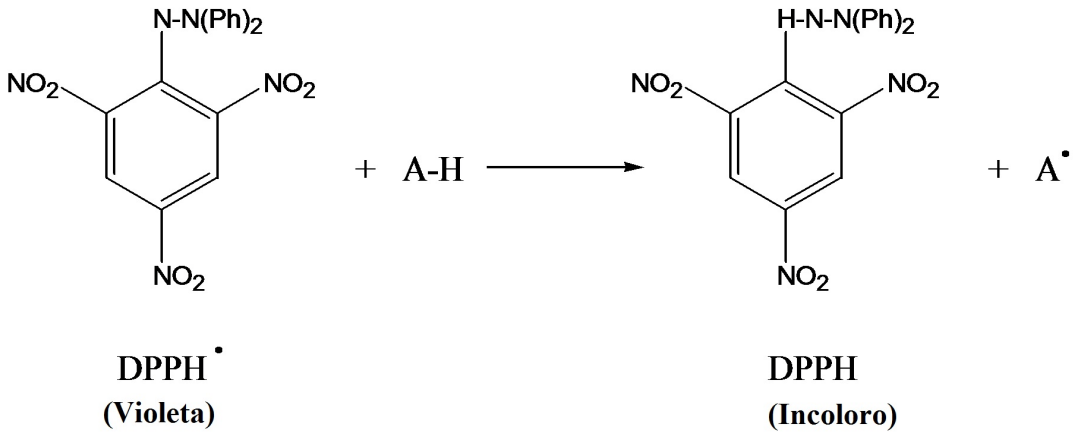

Figura 5. Método DPPH$^{\bullet}$

1.5. TÉCNICAS ANALÍTICAS BASADAS EN LA CROMATOGRAFÍA ACOPLADA A ESPECTROMETRÍA DE MASAS

En 1910, el botánico ruso M. Tswett introdujo por vez primera el término de "cromatografía" tras su aplicación a la separación de pigmentos de plantas, dándole dicho nombre en referencia a las bandas coloreadas de pigmentos que se separaban por su adsorción selectiva sobre columnas de yeso. Un hecho importante en el desarrollo de la cromatografía lo constituyó el desarrollo de la cromatografía gas-líquido (James y Martin, 1952), técnica que encontró rápidamente aplicaciones de gran importancia, lo que llevo a su vez al desarrollo de la teoría de la separación cromatográfica (Van Deemter *et al.,* 1956) así como al desarrollo de una instrumentación que permitía un mayor control de las condiciones de trabajo.

La cromatografía permite separar entre sí los componentes de una matriz compleja, encontrando que su gran aplicabilidad se debe a la variedad de condiciones que pueden utilizarse para separar dichos componentes. Se pueden utilizar diferentes fases móviles (gases, líquidos o fluidos supercríticos) y estacionarias (minerales, polímeros orgánicos e inorgánicos o sólidos recubiertos de líquidos) (Rubinson y Rubinson, 2001). Hoy en día, en casi todos los campos de las ciencias experimentales (química, biología, medicina, etc.) se utiliza la cromatografía en alguna de sus formas, tanto en su vertiente preparativa como en la analítica; por otra parte, el desarrollo del uso conjunto de la cromatografía con otras técnicas analíticas, así como el desarrollo de otros tipos de cromatografía hace previsible una extensión aún mayor de su uso.

La característica que distingue a la cromatografía de la mayoría de los métodos físicos y químicos de separación es que se ponen en contacto dos fases mutuamente inmiscibles (una estacionaria y otra móvil). La muestra se introduce en la fase móvil donde es transportada a lo largo de la columna que contiene la fase estacionaria. Los componentes de la muestra experimentan interacciones repetidas (repartos) entre la fase móvil y la fase estacionaria, provocando que los diferentes constituyentes de la muestra se separen gradualmente en bandas en la fase móvil. Al final del proceso los

componentes separados emergen en orden creciente de interacción con la fase estacionaria, el componente menos retenido emerge primero mientras el más afín con la fase estacionaria eluye el último.

En comparación con la cromatografía líquida (LC), la GC tiene la ventaja de disponer de detectores mucho más versátiles (por ejemplo, el de ionización de llama), por lo que permiten el análisis de un número mayor de especies diversas de analitos. Además, para numerosas aplicaciones los métodos son más simples, rápidos y sensibles que los correspondientes a HPLC. La instrumentación requerida para GC también es mucho más sencilla y económica que la empleada en HPLC. Sin embargo, en GC, la influencia de la temperatura sobre la estabilidad de los analitos es considerable, a diferencia de la HPLC, por lo que la GC se emplea cuando los componentes de la mezcla problema son volátiles o semivolátiles y térmicamente estables a temperaturas de hasta 350-400 ºC. En cambio, cuando los compuestos a analizar son poco volátiles y/o termolábiles, la técnica separativa adecuada suele ser HPLC (Gutiérrez y Doguet, 2002).

Por su parte, la espectrometría de masas es una herramienta analítica muy completa, de elevada capacidad y de aplicación muy general, pudiéndose utilizar en investigación básica, análisis de rutina, en controles de calidad entre otras aplicaciones. Se basa en la generación de los iones correspondientes a las moléculas de los analitos que constituyen la muestra para posteriormente, determinarlos de acuerdo con su relación masa/carga (*m/z*). Los espectros de masas suministran información sobre la estructura de especies moleculares complejas, las relaciones isotópicas de los átomos en las muestras y la composición cualitativa y cuantitativa de analitos orgánicos e inorgánicos en muestras complejas.

Existe diferentes tipos de espectrómetros de masas destacando los de simple y triple cuadrupolo, trampa de iones, tiempo de vuelo (TOF), sectores magnéticos, transformador de Fourier-ICR y orbitales. Una característica común a todos ellos es la necesidad de trabajar en condiciones de muy baja presión ($<10^{-4}$ Torr) así como la

separación de los iones se realiza en fase gaseosa en función de su relación *m/z*. Sin embargo, difieren en los medios empleados para llevar a cabo la ionización y separación, haciendo variar la sensibilidad y la información suministrada por cada uno de ellos en cuanto a la resolución de masas, la precisión, el rango de masas y la velocidad de escaneo.

El sistema de ionización más frecuente en GC es mediante impacto electrónico (sus siglas en inglés, EI), en el cual las moléculas neutras de la muestra se hacen colisionar con iones cargados con una energía de 70 eV, provocando la emisión de un electrón de las moléculas del analito y así ionizarlas mediante la generación de una carga residual positiva. Además de los iones moleculares (M^+) también se generan sus correspondientes iones fragmento debido a la fractura de su estructura molecular durante el proceso de ionización, lo cual será utilizado para la posterior identificación de los analitos estudiados. En el caso de compuestos no volátiles, la ionización se produce por otros métodos como la inducida por electrospray (ESI-MS), por ionización química (APCI-MS), por bombardeo con átomos rápidos (FAB-MS) y por ionización/desorción por láser (MALDI-MS).

Una vez ionizadas las moléculas estas son aceleradas y conducidas hacia el sistema de detección mediante campos eléctricos o magnéticos. La detección de los iones formados a partir de las moléculas de la muestra así como de sus correspondientes fragmentos tras aplicar diferentes condiciones de ruptura (normalmente por disociación inducida por colisión, CID, aunque recientemente han surgido otras vías como la ETD, disociación por transferencia de electrones) produce el espectro de masas característico de los constituyentes detectados.

El espectrómetro de masas además de ayudar en la identificación de compuestos a través de la generación de sus iones moleculares y espectros de fragmentación, actúa como detector cromatográfico al registrar la corriente iónica total (en inglés, TIC chromatogram) generada. La corriente iónica generada por todos los iones da lugar a picos gaussianos cuyas áreas bajo la curva están relacionadas con la concentración del

analito. En el caso de mezclas complejas, el cromatograma obtenido puede presentar muchos picos, algunos de ellos muy próximos o totalmente solapados, resultando difícil la identificación rápida y fiable de los compuestos implicados. Cuando se desea explícitamente localizar la presencia de uno o varios compuestos en concreto se recurre a la técnica de detección por seguimiento del ión aislado (SIM, del inglés Single Ion Monitoring). En esta modalidad de trabajo se visualizan únicamente las masas de interés y no todas como en el caso del TIC, aumentando por tanto la selectividad del método.

La introducción de la MS ha supuesto un gran avance en las técnicas analíticas por su gran sensibilidad y su alto grado de fiabilidad. Su principal ventaja sobre otras técnicas de detección (UV-Vis, fluorimetría, detección electroquímica) es por un lado, su capacidad para suministrar información útil desde el punto de vista cualitativo, teniendo que el espectro de masas pueda ser una prueba casi inequívoca de la identidad del compuesto considerado. Por otro lado, se trata de detectores universales basados en la separación de las especies cargadas de acuerdo con su relación *m/z*. La MS se presenta como uno de los métodos de detección más sensibles, específicos, fiables y de mayor capacidad para el análisis molecular.

1.5.1. Cromatografía de gases acoplada a espectrometría de masas (GC-MS)

La GC es una técnica que posee una inmejorable capacidad separativa (propiciada por la resolución cromatográfica de las columnas capilares empleadas), pudiendo analizar una gran variedad de compuestos termoestables, volátiles o susceptibles de serlo, en muestras complejas. Su sensibilidad y selectividad aumentan enormemente cuando ésta se combina con la MS.

El acoplamiento de la MS a la GC surge a finales de la década de 1950 (Abian, 1999). En la actualidad, esta metodología es robusta y se utiliza de forma rutinaria en los laboratorios de análisis, resultando ser una técnica de cribado indiscutible. Esto se debe a la gran reproducibilidad de la ionización por EI, dando lugar a la fragmentación estable de los compuestos independientemente de la instrumentación utilizada. Esto ha

posibilitado la creación de librerías que incorporan los espectros de masas característicos de una gran multitud de compuestos, pudiendo llevar a cabo labores de caracterización sistemática y automatizada de las muestras sometidas a estudio (Bogusz, 2000). Sin embargo, el principal inconveniente de la GC es la dificultad en el análisis de determinados compuestos, como sustancias poco volátiles, polares o termolábiles, haciéndose necesaria la utilización de laboriosos procedimientos de derivatización.

En GC-MS, la muestra se introduce en el analizador a través de un puerto de inyección calentado a elevada temperatura (alrededor de 250 ºC), siendo posteriormente arrastrado y conducido a la columna de separación mediante un gas portador (generalmente helio), la cual se encuentra dentro de un horno con programación de temperatura. Una vez separados generalmente mediante una rampa de temperatura, pasan al espectrómetro de masas donde son identificados. Cada uno de los componentes se registra en forma de pico cromatográfico, y por tanto integrable/cuantificable, llevando a cabo el proceso de identificación a partir de su respectivo espectro de masas.

Generalmente, la muestra a inyectar se encuentra en estado sólido o líquido, por lo que debe ser vaporizada. La temperatura óptima del inyector se determina experimentalmente y en general es igual o superior a la temperatura máxima alcanzada por la columna durante la separación.

Inyectar una muestra en una columna capilar de diámetro inferior a un milímetro es complicado porque el volumen de muestra debe ser pequeño para no causar una sobrecarga de la fase estacionaria. Para mantener la cantidad de muestra en el intervalo correcto se emplea el inyector en modo con o sin división (en inglés, split/splitless respectivamente), el cual permite reducir la cantidad de muestra que llega a la cabeza de la columna capilar. Las muestras con concentración baja de analito se inyectan por el método splitless y se arrastran mediante el gas acarreador a la columna. Por otro lado, si se utiliza el método split sólo una fracción del gas portador de muestra llega a la columna.

1.5.2. Cromatografía líquida de alta resolución con detector de fotodiodos acoplada a la espectrometría de masas con electroespray (HPLC-DAD/ESI-MS^n)

La separación por HPLC (aparecida en 1969) ha sido frecuentemente utilizada en bioquímica y química analítica para separar los componentes de una mezcla basándose en diferentes tipos de interacciones químicas que se dan entre los analitos, la columna cromatográfica y la fase móvil. Actualmente, es la técnica analítica más utilizada para la separación y caracterización de compuestos fenólicos en cualquier extracto natural. Esta técnica permite el acoplamiento de numerosos sistemas de detección como UV-Vis (espectroscopía ultravioleta-visible), detector de fotodiodos (en inglés, Diode Array Detector, DAD) (Chen *et al.*, 2006) y MS (Nicoletti *et al*., 2008), entre otros. El desarrollo de sistemas que permiten el acoplamiento entre un sistema HPLC y un detector de masas ha dado lugar a la gran expansión de esta metodología analítica en las últimas décadas, ya que en su origen aparecieron numerosos problemas debidos a la ionización a presión atmosférica de la muestra en fase líquida procedente del HPLC. Las principales interfaces generalmente usadas para ionizar a presión atmosférica (API) son: la ionización química a presión atmosférica y la ionización por electrospray (APCI y ESI, respectivamente, Vékey, 2001).

La fuente ESI ioniza las muestras en estado líquido mediante la formación de un espray de gotas, es decir, la evaporación e ionización del analito se producen simultáneamente. En ESI se puede trabajar en modo positivo o negativo (ESI^+ o ESI^-) en función de la polaridad del voltaje aplicado en el capilar de la sonda de ionización. Además del ion pseudomolecular, la presencia de ciertas especies iónicas procedentes del material de laboratorio (generalmente, cationes Na^+ y Ca^{2+}), del solvente (p.ej. ácido fórmico) y reacciones de polimerización (dimerización principalmente) puede dar lugar a la formación de aductos.

La respuesta originada en ESI depende en gran medida de la naturaleza del compuesto a analizar, permitiendo el análisis de compuestos de polaridad alta e intermedia. Una de sus principales aplicaciones es el análisis de biomoléculas polares de

elevado peso molecular y termolábiles como es el caso de péptidos y proteínas, ambos difícilmente analizables mediante otras técnicas.

Por otra parte, la tendencia más importante en el desarrollo de la cromatografía líquida desde sus inicios hasta la actualidad ha sido conseguir métodos de análisis cada vez más rápidos y eficientes. En la pasada década, se propusieron diferentes soluciones para mejorar la velocidad de análisis mediante LC, siendo este un reto importante para los instrumentalistas. En general, la tendencia se orienta hacia el uso de columnas con partículas cada vez de menor tamaño, con el correspondiente uso de presiones más elevadas. Las columnas más utilizadas son las de fase reversa (con diferentes rellenos, dimensiones y tamaños de partícula), quedando el uso de las de fase normal reducido a un limitado número de aplicaciones (compuestos muy polares como los azúcares). En este sentido, destacar que los avances (referidos principalmente a la electrónica implicada en el proceso de toma de medidas) orientados a aumentar la velocidad de muestreo de los detectores de masas han contribuido de manera esencial a acortar los tiempos de análisis.

1.6. AMDIS

Los detectores de masas generan una inmensa cantidad de datos experimentales que necesita ser procesada adecuadamente. Hasta hace poco, este análisis se llevaba a cabo de forma manual o semiautomática mediante el uso de algoritmos matemáticos ofrecidos por los propios fabricantes de las diferentes plataformas de análisis (tales como Xcalibur^{R} de Thermo Scientific o ChemStation^{R} de Agilent Technologies) permitiendo el procesado de datos de manera manual o semi-automático. Estos programas resultan ser bastante caros, tediosos, poco flexibles, complejos y requieren demasiado tiempo para el procesamiento de datos teniendo a su vez limitaciones operacionales en el caso de tener que procesar espectros contaminados con interferentes o bien, en el caso de iones procedentes de picos superpuestos (Colby, 1992; Halket *et al*., 1999; Stein, 1999).

Hoy en día, algunos fabricantes ofrecen softwares de procesamiento automático de alto rendimiento, con capacidad de deconvolución, capaces de procesar archivos MS en poco tiempo. En este contexto, el Automated Mass Spectral Deconvolution and Identification System (AMDIS, desarrollado por el National Institute of Standards and Technology, NIST) es un programa de descarga gratuita para el procesamiento automático de los datos obtenidos mediante el empleo de sistemas GC-MS, el cual puede procesar archivos generados por cualquier tipo de plataforma de análisis con independencia de su fabricante. Este programa elimina los sesgos y deconvoluciona los iones presentes en el TIC, extrayendo una serie de espectros de masas limpios, asociándolos a un único componente. Una vez que ha sido aislado el espectro de un componente, AMDIS lo compara conjuntamente con el tiempo de retención con los componentes recopilados en la librería de referencia correspondiente (comercial o creada por el propio investigador) donde se encuentran recogidos los espectros y tiempos de retención característicos de cada componente, obteniendo así la identificación del compuesto (NIST, 2014).

En definitiva, AMDIS trabaja en cuatro pasos:

- Análisis del ruido
- Percepción del componente
- Deconvolución espectral
- Identificación del compuesto

AMDIS se ha utilizado para la determinación de varios analitos como: marcadores urinarios de trastornos metabólicos, venenos y drogas (Meyer *et al.,* 2010), pesticidas (Zhang *et al.,* 2006), contaminantes (Gómez *et al*., 2010) y volátiles (Miladinovic *et al.*, 2014) entre otros.

Sin embargo, AMDIS puede crear falsos positivos cuando los picos son muy amplios o presentan varios máximos, ya que puede llevar a que un mismo componente sea identificado varias veces (Lu, H. *et al.*, 2008). En cambio, Smart y colaboradores (2010) señalan que AMDIS es fiable a la hora de realizar identificaciones correctas

incluso en los casos de picos parcialmente co-eluidos, pero fue incapaz de cuantificar con precisión muchos de los compuestos identificados. Así pues, la optimización de los parámetros y condiciones de análisis implicados en el funcionamiento del AMDIS resulta ser un reto de gran interés para conseguir emplear de manera fiable y eficaz (tanto cualitativa como cuantitativamente) este programa analítico.

BIBLIOGRAFÍA

2. BIBLIOGRAFÍA

Abian, J. (1999). The coupling of gas and liquid chromatography with mass spectrometry. *Journal of Mass Spectrometry*, 34(3), 157–168.

Acosta-Estrada, BA; Gutiérrez-Uribe, JA; Serna-Saldívar, SO. (2014). Bound phenolics in foods, a review. *Food Chemistry,* 152, 46-55.

Aguilar, CN; Aguilera-Carbo, A; Robledo, A; Ventura, J; Belmares, R; Martinez, D; Rodríguez-Herrera, R; Contreras, J. (2008). Production of Antioxidant Nutraceuticals by Solid-State Cultures of Pomegranate (*Punica granatum*) Peel and Creosote Bush (*Larrea tridentata*) Leaves. *Food Technology and Biotechnology*, 46(2), 218–222.

Arnal, L; del Río, MA. (2003). Removing Astringency by Carbon Dioxide and Nitrogen-Enriched Armospheres in Persimmon Fruit cv. "Rojo brillante". *Journal of Food Science*, 68(4), 1516-1518.

Arthur, CL; Killam, LM; Buchholz, KD; Pawliszyn, J; Berg, JR. (1992). Automation and optimization of solid-phase microextraction. *Analytical Chemistry*, 64(17), 1960-1966.

Barboni, T; Luro, F; Chiaramonti, N; Desjobert, JM; Muselli, A; Costa, J. (2009). Volatile composition of hybrids Citrus juices by headspace solid-phase micro extraction/gas chromatography/mass spectrometry. *Food Chemistry*, 116(1), 382-390.

Bellini, E; Giordani, E; Nin, S. (2008). Evolution of persimmon cultivation and use in Italy. *Advances in Horticultural Science*, 22(4), 233-238.

Benzie, IFF; Choi, SW. (2014). Chapter One - Antioxidants in Food: Content, Measurement, Significance, Action, Cautions, Caveats, and Research Needs. *Advances in Food and Nutrition Research*, 71, 1-53.

Besada, C; Arnal, L; Salvador, A. (2008). Improving storability of persimmon cv. Rojo Brillante by combined use of preharvest and postharvest treatments. *Postharvest Biology and Technology*, 50(2-3), 169-175.

Bogusz, MJ. (2000). Liquid chromatography-mass spectrometry as a routine method in forensic sciences: a proof of maturity. *Journal of Chromatography B: Biomedical Sciences and Applications*, 748(1), 3-19.

Brand-Williams, W; Cuvelier, ME; Berset, C. (1995). Use of a free radical method to evaluate antioxidant activity. *LWT - Food Science and Technology*, 28(1), 25-30.

Calín-Sánchez, Á; Carbonell-Barrachina, ÁA. (2012). LA FRUTA GRANADA CULTIVADA EN ESPAÑA. Punicalagina antioxidante del zumo de granada y el extracto de granada, en la alimentación funcional del futuro. *Departamento Tecnología Agroalimentaría, Universidad Miguel Hernández*.

Chen, L; Vigneault, C; Raghavan, GSV; Kubow, S. (2007). Importance of the phytochemical content of fruits and vegetables to human health. *Stewart Postharvest Review*, 3(3), 1-5.

Chen, L; Wang, Q; Liu, J. (2006). Simultaneous analysis of nine active components in Gegen Qinlian preparations by high-performance liquid chromatography with diode array detection. *Journal of Separation Science,* 29(14), 2203-2210.

Chen, XN; Fan, JF; Yue, X; Wu, XR; Li, LT. (2008). Radical scavenging activity and phenolic compounds in persimmon (*Dyospiros kaki* L. cv. Mopan). *Journal of Food Science*, 73(1), 24−28.

Colby, BN. (1992). Spectral Deconvolution For Overlapping Gc Ms Components. *Journal of the American Society for Mass Spectrometry*, 3(5), 558-562.

Cullum, A. (2003). Increasing fruit and vegetable consumption: the 5 A DAY programme. *Nutrition Bulletin*, 28(2), 159-163.

Daood, HG; Biacs, P; Czinkotai, B; Hoschke, Á. (1992). Chromatographic investigation of carotenoids, sugars and organic acids from *Diospyros kaki* fruits. *Food Chemistry*, 45(2), 151-155.

Dillard, CJ; German, JB. (2000). Phytochemicals: nutraceuticals and human health. *Journal of the Science of Food and Agriculture*, 80(12), 1744-1756.

Elkins, ER; Heuser, JR; Chin, H. (1988). Detection of adulteration in selected fruit juices, in Adulteration of fruit juice beverages. *National Food Processors Association*, 317-341.

El Kar, C; Ferchichi, A; Attia, F; Bouajila, J. (2011). Pomegranate (*Punica granatum*) Juices: Chemical Composition, Micronutrient Cations, and Antioxidant Capacity. *Journal of Food Science,* 76(6), 795-800.

FAOSTAT (2012). Base de datos estadísticos. http://faostat.fao.org.

Füzfai, Zs; Molnár-Perl, I. (2007). Gas chromatographic–mass spectrometric fragmentation study of flavonoids as their trimethylsilyl derivatives: Analysis of flavonoids, sugars, carboxylic and amino acids in model systems and in citrus fruits. *Journal of Chromatography A*, 1149(1), 88-101.

Giannakourou, MC; Taoukis, PS. (2003). Application of a TTI-based Distribution Management System for Quality Optimization of Frozen Vegetables at the Consumer End. *Journal of Food Science*, 68(1), 201-209.

Gil, MI; Tomas-Barberan, FA; Hess-Pierce, B; Holcroft, DM; Kader, AA. (2000). Antioxidant Activity of Pomegranate Juice and Its Relationship with Phenolic Composition and Processing. *Journal of Agricultural and. Food Chemistry,* 48(10), 4581-4589.

Giordani, E; Doumett, S; Nin, S; Del Bubba, M. (2011). Selected primary and secondary metabolites in fresh persimmon (*Diospyros kaki* Thunb.): A review of

analytical methods and current knowledge of fruit composition and health benefits. *Food Research International*, 44(7), 1752-1767.

Gómez, MJ; Gómez-Ramos, MM; Agüera, A; Mezcua, M; Herrera, S; Fernández-Alba, AR. (2010). Rapid automated screening, identification and quantification of organic micro-contaminants and their main transformation products in wastewater and river waters using liquid chromatography–quadrupole-time-of-flight mass spectrometry with an accurate-mass database. *Journal Chromatography A*, 1217(45), 7038-7054.

González-Mas, MC; Rambla, JL; Alamar, MC; Gutiérrez, A; Granell, A. (2011). Comparative Analysis of the Volatile Fraction of Fruit Juice from Different Citrus Species. *PLoS One*, 6(7): e22016, 1-11.

Gorinstein, S; Bartnikowska, E; Kulasek, G; Zemser, M; Trakhtenberg, S. (1998). Dietary persimmon improves lipid metabolism in rats fed diets containing cholesterol. *The Journal of Nutrition*, 128(11), 2023−2027.

Gorinstein, S; Martin-Belloso, O; Katrich, E; Lojek, A; Číž, M; Gligelmo-Miguel, N; Haruenkit, R; Park, YS; Jung, ST; Trakhtenberg, S. (2003). Comparison of the contents of the main biochemical compounds and the antioxidant activity of some Spanish olive oils as determined by four different radical scavenging tests. *The Journal of Nutritional Biochemistry*, 14(3), 154-159.

Granado, F; Olmedilla, B; Blanco, I. (2003). Nutritional and clinical relevance of lutein in human health. *British journal of nutrition*, 90(3), 487 -502.

Grassi, D; Desideri, G; Croce, G; Tiberti, S; Aggio, A; Ferri, C. (2009). Flavonoids, vascular function and cardiovascular protection. *Current Pharmaceutical Design*, 15(10), 1072-1084.

Gutiérrez, MC; Doguet, M. (2002). La cromatografía de gases y la espectrometría de masas: Identificación de compuestos causantes de mal olor. *Boletín intexter*, 122, 35-41.

Halket, JM; Przyborowska, A; Stein, SE; Mallard, WG; Down, S; Chalmers, RA. (1999). Deconvolution gas chromatography mass spectrometry of urinary organic acids - Potential for pattern recognition and automated identification of metabolic disorders. *Rapid Communications In Mass Spectrometry*, 13(4), 279-284.

Högnadóttir, Á; Rouseff, RL. (2003). Identification of aroma active compounds in orange essence oil using gas chromatography–olfactometry and gas chromatography–mass spectrometry. *Journal of Chromatography A*, 998(1-2), 201-211.

Jaiswal, V; DerMarderosian, A; Porter, JR. (2010). Anthocyanins and polyphenol oxidase from dried arils of pomegranate (*Punica granatum* L.). *Food Chemistry*, 118(1), 11-16.

James, AT; Martin, AJP. (1952). Gas-liquid partition chromatography: the separation and micro-estimation of volatile fatty acids from formic acid to dodecanoic acid. *Biochemical Journal*, 50(5), 679–690.

Kataoka, H; Lord, HL; Pawliszyn, J. (2000). Applications of solid-phase microextraction in food analysis. *Journal of Chromatography A*, 880(1), 35-62.

Katona, ZsF; Sass, P; Molnár-Perl, I. (1999). Simultaneous determination of sugars, sugar alcohols, acids and amino acids in apricots by gas chromatography–mass spectrometry. *Journal of Chromatography A*, 847(1), 91-102.

Kaur, C; Kapoor, HC. (2001). Antioxidants in fruits and vegetables – the millennium's health. *International Journal of Food Science & Technology,* 36(7), 703–725.

Krajcovicova-Kudlackova, M. (2005). Health benefits of plant food. *Klinicka Biochemie a Metabolismus*, 13(4), 168-171.

Lampe, JW. (1999). Health effects of vegetables and fruit: Assessing mechanisms of action in human experimental studies. *American Journal of Clinical Nutrition*, 70(3 SUPPL.), 475S-490S.

Lansky, EP; Newman, RA. (2007). *Punica granatum* (pomegranate) and its potential for prevention and treatment of inflammation and cancer. *Journal of Ethnopharmacology,* 109(2), 177-206.

Llácer, G; Badenes, ML. (2002). Situación actual de la producción de caquis en el mundo. *Agrícola Vergel: Fruticultura, horticultura, floricultura*, 242, 64-71.

Lock, O; Cabello D. (2006). Práctica VI análisis de flavonoides en plantas. *Pontificia Universidad católica del Perú*, 1-7. http://old.iupac.org/publications/cd/medicinal_chemistry/Practica-VI-6.pdf

Lu, H; Liang, Y; Dunn, WB; Shen, H; Kell, DB. (2008). Comparative evaluation of software for deconvolution of metabolomics data based on GC-TOF-MS. *TrAC Trends in Analytical Chemistry*, 27(3), 215-227.

Lu, J; Ding, K; Yuan, Q. (2008). Determination of punicalagin isomers in pomegranate husk. *Chromatographia*, 68(3-4), 303-306.

Machado, TB; Leal, ICR; Amaral, ACF; Dos Santos, KRN; De Silva, MG; Kuster, RM. (2002). Antimicrobial elagitanin of *Punica granatum* fruit. *Journal Brazilian Chemistry Society*, 13(5), 606-610.

MAGRAMA (2012). Ministerio de Agricultura, Alimentación y Medio Ambiente. Anuario de estadística año 2012. http://www.magrama.gob.es.

Marcotte, M; Stewart, B; Fustier, P. (1998). Abused Thermal Treatment Impact on Degradation Products of Chilled Pasteurized Orange Juice. *Journal of Agricultural and Food Chemistry*, *46*(5), 1991-1996.

Markham, KR. (1982). Techniques of Flavonoid Identification. *Academic Press*.

Martínez-Hernández, JA; Martí del Moral, AA. (2005). ¿Sabemos realmente que comemos?: alimentos transgénicos, ecológicos y funcionales. *ENUSA*.

Meyer, MR; Peters, FT; Maurer, HH. (2010). Automated Mass Spectral Deconvolution and Identification System for GC-MS Screening for Drugs, Poisons, and Metabolites in Urine. *Clinical Chemistry,* 56(4), 575-584.

Miguel, G; Dandlen, S; Antunes, D: Neves, A; Martins, D. (2004). The Effect of Two Methods of Pomegranate (*Punica granatum* L) Juice Extraction on Quality During Storage at 4ºC. *BioMed Research International*, 2004(5), 332-337.

Miladinovic, DL; Ilic, BS; Nikolic, DM; Markovic, MS; Nikolic, ND; Miladinovic, LC;. Miladinovic, MD. (2014). Volatile constituents of *Euphrasia stricta*. *Chemistry of Natural Compounds*, 49(6), 1149-1147.

Nagy, S; Rouseff, RL; Lee, HS. (1989). Chapter 31 - Thermally Degraded Flavors in Citrus Juice Products, in Thermal Generation of Aromas. *ACS Symposium series*, 409, 331–345.

Nakatsubo, F; Enokita, K; Murakami, K; Yonemori, K; Sungiura A; Utsumoniya, N; Subhadrabadhu, S. (2002). Chemical structures of the condensed tannins in the fruits of Diospyros species. *Journal of Wood Science*, 48(5), 414-418.

Nicoletti, I; Bello, C; De Rossi, A; Corradini, D. (2008). Identification and Quantification of Phenolic Compounds in Grapes by HPLC-PDA-ESI-MS on a Semimicro Separation Scale. *Journal of Agricultural and Food Chemistry*, 56(19), 8801-8808.

NIST (2014). National Institute of Standards and Technology. http://chemdata.nist.gov/dokuwiki/doku.php?id=chemdata:amdis.

Oey, I; Lille, M; Van Loey, A; Hendrickx, M. (2008). Effect of high-pressure processing on colour, texture and flavour of fruit- and vegetable-based food products: a review. *Trends in Food Science & Technology*, 19(6), 320-328.

Parada, J; Aguilera, J. (2007). Food microstructure affects the bioavailability of several nutrients. *Journal of Food Science*, 72(2), 21-32.

Pérez-Cacho, P; Rouseff, R. (2008). Processing and Storage Effects on Orange Juice Aroma: A Review. *Journal of Agricultural and Food Chemistry*, 56(21), 9785-9796.

Riu-Aumatell, M; Castellari, M; López-Tamames, E; Galassi, S; Buxaderas, S. (2004). Characterisation of volatile compounds of fruit juices and nectars by HS/SPME and GC/MS. *Food Chemistry*, 87(4), 627-637.

Roessner-Tunali, U; Hegemann, B; Lytovchenko, A; Carrari, F; Bruedigam, C; Granot, D; Fernie, AR. (2003). Metabolic Profiling of Transgenic Tomato Plants Overexpressing Hexokinase Reveals That the Influence of Hexose Phosphorylation Diminishes during Fruit Development. *Plant Physiology September*, 133(1), 84-99.

Rubinson, KA; Rubinson JF. (2001). Análisis Instrumental (Spanish Edition). *Pearson Publications Company*, 1st edition.

Santos-Buelga, C; Scalbert, A. (2000). Proanthocyanidins and tannin-like compounds, nature, occurrence, dietary intake and effects on nutrition and health. *Journal of the Science of Food and Agriculture*, 80(7), 1094-1117.

Scalbert, A; Manach, C; Morand, C; Rémésy, C; Jiménez, L. (2005). Dietary polyphenols and the prevention of diseases. *Critical Reviews in Food Science and Nutrition*, 45(4), 287-306.

Sendra, JM; Sentandreu, E; Navarro, JL. (2006). Reduction kinetics of the free stable radical 2,2-diphenyl-1-picrylhydrazyl ($DPPH^{\bullet}$) for determination of the antiradical activity of citrus juices. *European Food Research and Technology,* 223(5), 615-624.

Sentandreu, E; Carbonell, JV; Izquierdo, L. (2005). Effects of Heat Treatment Conditions on Fresh Taste and on Pectinmethylesterase Activity of Chilled Mandarin and Orange Juices. *Food Science and Technology International*, 11(3), 217-222.

Sentandreu, E; Carbonell, L; Rodrigo, D; Carbonell, JV. (2006). Pulsed Electric Fields Versus Thermal Treatment: Equivalent Processes To Obtain Equally Acceptable Citrus Juices. *Journal of Food Protection*, 69(8), 2016-2018.

Sentandreu, E; Navarro, JL; Sendra, JM. (2008). Reduction kinetics of the antiradical probe 2,2-diphenyl-1-picrylhydrazyl in methanol and acetonitrile by the antiradical activity of protocatechuic acid and protocatechuic acid methyl ester. *Journal of Agricultural and. Food Chemistry*, 56(13), 4928-4936.

Shepherd, T; Dobson, G; Verrall, SR; Conner, S; Griffiths, DW; McNicol, JW; Davies, HV; Stewart, D. (2007). Potato metabolomics by GC–MS: what are the limiting factors?. *Metabolomics*, 3(4), 475-488.

Smart, KF; Aggio, RBM; van Houtte, JR; Villas-Bôas, SG. (2010). Analytical platform for metabolome analysis of microbial cells using methyl chloroformate derivatization followed by gas chromatography–mass spectrometry. *Nature Protocols*, 5(10), 1709-1729.

Stashenko, EE; Martínez, JR. (2007). Sampling volatile compounds from natural products with headspace/solid-phase micro-extraction. *Journal of Biochemical and Biophysical Methods*, 70(2), 235-242.

Stein, SE. (1999). An integrated method for spectrum extraction and compound identification from gas chromatography/mass spectrometry data. *Journal of the American Society for Mass Spectrometry*, 10(8), 770-781

Thilakarathna, SH; Rupasinghe, HPV. (2013). Flavonoid Bioavailability and Attempts for Bioavailability Enhancement. *Nutrients,* 5(9), 3367-3387.

Torres, JA; Velázquez, G. (2005). Commercial opportunities & research challenges in the high pressure processing of foods. *Journal of Food Engineering*, 67(1-2), 95-112.

U.S. Department of Agriculture and U.S. Department of Health and Human Services. (2010). Dietary Guidelines for Americans 2010. *U.S. Government Printing Office*, 7th Edition.

Van Deemter, JJ; Zuiderweg, FJ; Klinkenberg, A. (1956). Longitudinal diffusion and resistance to mass transfer as causes of nonideality in chromatography. *Chemical Engineering Science*, 5, 271-289.

Vékey, K. (2001). Mass spectrometry and mass-selective detection in chromatography. *Journal of Chromatography A,* 921(2), 227-236.

Vervoort, L; Van der Plancken, I; Grauwet, T; Timmermans, RAH; Mastwijk, HC; Matser, AM; Hendrickx, ME; Van Loey, A. (2011). Comparing equivalent thermal, high pressure and pulsed electric field processes for mild pasteurization of orange juice: part II: impact on specific chemical and biochemical quality parameters. *Innovative Food Science and Emerging Technologies*, 12(4), 466–477.

Villaño, D; Fernández-Pachón, MS; Troncoso, AM; García-Parrilla, MC. (2006). Influence of enological practices on the antioxidant activity of wines. *Food Chemistry*, 95(3), 394-404.

Wright KP; Kader, AA. (1996). Effect of controlled-atmosphere storage on the ascorbate content and quality of strawberries and persimmons. *Postharvest Biology and Technology*, 10(1), 89-97.

Yamada, M; Giordani, E; Yonemori, K. (2012). Chapter 17 – Persimmon, in Fruit Breeding. *Handbook of Plant Breeding*, 8, 663-693.

Zhang, W; Wu, P; Li, C. (2006). Study of automated mass spectral deconvolution and identification system (AMDIS) in pesticide residue analysis. *Rapid Communications in Mass Spectrometry*, 20(10), 1563-1568.

Zhang, Z; Pawliszyn, J. (1993). Headspace solid-phase microextraction. *Analytical Chemistry*, 65(14), 1843-1852.

OBJETIVOS

3. OBJETIVOS

El objetivo fundamental de la presente Tesis Doctoral es llevar a cabo una aproximación metabolómica detallada de diferentes productos naturales (zumos cítricos, zumos de granada y pulpa de caqui) mediante el empleo de sistemas de LC-MS y GC-MS convencionales como son los espectrómetros de tipo trampa iónica tridimensional.

Este trabajo pretende demostrar como con una adecuada formación del investigador, tanto de la materia sujeta a estudio como de los equipos de análisis de rutina empleados, se pueden llevar a cabo estudios de elevada calidad científica. Así pues, los objetivos a realizar en esta tesis doctoral son los siguientes:

1. Optimización de los parámetros de muestreo y de análisis del sistema GC-MS y del procesado automático de datos mediante el AMDIS. Así pues, se plantea llevar a cabo el análisis masivo, rápido y fiable de los metabolitos detectados en las muestras estudiadas.

2. Caracterización de los zumos de naranja (*Citrus sinensis*) en fresco y procesados obtenidos mediante diferentes tratamientos (despulpado, pasteurización y homogenización a altas presiones) y almacenamiento refrigerado a través del análisis GC-MS/AMDIS de su composición en volátiles, azúcares, ácidos orgánicos y aminoácidos. Como consecuencia, se evaluarán los efectos del procesado y almacenamiento sobre la calidad (composicional/sensorial) de los zumos con el fin de obtener productos de elevado valor comercial con una prolongada vida útil.

3. Caracterización de los zumos de granada (*Punica granatum*) obtenidos de manera industrial en base a su perfil de compuestos fenólicos de bajo y elevado peso molecular (aductos) mediante una metodología HPLC-DAD/$ESI^{+/-}$-MS^n. Se

prestará especial atención a la elucidación estructural de compuestos no descritos con anterioridad en los zumos de granada.

4. Caracterización de fenoles de bajo y elevado peso molecular (aductos) procedentes de la pulpa de caqui *(Diospyros kaki*) mediante metodologías HPLC-DAD/ESI$^{+/-}$-MS^{n}. Se prestará especial atención a la elucidación estructural de compuestos no descritos con anterioridad en el caqui.

5. Correlación de los perfiles de compuestos fenólicos dilucidados en las muestras estudiadas con su capacidad y cinéticas de actividad antirradical *in vitro* mediante el empleo del DPPH$^{\bullet}$ como sonda antirradical.

JUSTIFICACIÓN DE LA UNIDAD TEMÁTICA Y PRESENTACIÓN DE LOS TRABAJOS

4. JUSTIFICACIÓN DE LA UNIDAD TEMÁTICA Y PRESENTACIÓN DE LOS TRABAJOS

Durante los últimos años, como ya se ha comentado en la Introducción, los diferentes sectores comerciales y políticas de mercado así como los propios consumidores han orientado sus posturas hacia la consecución de hábitos alimentarios equilibrados desde el punto de vista nutricional. En este sentido, los metabolitos presentes en frutas y sus derivados ejercen un papel esencial sobre la salud humana y su buena preservación. Sin embargo, la mayoría de las frutas tienen un perfil metabolómico muy complejo y variado por lo que se requiere el uso de metodologías de análisis de alto rendimiento para su estudio, destacando aquellas fundamentadas en la GC-MS y LC-MS.

En lo concerniente al estudio de la fracción aromática de los alimentos, el análisis GC-MS ha sido la solución analítica elegida de manera tradicional. Además, su uso ha permitido la determinación simultánea de compuestos polares no volátiles (azúcares, ácidos orgánicos y aminoácidos) presentes en los extractos naturales mediante la conversión de dichos compuestos en sus correspondientes TMS-derivados. Asimismo, la elevada sensibilidad de los detectores de masas genera una inmensa cantidad de datos experimentales que necesita ser procesada adecuadamente. Convencionalmente, el procesado de datos se ha llevado a cabo de forma manual o semiautomática mediante el uso de algoritmos matemáticos que se encuentran en los programas informáticos ofrecidos por los propios fabricantes de las diferentes plataformas de análisis (como Xcalibur^{R} de Thermo Scientific o ChemStation^{R} de Agilent Technologies). Estos programas informáticos son, normalmente, bastante caros, tediosos, incompatibles con otros fabricantes, poco intuitivos y no demasiado rápidos dada su complejidad, teniendo a su vez limitaciones operacionales en el caso de tener que procesar espectros contaminados con interferentes (p. ej. sangrado de columna y ruido de fondo) o bien, en el caso de iones procedentes de picos cromatográficos superpuestos (coelución de señales). De este modo e idealmente, se debería disponer de programas que permitieran el

procesado automático y simultáneo de los archivos generados por los detectores de masas además de ser baratos, fáciles de usar, versátiles, rápidos y capaces de aislar (deconvolucionar) picos solapados, lo que proporcionaría unos resultados fiables desde el punto de vista cualitativo y cuantitativo. En este contexto, el AMDIS (desarrollado por el NIST) es un programa de descarga gratuita para el procesado automático de los datos obtenidos mediante el empleo de cualquier sistema GC-MS con independencia del fabricante. Este programa elimina los sesgos y deconvoluciona los iones presentes en el TIC, extrayendo una serie de espectros de masas limpios que conjuntamente a los tiempos de retención, realiza la identificación de todos los componentes presentes en la muestra a cada tiempo considerado (espectros y tiempos de retención característicos se compilan en la correspondiente librería). En el **Capítulo 1**, se describe la optimización del AMDIS para su uso en el análisis masivo de volátiles y compuestos polares no volátiles en zumos cítricos.

En lo referente a la calidad composicional de los alimentos, la industria alimentaria está realizando durante los últimos años un gran esfuerzo para preservar aquellos compuestos de elevado valor nutricional y organoléptico presentes en los alimentos durante las etapas de procesado y almacenamiento. Para ello se buscan nuevos protocolos analíticos que permitan seguir, de manera rápida y sencilla, la evolución de un amplio espectro de analitos durante la manipulación de los alimentos, pudiéndose minimizar la pérdida de compuestos valiosos mediante la optimización de las operaciones tecnológicas empleadas. Como ejemplo ilustrativo tenemos el caso de los zumos de cítricos los cuales tras su extracción mecánica son sometidos a diferentes procesos tecnológicos como la tamización, centrifugación, estabilización (tradicionalmente mediante tratamiento térmico), envasado y almacenamiento. En esta línea, durante los últimos años el grupo de Zumos del IATA-CSIC ha estado trabajando en el desarrollo de nuevos procesos industriales encaminados a la obtención de zumos de mandarina y naranja de larga vida comercial (hasta tres meses en refrigeración) y de elevada calidad sensorial. Para ello, se ha desarrollado un nuevo procedimiento por el que los zumos de cítricos se estabilizan mediante una homogeneización dinámica a alta

presión (150 MPa) como alternativa a los métodos clásicos de pasterización. En el **Capítulo 2** se estudia la evolución de la calidad de zumos de naranja sometidos a diferentes procesos industriales y tiempos de almacenamiento en refrigeración. Para ello, se estudiaron los volátiles y compuestos polares no volátiles de los zumos aplicando la metodología desarrollada para su análisis en el **Capítulo 1**, esto es mediante el análisis por GC-MS y procesado automático de los datos mediante el AMDIS.

Por su parte, los sistemas LC-MS facilitan el estudio detallado de aquellos compuestos que no pueden ser analizadas por metodologías GC-MS, es decir, analitos con escasa volatilidad y/o estabilidad térmica como es el caso de los compuestos fenólicos. Por tanto, se ha estudiado el perfil de compuestos fenólicos de los zumos de granada (**Capítulo 3**) y de los extractos procedentes de la pulpa de caqui (**Capítulo 4**) con el claro objetivo de identificar nuevos compuestos anteriormente no descritos mediante el empleo de un sistema rutinario de análisis como es una trampa iónica tridimensional.

Teniendo en cuenta todo lo anterior, la presente Tesis Doctoral plantea llevar a cabo una aproximación metabolómica de diferentes extractos naturales (zumos de naranja, zumos de granada y pulpa de caqui) mediante el empleo de sistemas GC-MS y LC-MS de rutina. Así pues, este trabajo pretende demostrar como a través de una formación adecuada del investigador, tanto en lo referente a la materia sujeta a estudio como de los equipos de análisis convencionales empleados, se pueden llevar a cabo actividades de máxima calidad científica.

Los resultados obtenidos en este trabajo de tesis doctoral han dado lugar a las siguientes publicaciones científicas:

Capítulo 1. Optimización de los parámetros de muestreo y de análisis del sistema GC-MS/AMDIS.

1.1. **Gas chromatography coupled to mass spectrometry analysis of volatiles, sugars, organic acids and aminoacids in Valencia Late orange juice and reliability of the Automated Mass Spectral Deconvolution and Identification System for their automatic identification and quantification**. (2012). *Journal of Chromatography A*, 1241, 84– 95.

Capítulo 2. Caracterización del perfil de volátiles y compuestos polares no volátiles de los zumos de naranja (*Citrus sinensis*).

2.1. **Valencia Late orange juice preserved by pulp reduction and high pressure homogenization: Sensory quality and gas chromatography-mass spectrometry analysis of volatiles**. (2013). *LWT - Food Science and Technology*, 51(2), 476-483.

2.2. **Evaluation of minimal processing of orange juice by automated data analysis of volatiles and nonvolatile polar compounds determined by gas chromatography coupled to mass spectrometry**. (2014). *International Journal of Food Science and Technology*, 49(6), 1432-1440.

Capítulo 3. Caracterización del perfil de fenoles de los zumos de granada (*Punica granatum*) de la variedad "Wonderful".

3.1. **Phenolic profile characterization of pomegranate (*Punica granatum*) juice by high-performance liquid chromatography with diode array detection coupled to an electrospray ion trap mass analyzer**. (2013). *Journal of Food Composition and Analysis*, 30(1), 32–40.

3.2. **Determination of the antiradical activity and kinetics of pomegranate juice using 2,2-diphenylpicyrl-1-hydrazyl as the antiradical probe**. (2014). *Food Science and Technology International.* (En prensa).

Capítulo 4. Caracterización del perfil de fenoles de la pulpa de caqui (*Diospyros kaki*) de la variedad "Rojo Brillante".

4.1. **Metabolite profiling of pigments from acid-hydrolyzed persimmon (*Diospyros kaki*) extracts by HPLC-DAD/ESI-MS^n analysis**. (2014). *Journal of Food Composition and Analysis.* (Aceptado para su publicación).

4.2. **Rapid screening of low molecular weight phenols from persimmon (*Diospyros kaki*) pulp using liquid chromatography-UV/Vis-electrospray mass spectrometry analysis**. (2014). *Journal of the Science of Food and Agriculture.* (En prensa).

RESULTADOS

CAPÍTULO 1

Optimización de los parámetros de muestreo y de análisis de la metodología GC- MS/AMDIS.

1. **Gas chromatography coupled to mass spectrometry analysis of volatiles, sugars, organic acids and aminoacids in Valencia Late orange juice and reliability of the Automated Mass Spectral Deconvolution and Identification System for their automatic identification and quantification.** (2012). *Journal of Chromatography A,* 1241, 84– 95. Impact Factor: 4.258.

Journal of Chromatography A, 1241 (2012) 84–95

Contents lists available at SciVerse ScienceDirect

Journal of Chromatography A

journal homepage: www.elsevier.com/locate/chroma

Gas chromatography coupled to mass spectrometry analysis of volatiles, sugars, organic acids and aminoacids in Valencia Late orange juice and reliability of the Automated Mass Spectral Deconvolution and Identification System for their automatic identification and quantification

Manuela Cerdán-Calero, José María Sendra, Enrique Sentandreu*

Instituto de Agroquímica y Tecnología de Alimentos (IATA-CSIC), Avd. Agustín Escardino 7, 46980, Paterna, Valencia, Spain

ARTICLE INFO

Article history:
Received 11 January 2012
Received in revised form 2 April 2012
Accepted 3 April 2012
Available online 11 April 2012

Keywords:
AMDIS
Orange juice
GC–MS
Metabolite profiling
Volatile compounds
TMS derivatives

ABSTRACT

Neutral volatiles and non-volatile polar compounds (sugars, organics acids and aminoacids) present in Valencia Late orange juice have been analysed by Gas Chromatography coupled to Mass Spectrometry (GC–MS). Before analysis, the neutral volatiles have been extracted by Headspace-Solid Phase Microextraction (HS-SPME), and the non-volatile polar compounds have been transformed to their corresponding volatile trimethylsilyl (TMS) derivatives. From the resulting raw GC–MS data files, the reliability of the Automated Mass Spectral Deconvolution and Identification System (AMDIS) to perform accurate identification and quantification of the compounds present in the sample has been tested. Hence, both raw GC–MS data files have been processed automatically by using AMDIS and manually by using Xcalibur™, the manufacturer's data processing software for the GC–MS platform used. Results indicate that the reliability of AMDIS for accurate identification and quantification of the compounds present in the sample strongly depends on a number of operational settings, for both the MS and AMDIS, which must be optimized for the particular type of assayed sample. After optimization of these settings, AMDIS and Xcalibur™ yield practically the same results. A total of 85 volatiles and 22 polar compounds have been identified and quantified in Valencia Late orange juice.

1. Introduction

Gas Chromatography coupled to Mass Spectrometry (GC–MS) is the analytical methodology of choice for the separation and further determination (identification and quantification) of volatiles present in complex matrices. Until recently, this determination was mainly performed by using dedicated mathematical algorithms offered by the manufacturers for their own GC–MS platforms (such as Xcalibur™ from Thermo Scientific), allowing only manual or semi-automatic data processing of the raw GC–MS data files, and that were incompatible within them. Moreover, these older algorithms are normally rather expensive, quite tedious and long time consuming for data processing [1], and even could become almost useless if the acquired spectra are contaminated with ions from overlapping peaks, column bleeding or ionization-chamber contaminants, which turn the manual or semi-automatic interpretation process of data from very complex up to nearly impossible [2–4]. Today, many GC/MS manufacturers offer dedicated data processing software with automatic high-throughput capabilities (automatic de-skewing of mass spectra, deconvolution capability, etc.), thus being able to process the raw GC–MS data files in a quite short time and yielding unambiguous identification and quantification of the compounds present in the assayed sample. However, although these new dedicated software are quite easy to use, they are normally incapable to operate with independence of the particular GC–MS platform used, that is, with independence of the origin of the GC–MS raw data file and, what is not of minor importance, they are quite expensive.

In this context, the National Institute of Standards and Technology-Automated Mass Spectral Deconvolution and Identification System (NIST-AMDIS) is a free of charge downloadable software (http://chemdata.nist.gov/mass-spc/amdis/downloads) for data processing of raw GC–MS data files, which incorporates automatic high-throughput capabilities and operates with almost any GC–MS raw data file, with independence of its origin. AMDIS de-skews and deconvolutes the ions of the TIC (Total Ion Chromatogram) from a raw GC–MS data file, extracts a series of "cleaned" mass spectra ("components"), as well as their corresponding retention times, and identifies the compounds present in the sample (targets) by matching the mass spectra of the "components", and optionally also their retention times, against a reference library, either commercial such as the NIST™ libraries or

* Corresponding author. Tel.: +34 963 90 00 22; fax: +34 963 63 63 01.
E-mail address: elcapi@iata.csic.es (E. Sentandreu).

0021-9673/$ – see front matter © 2012 Elsevier B.V. All rights reserved.
http://dx.doi.org/10.1016/j.chroma.2012.04.014

shelf-built by the operator [5]. The deconvolution and extraction of the "cleaned" mass spectra and corresponding retention times can be performed either manually by the operator or automatically, although in this later case a number of settings are to be optimized to assure correct determinations. Moreover, once AMDIS has identified a "component" as a target, that is, a compound present in the analysed sample, it is quantified by extraction of its ion model from all the corresponding "cleaned" mass spectra and integration of the area under the resulting chromatographic peak. As in the case of the checking of the "components" as possible targets, the accurate automatic quantification of the identified targets also requires the previous optimization of a number of settings for both the MS and AMDIS.

AMDIS has been used for the determination of urinary markers in metabolic disorders, poisons and drugs [1,6,7], of pollutants in water and vegetables [8–11], of steroids in sedimentary matrix [12], of polar compounds and pesticides in vegetables [13–15], and of volatiles in tomato [16], among others, without reported problems about its reliability for accurate identification and quantification of the compounds present in the samples. However, some limitations of AMDIS to perform accurate determinations in multiple metabolite analysis have also been reported. Hence, Lu et al. [17] compared the reliability of three deconvolution software, including AMDIS, for the identification and quantification of a test-mixture of 36 endogenous metabolites with a wide range of relative concentration ratios, which were analysed by GC–MS, using a time-of-flight MS as the mass analyzer. From the results, the authors concluded that AMDIS tends to produce a large number of false positives. In contrast, Smart et al. [18] when analyzing intra- and extracellular metabolites of microbial cell by GC–MS, using a single-quadrupole MS as the mass analyzer, found that AMDIS was reliable to provide correct identifications even for partially co-eluted peaks, thanks to its deconvolution capability, but was unable to accurately quantify many of the identified compounds present in the assayed samples. Hence, the authors suggested the use of free supplementary software for AMDIS, named R (http://www.r-project.org), to overcome quantification mismatches.

Orange juice is a complex matrix containing different groups of metabolites which exhibit rather different polarities. Phenolics, vitamins, sugars, aminoacids and organic acids are the major ones within the groups of medium-high polarity, whilst carotenoids and volatiles, both linked to the pulp, are the major ones within the non-polar groups.

Volatiles in citrus juices have usually been determined by combining Headspace-Solid Phase Microextraction with Gas Chromatography-Mass Spectrometry (HS-SPME/GC–MS). The resulting chromatograms are rather complex and the total number of determined volatiles lies within the range 50–90 [19–22]. Sugars, organic acids and aminoacids, in their turn, have simultaneously been determined in vegetables by GC–MS after their conversion in volatile trimethylsilyl derivatives (TMS) [23–25], but their determination in citrus juices is rather scarce [26].

The flavour and taste characteristics of an orange juice are essential factors for its commercial viability. Hence, the knowledge of its profiling for those compounds affecting such factors, mainly volatiles, sugars and organic acids, is of major importance for both fresh and processed juices. A major contributor to the fresh taste and aroma of citrus juices is the group of terpenes. This group is mainly constituted by volatile compounds located into the flavedo sacs (peel oil) of the fruit and that partially migrate to the juice during its mechanical extraction. However, also the "aged" or "cooked" flavour in altered juices is mainly attributed to an excessive content of some terpenes, such as 1-terpinen-4-ol and α-terpineol [27]. Moreover, the acceptability of an orange juice is also strongly affected by the ratio between its content in sugars (mainly glucose, fructose and sucrose), and organic acids (mainly citric acid).

The aim of this work is double. Firstly, to develop an easy, robust, reliable and exhaustive methodology for the determination of those compounds involved in the flavour and taste of citrus juices. Secondly, to test the reliability of AMDIS, after optimization of the main operating settings for both the MS and AMDIS, for automatic identification and quantification of the compounds present in rather complex matrices. For this goal, the raw GC–MS data files from both the volatiles and TMS derivatives were processed automatically by using AMDIS and manually by using Xcalibur™, the manufacturer's data processing software for the GC–MS platform used, and the results compared.

2. Experimental

2.1. Reagents and standards

HPLC gradient grade methanol was from Scharlab (Scharlab S.L., Barcelona, Spain). Analytical grade standards of non-volatile polar compounds (listed in Table 2), volatiles (listed in Table 3) and reagents: 99% pyridine, methoxyl-amine hydrochloride (MEOX) and N-methyl-N-(trimethylsilyl)-trifluoroacetamide (MSTFA) were from Sigma (Sigma–Aldrich Co., St. Louis, MO, USA).

2.2. Extraction of the juice from oranges and mandarines

Fruits of Valencia Late [*Citrus sinensis* (L.) Osb.]; Lane Late [*Citrus sinensis* (L.) Osb.]; Nova (*Citrus reticulata* Blanco) which is a hybrid between Clementine (*Citrus clementina* Hort. ex Tan.) × tangelo Orlando (*Citrus paradisi* Macf. × *Citrus tangerina* Hort. ex Tan.); Ortanique, hybrid between mandarin (*Citrus reticulata* Blanco) × orange [*Citrus sinensis* (L.) Osb.], and Clemenules (*Citrus clementina* Hort. ex Tan.) were from a local orchard located in Líria, Valencia, Spain. Juices were obtained using an industrial extractor (Luzyssa, El Puig, Valencia, Spain), sieved (0.4 mm hole diameter) using a paddle finisher and immediately stored at −30 °C until analysis.

2.3. Extraction of the volatiles by HS-SPME

Preliminary experiments were carried out to optimize the different parameters affecting the extraction of the volatiles. The optimized final protocol was as follows.

Five mL of juice plus 50 μL of a methanolic solution (10.24 μg/mL) of ethyl nonanoate (internal standard) and 1.5 g of NaCl were poured into a 15 mL glass vial. The vial was end-capped and sealed with a Teflon septum, vortexed and then equilibrated overnight at 4 °C. After equilibration, the mixture was magnetically stirred at 500 rpm during 30 min and then placed in a water bath at 40 °C for 15 min under the same magnetic stirring. After this time, the volatiles at the vial headspace were extracted during 60 min by HS-SPME using a fibber of 10 mm length coated with 100 μm of polydimethylsiloxane (PDMS) (Sigma–Aldrich Co., St. Louis, MO, USA). Finally, the volatile compounds were desorbed at 230 °C for 25 min from the SPME fibber into the injector port of the GC–MS system. The aim of this long resident time into the GC injector was for pre-conditioning the fibber for the next extraction of volatiles. Volatiles were analysed in triplicate.

2.4. Derivatisation of non-volatile polar metabolites

Non-volatile polar metabolites (sugars, organic acids and aminoacids) were transformed to volatile TMS derivatives before their determination by GC–MS. Hence, preliminary experiments were carried out to optimize the derivatisation process. The final optimized protocol was as follows.

Five mL of juice was centrifuged at 5000 rpm, the supernatant was filtered through a 0.45 μm nylon filter, 10 μL of the resulting serum was poured into a 250 μL glass insert and then 40 μL of a methanolic solution (1 mg/mL) of ribitol (internal standard) was added. The insert was placed into a GC glass vial, which was end-capped and sealed, vortexed, open and then the mixture exhaustively dried under vacuum using a speed-vac system (ThermoScientific, San Jose, CA, USA). After draying, 30 μL of a MEOX solution (20 mg/mL in pyridine) was poured into the insert, the GC glass vial was end-capped and sealed, vortexed and then the mixture incubated at 40 °C for 1 h. After this first incubation, the GC glass vial was open, 80 μL of MSTFA was added into the insert, the vial was end-capped and sealed again, vortexed and then the mixture incubated at 40 °C for 1 h. Finally, the GC glass vial was placed into the automatic injector of the GC–MS system for analysis. Polar metabolites were analysed in triplicate.

2.5. De-aromatisation of a citrus juice

To test the reliability of AMDIS for the identification, quantification and its linearity for the assayed standards of volatile compounds, five different concentrations of commercial standards of volatiles plus a constant concentration of internal standard were dissolved in a de-aromatised citrus juice, extracted and analysed. To select the best citrus juice to be de-aromatised, the aromatic profiles of fresh juices from Valencia Late, Lane Late, Nova, Ortanique, and Clemenules were compared. Finally, the juice from Nova was selected due to its poorer aromatic profile. Hence, 25 mL of Nova juice were centrifuged at 5000 rpm during 5 min, filtered through Whatman paper #4 and percolated twice through a C-18 Sep-pak cartridge (Waters Co., Milford, MA, USA) to obtain the de-aromatised juice. Five different amounts (see Table 3) of commercial standards of volatiles (from methanolic solutions) and 60 μL of a methanolic solution of ethyl nonanoate (internal standard, 0.84 μg/mL) were added to 5 mL of de-aromatised juice up to a total volume of 6 mL (additional de-aromatised juice was added when necessary). Then the mixture was equilibrated overnight at 4 °C and the volatiles from 5 mL of the mixture were extracted and analysed in the same way that the assayed samples of citrus juices.

2.6. GC–MS analysis of volatiles and TMS derivatives

Gas Chromatography was performed on a ThermoFinnigan (ThermoScientific, San José, CA, USA) Trace GC system equipped with an autosampler. The column used was a HP-5MS (5% phenyl/95% methylpolysiloxane) capillary column, 30 m × 0.25 mm i.d., 0.25 μm film thickness, from Agilent (Agilent Technologies, Palo Alto, CA, USA). MS analysis was performed on a ThermoFinnigan (ThermoScientific, San José, CA, USA) Polaris Q ion trap mass analyzer.

2.6.1. Volatile compounds

The GC parameters for the analysis of volatiles were: carrier gas, helium at flow rate (constant mode) of 1.6 mL/min; injector temperature, 230 °C [equipped with a SPME inlet liner (Sigma–Aldrich Co., St. Louis, MO, USA)]; injection, splitless mode during the first 4 min and then turned to split mode (1:50) until the end of the analysis; oven temperature ramp, initial temperature 40 °C, held for 4 min, then heating at 1 °C/min up to 73 °C, held for 10 min, then heating at 2 °C/min up to 192 °C, and finally heating at 20 °C/min up to 250 °C and held for 5 min. The total chromatographic time was 103 min. The fixed MS settings for the analysis of volatile compounds were: transfer line temperature, 280 °C; ion source temperature, 250 °C; scan mode, full with mass range m/z 41–250; ionization mode, electron impact at 70 eV; data file format, Xcalibur™ Raw Data File.

2.6.2. TMS derivatives

The GC parameters for the analysis of TMS derivatives were: carrier gas, helium at flow rate (constant mode) of 1.1 mL/min; injector temperature, 230 °C; injection, split mode (1:10); injection volume, 1 μL; oven temperature ramp, initial temperature 70 °C, held for 5 min, then heating at 4 °C/min up to 325 °C. The total chromatographic time was 74 min. The fixed MS settings for the analysis of the TMS derivatives were: transfer line temperature, 300 °C; ion source temperature, 250 °C; scan mode, full with mass range m/z 60–650; ionization mode, electron impact at 70 eV; data file format, Xcalibur™ Raw Data File.

2.7. Software for data processing of raw GC–MS data files

The last free available version of the AMDIS program (v. 2.69) was downloaded from the NIST™ website (http://chemdata.nist.gov/mass-spc/amdis/). The dedicated software for the GC–MS platform used was Xcalibur™ (v. 2.07) (ThermoScientific, San José, CA, USA).

2.8. Shelf-build AMDIS GC–MS libraries

2.8.1. Preliminary AMDIS GC–MS library for volatiles

To elucidate the influence of the AMDIS settings on the automatic determination of volatiles, a preliminary AMDIS library (with extension .MSL) was build. In a first step, the commercially available standards of those volatiles that have already been reported in citrus juices (39, see Table 3) were analysed and their characteristic mass spectrum and chromatographic retention time (extracted by manual deconvolution) were incorporated into the preliminary library. In a second step and with the aim to complete the preliminary library with those citrus volatiles that are not commercially available, samples of Valencia Late, Nova, Lane Late, Ortanique and Clemenules juices were also analysed. In these cases, AMDIS identifications were carried out by means of the NISTFF.MSL library for flavour and fragrances (provided by NIST™ 2005) and, when necessary, with the help of additional bibliographic information concerning the chromatographic elution order of the volatiles present in citrus juices [19]. Once a compound was positively identified, both its mass spectrum and chromatographic retention time were incorporated into the preliminary library. The total of volatile compounds incorporated was 110. The demanded minimum match factor was 80% (only considering reverse search) which, as pointed out by Stein [3], is enough to exclude false positives.

2.8.2. Preliminary AMDIS GC–MS library for TMS derivatives

In a similar way, it was built a preliminary library for the TMS derivatives of sugars, acids and aminoacids reported in citrus juices. The available standards (45, see Table 2) were derivatised, analysed by GC–MS, the resulting TIC manually deconvoluted and the extracted mass spectra and chromatographic retention times added to the preliminary library.

2.8.3. Ion model selection

The quantification by AMDIS of an identified compound from a raw GC–MS data file requires the previous selection of a significant ion (ion model) present in its mass spectrum (SIM-like quantification). Among all the ions generated at the ionization source of the mass analyzer for every single compound, the right choice of its ion model results crucial for its accurate quantification. The goal is to maximize selectivity, and so minimize problems in the case of its chromatographic co-elution with some other compounds present in the sample, as well as sensitivity, by choosing, if possible, an ion with high relative abundance.

2.8.4. Final shelf-build AMDIS GC–MS libraries

The preliminary AMDIS libraries described above for volatiles and TMS derivates were completed by including the corresponding ion model for the assayed compounds. It must be noted that the shelf-built libraries are easily exportable to other users and platforms as well as easily upgraded with data from other AMDIS libraries.

2.9. Optimization of MS and AMDIS operating settings

The results of the data processing performed by AMDIS depend on a number of settings for both the MS and AMDIS, which modulate the deconvolution, identification, integration and quantification steps, as well as the loaded AMDIS GC–MS library. In the present work, the following identification settings were fixed as default: minimum match factor for reverse search, 80%; use of chromatographic retention time, on; retention time window, 0.25 min; match factor penalty, average; maximum penalty, 20; No. of RT in Library, 10; instrument threshold, medium; data file format, Xcalibur™ raw file; instrument type, ion trap. It must be noted that the use of both the mass spectrum and the chromatographic retention time as criterions for identification greatly enhances the accuracy of the determinations, making rather improbable to obtain mismatched assignments [15].

2.9.1. MS scan rate (sampling rate)

To test the dependence of AMDIS reliability on the sampling rate of the MS, different MS scan rates for both the volatiles and TMS derivatives of polar compounds were assayed using samples of Valencia Late juice. As a general rule, the scan time in an ion trap mass analyzer is a function of both the ion injection time, which determines the accumulation time of ions, and the number of microscans, which determines the overall scan time. Theory states that for the detection of an analyte at small concentration, the number of microscans must be low (or just one in extreme cases), whilst the ion injection time has to be increased until a value that still allows an enough number of scans (data points) per chromatographic peak. Usually, the setting for ion injection time is a default value recommended by the manufacturer in order to avoid sensitivity problems. Consequently, when using this default value, it is the number of microscans which determines the final value of the sampling rate, and so the settled value for it can become critical for the quality of the resulting mass spectral data. Values excessively low produce short scan times and consequently high sampling rates but also poor signal-to-noise ratios, whereas values excessively high produce rather long scan times and consequently low sampling rates, with the net result of an insufficient number of data points across the chromatographic peaks and the consequent ruining of both the peak shape and chromatographic resolution. In the present work, the ion injection time used was that recommended by the manufacturer, namely 25 ms, whilst three different microscan settings, 3, 6 and 9 microscan/scan, were tested for both the volatiles and TMS derivatives.

2.9.2. AMDIS deconvolution settings

Main AMDIS deconvolution settings, namely sensitivity, shape requirement and resolution, were tested to elucidate their effects on data processing. Sensitivity modulates how AMDIS deals with the width and noise of chromatographic peaks; shape requirement modulates how the program deals with the shape of chromatographic peaks; and finally resolution modulates how the algorithm of analysis deals with the resolution of chromatographic peaks. In addition, some minor AMDIS deconvolution settings were also tested, namely, component width and adjacent peak subtraction, which also affect the data processing but in a lesser extend. The former is related with the width of the chromatographic peaks (expressed in scans, not in time), whilst the latter refers to the degree at which the interfering ions in co-eluted chromatographic peaks may be subtracted.

2.10. Xcalibur™ settings

After each optimization step, the results obtained automatically from AMDIS were tested by comparison against those obtained manually by using Xcalibur™. The program Xcalibur™ also includes a setup option that allows automatic processing of raw GC–MS data files, but requires a rather intricate procedure of customization and, what is worse, since it lacks of de-skewing and deconvolution capabilities, it becomes very prone to mismatched identifications and erroneous quantifications, even in cases of moderate peak overlapping. For these reasons, the identification and quantification of compounds were done manually when using Xcalibur™. As a consequence, only the smooth factor needed to be optimized and a final averaged value of 7 was selected.

3. Results and discussion

3.1. Effect of the MS scan rate on AMDIS reliability

The effects of overlapping levels and concentration ratios of overlapping compounds and of the MS scan rates, on the AMDIS reliability was discussed by Zhang et al. [10]. The authors found that for the testing mixture of two pesticides (PCNB and β-HCH), only those scan rates within the range 0.4–0.95 s/scan allowed AMDIS to perform reliable qualitative and quantitative analysis. Below a scan rate of 0.4 s/scan there is a degradation of the ion profile, which specially affects the analytes at low concentration, thus inducing AMDIS to perform incorrect identifications and quantifications. Above a scan rate of 0.95 s/scan, there is an excessive reduction of data points across the chromatographic peaks, thus inducing AMDIS to incorrect (under-measured) quantitative results and problems for identifying overlapped peaks. Moreover, at a scan rate within the optimum range and a concentration ratio 1:1 of PCNB:β-HCH, it is enough a difference of 3 scans between the retentions times of both pesticides to allow AMDIS performs ideally qualitative and quantitative analysis. Finally, at a scan rate within the optimum range and chromatographic resolution of only 2 scans, AMDIS provided excellent resolving ability when the concentration ratios were in the range from 10:2 to 1:10 of PCNB:β-HCH.

As a general rule, in GC–MS the MS scan rate for a given assayed sample must always be settled as a direct function of the width of the chromatographic peaks and even, if necessary, resettled accordingly along the chromatogram. The accuracy of the mathematical algorithms for the integration of chromatographic peaks is quite dependent on the number of data points across them or, in other words, on the sampling rate at which the data points have been acquired. It is widely accepted that a digitalized chromatographic peak would approximately contain within 15–25 data points to be mathematically well reconstituted (as it was analogical) and thus accurately integrated. An excessive number of data points per peak (excessively fast scan rate) can lead to a minimum variation of the "discriminant" measured parameter between two successive data points. As a consequence and depending on the settled value for the signal threshold (or an equivalent parameter), the algorithm could be unable to correctly detect the beginning and the ending of the peaks or, alternatively, to detect an almost infinite number of peaks from the chromatographic background (noise). Moreover and in some minor cases, if during the elution of a pure peak there is a fortuitous and sudden fluctuation (increase and decrease) of the "discriminant" parameter, the algorithm could consider this pure peak as the sum of two overlapping peaks (splitting) and proceeds

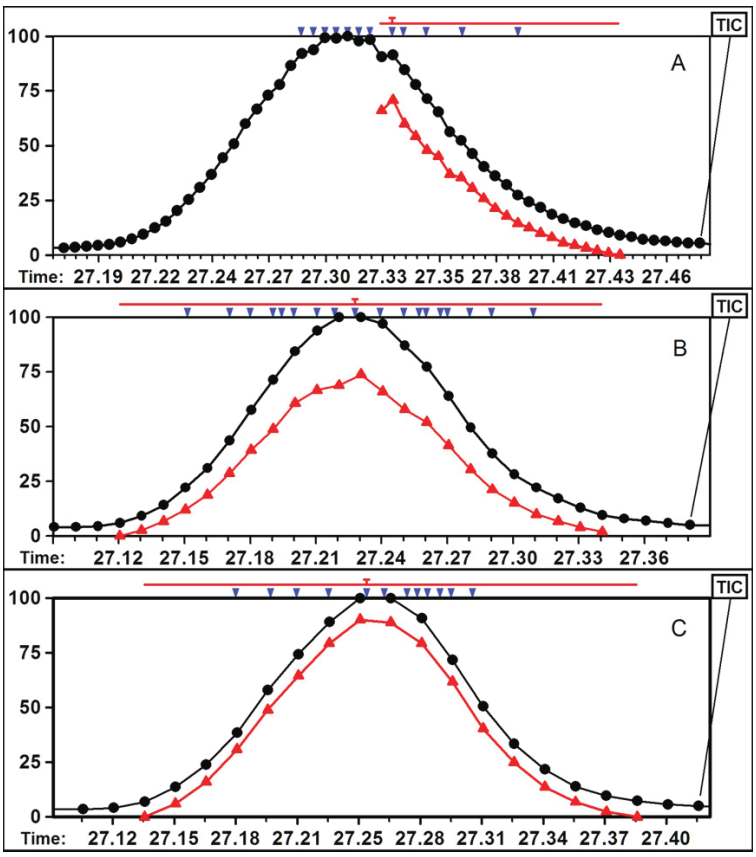

Fig. 1. Identification and quantification by AMDIS of pure 1-terpinen-4-ol (ion model *m*/*z* 71) from three raw GC–MS data files of a sample of orange juice, which were acquired at sampling rates of 0.34 (A), 0.62 (B), and 0.93 s/scan (C), respectively. (●) TIC from the sample, (▲) extracted ion model by AMDIS.

consequently. In contrast, an insufficient number of data points per peak (excessively slow scan rate) could prevent the algorithm to mathematically reconstitute the true (analogical) peaks and adequately deconvolute overlapping peaks, thus yielding erroneous identifications and integrations.

In Fig. 1A, the dots are the experimental data points (scan points) corresponding to pure 1-terpinen-4-ol from the TIC of a real sample of orange juice, when it was acquired at a scan rate of 3 microscan/scan, which corresponds to 0.34 s/scan for the scanned *m*/*z* 41–250 mass range. The triangles is the representation by AMDIS (with the "show component on chromatogram" option activated) of the extracted ion at *m*/*z* 71 (the ion model for 1-terpinen-4-ol) from the deconvoluted mass spectra of the identified compound. Fig. 1B and C are all similar to Fig. 1A, excepting that the scan rates were 6 microscan/scan, equivalent to 0.62 s/scan, and 9 microscan/scan, equivalent to 0.93 s/scan, respectively. The range of scans forming the extracted peak is represented at the top of the chromatogram as a horizontal bar which just extends the width of the identified peak; the down triangles mark the "components" that have been extracted by AMDIS to be checked against the library before final compound identification and quantification, and the symbol "T" (target) indicates that this "component" has been identified as a compound present in the analysed sample. In both cases, the chromatographic peaks have roughly been reconstituted by means of straight lines connecting the dots and the triangles, respectively.

As can be seen in Fig. 1A, the width of the chromatographic peak from the TIC (line connecting dots) is about 0.21 min and at the assayed scan rate (0.34 s/scan) it contains about 46 data points, which are in excess from the optimal range. It was rather striking that the shape of this peak from the AMDIS representation (line connecting triangles) was quite different. This difference can be attributed to the fortuitous and short time fluctuation (increase and decrease) of the signal between the TIC data points at 27.325 and 27.335 min. In this case, it seems that AMDIS dealt with this "singular" peak as if it was not pure but the result of two overlapping peaks. After the inevitable failed deconvolution, the "first" compound could neither be identified (its mass spectrum practically lacked of ions) nor quantified, whilst the "second" compound could be identified and quantified, but the quantification value given for this pure compound was clearly erroneous. It seems evident that a slower scan rate would normally prevent this type of problems. In Fig. 1B and C, the chromatographic peak from the TIC contains 23 (sampling rate 0.62 s/scan) and 17 (sampling rate 0.93 s/scan) data points, respectively. Moreover, the shape of the peak from both the TIC and the AMDIS representations was very similar and thus it was accurately identified and quantified in both cases. Taking into account that the width of all the chromatographic peaks from the volatiles was practically the same, and that 17 data points per peak is enough for an accurate quantification, a sampling rate of 9 microscan/scan, equivalent to 0.93 s/scan, was finally selected. An additional reason for selecting this scan rate was that a suited but slower scan rate improves the library matching of the mass spectra [10].

Similarly to the volatile compounds, Fig. 2A–C show the experimental data for the TMS derivative of malic acid (ion model *m*/*z*

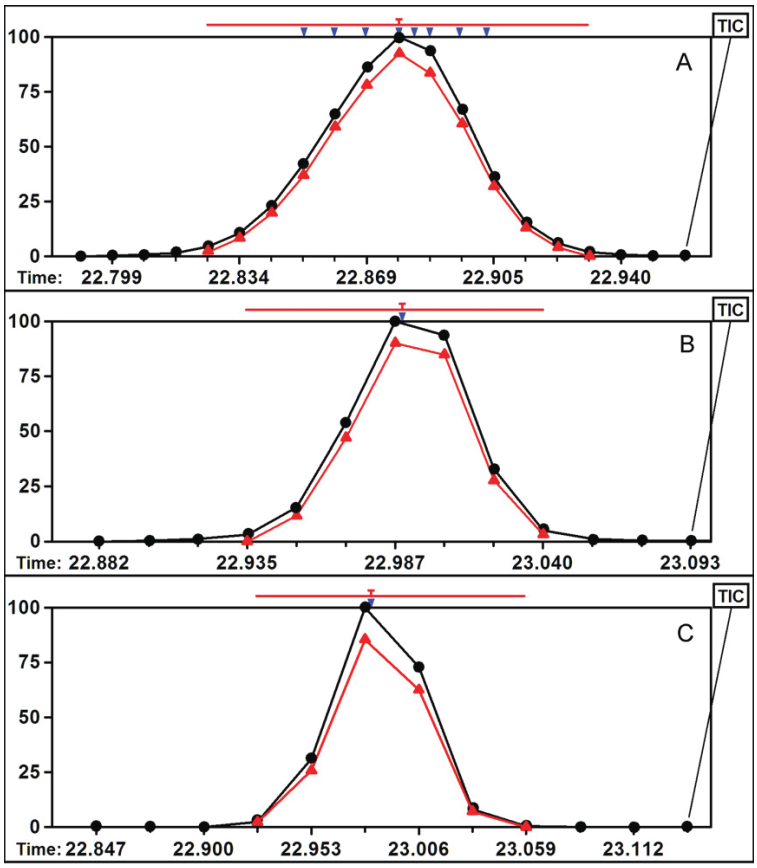

Fig. 2. Identification and quantification by AMDIS of the TMS derivative of pure malic acid (ion model *m*/*z* 245) from three raw GC–MS data files of a sample of orange juice, which were acquired at sampling rates of 0.58 (A), 1.08 (B), and 1.58 s/scan (C), respectively. (●) TIC from the sample, (▲) extracted ion model by AMDIS.

245) from both the TIC (dots) and AMDIS (triangles) representations, when acquired at sampling rates of 3, 6 and 9 microscan/scan, corresponding to 0.58, 1.08 and 1.58 s/scan, respectively, for the assayed *m*/*z* 60–650 mass range. It must be noted that the width of the chromatographic peak of the TMS derivative of malic acid (≈0.11 min) is about half of that of 1-terpinen-4-ol (≈0.21 min). Therefore, the chromatographic peak in Fig. 2A–C only contains 13, 7 and 6 data points, respectively, and it was identified and quantified in all cases. However, it seems clearly evident that the true analogical shape of the chromatographic peak cannot mathematically be reconstituted from only 6 or 7 data points and so accurately integrated, but it could be from 13 data points, although this number is at the lower limit. Consequently and taking into account that the width of all the chromatographic peaks from the TMS derivatives of polar compounds was practically the same, a sampling rate of 3 microscan/scan, equivalent to 0.58 s/scan, was selected for their determination.

3.2. Optimization of AMDIS deconvolution settings for data processing

3.2.1. Volatile compounds

All the possible 45 combinations of settings for sensitivity, shape requirement and resolution were tested. Hence, sensitivity was ranged from very low to very high, shape requirement was ranged from low to high, and resolution was ranged from low to high. Table 1 shows the results obtained by combining the different assayed deconvolution settings, which are expressed as "components" (the number of extracted potential compounds that could be present in the sample), and targets (the real number of positively identified compounds in the sample). As a general rule, a decrease of the number of "components" also decreases the probability of the targets to be detected and identified; on the contrary, an increase of the number of "components" also increases the probability that some more targets could be detected but with the risking of obtaining false positives or incorrect identifications. Thus, the challenge is to customize AMDIS as much as possible, in such a way that from a single run it could correctly identify and quantify the maximum number of true targets with a minimum number of "components".

As it is shown in Table 1, the number of targets and "components" varied within the ranges 65–88 and 255–1678, respectively. Results indicate that the best performance is achieved when sensitivity was set to medium, shape requirements was set to low, and resolution was set to low, since with this combination of settings the number of correct targets was 87 and the number of "components" was only 428. Moreover, for those combinations of settings giving a number of "components" of 800 or greater, it was observed the existence of a direct correlation between the number of incorrect quantifications and the number of "components". It seems, therefore, that the best choice is to ensure the accuracy of the quantifications even at the expense of "sacrifice" the possible detection of some more targets, although in practice only a few very minor targets would be lost as a maximum.

Table 1
Influence of AMDIS deconvolution settings on identification efficiency.

Sensitivity	Shape requirement	Resolution					
		High		Medium		Low	
		Targets	Components	Targets	Components	Targets	Components
Very high	High	78	1441	77	959	78	608
	Medium	87	1656	85	1115	84	739
	Low	88	1678	87	1136	87	756
High	High	80	1195	79	801	80	523
	Medium	85	1309	85	864	84	576
	Low	87	1315	87	871	87	580
Medium	High	77	926	76	618	77	412
	Medium	86	975	85	639	85	430
	Low	88	979	87	639	87	428
Low	High	70	722	69	475	70	316
	Medium	79	765	78	492	78	334
	Low	81	770	80	493	79	334
Very low	High	64	565	65	368	65	255
	Medium	73	603	73	385	72	268
	Low	76	603	76	382	75	268

There were also tested the settings for component width (range 5–30) and adjacent peak subtraction (range 0–2). The default value for the component width is 12, but it was found that the optimum value ranged within 12–20. Below the value 12, the number of "components" and targets decreased; above the value 20, the number of "components" increased but the number of targets remained constant. Therefore, the value of 20 was selected. The default value for adjacent peak subtraction is 1. When this value was set to 0, the number of targets decreased; when it was set to 2, the number of "components" increased but without an increase of the number of targets. Therefore, the default value of 1 was selected.

3.2.2. TMS derivatives of polar compounds

Concerning to the optimization of AMDIS settings for data processing of the TMS derivatives, it was found that the optimized settings coincided with those obtained from the volatiles.

3.3. Testing of AMDIS for deconvolution of overlapped chromatographic peaks

The reliability of AMDIS to deconvolute overlapped chromatographic peaks was tested using the above optimized deconvolution settings. Fig. 3A shows a simple example of two partially overlapped peaks from a sample of orange juice, which correspond to the volatiles carvone and neral. The dots correspond to the data points from the TIC of the sample, and the peaks are roughly reconstituted by the straight lines connecting them. After AMDIS deconvolution and processing, two compounds were detected, identified and quantified. The down triangles (▼) correspond to the peak generated from the extraction of the ion model (at m/z 54) of the identified carvone, whilst the up triangles (▲) correspond to the peak generated from the extraction of the ion model (at m/z 119) of the identified neral, which were used to perform the corresponding quantification. The identified compounds are marked with the

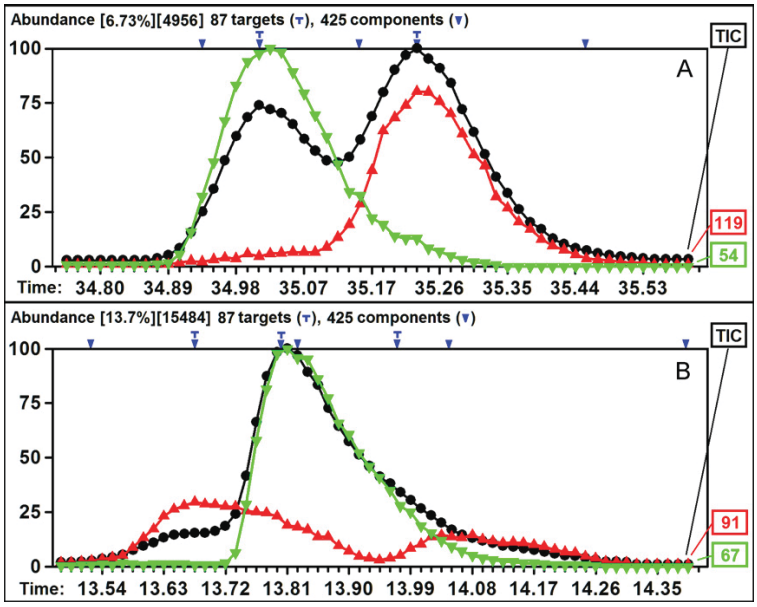

Fig. 3. Deconvolution, identification and quantification by AMDIS of the compounds present in partially co-eluted chromatographic peaks. (A) Two co-eluting chromatographic peaks, (●) TIC of the sample, (▲) neral (ion model m/z 119), (▼) carvone (ion model m/z 54). (B) Three co-eluting chromatographic peaks, (●) TIC of the sample, (▲) α-fellandrene (Rt = 13.59 min, ion model m/z 91) and δ-3-carene (Rt = 14.02 min, ion model m/z 91), and (▼) octanal (ion model m/z 67).

Table 2
Retention time, ion model, weight interval, relative response factor, and linearity of the concentration response from Xcalibur™ and AMDIS for the assayed TMS derivatives of polar commercial standards.

TMS derivative	Rt (min)	Ion model (*m*/*z*)	[a]Weight interval (mg)	Xcalibur™		AMDIS	
				[b]$F_{x,is}$	[c]R^2	[b]$F_{x,is}$	[c]R^2
Sugars							
L-Xylose $(TMS)_4$	27.90	307	0.0126–0.0630	1.90	0.995	1.91	0.993
Arabinose $(TMS)_4$	28.29	307	0.0113–0.0565	1.71	0.994	1.67	0.991
Ribose $(TMS)_4$	28.71	307	0.0107–0.0535	1.39	0.990	1.36	0.990
Rhamnose $(TMS)_4$	29.80	117	0.0121–0.0604	0.67	0.992	0.68	0.994
[d]Fructose $(TMS)_5$	33.92/34.18	307	0.0120–0.1180	1.11	0.996	1.16	0.994
[d]Glucose $(TMS)_5$	34.52/34.93	319	0.0111–0.1140	0.71	0.997	0.70	0.993
Mannitol $(TMS)_6$	35.27	319	0.0126–0.0630	0.41	0.997	0.41	0.996
Sorbitol $(TMS)_6$	35.45	319	0.0107–0.0535	0.44	0.997	0.44	0.997
Scyllo-Inositol $(TMS)_6$	35.54	318	0.0082–0.0410	0.25	0.999	0.25	0.996
Myo-Inositol $(TMS)_6$	38.88	305	0.0123–0.0615	0.18	0.993	0.18	0.990
Sucrose $(TMS)_8$	50.47	361	0.0107–0.5544	0.19	0.995	0.19	0.998
Maltose $(TMS)_8$	52.31	361	0.0109–0.0547	0.70	0.993	0.70	0.994
Raffinose $(TMS)_{11}$	62.91	361	0.00967–0.04840	0.95	0.995	1.02	0.998
Organic acids							
Oxalic Acid $(TMS)_2$	10.71	147	0.0109–0.0545	0.26	0.995	0.26	0.994
Succinic Acid $(TMS)_2$	16.96	247	0.0138–0.0690	4.50	0.997	4.40	0.997
Fumaric Acid $(TMS)_2$	18.06	245	0.0104–0.0520	0.25	0.994	0.25	0.993
Malic Acid $(TMS)_3$	22.89	245	0.0104–0.0520	1.88	0.991	1.86	0.995
Tartaric Acid $(TMS)_4$	27.52	189	0.0132–0.0660	0.56	0.991	0.56	0.994
Citric Acid $(TMS)_4$	32.26	273	0.0235–0.1175	0.27	0.995	0.30	0.998
Quinic Acid $(TMS)_5$	33.46	345	0.0122–0.0610	0.17	0.993	0.17	0.995
Glucaric Acid $(TMS)_4$	35.51	244	0.0103–0.0512	2.15	0.995	1.95	0.994
Galacturonic Acid $(TMS)_5$	35.61	333	0.0166–0.0830	0.36	0.998	0.35	0.995
Aminoacids							
D-Alanine $(TMS)_2$	9.52	116	0.0122–0.0488	0.36	0.994	0.36	0.990
L-Valine $(TMS)_2$	13.62	144	0.0123–0.0615	0.22	0.995	0.21	0.995
L-Leucine $(TMS)_2$	15.62	158	0.0126–0.0504	0.30	0.997	0.30	0.990
L-Proline $(TMS)_2$	16.31	142	0.0128–0.0512	0.25	0.995	0.26	0.993
L-Isoleucine $(TMS)_2$	16.36	158	0.0132–0.0660	0.21	0.994	0.21	0.990
Glycine $(TMS)_3$	16.70	174	0.0139–0.0556	0.19	0.997	0.20	0.997
L-Serine $(TMS)_3$	18.79	204	0.0116–0.0580	0.22	0.995	0.22	0.992
L-Threonine $(TMS)_3$	19.67	101	0.0111–0.0555	0.50	0.997	0.51	0.997
L-Methionine $(TMS)_2$	23.49	128	0.0113–0.0452	0.41	0.996	0.39	0.998
L-Aspartic acid $(TMS)_3$	23.80	232	0.0118–0.0472	0.37	0.999	0.36	0.996
Hydroxy-L-proline $(TMS)_3$	23.90	230	0.0106–0.0530	0.19	0.999	0.19	0.990
L-Cysteine $(TMS)_3$	24.71	220	0.0109–0.0436	0.40	0.998	0.40	0.998
Arginine $(TMS)_2$	26.44	142	0.0146–0.0730	5.37	0.991	5.18	0.994
L-Phenylalanine $(TMS)_2$	26.51	218	0.0123–0.0615	0.53	0.993	0.55	0.991
D-Glutamic Acid $(TMS)_3$	26.64	246	0.0137–0.0548	0.60	0.997	0.56	0.996
L-Asparragine $(TMS)_3$	28.06	188	0.0116–0.0464	4.04	0.993	4.06	0.992
Glutamine $(TMS)_3$	30.75	156	0.0098–0.0490	1.75	0.994	1.75	0.997
L-Histidine $(TMS)_3$	34.48	254	0.0108–0.0540	5.91	0.997	5.90	0.995
L-Lysine $(TMS)_3$	34.51	156	0.0106–0.0530	0.14	0.998	0.13	0.990
D-Tirosyne $(TMS)_3$	34.89	218	0.0109–0.0545	0.35	0.993	0.37	0.994
L-Tryptophan $(TMS)_3$	40.74	202	0.0135–0.0640	2.31	0.993	2.30	0.992
Others							
Putrescine $(TMS)_4$	29.60	174	0.0194–0.0582	0.28	0.994	0.28	0.991
Cadaverine $(TMS)_4$	32.13	174	0.0172–0.0860	0.39	0.996	0.39	0.996

[a] Diluted in 110 μL of MEOX-MSTFA solution.
[b] Relative response factor of compound "x" against the internal standard "is" (ribitol).
[c] Correlation coefficients from five different assayed concentrations.
[d] Fructose and glucose appear as α- and β-isomers.

symbol "T", at the top of the chromatogram, at their corresponding retention time. Fig. 3B shows a rather more complex overlapping case. The TIC representation (●) suggests the presence of a major peak and a couple of shoulders, that is, a total of three partially co-eluted compounds. After deconvolution and processing, AMDIS accurately extracted, identified and quantified three compounds: α-fellandrene (▲, Rt = 13.59 min, ion model *m*/*z* 91), octanal (▼, ion model *m*/*z* 67) and δ-3-carene (▲, Rt = 14.02 min, ion model *m*/*z* 91).

3.4. Linearity of the AMDIS quantification response

The absolute quantification of the polar compounds present in the juice, namely, sugars, organic acids and aminoacids, is rather straightforward because they are derivatised from a dried sample of orange juice, without any loss by evaporation. Hence, the previous addition of a known amount of internal standard (ribitol) to the sample, before its drying and derivatisation, allows their absolute quantification using the known formula

$$W_x = F_{x,is}\frac{A_x}{A_{is}}W_{is}$$

where W_x and A_x are, respectively, the weight (in mg) and the area under the peak corresponding of the identified compound; W_{is} and A_{is} are, respectively, the weight (in mg) of added internal standard and the area under its corresponding peak; and $F_{x,is}$ is the relative response factor of the identified compound against

Table 3
Retention time, ion model, weight interval, relative response factor, and linearity of the concentration response from Xcalibur™ and AMDIS for the assayed commercial volatile standards.

Compound	Rt (min)	Ion model (*m*/*z*)	[a]Weight interval (μg)	Xcalibur™		AMDIS	
				[b]Rf	[c]R^2	[b]Rf	[c]R^2
Z-3-Hexenal	3.92	43	0.06–0.30	39.13	0.994	36.23	0.990
Ethyl butyrate	4.01	88	0.10–0.50	31.40	0.999	28.34	0.994
Heptanal	7.68	43	0.06–0.30	7.85	0.987	6.55	0.990
α-Pinene	9.18	91	0.30–1.50	17.57	0.998	14.28	0.990
β-Pinene	11.67	93	0.50–4.00	4.95	0.998	4.75	0.999
α-Felandrene	13.61	91	0.06–0.30	25.50	0.990	29.33	0.981
Octanal	13.82	67	0.20–1.00	4.99	0.992	4.65	0.990
δ-3-Carene	14.02	91	0.06–0.30	10.54	0.999	8.78	0.996
α-Terpinene	14.73	93	0.06–0.30	4.83	0.988	3.85	0.998
trans-β-Ocimene	17.43	91	0.30–1.50	10.02	0.993	10.04	0.982
γ-Terpinene	17.93	91	0.30–1.50	6.18	0.997	5.72	0.990
1-Octanol	19.28	55	0.30–1.50	1.59	0.986	1.75	0.987
α-Terpinolene	20.01	93	0.05–0.25	0.73	0.961	0.74	0.981
Linalool	21.55	93	1.00–5.00	4.66	0.995	4.79	0.990
Nonanal	21.82	67	0.10–0.50	0.85	0.990	0.91	0.987
Camphor	24.25	95	0.06–0.30	1.97	0.990	1.85	0.985
Citronellal	24.88	79	0.06–0.30	53.89	0.990	55.07	0.990
1-Terpinen-4-ol	27.43	71	0.30–1.50	2.23	0.979	2.77	0.973
α-Terpineol	29.02	59	0.60–3.00	5.11	0.991	5.74	0.994
Decanal	31.38	41	0.40–2.00	0.62	0.998	0.69	0.999
cis-Carveol	32.02	109	0.06–0.30	6.54	0.981	7.28	0.987
ι-carveol	32.53	91	0.06–0.30	18.35	0.995	22.20	0.992
Nerol	33.63	91	0.06–0.30	2.72	0.990	2.85	0.991
β-Citronellol	34.12	67	0.004–0.020	0.04	0.990	0.03	0.992
Carvone	35.05	54	0.20–1.00	4.15	0.999	4.01	0.994
Perillaldehyde	39.01	79	0.10–0.50	1.68	0.986	1.79	0.981
Geranial	39.53	41	0.20–1.00	2.56	0.989	2.17	0.982
1-Decanol	40.42	41	0.08–0.40	0.27	0.994	0.33	0.999
2,4-Decadienal	44.41	81	0.06–0.30	0.28	0.991	0.26	0.987
α-Terpenyl acetate	47.47	93	0.06–0.30	0.21	0.991	0.27	0.997
Citronellyl acetate	48.32	67	0.06–0.30	0.45	0.997	0.37	0.987
Neryl Acetate	49.37	93	0.06–0.30	0.40	0.998	0.41	0.994
Camphene	51.01	41	0.06–0.30	0.79	0.993	0.56	0.999
β-Caryophyllene	52.45	91	0.10–0.50	3.21	0.995	3.00	0.982
Geranyl acetate	52.71	41	0.06–0.30	40.25	0.991	33.71	0.980
allo-Aromadendrene	53.90	105	0.10–0.50	5.01	0.998	5.24	0.993
α-Caryophyllene	55.03	93	0.10–0.50	0.36	0.995	0.33	0.997
Valencene	58.02	105	0.06–0.30	0.18	0.999	0.18	0.999
Nootkatone	75.91	146	0.06–0.30	24.94	0.991	22.48	0.981

[a] Diluted in 6 mL of MeOH.
[b] Relative response factor of compound "x" against the internal standard "is" (ethyl nonanoate).
[c] Correlation coefficients from five different assayed concentrations.

the internal standard. Table 2 shows the assayed TMS derivatives of polar commercial standards, their chromatographic retention time, ion model, weight range assayed (five different added weights), relative response factor against ribitol (internal standard) and the linearity of the response when quantified by using AMDIS and Xcalibur™ (glucose and fructose appear as two peaks corresponding to their α- and β-isomers). As can be seen, the determined response factors and correlation coefficients (>0.990 in all cases) were practically identical from both analyses, thus suggesting that AMDIS and Xcalibur™ should yield similar quantifications when processing orange juice samples.

The absolute quantification of the volatiles in the juice, on the contrary, is extremely difficult. At the ending of the extraction by HS-SPME, each one of the volatiles is shared out within the pulp, the juice serum, the head space and the extraction fibber according to their specific distribution coefficient constants between pulp/serum, serum/head space and head space/fibber. Since these constants are unknown, it becomes unrealistic any attempting to determine their absolute concentration in the juice from the determination of their concentration in the extraction fibber. Nevertheless, the extraction of volatiles with the fibber and their further identification and "quantification" has several advantages. Firstly, this allows to have an insight on its volatile composition and on the relative concentrations of these volatiles; secondly and very important, it allows to monitor the changes in volatile composition due to industrial processes or to storage. In this work, the goal of the extraction of volatiles by HS-SPME from a de-pulped and de-aromatised juice, previously spiked with different amounts of volatile standards and internal standard, was for comparison of the identification, quantification and linearity of the quantification responses from AMDIS and Xcalibur™. Table 3 lists the assayed commercial volatile standards, their chromatographic retention time, ion model, weight range assayed (five different added weights), relative response factor against ethyl nonanoate (internal standard) and linearity of the response when quantified using AMDIS and Xcalibur™. As in the case of TMS derivates, the relative response factors and correlation coefficients (>0.990 for almost all volatiles) determined by AMDIS and Xcalibur™ were practically identical, thus suggesting also similar quantifications when analyzing juice samples. The above determined relative response factors are useless for absolute quantification of volatiles in orange juices, as indicated previously, but similarly to the spiked de-aromatised juice, relative quantifications can be carried out. This can be accomplished by the addition of a known amount of internal standard to the citrus juice and let it to equilibrate before volatile extraction (Section 2.3). In must be noted that to obtain a similar TIC response, the constant added weight of internal standard (50 μL of a methanolic solution of 10.24 μg/L) to 5 mL of juice

Table 4
Aroma profile of fresh Valencia Late juice determined by Xcalibur™ and AMDIS.

No	Compound	Rt (min)	Ion model (*m*/*z*)	[a]Relative content (mean ± SD)	
				Xcalibur™	AMDIS
1	Z-3-Hexenal	3.96	43	1.10 ± 0.11	0.99 ± 0.05
2	Ethyl butyrate	4.07	88	2.04 ± 0.20	2.29 ± 0.24
3	E-2-Hexenal	5.56	41	0.11 ± 0.01	0.11 ± 0.01
4	Heptanal	7.63	43	0.30 ± 0.05	0.33 ± 0.03
5	α-Thujene	8.83	91	0.50 ± 0.02	0.54 ± 0.04
6	α-Pinene	9.09	91	76.56 ± 3.04	79.21 ± 0.46
7	Sabinene	9.89	93	0.47 ± 0.06	0.50 ± 0.05
8	β-Pinene	11.57	93	8.30 ± 0.86	8.65 ± 1.08
9	β-Mircene	12.95	93	263.62 ± 3.51	258.23 ± 26.49
10	α-Fellandrene	13.59	91	13.79 ± 1.50	9.36 ± 1.12
11	Octanal	13.79	67	31.19 ± 1.72	32.38 ± 3.08
12	δ-3-Carene	13.96	91	6.27 ± 0.15	6.07 ± 0.13
13	α-Terpinene	14.50	93	6.75 ± 0.11	7.08 ± 0.26
14	trans-β-Ocimene	17.33	91	9.66 ± 0.20	9.77 ± 0.40
15	γ-Terpinene	17.92	91	24.50 ± 0.26	21.24 ± 1.31
16	1-Octanol	19.21	55	37.90 ± 2.69	40.25 ± 0.83
17	α-Terpinolene	20.06	93	6.15 ± 0.73	6.42 ± 0.67
18	6-Camphenone	20.53	93	1.78 ± 0.21	1.78 ± 0.14
19	Linalool	21.55	93	260.51 ± 3.24	258.05 ± 7.05
20	Nonanal	21.76	67	7.44 ± 0.21	7.51 ± 0.36
21	p-Mentha-1,3,8-triene	21.89	119	0.84 ± 0.07	0.86 ± 0.04
22	trans-p-Mentha-2,8-dienol	22.65	91	2.82 ± 0.20	3.01 ± 0.08
23	4-Acetyl-1-methyl-1-cyclohexene	23.55	95	0.69 ± 0.05	0.73 ± 0.05
24	cis-p-Mentha-2,8-dienol	23.85	91	1.69 ± 0.13	1.61 ± 0.07
25	Ethyl 3-hydroxyhexanoate	24.20	77	0.48 ± 0.02	0.51 ± 0.01
26	Camphor	24.27	95	0.37 ± 0.03	0.36 ± 0.04
27	Citronellal	24.64	79	1.01 ± 0.08	1.05 ± 0.05
28	Eucalyptol	24.88	93	0.89 ± 0.04	0.88 ± 0.05
29	β-Terpineol	25.06	91	1.32 ± 0.07	1.32 ± 0.05
30	Z-Limonene oxide	26.03	123	1.06 ± 0.11	1.07 ± 0.09
31	E-Limonene oxide	26.46	91	1.29 ± 0.09	0.90 ± 0.10
32	1-Terpinen-4-ol	27.44	71	60.78 ± 4.43	63.74 ± 3.01
33	Nonanol	27.61	55	3.17 ± 0.22	3.27 ± 0.13
34	Thymol	28.48	135	0.27 ± 0.02	0.27 ± 0.03
35	α-Terpineol	28.75	59	7.09 ± 0.32	7.26 ± 0.47
36	cis-Carvyl acetate	29.73	91	1.49 ± 0.20	1.48 ± 0.12
37	Dihydrocarvone	30.04	67	1.21 ± 0.07	1.16 ± 0.16
38	Decanal	31.04	41	20.67 ± 1.58	21.69 ± 1.22
39	p-Menth-1-en-9-al	31.60	94	0.78 ± 0.05	0.71 ± 0.07
40	cis-Carveol	32.01	109	2.74 ± 0.12	2.86 ± 0.36
41	ι-Carveol	32.54	91	2.40 ± 0.11	2.34 ± 0.13
42	Nerol	33.46	91	7.58 ± 0.47	7.24 ± 0.56
43	β-Citronellol	34.04	67	12.78 ± 0.87	12.65 ± 0.45
44	Carvone	35.03	54	4.66 ± 0.33	4.14 ± 0.36
45	Neral/cis-Citral	35.34	119	4.14 ± 0.19	4.37 ± 0.25
46	Piperitone	36.39	95	0.18 ± 0.01	0.22 ± 0.02
47	Geraniol	37.64	91	4.16 ± 0.32	4.04 ± 0.17
48	Lynalyl acetate	37.96	93	0.75 ± 0.03	0.77 ± 0.03
49	Perillaldehyde	38.86	79	4.53 ± 0.39	4.41 ± 0.31
50	Geranial	39.42	41	7.46 ± 0.46	7.58 ± 0.44
51	1-Decanol	40.06	41	3.10 ± 0.18	3.11 ± 0.08
52	2,4-Decadienal	44.33	81	1.26 ± 0.09	1.38 ± 0.09
53	α-Selinene	46.33	95	1.18 ± 0.11	1.08 ± 0.10
54	α-Terpenyl acetate	47.32	93	2.62 ± 0.25	2.64 ± 0.18
55	Citronellyl acetate	48.22	67	2.08 ± 0.05	2.17 ± 0.09
56	α-Copaene	49.03	105	13.21 ± 0.9	13.71 ± 0.87
57	Neryl acetate	49.22	93	1.81 ± 0.05	1.81 ± 0.12
58	α-Cubebene	50.40	105	9.63 ± 0.11	9.46 ± 0.63
59	β-Elemene	50.63	93	5.37 ± 0.50	5.26 ± 0.30
60	Camphene	50.86	41	0.49 ± 0.04	0.45 ± 0.04
61	Isolongifolene	51.36	79	0.19 ± 0.02	0.20 ± 0.02
62	β-Caryophyllene	52.45	91	6.65 ± 0.11	6.41 ± 0.16
63	Geranyl acetate	52.62	41	3.25 ± 0.19	3.05 ± 0.14
64	Longifolene-(V4)	53.18	105	8.54 ± 0.29	8.68 ± 0.13
65	allo-Aromadendrene	54.09	105	0.22 ± 0.02	0.23 ± 0.02
66	p-Menth-1-en-9-ol	54.39	91	0.72 ± 0.06	0.74 ± 0.04
67	α-Caryophyllene	54.88	93	3.47 ± 0.15	3.43 ± 0.09
68	Aromadendrene	55.78	91	1.57 ± 0.12	1.78 ± 0.22
69	(Z)-β-Guaiene	56.11	120	2.38 ± 0.14	2.47 ± 0.13
70	β-Selinene	56.48	107	0.96 ± 0.01	0.95 ± 0.09
71	Viridiflorene	56.71	133	0.58 ± 0.04	0.58 ± 0.03
72	Germacrene-D	56.93	105	7.94 ± 0.38	8.39 ± 0.27
73	Valencene	57.78	105	101.87 ± 3.75	103.06 ± 4.34
74	y-Elemene	58.02	93	1.59 ± 0.10	1.63 ± 0.14
75	α-Muurolene	58.54	105	4.54 ± 0.26	4.63 ± 0.13
76	ε-Guaiene	58.79	107	0.24 ± 0.02	0.23 ± 0.01
77	Selina-3,7(11)-diene	59.39	105	4.58 ± 0.29	4.54 ± 0.12
78	α-Farnesene	59.61	91	3.20 ± 0.14	3.33 ± 0.04
79	Cadinene	60.08	119	19.59 ± 1.74	19.96 ± 1.51
80	Germacrene-B	60.24	41	0.49 ± 0.01	0.49 ± 0.04
81	Caryophyllene oxidade	63.41	79	0.61 ± 0.02	0.61 ± 0.02
82	α-Guaiene	67.19	105	0.33 ± 0.01	0.32 ± 0.02
83	β-Sinensal	70.69	91	9.09 ± 0.09	9.48 ± 0.87
84	α-Sinensal	73.73	91	1.29 ± 0.13	1.34 ± 0.15
85	Nootkatone	75.81	146	1.48 ± 0.12	1.44 ± 0.12

[a] Values are the average of three replicates.

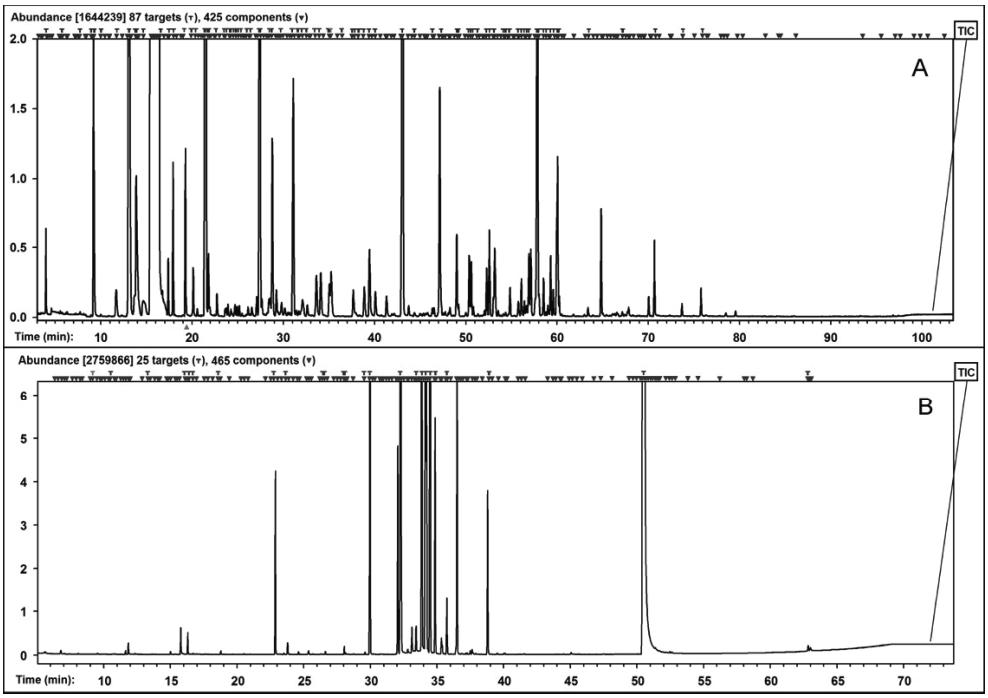

Fig. 4. TIC profiles from the GC–MS analysis of volatiles (A) and TMS derivatives of sugars, acids and aminoacids (B) in Valencia Late juice.

has to be greater by far than that added (60 μL of a methanolic solution of 0.84 μg/L) to 6 mL of de-aromatised juice (Section 2.5), since the citrus juices contain pulp which sequestrates most of the internal standard. Assuming thus that the relative response factor is the same for all the volatiles and equal to unity, the relative quantification of volatiles was done according to the formula

$$W_x = 100\frac{A_x}{A_{is}}$$

where the multiplying factor 100 has been included exclusively to obtain more easy-to-use numbers.

3.5. GC–MS analysis and compounds determination of orange juice samples

Fig. 4A and B show the TIC profiles from the GC–MS analysis of volatiles and TMS derivatives of sugars, organic acids and aminoacids in Valencia Late juice, respectively. Both raw GC–MS

Table 5
Polar metabolites in fresh Valencia Late juice as determined by Xcalibur™ and AMDIS.

No	[b]Compound	Rt (min)	Ion model (*m*/*z*)	[a]g/L (mean ± SD)	
				Xcalibur™	AMDIS
1	D-Alanine $(TMS)_2$	9.52	116	0.0873 ± 0.0040	0.0865 ± 0.0076
2	L-Valine $(TMS)_2$	13.62	144	0.0108 ± 0.0008	0.0114 ± 0.0017
3	L-Leucine $(TMS)_2$	15.62	158	0.0055 ± 0.0004	0.0005 ± 0.0001
4	L-Proline $(TMS)_2$	16.31	142	1.6458 ± 0.1528	1.6534 ± 0.1802
5	L-Isoleucine $(TMS)_2$	16.36	158	0.0065 ± 0.0004	0.0068 ± 0.0002
6	Glycine $(TMS)_3$	16.70	174	0.0093 ± 0.0003	0.0093 ± 0.0009
7	L-Serine $(TMS)_3$	18.79	204	0.1046 ± 0.0015	0.1078 ± 0.0124
8	L-Threonine $(TMS)_3$	19.67	101	0.0098 ± 0.0005	0.0101 ± 0.0010
9	Malic acid $(TMS)_3$	22.89	245	2.5325 ± 0.2090	2.5957 ± 0.0537
10	L-Aspartic acid $(TMS)_3$	23.80	232	0.0736 ± 0.0098	0.0755 ± 0.0087
11	L-Phenylalanine $(TMS)_2$	26.51	218	0.0177 ± 0.0022	0.0176 ± 0.0023
12	D-Glutamic acid $(TMS)_3$	26.64	246	0.0647 ± 0.0044	0.0621 ± 0.0010
13	L-Asparragine $(TMS)_3$	28.06	188	0.3614 ± 0.0437	0.3537 ± 0.0478
14	Putrescine $(TMS)_4$	29.60	174	0.0690 ± 0.0089	0.0698 ± 0.0088
15	Citric acid $(TMS)_4$	32.26	273	12.1023 ± 0.0722	12.2253 ± 1.1132
16	Quinic acid $(TMS)_5$	33.46	345	0.1511 ± 0.0034	0.1487 ± 0.0057
17	[c]Fructose $(TMS)_5$	33.92/34.18	307	14.6200 ± 0.3074	14.1320 ± 2.0961
18	[c]Glucose $(TMS)_5$	34.52/34.93	319	12.5202 ± 0.8119	12.6906 ± 1.4073
19	Scyllo-inositol $(TMS)_6$	35.54	318	0.7300 ± 0.0179	0.7337 ± 0.0050
20	Myo-inositol $(TMS)_6$	38.88	305	0.7570 ± 0.0342	0.7539 ± 0.0905
21	Sucrose $(TMS)_8$	50.47	361	73.1024 ± 1.5549	72.8949 ± 7.1546
22	Raffinose $(TMS)_{11}$	62.91	361	0.2623 ± 0.0354	0.2591 ± 0.0354

[a] Values are the average of three replicates.
[b] TMS, trimethylsilyl.
[c] Fructose and glucose appears as two peaks corresponding to the α- and β-isomers.

data files were automatically processed by using AMDIS, which operated under all the optimized settings described previously, as well as manually by using Xcalibur™. As it was indicated previously, at the top of the chromatograms the "components" are marked with down triangles whilst the identified compounds (targets) are marked with the symbol "T".

From a single GC–MS run of volatiles, AMDIS was able to automatically identify and quantify 85 volatiles (87 targets taking into account the internal standard plus limonene, which is always present at saturation level in orange and mandarin juices), the same results that were obtained manually by using Xcalibur™. Table 4 shows the volatiles identified in Valencia Late juice, their retention time, ion model, and relative concentration determined by using Xcalibur™ and AMDIS. As expected, both analyses gave very similar results.

Similarly and from a single GC–MS run of the TMS derivatives, AMDIS was able to automatically identify and quantify 22 TMS derivatives (25 targets taking into account the internal standard and that the α- and β-isomers of glucose and fructose elute as separated peaks), the same results that were obtained manually by using Xcalibur™. Table 5 shows the TMS derivatives identified in Valencia Late juice, their retention time, ion model, and absolute concentration determined by using Xcalibur™ and AMDIS.

4. Conclusions

This work indicates that from a well acquired raw GC–MS data file and provided that the deconvolution settings are optimized, AMDIS is able to automatically provide fast and accurate results for both the identification and quantification of the compounds present in complex matrices. However, if the sampling rate of the MS is not adequate for the width of the chromatographic peaks, or the main deconvolution settings of AMDIS are not optimized for the particular sample assayed, most probably there would be a noticeable probability to obtain false identifications and erroneous quantifications.

The optimization of the AMDIS deconvolution settings is certainly tedious and time consuming since the results obtained by AMDIS, after each optimization step, must be compared with those obtained manually. Therefore, for data processing of only one raw GC–MS data file from a single sample, it seems not a good idea the use of AMDIS for automatic identification and quantification of its compounds. However, if a set of raw GC–MS data files from similar samples are to be processed, the previous customization of AMDIS could be a very great advantage. One must taken into account that the manual processing of data is very tedious, prone to errors from the analyst and very time consuming, from several hours to several days, whilst AMDIS automatically performs the whole data processing and gives the results in only a few minutes.

Acknowledgements

This research was supported by the Ministerio de Ciencia e Innovación (Spain), project AGL2009-11805. Authors acknowledge the financial support for the contracts of E. Sentandreu (JAEdoc Program, CSIC-FEDER funds) and M. Cerdán-Calero (JAE-predoc program, CSIC-FEDER funds). The authors are grateful to Prof. John M. Halket, Dr. Paul D. Fraser and Prof. Peter M. Bramley for initial AMDIS familiarization and to Prof. José L. Navarro for GC–MS technical assistance.

References

[1] J.M. Halket, A. Przyborowska, S.E. Stein, W.G. Mallard, S. Down, R.A. Chalmer, Rapid Commun. Mass Spectrom. 13 (1999) 279.
[2] B.N. Colby, J. Am. Soc. Mass Spectrom. 3 (1992) 558.
[3] S. Stein, J. Am. Soc. Mass Spectrom. 10 (1999) 770.
[4] S. Lee, H.K. Choi, S.K. Cho, Y.S. Kim, J. Chromatogr. B 878 (2010) 2983.
[5] http://chemdata.nist.gov/mass-spc/amdis.
[6] M.R. Meyer, F.T. Peters, H.H. Maurer, Clin. Chem. 56 (2010) 575.
[7] M.R. Meyer, J. Wilhelm, F.T. Peters, H.H. Maurer, Anal. Bioanal. Chem. 397 (2010) 1225.
[8] S. Dagan, J. Chromatogr. A 868 (2000) 229.
[9] V. Furtula, G. Derksen, J. Environ. Sci. Health, Part B 41 (2006) 1259.
[10] W. Zhang, P. Wu, C. Li, Rapid Commun. Mass Spectrom. 20 (2006) 1563.
[11] M.J. Gómez, M.M. Gómez-Ramos, A. Agüera, M. Mezcua, S. Herrera, A.R. Fernández-Alba, J. Chromatogr. A 1216 (2009) 4071.
[12] Y. Finck, N. Aydin, C. Pellaton, G. Gorin, F. Gülaçar, J. Chromatogr. A 1049 (2004) 227.
[13] S. Lee, H.-K. Choib, S.K. Choc, Y.-S. Kim, J. Chromatogr. B 878 (2010) 2983.
[14] A. Kende, Z. Csizmazia, T. Rikker, V. Angyal, K. Torkos, Microchem. J. 84 (2006) 63.
[15] H.R. Norli, A. Christiansen, B. Holen, J. Chromatogr. A 1217 (2010) 2056.
[16] Y. Tikunov, A. Lommen, C.H. Ric de Vos, H.A. Verhoeven, R.J. Bino, R.D. Hall, A.G. Bovy, Plant Physiol. 139 (2005) 1125.
[17] H. Lu, Y. Liang, W.B. Dunn, H. Shen, D.G. Kell, Trends Anal. Chem. 27 (2008) 215.
[18] K.F. Smart, R.B.M. Aggio, J.R. van Houtte, S.G. Villas-Bôas, Nat. Protoc. 5 (2010) 1709.
[19] A. Högnadóttir, R.L. Rouseff, J. Chromatogr. A 998 (2003) 201.
[20] M. Riu-Aumatell, M. Castellari, E. López-Tamames, S. Galassi, S. Buxaderas, Food Chem. 87 (2004) 627.
[21] M.C. González-Mas, J.L. Rambla, M.C. Alamar, A. Gutiérrez, A. Granell, PLoS ONE 6 (2011) e22016.
[22] T. Barboni, F. Luro, N. Chiaramonti, J.-M. Desjobert, A. Muselli, J. Costa, Food Chem. 116 (2009) 382.
[23] T. Sheperd, G. Dobson, S.R. Verrall, S. Conner, D.W. Griffiths, J.W. McNicol, H.V. Davies, D. Steward, Metabolomics 3 (2007) 475.
[24] U. Roessner-Tunali, B. Hegemann, A. Lytovchenko, F. Carrari, C. Bruedigam, D. Granot, A.R. Fernie, Plant Physiol. 133 (2003) 84.
[25] Zs.F. Katona, P. Sass, I. Molnár-Perl, J. Chromatogr. A 847 (1999) 91.
[26] Zs. Füzfai, I. Molnár-Perl, J. Chromatogr. A 1149 (2007) 88.
[27] A.J. Pérez-López, A.A. Carbonell-Barrachina, J. Sci. Food Agric. 86 (2006) 2404.

CAPÍTULO 2

Caracterización del perfil de volátiles y compuestos polares no volátiles de los zumos de naranja (*Citrus sinensis*).

1. **Valencia Late orange juice preserved by pulp reduction and high pressure homogenization: Sensory quality and gas chromatography-mass spectrometry analysis of volatiles**. (2013). *LWT - Food Science and Technology*, 51(2), 476-483. Impact Factor: 2.468.

2. **Evaluation of minimal processing of orange juice by automated data analysis of volatiles and nonvolatile polar compounds determined by gas chromatography coupled to mass spectrometry**. (2014). *International Journal of Food Science and Technology*, 49(6), 1432-1440. Impact Factor: 1.354.

LWT - Food Science and Technology 51 (2013) 476–483

Contents lists available at SciVerse ScienceDirect

LWT - Food Science and Technology

journal homepage: www.elsevier.com/locate/lwt

Valencia Late orange juice preserved by pulp reduction and high pressure homogenization: Sensory quality and gas chromatography–mass spectrometry analysis of volatiles

Manuela Cerdán-Calero, Luís Izquierdo, Enrique Sentandreu*

Instituto de Agroquímica y Tecnología de Alimentos (IATA-CSIC), Avda. Agustín Escardino 7, 46980 Paterna, Valencia, Spain

ARTICLE INFO

Article history:
Received 18 May 2012
Received in revised form
9 November 2012
Accepted 19 November 2012

Keywords:
Orange juice stabilization
High-pressure homogenization
Fresh flavour
GC–MS analysis
AMDIS data processing

ABSTRACT

Low pulp Valencia Late orange juice was obtained by high-pressure homogenization (HPH) at 150 MPa as an alternative to thermal pasteurization processes. Colour and cloudiness were improved through a soft pre-homogenization at 20 MPa applied before centrifugation. Initially and until 0.5 months of refrigerated storage, it was not distinguishable from the fresh juice and was more acceptable than its counterpart pasteurized at 85 °C for 15 s. At 1.5 months onwards of storage (till 3.5 months), acceptability, colour and transmittance of both juices became similar. Moreover, the effects of processing and storage on the aroma profile of juices were evaluated by Gas Chromatography coupled to Mass Spectrometry (GC–MS) analysis with an automated data processing performed by the Automated Mass Spectral Deconvolution and Identification System (AMDIS). There were determined a total of 88 volatiles, following the evolution of 32 aroma descriptors. Compared with the pasteurized sample, the aroma profile of the double homogenized juice was initially closer to fresh juice and presented lower concentrations in off flavour compounds during storage.

1. Introduction

Commercial pasteurized chilled citrus juices are usually obtained by mechanical extraction of the whole fruit, removal of membrane debris and coarse pulp and thermal pasteurization at 90–92 °C for 30–60 s. Since pectinmethylesterase (PME) activity of citrus juices, responsible of their clarification, is by far more thermoresistant than the spoilage microorganisms, these strong pasteurization conditions are needed to reduce PME activity until a residual level compatible with refrigerated storage. As a consequence of thermal pasteurization, a decrease of "freshness" and sensory quality of juice is inevitable, appearing a perceptible "cooked" smell and taste (Berry & Veldhuis, 1997) promoted by the apparition of off flavour compounds.

A way to avoid this loss of freshness is the use of non-thermal processes such as pulsed electric fields (Sentandreu, Carbonell, Rodrigo, & Carbonell, 2006; Walkling-Ribeiro, Noci, Cronin, Lyng, & Morgan, 2009) or high hydrostatic (Katsaros, Tsevdou, Panagiotou, & Taoukis, 2010) and dynamic pressures (high-pressure homogenization, HPH, Donsi, Ferrari, & Maresca, 2010). All these processes minimally affect sensory quality of juices and seem to be effective for their microbial inactivation, but their effectiveness on the reduction of PME activity is reasonably low. Welti-Chanes, Ochoa-Velasco, and Guerrero-Beltrán (2009) achieved a decrease of only 50% in PME activity after a single pass through an HPH system working at 250 MPa meanwhile Lacroix, Fliss, and Makhlouf (2005) reported a decrease of only 20% after three passes through a homogenizer working at 170 MPa. Similarly, Katsaros et al. (2010) achieved a maximum inactivation of 85% in Valencia Late orange juice but under severe static pressure conditions (350 MPa at 35 °C for 2 min).

In a high-pressure homogenizer, suspended particles of juice suffer breakdowns caused by shear forces, impacts and sudden pressure drop. Part of the liberated energy in the homogenizer is consumed to break droplets and solids meanwhile the remaining energy is converted into friction heat, increasing the temperature of the sample. In this line, Belloch, Gurrea, Tárrega, Sampedro, and Carbonell (2012) described how in Valencia Late orange juice, the combined effect of pressure and temperature generated during the HPH treatment achieved an inactivation level higher than 5 log cycles in *Listeria innocua* (working at 110 MPa and 48 °C during 2 s) and in *Lactobacillus plantarum* (working at 150 MPa and 56 °C for 20 s).

Homogenization at 150 MPa increases up to 60–65 °C the temperature of a juice fed to the system at 22–28 °C. A temperature

* Corresponding author. Tel.: +34 963900022; fax: +34 963636301.
E-mail address: elcapi@iata.csic.es (E. Sentandreu).

0023-6438/$ – see front matter © 2012 Elsevier Ltd. All rights reserved.
http://dx.doi.org/10.1016/j.lwt.2012.11.016

of 60 °C (held for 15 s) produced enough microbial inactivation in short life chilled juices (Torres, Bayarri, Sampedro, Martinez, & Carbonell, 2008) without thermal damage, since as pointed out by Sentandreu, Carbonell, Carbonell, and Izquierdo (2005) juices treated at temperatures below 70 °C did not differ in sensory acceptability from the original fresh juice. Nevertheless, heating at 60–65 °C does not induce efficient PME inactivation. Torres et al. (2008) reported that a treatment at 60 °C for 15 s reduced PME activity of a clementine juice around 50% of its initial value, far away the recommended 90% for short life chilled citrus juices (Irwe & Olson, 1994).

But there is an alternative way to reduce PME activity in citrus juices that consists in reducing the pulp content by centrifugation, since PME is cell-wall enzymes associated with pulp (Rouse, 1953). The pulp content reduction caused by centrifugation can lead to juices with less colour and cloudiness, a problem that can be easily avoided by converting part of the suspended pulp into coloidal pulp. This conversion decreases the particle size of pulp and can be achieved through a soft homogenization of the whole juice before centrifugation.

Evidently, technological processes aiming to stabilize orange juices can significantly modify their chemical composition, mainly for heat sensitive compounds and/or those directly linked to the pulp of juices such as volatile constituents. Compositional modifications affect flavour characteristics of the resultant products, having a key role in their acceptability by consumers. However, orange juice has a very complex aroma profile needing the use of high-throughput methodologies of analysis for its study, having Gas Chromatography coupled to Mass Spectrometry (GC–MS) as the traditional election of choice. But in addition to the intricate aroma composition of juices, the high sensitivity of GC–MS systems generates an immense quantity of experimental data that needs to be appropriately processed, with the subsequent consumption of time. To overcome this problem, bioinformatics can help analysts in their task of performing an accurate processing of such quantity of raw data. Ideally, analytical programs should be cheap, easy to use, versatile, fast and able to deconvolute overlapped chromatographic peaks, thus providing reliable qualitative and quantitative results. Currently, the National Institute of Standards and Technology-Automated Mass Spectral Deconvolution and Identification System (NIST-AMDIS) satisfies all these requirements.

Recently, Cerdán-Calero, Sendra, and Sentandreu (2012) demonstrated the utility of AMDIS to determine the aroma profile of freshly squeezed Valencia Late orange juice through Head Space Solid-Phase Microextraction (HS-SPME) and GC–MS analysis. Authors clearly remarked that the reliability of the automated analysis performed by AMDIS strongly depends on the optimization of different settings and conditions of analysis (belonging to AMDIS and the considered platform of analysis). Moreover, it was also concluded that although AMDIS was a very reliable system of analysis, the requested optimization as well as the generation of the customized in-house libraries needed to perform an automated and reliable data processing was tedious, only recommending AMDIS for bulky data analysis.

This research aims to study the residual PME activity, cloudiness, colour, acceptability and aroma composition of a chilled orange juice pre-homogenized at 20 MPa, partially depulped by centrifugation and homogenized at 150 MPa (with an outlet temperature of 65 °C for 15 s). Flavour and physicochemical properties of this juice were evaluated during its refrigerated storage taking as reference two partially depulped juices, one treated in a similar way but without pre-homogenization and the other one pasteurised in a heat exchanger at 85 °C for 15 s. Additionally, reliability of AMDIS to perform multiple data processing was tested, determining the aroma profiles of the assayed juices.

2. Material and methods

2.1. Sample preparation

Valencia Late orange (*Citrus sinesnsis* L. Osb.) fruits were harvested in June 2010 from an orchard located in Lliria (Valencia, Spain). Fruits (400 kg) were washed by immersion in tap water, drained, sized and squeezed in an industrial extractor with finger cups (Exzel, Luzzysa; El Puig, Valencia, Spain). Raw juice (180 L) was sieved in a paddle finisher (Ø 0.4 mm, Luzzysa) giving sample A as shown in Fig. 1 (scheme of operations to obtain the different juices studied). To prepare samples E and F, part of raw juice (100 L) was pre-homogenized with a Manton–Gaulin homogenizer (model 15M8TBA) working at 20 MPa, meanwhile the remaining juice (to prepare sample D) was not. Low pulp juices (LPJs, samples B and C) were obtained using a Westfalia centrifuge (model SAOH 205) fed at 60 L/h, finally blending 75% of centrifuged with 25% of non-centrifuged juice. Sample F was from the pasteurization of sample C using a plate heat-exchanger (model Junior, APV Ibérica S. A., Madrid) fed at 1 L/min in where the juice was heated at 85 °C for 15 s and finally cooled at 7 °C for 10 s. By their hand, samples D and E were from the homogenization at 150 MPa of samples B and C respectively using a GEA Niro-Soavi homogenizer, model NS3015 H with 420 mL of residence volume (GEA Niro Soavi S.p.A. Via da Erba Edoari 29, Parma, Italy). The homogenizer was fed at 100 L/h at 28 °C, reaching an outlet temperature of 65 °C for 15 s during the HPH treatment and finally cooling the juice at 7 °C in the cooling section of the system. Samples D, E and F were aseptically packed in 946 mL glass jars with twist-off cups that were previously sterilized with fluent steam. Delay between extraction and packaging of juices was about 40 min at room temperature (20 °C). Finally, samples were stored at 3 °C and analysed after 0, 0.5, 1.5, 2.5 and 3.5 months of storage.

2.2. Reagents and standards

HPLC gradient grade methanol was from Scharlab (Scharlab S. L., Barcelona, Spain). Analytical grade ethyl nonanoate standard was from Sigma (Sigma–Aldrich Co., St. Louis, MO, USA).

2.3. °Brix, acidity and pH

Total soluble solids were measured as °Brix with a digital refractometer (Pal-1; Atago Co., Ltd., Tokyo, Japan). Total acidity

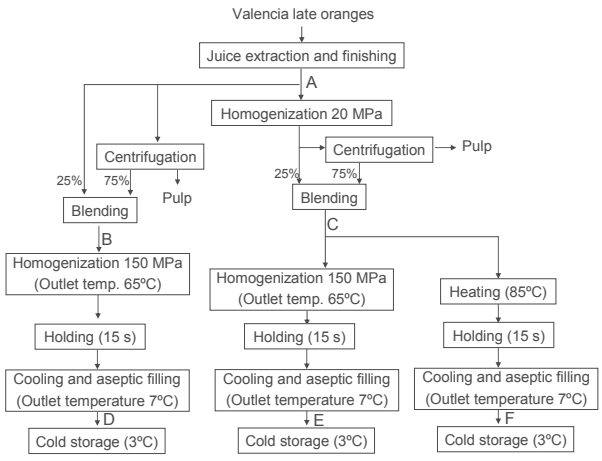

Fig. 1. Diagram of treatments applied to obtain the different Valencia Late orange juices (see Table 1 for nomenclature).

Table 1
Values[a] of suspended pulp, transmittance, PME activity, mean volume diameter and total colour differences of juices assayed (see Fig. 1).

Product	Suspended pulp[c]	Transmittance[d]	PME activity[e]	$D[4,3]$, μm	Total colour difference[b] (ΔE^*)
Fresh juice (A)	12.0 ± 0.5	15.43 ± 0.12	1.720 ± 0.125	478.46 ± 33.77	–
Fresh low pulp juice from non-homogenized juice (B)	4.0 ± 0.3	13.41 ± 0.15	0.412 ± 0.039	–	25.82 ± 0.45
Fresh low pulp juice from pre-homogenized juice (C)	4.5 ± 0.3	9.48 ± 0.25	0.396 ± 0.031	–	7.89 ± 0.69
Sample B homogenized at 150 MPa (D)	3.5 ± 0.2	12.46 ± 0.65	0.084 ± 0.006	49.44 ± 3.99	19.52 ± 0.33
Sample C homogenized at 150 MPa (E)	3.0 ± 0.2	5.11 ± 0.03	0.060 ± 0.005	22.28 ± 0.48	5.20 ± 0.47
Sample C pasteurized at 85 °C − 15 s (F)	3.5 ± 0.3	1.57 ± 0.05	0.014 ± 0.001	81.99 ± 1.31	3.36 ± 0.71

[a] Average of three replicates ± standard deviation.
[b] ΔE^* indicates the magnitude of the colour differences between fresh and treated juices ($P < 0.05$). Values of $\Delta E^* \geq 2$ would indicate a noticeable visual difference (Francis & Clydesdale, 1975).
[c] Expressed as percentage on volume basis (mL pulp/mL sample).
[d] Expressed as the percentage of incident radiation at 650 nm transmitted through the sample (water was used as reference with value of 100%).
[e] Expressed as nkatal/mL.

was assessed by titration with 0.1 N NaOH and expressed as percentage of citric acid meanwhile pH was determined by potentiometric measurement using a Crison GLP 21 pH-meter (Crison Inst. S. A., Barcelona, Spain).

Samples were analysed in triplicate.

2.4. Suspended pulp and cloudiness

A graduated centrifuge tube with a conical bottom was filled with 10 mL of juice, then centrifuged at 370 *g* for 10 min at 22 °C and finally the pulp volume was read. The supernatants were collected, and their transmittance was analysed for cloudiness at 650 nm (Cheng, 2002) in a UV/visible spectrophotometer (Ultrospec 3300 pro; Amersham Bioscience, Piscataway, NJ, USA).

Samples were analysed in triplicate.

2.5. PME activity

It was determined according to Carbonell, Contreras, Carbonell, and Navarro (2006) using a modification of the traditional procedure based on titration of carboxylic groups generated by PME activity during the hydrolysis of a commercial pectin solution (Rouse & Atkins, 1955).

Samples were analysed in triplicate.

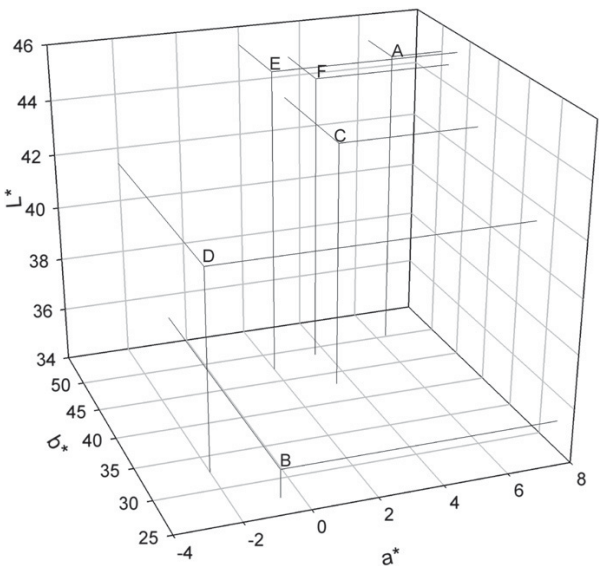

Fig. 2. CIELab* colour parameters of the Valencia Late orange juices (see Table 1 for nomenclature).

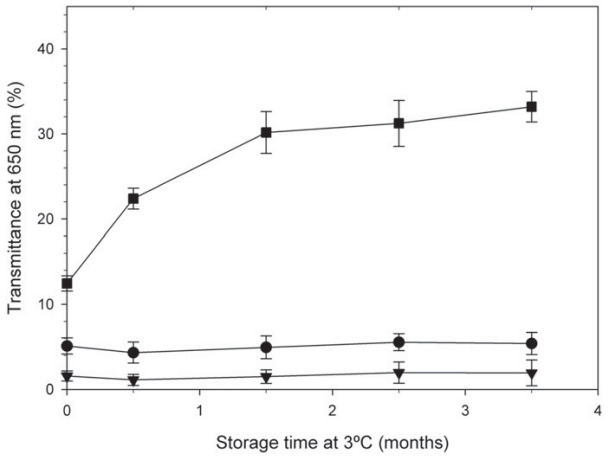

Fig. 3. Evolution of cloudiness of low pulp Valencia Late orange juices during the storage time (see Table 1 for nomenclature): sample D (■), sample E (●) and sample F (▼). Error bars correspond to standard deviations of three replicates.

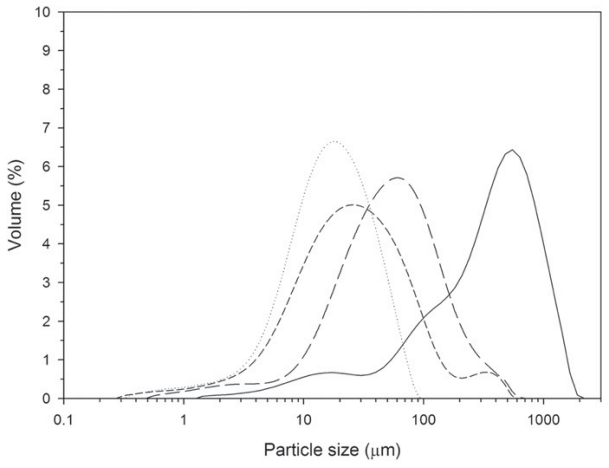

Fig. 4. Particle size distribution of fresh and low pulp Valencia Late orange juices (see Table 1 for nomenclature): sample A (solid line), sample D (short dashed line), sample E (dotted line) and sample F (long dashed line).

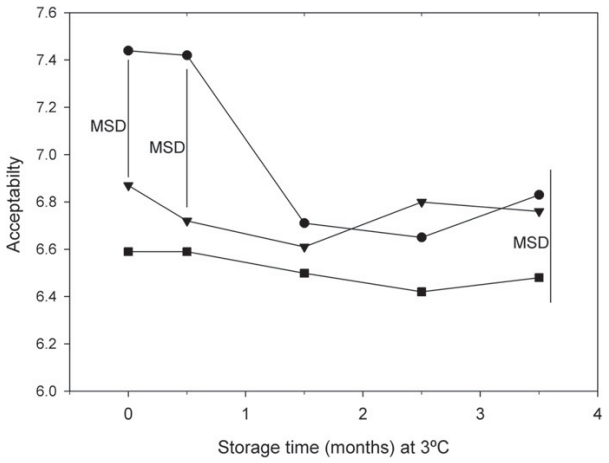

Fig. 5. Mean acceptability scores (average for all assessors) of low pulp Valencia Late orange juices during storage (see Table 1 for nomenclature): sample D (■), sample E (●) and sample F (▼). Minimum significant difference (MSD).

2.6. Colour

It was measured with a Hunter colorimeter (Labscan II model) as described by Bayarri, Calvo, Costell, and Durán (2001). Samples were poured in optical glass cells (3.8 cm high and 6 cm diameter) and results were expressed in a CIELab* system for illuminant D65 and a 10° angle of vision. Recorded parameters were: L^* (brightness), a^* (red–green component) and b^* (yellow–blue component). The total colour differences were calculated as $\Delta E^* = \sqrt{\Delta L^{*2} + \Delta a^{*2} + \Delta b^{*2}}$

Samples were analysed in triplicate.

2.7. Particle size

Particle size distribution was determined using a Malvern Mastersizer 2000 system (Malvern Instruments Limited, Worcestershire, U.K.), with a short wavelength blue light source in conjunction with forward and backscatter detection to enhance sizing performance in the range 0.02–2000 μm. The values 1.73 and 1.33 were used as the refractive indexes of the juice and the dispersant (water) respectively, setting 0.1 for the absorption index of cloud particles (Corredig, Kerr, & Wicker, 2001).

The equivalent volume mean diameter $D[4,3]$ was calculated by the equation

$$D[4,3] = \sum_i n_i d_i^4 / \sum_i n_i d_i^3$$

where n_i is the number of particles with diameter d_i.

Samples were analysed in triplicate.

Table 2
Aroma descriptors monitored from Valencia Late orange juices[a] determined[b] by AMDIS initially and during refrigerated storage.

Compound	Retention time (min)	Ion model (m/z)	Fresh juice[e]	Sample D			
			0 Months	0 Months	0.5 Months	1.5 Months	3.5 Months
1 Z-3-Hexenal	3.96	43	0.993 ± 0.053	1.019 ± 0.208[c]	0.863 ± 0.021[d]	0.842 ± 0.028[d]	0.835 ± 0.048[d]
2 Ethyl butyrate	4.07	88	2.288 ± 0.237	1.757 ± 0.153[c]	1.682 ± 0.048	1.661 ± 0.034	1.680 ± 0.111
3 E–2-Hexenal	5.56	41	0.110 ± 0.011	ND	ND	ND	ND
4 α-Pinene	9.09	91	79.214 ± 0.460	31.536 ± 3.983[c]	27.671 ± 0.541[d]	22.930 ± 2.100[d]	21.731 ± 1.232[d]
5 β-Pinene	11.57	93	8.654 ± 1.077	1.765 ± 0.158[c]	1.643 ± 0.108	1.426 ± 0.012[d]	1.418 ± 0.188[d]
6 β-Myrcene	12.95	93	258.266 ± 26.493	115.771 ± 14.420[c]	170.031 ± 8.917[d]	170.905 ± 8.626[d]	171.198 ± 6.485[d]
7 Octanal	13.79	67	32.379 ± 3.081	26.495 ± 3.381[c]	18.515 ± 0.702[d]	16.534 ± 2.140[d]	15.149 ± 0.209[d]
8 γ-Terpinene	17.92	91	21.239 ± 1.310	11.076 ± 1.480[c]	5.868 ± 0.393[d]	5.795 ± 0.495[d]	4.950 ± 0.618[d]
9 1-Octanol	19.21	55	40.245 ± 0.827	38.125 ± 2.932	35.443 ± 2.504	32.279 ± 1.896[d]	30.498 ± 0.579[d]
10 α-Terpinolene	20.06	93	6.419 ± 0.668	2.741 ± 0.368[c]	2.445 ± 0.094	2.708 ± 0.150	4.351 ± 0.365[d]
11 Linalool	21.55	93	258.050 ± 7.048	320.577 ± 7.496[c]	313.461 ± 11.648	300.334 ± 31.84	295.387 ± 13.536
12 Nonanal	21.76	67	7.512 ± 0.358	6.284 ± 0.856[c]	4.722 ± 0.218[d]	3.738 ± 0.112[d]	3.062 ± 0.415[d]
13 Ethyl 3-hydroxyhexanoate	24.20	77	0.513 ± 0.009	0.489 ± 0.026	0.746 ± 0.021[d]	0.965 ± 0.067[d]	1.296 ± 0.150[d]
14 Citronellal	24.64	79	1.051 ± 0.045	1.337 ± 0.113	2.376 ± 0.185[d]	3.542 ± 0.417[d]	6.612 ± 0.369[d]
15 β-Terpineol	25.06	91	1.324 ± 0.051	1.750 ± 0.210[c]	1.800 ± 0.018	1.947 ± 0.078	2.206 ± 0.263[d]
16 1-Terpinen-4-ol	27.44	71	63.743 ± 3.006	39.206 ± 0.400[c]	41.372 ± 3.746	43.897 ± 1.648[d]	45.218 ± 2.025[d]
17 α-Terpineol	28.75	59	7.258 ± 0.465	9.010 ± 0.488[c]	15.092 ± 1.063[d]	19.281 ± 1.032[d]	29.934 ± 0.578[d]
18 Decanal	31.04	41	21.691 ± 1.218	4.204 ± 0.420[c]	3.354 ± 0.253[d]	2.948 ± 0.212[d]	1.898 ± 0.166[d]
19 cis-Carveol	32.01	109	2.864 ± 0.360	4.299 ± 0.359[c]	5.386 ± 0.331[d]	5.642 ± 0.236[d]	6.571 ± 0.099[d]
20 Nerol	33.46	91	7.241 ± 0.557	9.073 ± 0.226[c]	1.954 ± 0.112[d]	1.553 ± 0.121[d]	0.742 ± 0.014[d]
21 β-Citronellol	34.04	67	12.653 ± 0.445	16.535 ± 0.536[c]	16.290 ± 0.184	15.156 ± 0.753[d]	15.138 ± 0.167[d]
22 Carvone	35.03	54	4.142 ± 0.364	5.626 ± 0.110[c]	6.016 ± 0.610	6.489 ± 0.192[d]	6.998 ± 0.607[d]
23 Neral/cis-citral	35.34	119	4.365 ± 0.251	5.047 ± 0.617[c]	0.658 ± 0.040[d]	0.088 ± 0.010[d]	ND
24 Geraniol	37.64	91	4.040 ± 0.172	4.697 ± 0.194	4.666 ± 0.062	4.832 ± 0.093	5.257 ± 0.405[d]
25 Perillaldehyde	38.86	79	4.406 ± 0.314	6.978 ± 0.080[c]	6.677 ± 0.405	6.441 ± 0.330	6.278 ± 0.540
26 Geranial	39.42	41	7.580 ± 0.441	3.156 ± 0.051[c]	1.410 ± 0.074[d]	0.105 ± 0.008[d]	ND
27 1-Decanol	40.06	41	3.107 ± 0.079	0.887 ± 0.091[c]	0.941 ± 0.051	1.049 ± 0.071[d]	1.107 ± 0.062[d]
28 2,4-Decadienal	44.33	81	1.378 ± 0.094	1.076 ± 0.092[c]	0.313 ± 0.039[d]	0.178 ± 0.021[d]	0.084 ± 0.002[d]
29 Valencene	57.78	105	103.062 ± 4.340	25.930 ± 3.411[c]	32.604 ± 3.257[d]	34.028 ± 1.208[d]	38.303 ± 0.560[d]
30 β-Sinensal	70.69	91	9.476 ± 0.872	5.581 ± 0.358[c]	4.747 ± 0.587[d]	3.435 ± 0.604[d]	3.341 ± 0.121[d]
31 α-Sinensal	73.73	91	1.341 ± 0.153	0.840 ± 0.059[c]	0.594 ± 0.081[d]	0.346 ± 0.022[d]	0.338 ± 0.037[d]
32 Nootkatone	75.81	146	1.442 ± 0.119	1.757 ± 0.035[c]	1.730 ± 0.187	1.718 ± 0.114	1.688 ± 0.110

ND: not detected.
[a] Samples were fresh and processed low pulp juices (see Table 1 for nomenclature).
[b] Relative quantifications are the average of three replicates (mean ± std.dev.) using ethyl nonanoate as internal standard.
[c] Superscript indicates significant ($P < 0.05$) differences between fresh juice with samples D, E and F initially (0 months of storage).
[d] Superscript indicates significant ($P < 0.05$) differences between samples D, E and F during the storage time (0.5, 1.5 and 3.5 months).
[e] Results of fresh Valencia Late orange juice were from Cerdán-Calero et al. (2012).

2.8. Sensory analysis

To check if homogenization at 150 MPa (with its induced temperature of 65 °C for 15 s) affected acceptability of juices, sample E (see Fig. 1) was compared with freshly squeezed juice in a triangle test performed by 45 assessors. To make more similar both samples, the fresh juice was also homogenized at 20 MPa.

To analyse taste stability during storage, samples D, E and F (see Fig. 1) were compared after 0, 0.5, 1.5, 2.5 and 3.5 months of storage at 3 °C. Comparisons were performed in four independent sessions, one for each period of storage. The assessors (which number varied among sessions from 42 to 48) evaluated the acceptability of the three samples according to an unstructured scale from 0 to 10.

All sessions were carried out in a standardised test room (ISO, 2007) meanwhile data acquisition and analysis were performed using Compusense® five release 4.6 (Compusense Inc., Guelph, ON, Canada). Data was analysed by 2-way ANOVA considering the single effects of samples and assessors. Differences between particular samples were analysed by the Newman–Keuls test.

2.9. Sample preparation for the extraction of volatiles by HS-SPME

Samples were prepared as described by Cerdán-Calero et al. (2012). Volatiles were extracted with a 10 mm length fibre coated with 100 μm of polydimethylsiloxane (PDMS) (Sigma–Aldrich Co., St. Louis, MO, USA).

2.10. GC–MS and AMDIS conditions of analysis

The last free available version of the AMDIS program (v. 2.69) was downloaded from NIST™ website (http://chemdata.nist.gov/mass-spc/amdis/).

Gas Chromatography was performed on a ThermoFinnigan (ThermoScientific, San José, CA, USA) Trace GC system equipped with an autosampler. The column used was an HP-5MS (5% phenyl/95% methylpolysiloxane) capillary column, 30 mm × 0.25 mm i.d., 0.25 μm film thickness from Agilent (Agilent Technologies, Palo Alto, CA, USA). MS analysis was performed on a ThermoFinnigan (ThermoScientific, San José, CA, USA) PolarisQ ion trap mass analyser.

Optimized GC–MS and AMDIS settings and conditions of analysis used were from Cerdán-Calero et al. (2012).

Samples were analysed in triplicate and the generated GC–MS raw data files (39, initially and during storage) were simultaneously processed by AMDIS through a "batch job" analysis. Volatiles were relatively quantified using ethyl nonanoate as internal standard.

2.11. Statistical analysis of GC–MS data

Data of concentrations in volatile compounds was studied for each constituent by two-way analysis of variance (ANOVA) considering as factors the type of sample and the storage time. Significance (95% confidence level) of the differences between individual samples was analysed by Tukey's test.

Sample E				Sample F			
0 Months	0.5 Months	1.5 Months	3.5 Months	0 Months	0.5 Months	1.5 Months	3.5 Months
1.013 ± 0.027^{c}	1.109 ± 0.063^{d}	1.008 ± 0.066	0.521 ± 0.025^{d}	1.597 ± 0.150^{c}	1.104 ± 0.040^{d}	1.022 ± 0.029^{d}	0.966 ± 0.074^{d}
1.569 ± 0.041^{c}	1.909 ± 0.143^{d}	1.946 ± 0.246^{d}	2.023 ± 0.071^{d}	2.024 ± 0.303^{c}	2.043 ± 0.128	2.248 ± 0.122	3.047 ± 0.297^{d}
0.112 ± 0.014	ND	ND	ND	0.033 ± 0.005^{c}	ND	ND	ND
58.039 ± 2.949^{c}	52.559 ± 2.678^{d}	50.495 ± 0.975^{d}	49.495 ± 2.235^{d}	63.134 ± 7.553^{c}	57.857 ± 2.792	50.099 ± 1.847^{d}	48.955 ± 4.944^{d}
3.021 ± 0.283^{c}	2.671 ± 0.155	2.257 ± 0.144^{d}	2.081 ± 0.298^{d}	2.878 ± 0.256^{c}	2.868 ± 0.032	2.852 ± 0.211	2.843 ± 0.292
192.127 ± 14.309^{c}	227.629 ± 16.972	237.647 ± 21.632^{d}	265.987 ± 32.981^{d}	190.008 ± 16.854^{c}	247.952 ± 25.327^{d}	264.064 ± 30.853^{d}	278.933 ± 2.502^{d}
21.003 ± 1.294^{c}	19.969 ± 0.536	19.118 ± 0.875^{d}	10.247 ± 0.335^{d}	25.415 ± 2.687^{c}	24.530 ± 2.086	24.011 ± 1.579	20.141 ± 1.955^{d}
12.625 ± 0.657^{c}	12.559 ± 0.484	12.157 ± 0.119	11.229 ± 0.176^{d}	14.148 ± 1.793^{c}	13.659 ± 0.093	12.503 ± 0.453	12.345 ± 0.250^{d}
37.696 ± 4.695	41.904 ± 1.905	42.234 ± 3.669	43.767 ± 1.791	39.392 ± 3.051	44.376 ± 1.722	50.439 ± 4.542^{d}	54.975 ± 5.261^{d}
4.490 ± 0.258^{c}	4.562 ± 0.147	4.873 ± 0.267	5.904 ± 0.314^{d}	5.215 ± 0.470^{c}	6.070 ± 0.244^{d}	6.098 ± 0.324^{d}	6.345 ± 0.219^{d}
277.801 ± 28.484^{c}	301.667 ± 7.578	308.041 ± 27.663	340.728 ± 14.858^{d}	310.172 ± 27.545	364.734 ± 13.216	409.960 ± 25.83^{d}	468.385 ± 43.543^{d}
6.342 ± 0.515	6.039 ± 0.272	3.721 ± 0.105^{d}	1.948 ± 0.136^{d}	7.948 ± 0.622^{c}	6.764 ± 0.638^{d}	5.776 ± 0.055^{d}	2.630 ± 0.287^{d}
0.691 ± 0.028^{c}	0.990 ± 0.043^{d}	1.034 ± 0.092^{d}	1.314 ± 0.065^{d}	0.727 ± 0.091^{c}	0.855 ± 0.087	1.398 ± 0.025^{d}	2.737 ± 0.178^{d}
1.728 ± 0.303^{c}	2.578 ± 0.137^{d}	4.540 ± 0.193^{d}	5.591 ± 0.275^{d}	2.202 ± 0.066^{c}	2.897 ± 0.088	7.091 ± 0.982^{d}	9.917 ± 0.985^{d}
1.953 ± 0.157^{c}	2.035 ± 0.007	2.128 ± 0.096	2.195 ± 0.038^{d}	2.187 ± 0.193^{c}	2.166 ± 0.074	2.296 ± 0.268	2.881 ± 0.195^{d}
65.657 ± 8.422	85.446 ± 3.917^{d}	86.396 ± 2.532^{d}	87.462 ± 3.756^{d}	67.433 ± 4.849	79.636 ± 4.941	100.425 ± 11.92^{d}	122.690 ± 10.473^{d}
10.117 ± 1.440^{c}	14.088 ± 0.699	21.584 ± 3.013^{d}	39.889 ± 2.495^{d}	10.345 ± 0.772^{c}	15.203 ± 0.324	31.430 ± 3.997^{d}	46.096 ± 4.934^{d}
16.228 ± 1.217^{c}	7.029 ± 0.673^{d}	5.859 ± 0.649^{d}	5.458 ± 0.459^{d}	5.563 ± 0.149^{c}	4.798 ± 0.161^{d}	4.213 ± 0.134^{d}	3.247 ± 0.336^{d}
4.601 ± 0.252^{c}	5.105 ± 0.239	6.776 ± 0.602^{d}	8.368 ± 0.210^{d}	5.588 ± 0.629^{c}	7.487 ± 0.173^{d}	9.122 ± 0.741^{d}	9.619 ± 0.269^{d}
8.357 ± 1.123^{c}	10.072 ± 0.407^{d}	8.366 ± 0.374	8.693 ± 0.167	8.856 ± 0.360	10.752 ± 0.418^{d}	12.263 ± 1.349^{d}	14.351 ± 0.226^{d}
15.030 ± 2.338	15.640 ± 0.661	16.128 ± 0.601	17.043 ± 0.686	14.314 ± 0.486^{c}	16.690 ± 0.524^{d}	17.331 ± 0.226^{d}	17.494 ± 0.844^{d}
6.873 ± 0.530^{c}	6.913 ± 0.019	7.243 ± 0.587	8.038 ± 0.387^{d}	7.709 ± 0.358^{c}	11.376 ± 0.836^{d}	11.393 ± 1.215^{d}	15.021 ± 1.405^{d}
3.473 ± 0.357	0.900 ± 0.013^{d}	0.104 ± 0.004^{d}	ND	4.598 ± 0.429^{c}	1.091 ± 0.080^{d}	0.187 ± 0.010^{d}	ND
4.304 ± 0.604	4.462 ± 0.070	4.510 ± 0.209	4.802 ± 0.037	4.648 ± 0.184	5.014 ± 0.295	5.639 ± 0.663^{d}	7.663 ± 0.288^{d}
6.398 ± 0.819^{c}	6.290 ± 0.445	6.054 ± 0.375	5.847 ± 0.245	6.774 ± 0.286^{c}	7.898 ± 0.472	8.187 ± 0.988^{d}	8.900 ± 0.665^{d}
6.599 ± 0.973^{c}	0.832 ± 0.008^{d}	0.138 ± 0.007^{d}	0.078 ± 0.004^{d}	2.451 ± 0.075	0.918 ± 0.022^{d}	0.175 ± 0.014^{d}	ND
3.133 ± 0.500^{c}	3.178 ± 0.034	3.180 ± 0.006	3.187 ± 0.319	1.067 ± 0.020	1.895 ± 0.118^{d}	2.509 ± 0.271^{d}	2.783 ± 0.325^{d}
1.024 ± 0.151^{c}	0.377 ± 0.005^{d}	0.211 ± 0.014^{d}	0.211 ± 0.011^{d}	1.000 ± 0.023^{c}	0.491 ± 0.023^{d}	0.262 ± 0.020^{d}	0.229 ± 0.021^{d}
50.666 ± 3.101^{c}	52.946 ± 2.487	54.954 ± 2.928	86.318 ± 0.531^{d}	46.856 ± 0.688^{c}	48.614 ± 4.999	52.907 ± 2.341	79.461 ± 8.275^{d}
6.799 ± 0.001^{c}	5.687 ± 0.602^{d}	4.685 ± 0.006^{d}	4.585 ± 0.058^{d}	7.613 ± 0.495^{c}	7.411 ± 0.963	6.815 ± 0.576	4.361 ± 0.412^{d}
0.914 ± 0.018	0.625 ± 0.053^{d}	0.543 ± 0.037^{d}	0.540 ± 0.051^{d}	1.187 ± 0.150^{c}	0.860 ± 0.045^{d}	0.737 ± 0.082^{d}	0.436 ± 0.053^{d}
1.177 ± 0.048^{c}	1.079 ± 0.042^{d}	1.078 ± 0.016^{d}	1.057 ± 0.059^{d}	1.937 ± 0.121^{c}	1.955 ± 0.058	1.917 ± 0.119	1.915 ± 0.226

3. Results and discussion

3.1. Physicochemical properties

Fresh Valencia Late orange juice had 14 °Brix and 1.13% of acidity (Brix/Acidity ratio of 12.5) with a pH of 3.50. Table 1 shows some properties of the different juices studied at the stages described in Fig. 1.

The decrease in the observed values of suspended pulp belonging to processed samples in relation with fresh juice (sample A in Table 1) was the consequence of two complementary effects, the removal of pulp by centrifugation (sample B) and the particle size reduction produced by HPH at 150 MPa (samples D and E). In addition, pre-homogenization at 20 MPa also converted part of the suspended pulp into smaller particles, hardly separated by centrifugation, what increased light dispersion, thus lowering transmittance values. This effect was observed before (sample B vs. C) and after (sample D vs. E) the HPH treatment. In any case, transmittance values in all samples were lower than 24%, corresponding to orange juices with an acceptable cloudiness (Cheng, 2002).

On the other hand, PME activity greatly decreased as a result of the pulp content reduction produced by centrifugation and also by the effects of pressure and temperature during the HPH treatment. As shown in Table 1, fresh juice (sample A) had a suspended pulp content of 12%, which was reduced to about 4% in centrifuged samples C and B, decreasing PME activity from 1.72 (sample A) to about 0.4 nkatal/mL (samples B and C). Moreover, the combined effects of pressure at 150 MPa and its inherent heat induction (65 °C for 15 s) led to a second reduction of PME activity, reaching the value of 0.084 nkatal/mL in sample D (from the homogenization of sample B) and to 0.06 nkatal/mL in sample E (from the homogenization of sample C). To estimate the influence of pressure and temperature generated during the HPH treatment on PME activity, 10 L of sample B were just heated at 65 °C for 15 s (in the same plate heat-exchanger described above) giving a residual PME activity (not shown in tables) of 0.19 nkatal/mL (practically 50% of the residual PME activity of B). Thus, we can conclude that the reduction of PME activity promoted by HPH at 150 MPa was equally contributed by pressure and temperature generated during the process.

Sample F was obtained by conventional pasteurization at 85 °C for 15 s presenting maximum cloudiness and minimum residual PME activity. Nevertheless, its flavour properties (discussed below) were not as good as showed by the HPH juice (sample E).

Table 1 contains the total colour differences and Fig. 2 shows the CIELab parameters of assayed juices. In spite of their low pulp content, colour parameters of samples previously pre-homogenized at 20 MPa (C, E. F) were near to those of the original fresh juice (sample A, taken as a reference). Pre-homogenization converts suspended pulp into colloidal pulp, less efficiently removed by centrifugation. Consequently, the low pulp fraction of a pre-homogenized juice is richer in pulp than in its non pre-homogenized counterpart and thus, richer in carotenoids, that are correlated with parameter a^* (Meléndez-Martínez, Gómez-Robledo, Melgosa, Vicario, & Heredia, 2011), explaining the higher value of parameter a^* in samples C, E and F in contrast to samples B and D. Homogenization at 150 MPa increased the L^* parameter and decreased the a^* parameter in all samples (D vs B; E and F vs C), what indicates that HPH increases lightness and reduces redness. The change was more important in sample D, more similar than B to sample A, but still too different.

Fig. 3 shows the changes in transmittance of final juices (D, E and F) during storage. According to Cheng (2002), the scale that is commonly used by citrus industries to evaluate the clarification of an orange juice (expressed as % of light transmission) is: none, 0–24%; slight, 25–35%; definite, 36–60%; extreme, 61–100%. Thus, pre-homogenized juices at 20 MPa (samples E and F) preserved an acceptable cloudiness during the assayed storage period (3.5 months). However, the non pre-homogenized juice (sample D) presented a fast loss of cloudiness, reaching the zone of slight clarification after about 1.5 months of storage.

Fig. 4 shows the size distribution of suspended particles in the original fresh juice (A) and in final juices D, E and F (values of the volume mean diameter weighted of each one are shown in Table 1). As observed, either a soft homogenization (sample F, just pre-homogenized) or a hard homogenization at 150 MPa (sample D) highly decreased the particle size, making both processed samples similar. By its hand, sample E received two homogenization treatments (20 and 150 MPa) presenting a smaller particle size than sample D. Nevertheless, the big differences found for colour (Fig. 2) and cloud stability (Fig. 3) between samples D and E seemed not to be appropriately justified by their different particle size (not too different).

3.2. Sensory analysis

Triangle tests comparing sample E with fresh juice produced 20 correct and 34 non correct responses. The critical value of correct responses for significance of the differences between samples at the 95% confidence level was 25. This indicates that sample E (heated at 65 °C) did not significantly differ from fresh juice homogenized at 20 MPa. Comparable results were obtained by Sentandreu et al. (2005) when demonstrating that heat treatments below 70 °C did not affect fresh taste of citrus juices (reporting a significant decrease of freshness over this temperature).

Fig. 5 shows the mean acceptability (average for all assessors) of juices D, E and F during refrigerated storage and the minimum significant difference (MSD) according to Newman–Keuls test between two consecutive ordered means. This MSD presented slightly different values among evaluations since, as mentioned in the Materials and methods section, ANOVA was independently applied to data corresponding to each period of storage and the error variance varied among independent ANOVA tests (ranging from 1.42 to 2.27). Also, the number of assessors differed among sensory evaluations. As observed in Fig. 5, samples F and D did not significantly differed during storage, whereas sample E was significantly preferred at the beginning of the storage (0 and 0.5 months). However, after 1.5 months onwards samples D, E and F did not show differences in acceptability. This means that the process used to prepare sample E can be interesting to produce very high quality juices, undistinguishable from fresh juices but with a very short shelf life, becoming similar to a pasteurized juice (sample F) in a period between 0.5 and 1.5 months of storage.

3.3. Volatile composition of juices by GC–MS and AMDIS analysis

Automated data processing performed by AMDIS determined 88 volatiles but for simplification purposes, only those compounds (named as target aroma descriptors, listed in Table 2) previously reported as odour active descriptors in orange juice (Arena, Guarrera, Campisi, & Asmundo, 2006; Pérez-Cacho & Rouseff, 2008; Seideneck & Schieberle, 2011; Tonder, Petersen, Poll, & Olsen, 1998) were considered. As we can see in Table 2, the aroma composition of juices mainly changed as a consequence of storage.

To obtain a global picture of the effects that processes and storage have on volatile contents, Principal Component Analysis (PCA) was applied to the concentrations from the 32 targeted aroma descriptors. Fig. 6 shows the joined representation of samples and volatiles (numbered as listed in Table 2) according to the first two axes that, respectively, explained 43.5% and 30.9% of total variability.

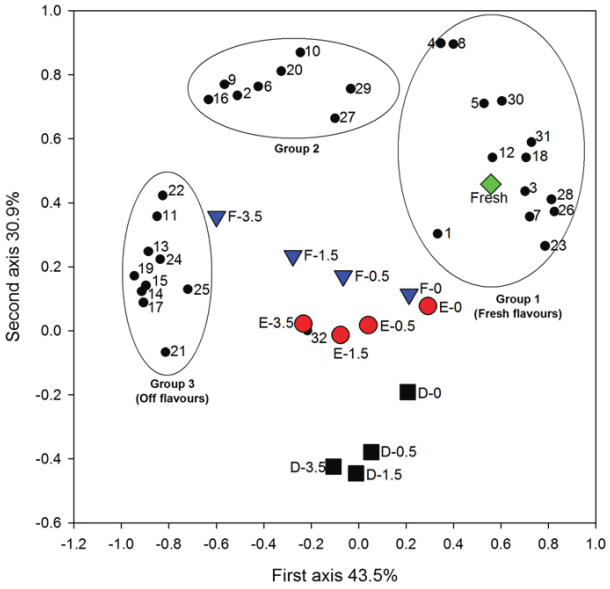

Fig. 6. PCA analysis from the contents of targeted aroma descriptors (numbered as listed in Table 2) determined in Valencia Late orange juices (see Table 1 for nomenclature): sample A (◆), sample D (■), sample E (●) and sample F (▼) stored at 0, 0.5, 1.5 and 3.5 months at 3 °C. Ellipses correspond to the group of characteristic aroma descriptors according to their relation with flavour.

Taking into account that flavour is influenced by the aroma, one could expect to find a correlation between the results showed in Figs. 5 and 6. At initial time of storage, samples E and F were closely represented in Fig. 6, showing maximum proximity to fresh juice and to the group 1 of volatiles (more related to fresh taste), although sample E was slightly closer considering the weight of the first axis. As storage time increased, the scores of both samples in the first axis decreased (but more in the case of the pasteurized sample F), showing a reduction in the concentration of volatiles belonging to group 1 with an increase in the concentration of volatiles belonging to group 2 and specially, to group 3 (where off flavour descriptors were included). This change in the volatile concentrations during storage is in concordance with the loss of acceptability of sample E. Separately, sample D showed a similar trend with storage but its representation in Fig. 6, with maximum distances from all groups of volatiles, indicates that this sample had the poorest aroma, what can be related with its lower scores in acceptability. These results confirm the influence that aroma exerts on acceptability of orange juices. However, further studies regarding the specific role of key aroma descriptors found on acceptability of juices are needed to refine our knowledge.

Assuming that volatiles are intimately linked with pulp, we can conclude that pre-homogenization at 20 MPa before centrifugation helped (by promoting colloidal particles in their pulpy fractions) to preserve the characteristic orange juice aroma of samples E and F.

4. Conclusions

Juices pre-homogenized at 20 MPa, partially depulped by centrifugation and finally homogenized at 150 MPa gave a resultant product with fresh taste, colour, cloudiness and aroma composition close to those of the original fresh juice. These quality properties were preserved for 15 days under refrigerated storage. Pre-homogenization at 20 MPa was necessary to preserve the original colour and cloudiness, not affecting the aroma profile of the resultant juice. This methodology can be easily implanted by citrus industry as an alternative to thermal treatments, resulting specially indicated to obtain short-time chilled orange juices with very high quality.

Moreover, AMDIS analysis provided reliable information with minimum time consumption making possible to correlate the acceptability of fresh, processed and stored orange juices with their volatile composition.

Acknowledgements

Authors thank MICIN (Spanish Government, project AGL 2009-11805ALI) and the JAEdoc and JAE-PREdoc programs (CSIC-FEDER funds) for the financial support for the contracts of E. Sentandreu and M. Cerdán-Calero respectively.

References

AMDIS. (2012). *Automated mass spectral deconvolution and identification system*. Gaithersburg, MD: National Institute of Standards and Technology. http://chemdata.nist.gov/mass-spc/amdis.

Arena, E., Guarrera, N., Campisi, S., & Asmundo, C. N. (2006). Comparison of odour active compounds detected by gas-chromatography-olfactometry between hand-squeezed juices from different orange varieties. *Food Chemistry, 98*(1), 59–63.

Bayarri, S., Calvo, C., Costell, E., & Durán, L. (2001). Influence of color on perception of sweetness and fruit flavour of fruit drinks. *Food Science and Technology International, 7*, 399–404.

Belloch, C., Gurrea, M. C., Tárrega, A., Sampedro, F., & Carbonell, J. V. (2012). Inactivation of microorganisms in orange juice by high pressure homogenization combined with its inherent heating effect. *European Food Research and Technology, 234*, 753–760.

Berry, R. E., & Veldhuis, M. K. (1997). Processing of oranges, grapefruit and tangerines. In S. Nagy, P. E. Shaw, & M. K. Veldhuis (Eds.), *Citrus science and technology, Vol. 2* (pp. 177–252). Connecticut: Avi Publishing Company Inc.

Carbonell, J. V., Contreras, P., Carbonell, L., & Navarro, J. L. (2006). Pectin methylesterase activity in juices from mandarins, oranges and hybrids. *European Food Research and Technology, 222*, 83–87.

Cerdán-Calero, M., Sendra, J. M., & Sentandreu, E. (2012). Gas chromatography coupled to mass spectrometry analysis of volatiles, sugars, organic acids and aminoacids in Valencia Late orange juice and reliability of the automated mass spectral deconvolution and identification system for their automatic identification and quantification. *Journal of Chromatography A, 1241*(8), 84–95.

Cheng, G. (2002). *Procedures for analysis of citrus products* (4th ed.) (pp. 52–53). In Citrus systems Florida: FMC Technologies Inc.

Corredig, M., Kerr, W., & Wicker, L. (2001). Particle size distribution of orange juice cloud after addition of sensitized pectin. *Journal of Agricultural and Food Chemistry, 48*, 4918–4923.

Donsi, G., Ferrari, G., & Maresca, P. (2010). Pasteurization of fruit juices by means of a pulsed high pressure process. *Journal of Food Science, 75*, 169–177.

Francis, F. J., & Clydesdale, F. M. (1975). *Food colorimetry: Theory and applications*. Westport, CT: The AVI Publishing Co., Inc.

Irwe, S., & Olson, I. (1994). Reduction of pectinesterase activity in orange juice by high-pressure treatment. In R. P. Sing, & F. A. R. Oliveira (Eds.), *Minimal processing of foods and process optimization* (pp. 35–42). Florida: CRC Press.

ISO, International Organization for Standardization. (2007). *General guidance for the design of test room*. Standard no 8589. Geneva.

Katsaros, G. I., Tsevdou, M., Panagiotou, T., & Taoukis, P. S. (2010). Kinetic study of high pressure microbial and enzyme inactivation and selection of pasteurisation conditions for Valencia orange juice. *International Journal of Food Science and Technology, 45*, 1119–1129.

Lacroix, N., Fliss, I., & Makhlouf, J. (2005). Inactivation of pectin methylesterase and stabilization of opalescence in orange juice by dynamic high pressure. *Food Research International, 38*, 569–576.

Meléndez-Martínez, A. J., Gómez-Robledo, L., Melgosa, M., Vicario, J. M., & Heredia, F. J. (2011). Color of orange juices in relation to their carotenoid contents as assessed from different spectroscopic data. *Journal of Food Composition and Analysis, 24*, 837–844.

Pérez-Cacho, P., & Rouseff, R. (2008). Fresh squeezed orange juice odor: a review. *Critical Reviews in Food Science and Nutrition, 48*, 681–695.

Rouse, A. H. (1953). Distribution of pectinesterase and total pectin in component parts of citrus fruits. *Food Technology, 7*, 360–362.

Rouse, A. H., & Atkins, C. D. (1955). Pectinesterase and pectin in commercial orange juice as determined by methods used at the citrus experiment station. *Florida Agricultural Experiment Station Bulletin, 570*, 1–19.

Seideneck, R., & Schieberle, P. (2011). Comparison of the key aroma compounds in hand-squeezed and unpasteurised, commercial NFC juices prepared from Brazilian Pera Rio oranges. *European Food Research and Technology, 232*, 995–1005.

Sentandreu, E., Carbonell, L., Carbonell, J. V., & Izquierdo, L. (2005). Effects of heat treatment conditions on fresh taste and on pectinmethylesterase activity of chilled Mandarin and orange juices. *Food Science and Technology International, 11*, 217–222.

Sentandreu, E., Carbonell, L., Rodrigo, D., & Carbonell, J. V. (2006). Pulsed electric fields versus thermal treatment: equivalent processes to obtain equally acceptable citrus juices. *Journal of Food Protection, 69*, 2016–2018.
Tonder, D., Petersen, A., Poll, L., & Olsen, C. (1998). Discrimination between freshly made and stored reconstituted orange juice using GC odour profiling and aroma values. *Food Chemistry, 61*, 223–229.
Torres, E. F., Bayarri, S., Sampedro, F., Martinez, A., & Carbonell, J. V. (2008). Improvement of the fresh taste intensity of processed clementine juice by separate pasteurization of its serum and pulp. *Food Science and Technology International, 14*, 525–529.
Walkling-Ribeiro, M., Noci, F., Cronin, D. A., Lyng, J. G., & Morgan, D. J. (2009). Shelf life and sensory evaluation of orange juice after exposure to thermosonication and pulsed electric fields. *Food and Bioproducts Processing, 87*, 102–107.
Welti-Chanes, J., Ochoa-Velasco, C. E., & Guerrero-Beltrán, J. A. (2009). High-pressure homogenization of orange juice to inactivate pectinmethylesterase. *Innovative Food Science and Emerging Technologies, 10*, 457–462.

International Journal of Food Science & Technology
www.ifst.org
1432 International Journal of Food Science and Technology 2014, **49**, 1432–1440

Original article

Evaluation of minimal processing of orange juice by automated data analysis of volatiles and nonvolatile polar compounds determined by gas chromatography coupled to mass spectrometry

Manuela Cerdán-Calero,[1] Luís Izquierdo[1], John M. Halket[2,3] & Enrique Sentandreu[1]*

1 Instituto de Agroquímica y Tecnología de Alimentos (IATA-CSIC), Avda. Agustín Escardino 7, 46980 Paterna, Valencia, Spain
2 Mass Spectrometry Facility/Drug Control Centre, King's College London, Franklin-Wilkins Building, 150 Stamford Street, London SE1 9NH, UK
3 Specialist Bioanalytical Services Ltd, Egham, Surrey TW20 9LZ, UK

(Received 29 November 2013; Accepted in revised form 11 February 2014)

Summary The effects of minimal processing on the metabolite composition of orange juice were studied. Volatiles and nonvolatile polar compounds in Lane Late orange juices, with different pulp contents, treated by high-pressure homogenisation (HPH) at 150 MPa (at 58, 63 and 68 °C) and stored for 3 months at 3 °C were analysed by gas chromatography coupled to mass spectrometry (GC-MS) with automated data processing. A total of 92 volatiles and 22 polar components (trimethylsilyl, TMS, derivatives of sugars, organic acids and amino acids) were determined in fresh, processed and stored juices. Initially, concentration of fresh flavours (hydrocarbon terpenes and aldehydes) determined in the homogenised samples with the original pulp content was higher than that determined in fresh juice. During storage, desirable descriptors were better preserved in the juice processed at 68 °C with the lowest increase in off-flavours (alcohols and ketones). Generally, operations assayed did not exert a significant influence on polar metabolites, showing no effect on their decrease with time.

Keywords AMDIS, automated data processing, GC-MS analysis, high-pressure homogenisation, metabolite profiling, minimally processed orange juice, pulp reduction.

Introduction

The food industry has the recurrent dilemma of finding balanced solutions to obtain safe and profitable high-quality products. In the particular case of commercial citrus juices, traditional stabilisation processes are based on thermal treatments, thus giving stable products but with their organoleptic properties seriously compromised (Pérez-Cacho & Rouseff, 2008b). High-pressure homogenisation (HPH) is a promising technology proposed inactivating vegetative microorganisms in orange juice (Belloch *et al*., 2012). However, HPH does not warrant a satisfactory inactivation level of pectinmethylesterases (PMEs) (Lacroix *et al*., 2005; Welti-Chanes *et al*., 2009), negatively affecting their cloud stability during storage. Carbonell *et al*. (2013) studied the extension of shelf-life by minimally processing Lane Late orange juices by combining HPH (150 MPa at 58, 63 and 68 °C, single pass) and pulp reduction (50% and 25%). Low-pulp juices (LPJs), even with an initial low residual PME activity (about 10% than that of fresh juice), did not preserve their cloudiness during refrigerated storage (3 months at 3 °C). Furthermore, homogenisation temperatures assayed in this study did not affect the acceptability of HPH-processed juices with no pulp reduction (whole juices, WJs). Treated products were indistinguishable from fresh juice initially and during refrigerated storage. Finally and as a very interesting finding, the whole juice homogenised at 68 °C maintained its cloudiness after 3 months at 3 °C even with a high residual PME activity of around 25%, in contrast to the results from Cerdán-Calero *et al*. (2013) describing how a low-pulp (prehomogenised at 20 MPa before centrifugation) Valencia Late orange juice homogenised at 150 MPa (65 °C) preserved its fresh taste, colour and cloudiness for only 15 days of refrigerated storage. Although sensory and turbidity properties of

*Correspondent: Fax: +34 963636301; e-mail: elcapi@iata.csic.es

doi:10.1111/ijfs.12539

Lane Late orange juices reported by Carbonell *et al.* (2013) were studied in detail, evaluation of the effects propitiated by the assayed processing conditions cannot be considered completed as possible alterations suffered by the metabolite composition of treated samples were not investigated.

Orange juice is a rather complex matrix with an intricate profile of volatiles and nonvolatile polar compounds (Vervoort *et al.*, 2011, 2012). Obviously, the determination of a small quantity of components in a convoluted sample, facilitated by the manual or semi-automatic analysis of the experimental data, can limit the quality of conclusions when studying the effect of processing and storage on foodstuffs. For this reason, Cerdán-Calero *et al.* (2012) proposed an exhaustive metabolite profiling of volatiles and polar compounds (determined as their respective trimethylsilyl, TMS, derivatives) in fresh Valencia Late orange juice by GC–MS analysis combined with automated data processing. This procedure was used in the aforementioned study of Cerdán-Calero *et al.* (2013) to demonstrate how the volatile profile of a twice-HPH-treated and pulp-reduced orange juice was initially closer to fresh juice than when pasteurised at 85 °C for 15 s.

This research aims to evaluate the metabolite profile of minimally processed Lane Late orange juices treated by high-pressure homogenisation at 150 MPa (single pass at 58, 63 and 68 °C, respectively) and then stored at 3 °C for 3 months. To achieve this goal, volatiles and nonvolatile polar compounds (sugars, organic acids and amino acids) of fresh, processed and stored juices were determined by GC–MS analysis with automated data processing.

Materials and methods

Orange juice preparation

Lane Late orange (*Citrus sinensis* L. Osb.) juices assayed were the same as described in the research of Carbonell *et al.* (2013). Briefly, entire and pulp-reduced (50% and 25% of the original pulp content) juices were homogenised (single pass) at 150 MPa at 58, 63 and 68 °C for 15 s. Bottling of juices was in 220 mL filled with no headspace for refrigerated samples but 40 mL for frozen samples with twist-off caps, previously sterilised with steam. Refrigerated samples were kept at 3 °C and evaluated after 0, 1.5 and 3 months of storage. Fresh and processed juice samples were frozen at time 0 and stored at −20 °C until analysed.

Solvents and chemicals

HPLC-gradient-grade methanol was from Scharlab S. L. (Barcelona, Spain) while the analytical grade standards ethyl nonanoate, ribitol, methoxylamine hydrochlorhide (MEOX) and N-methyl-N-(trimethylsilyl)-trifluoroacetamide (MSTFA) were from Sigma–Aldrich Co. (St. Louis, MO, USA).

Total soluble solids, acidity, pH and suspended pulp

Total soluble solids were measured as °Brix using a digital refractometer (Pal-1; Atago Co., Ltd., Tokyo, Japan). Total acidity was determined by titration with 0.1 N NaOH and expressed as% citric acid meanwhile pH was determined at 22 °C using a Crison GLP 21 pH-meter equipped with a temperature compensation sensor.

Suspended pulp was determined following the methodology proposed by Cheng (2002). A graduated centrifuge tube with a conical bottom was filled with 10 mL of juice centrifuged at 22 °C for 10 min at 370 ***g***. Suspended pulp values were estimated by reading the pulp volume after centrifugation and expressing the result as a percentage (mL pulp per mL sample × 100).

Freshly prepared Lane Late orange juice (WJ) had a °Brix to acid ratio of 13.8 and pH 3.74 while the suspended pulp of processed juices with 100%, 50% and 25% of pulp content before the HPH treatment was 8.5%, 4.2% and 2.1%, respectively (Carbonell *et al.*, 2013).

Extraction of volatile compounds and derivatization of nonvolatile polar metabolites

Sample preparation for GC–MS analysis of volatiles and TMS derivatization of sugars, organic acids and amino acids followed the methodologies described by Cerdán-Calero *et al.* (2012). Volatiles were extracted by headspace solid-phase microextraction (HS-SPME) using a 10-mm-long fibre coated with 100 μm of polydimethylsiloxane (PDMS, Sigma–Aldrich Co.). During extraction, 50 μL of a methanolic solution of the internal standard (ethyl nonanoate, 10.24 μg mL^{-1}) were added to samples. Nonvolatile sugars, organic acids and amino acids were converted into their respective TMS derivatives using MEOX and MSTFA reagents, during the extraction procedure 40 μL of a methanolic solution of the internal standard (ribitol, 1 mg mL^{-1}) were added.

GC–MS analysis and automated data processing

Gas chromatography was performed on a Thermo-Finnigan (ThermoScientific, San José, CA, USA) Trace GC system equipped with an autosampler. The column used was a HP-5MS (5% phenyl/95% methylpolysiloxane) capillary column, 30 m × 0.25 mm i.d., 0.25 μm film thickness (Agilent Technologies, Palo Alto, CA, USA). MS analysis was carried out on a

PolarisQ ion trap mass analyzer (ThermoScientific) operating in electron impact mode at 70 eV.

Optimised settings regarding the GC–MS device and the automated data processing analysis of samples (Mass Spectral Deconvolution and Identification System, AMDIS, version 2.71 downloaded from the National Institute of Standards and Technology, NIST, website http://chemdata.nist.gov/mass-spc/amdis/downloads), including the in-house libraries for volatiles and nonvolatile polar compounds, were from Cerdán-Calero *et al*. (2012). Positive assignments were based on the specific retention time and mass spectra recorded in libraries for all detected components (which also contained the ion model selected for each single metabolite listed to perform quantitative analysis).

All samples (fresh and homogenised WJs and LPJs) were analysed in triplicate at 0, 1.5 and 3 months of refrigerated storage, generating a total of 168 chromatographic runs (84 for volatiles and 84 for TMS derivatives) which were automatically processed by AMDIS through a 'batch job' analysis. As explained by Cerdán-Calero *et al*. (2012), absolute quantification of volatiles in juices is rather difficult due to their specific distribution coefficient constants between pulp/serum, serum/head space and head space/fibber are unknown. But the extraction of volatiles with a fibber, and using an appropriate internal standard, leads to have an insight into their relative concentrations in juices, allowing the comparison between samples analysed under the same experimental conditions. So, volatiles were relatively quantified using ethyl nonanoate as internal standard. Absolute quantifications were carried out for TMS derivatives of sugars, organic acids and amino acids through their respective relative response factors using ribitol as internal standard (from Cerdán-Calero *et al*., 2012).

Statistical analysis of GC–MS data

Three-way univariate analysis of variance (ANOVA) was applied to data of volatile and nonvolatile polar constituent contents of processed juices (81 samples, excluding fresh juice) analysing the effects of three single factors (pulp content, storage time and homogenisation temperature) and their double and triple interactions. One-way ANOVA was also applied considering all samples (84, including fresh juice). Error variance was estimated from the three replicates of each sample, and the significance (95% confidence level) of the differences between individual samples was computed according to Tukey's test. Principal component analysis (PCA) was applied to mean concentration values of volatile and of nonvolatile polar compounds to visualise the influence of the pulp content, HPH processes and storage time on their concentration changes.

Results and discussion

Volatiles in Lane Late orange juices

Figure 1 represents the total ion current (TIC) profile obtained by GC–MS analysis of volatiles in Lane Late orange juices studied as identified by AMDIS. A total of 94 volatiles were identified, but only 92 were quantified (Table S1) when excluding the internal standard and limonene. The latter is not considered a direct aroma contributor in orange juice (Pérez-Cacho & Rouseff, 2008a) due to its high odour threshold. However, only thirty-three targeted volatiles, shown in bold in Table S1 and most commonly cited as active odour descriptors for orange juice (Tonder *et al*., 1998; Arena *et al*., 2006; Pérez-Cacho & Rouseff, 2008b; Seideneck & Schieberle, 2011), were considered for further statistical analysis. Volatiles in orange juice can be generally classified as fresh flavours, which are mainly contributed by hydrocarbon terpenes and aldehydes, while alcohols and ketones are generally considered off-flavours. An important exception to this classification is β-myrcene (the second most abundant terpene and considered as a mild-level odorant) that is thought to contribute negatively to processed orange juice aroma (Ahmed *et al*., 1978; Pérez-Cacho & Rouseff, 2008b).

The concentration of the selected thirty-three targeted volatiles was analysed by three-way ANOVA considering as factors the level of pulp content, storage period, HPH temperature and also their interactions (Table 1). All single effects and interactions were significant with the exception of β-pinene (#8) for the double-interaction pulp temperature and temperature time as well as for the triple-interaction pulp temperature time as in the case of α-terpinolene (#17), β-sinensal (#90) and α-sinensal (#91). This is not surprising as experimental results were very precise, leading to detect as significant very small differences. Thus, discussion will be centred in the relative weights of experimental F values more than in their significance. In this sense, it must be noted that F values regarding pulp content and storage time were generally greater and, in most cases, much greater than F values from HPH temperatures. Nevertheless, in the cases of linalool (#19), β-citronellol (#47), geraniol (#51) and 2,4-decadienal (#58) in which the effect of pulp content was relatively low, the effect of temperature was higher. This in general, lower effect of temperature on volatiles was logical as the experimental HPH temperatures differed by 10 °C, whereas the relative differences in pulp content and storage time were larger. Volatile (fresh and off-flavours) concentrations were boosted by increasing the pulp content of juices (Table S1). The effect of storage time on volatiles was as expected results in practically all cases, that is, fresh

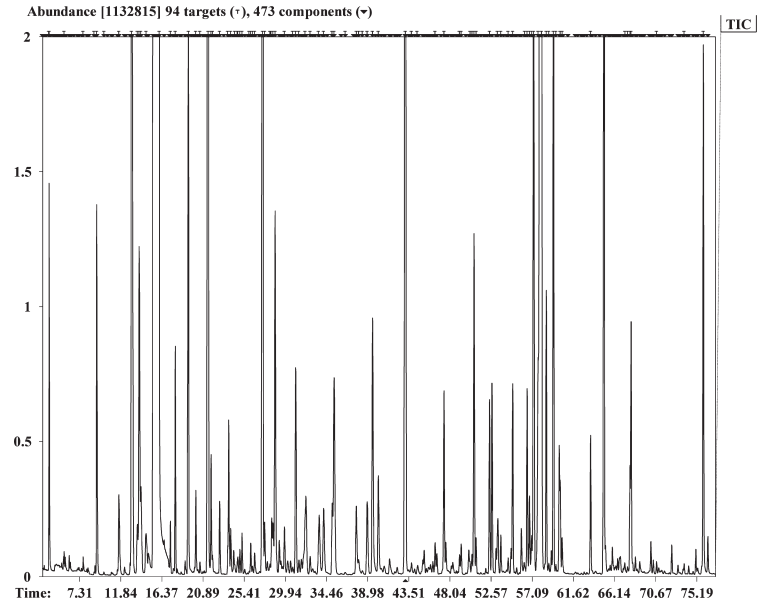

Figure 1 Total ion current (TIC) profile from the GC–MS analysis of volatiles in fresh Lane Late orange juice showed by AMDIS. Positive assignments (from the respective in-house library detailed by Cerdán-Calero *et al.*, 2012) are represented as targets (T) in the chromatogram.

flavour volatiles decreased with time while off-flavours increased during refrigerated storage.

Regarding triple interactions between pulp content, HPH temperature and storage time, they presented smaller F values than those for single effects with some exceptions. For instance, the interaction pulp time determined for 2,4-decadienal (#58) was higher than just corresponding to pulp content (243 vs. 42, see Table 1). Figure 2a can help clarify this finding. The single effect of pulp content was computed pooling together the concentrations (mean values from Table S1) from all storage times at each respective level of pulp, although a detailed representation of concentrations at each time showed significant differences in the behaviour of samples. So, WJs initially presented higher 2,4-decadienal concentrations than LPJs, but they also showed a higher decreasing rate for this analyte during storage.

Octanal (#11) is a clear example of a stronger interaction temperature–time effect than only temperature (F values of 86 vs. 47, respectively, Table 1). Curiously, Fig. 2b shows HPH treatment at 58 °C preserved better, and as expected, this desirable flavour descriptor but its loss was faster when compared to samples treated at higher temperatures. This finding can be explained considering the temperature-dependent inactivation of the enzymatic loading of orange juices, which is involved in chemical reactions causing a loss of the original odour or developments of odours foreign to fresh juice (Pérez-Cacho & Rouseff, 2008a). Finally, the interaction pulp temperature found for β-terpineol (#29) was stronger than for temperature alone (F values of 39 vs. 24, respectively, see Table 1). The effect of pulp content for this off-flavour was high ($F = 846$) as observed in Fig. 2c showing the highest concentrations for WJs. Although the effect of temperature on β-terpineol (#29) was not too important for any level of pulp, WJs presented a clear increase in this compound as HPH temperature increased (most probably as consequence of their higher limonene contents, whose breakdown is temperature favoured as reported by Petersen *et al.* (1998) in stored commercial orange juices).

In this study, PCA was applied to data from targeted volatile compounds considering average concentrations. Figure 3 illustrates the representation of fresh and processed juices with volatiles, numbered as listed in Table S1, according to the first two principle components explaining 45.7% and 31.0% of total variability, respectively. Fresh flavour hydrocarbon terpenes (except β-myrcene, compound #9) and aldehydes clustered around fresh and unstored WJs (actually closer than fresh juice, improving the results from Cerdán-Calero *et al.* (2013) regarding low-pulp HPH orange juices with short shelf-life), clearly suggesting that homogenisation at 150 MPa improved the volatile quality of homogenised samples with the original pulp content. This can be explained by the particle size reduction caused by the HPH treatment (that converted suspended pulp into colloidal pulp as pointed out by Carbonell *et al.*, 2013), thus boosting the surface area of pulp.

Table 1 Summary of ANOVA results on targeted volatile concentrations. Experimental F values from the effects of pulp content (P), storage time (t) and homogenisation temperature (T) and their interactions

		Experimental *F* values								
		Single factors			Double interaction			Triple interaction		
Peak No.[a]	Compound[b]	P	t	T	P-t	P-T	t-T	P-t-T	P[c]	t[c]
1	[F]*Z*-3-Hexenal	3210	822	57	243	104	22	28	I	D
2	[O]Ethyl butyrate	1236	266	232	45	87	35	23	I	I
3	[F]*E*-2 Hexenal	1808	939	135	809	176	71	71	I	D
6	[F]α-Pinene	4192	187	22	59	12	11	7	I	D
8	[F]β-Pinene	2062	798	4	234	1	2	1	I	D
9	[O]Myrcene	1954	116	12	14	4	6	3	I	I
11	[F]Octanal	118	459	47	12	77	86	11	I	D
15	[F]γ-Terpinene	2075	127	14	6	5	9	5	I	D
16	[O]1-Octanol	466	295	184	2	13	19	8	I	I
17	[F]α-Terpinolene	1742	84	25	9	12	10	2	I	D
19	[O]Linalool	30	187	98	5	8	15	3	I	I
20	[F]Nonanal	118	282	43	28	55	23	14	I	D
25	[O]Ethyl 3-hidroxyhexanoate	468	1257	59	21	12	32	5	I	I
27	[O]Citronellal	57	2022	51	12	23	18	5	I	D
29	[O]β-Terpineol	846	38	24	27	39	6	5	I	I
33	[O]1-Terpinen-4-ol	1941	251	197	24	35	27	9	I	I
34	[O]Nonanol	383	219	107	32	5	18	6	I	I
37	[O]α-Terpineol	716	1505	170	161	53	46	18	I	I
42	[F]Decanal	565	369	5	186	27	33	14	I	D
44	[O]*cis*-Carveol	524	401	118	10	19	46	5	I	I
46	[O]Nerol	25	596	17	23	379	57	89	I	I
47	[O]β-Citronellol	39	267	81	19	18	22	6	I	I
48	[O]Carvone	1313	322	67	17	14	11	3	I	I
49	[F]Neral/*cis*-Citral	8	4193	22	8	5	18	5	I	D
51	[O]Geraniol	37	247	172	4	7	15	6	I	I
54	[F]Perillaldehyde	93	48	41	6	28	16	11	I	D
55	[F]Geranial	175	5941	24	238	6	24	6	I	D
56	[O]1-Decanol	265	240	11	60	70	27	10	I	I
58	[F]2,4-Decadienal	42	1707	122	243	4	70	35	I	D
78	[O]Valencene	1462	86	77	6	35	10	4	I	I
90	[F]β-Sinensal	940	94	9	52	2	8	2	I	D
91	[F]α-Sinensal	973	221	9	113	3	6	2	I	D
92	[O]Nootkatone	81	162	26	37	13	9	4	I	I
Critical *F* value ($P = 0.05$)		3.11	3.11	3.11	2.49	2.49	2.49	2.06		

[a]Peak number of targeted volatiles as listed in Table S1.
[b]Superscripts are related to classification of compounds as fresh (F) and off-flavour (O) aroma descriptors.
[c]Effect exerted on volatile concentration by pulp content and storage time assayed (from Table S1): I, increase; D, decrease.

However, HPH did not compensate the negative effect caused by the pulp reduction in the volatiles composition of LPJs. As expected, pulp-reduced juices showed poorer volatile profiles (either for fresh or off-flavours) when compared to fresh and WJs at any storage time studied (see Table S1 and Fig. 3). Figure 3 shows how the content of desirable descriptors decreased while off-flavours increased with time in all samples assayed. However, it has to be remarked that among WJs, the sample homogenised at 68 °C better preserved fresh flavours and showed lower concentrations of undesirable volatiles during storage than its counterparts homogenised at 63 °C and 58 °C (see Fig. 3). This finding is particularly relevant considering previous results from Carbonell *et al.* (2013) regarding the exceptional acceptance and cloudiness preservation showed by this juice during refrigerated storage.

Nonvolatile polar compounds in Lane Late orange juices

The TIC profile (as showed by AMDIS) from the GC–MS analysis of TMS derivatives of sugars, organic acids and amino acids in the assayed Lane

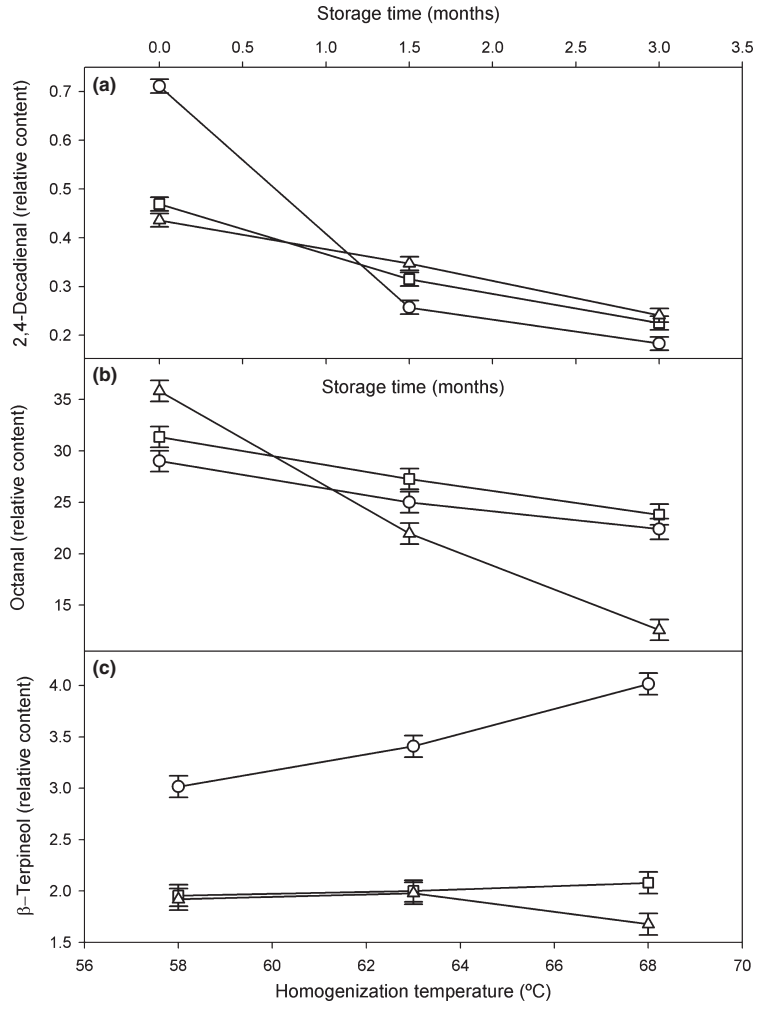

Figure 2 (a) Effect of interaction pulp content storage time on 2,4-decadienal concentration (●, 100% pulp; ■, 50% pulp; ▲, 25% pulp); (b) Effect of interaction homogenisation temperature storage time on octanal concentration (▲, 58 °C; ■, 63 °C; ●, 68 °C); (c) Effect of the interaction pulp content homogenisation temperature on β-terpineol concentration (●, 100% pulp; ■, 50% pulp; ▲, 25% pulp). Concentrations (mean values) are from Table S1.

Late orange juices is represented in Fig. 4 for fresh juice. Including the internal standard and α/β isomers of glucose and fructose, twenty-five compounds were identified out of which twenty-two were quantified (Table S2). As in the case of volatiles, their minimum significant differences are also shown to facilitate the individual comparison as a function of processing and storage time. However, nonvolatile polar compounds (Table S2) were significantly less affected by treatments and storage time when compared to volatiles.

Figure 5 shows quantified TMS derivatives (black dots numbered as listed in Table S2) according to the first two principle components explaining 52.8% and 10.9% of total variability, respectively. So, samples were grouped in accordance with storage time (bounded by vertical dashed lines) due to the low weight of the second latent variable. Moreover, temperatures reached during HPH treatments did not induce noticeable differences within samples with the same pulp content at any tested time. The analysis of the effect of juice processing (0 months of storage) showed that in general, the HPH treatments included in this study did not exert a significant influence on the nonvolatile polar fraction with the exceptions of glutamic acid (#12), asparragine (#13) and raffinose (#22) which decreased significantly (Table S2). The analysis of storage time showed that the concentration of alanine (#1), malic acid (#9), glutamic acid (#12), asparagine (#13) and raffinose (#22) increased noticeably with storage time (Fig. 5).

The changes in the concentration of nonvolatile polar constituents can be explained by the hydrolytic

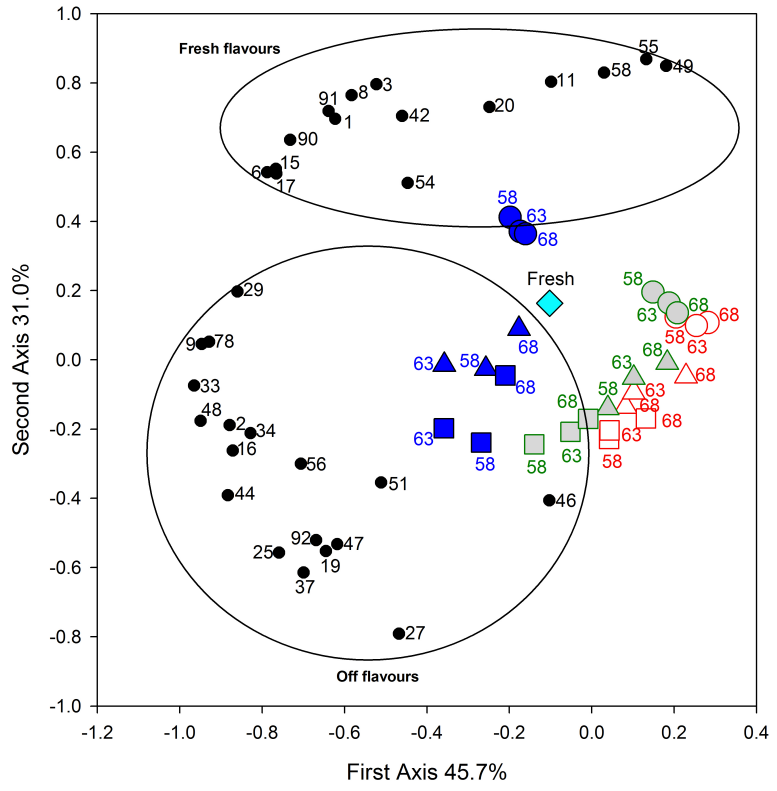

Figure 3 Principal component analysis (PCA) from the contents of targeted aroma descriptors (black dots numbered as listed in Table S1) determined in Lane Late orange juices: fresh (♦); high-pressure homogenised (HPH) juices with 100% of pulp content (solid filled); HPH juices with 50% of pulp content (grey filled); HPH juices with 25% of pulp content (white filled). Storage time at 3 °C is represented as: (●) 0 months, (▲) 1.5 months and (■) 3 months. Temperatures reached (58, 63 and 68 °C for 15 s) during homogenisation at 150 MPa appear beside each sample. Ellipses correspond to the group of characteristic aroma descriptors according to their relation with flavour.

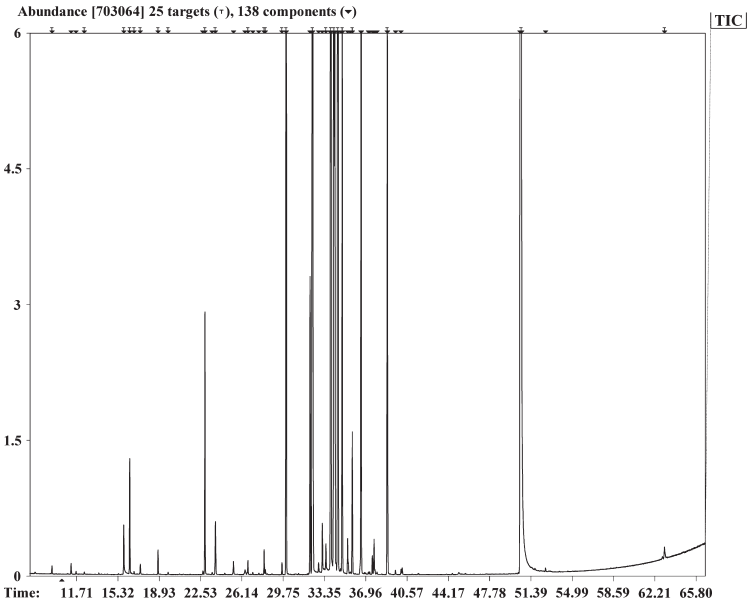

Figure 4 Total ion current (TIC) profile from the GC–MS analysis of trimethylsilyl (TMS) derivatives of sugars, organic acids and amino acids in fresh Lane Late orange juice showed by AMDIS. Positive assignments (from the respective in-house library detailed by Cerdán-Calero *et al.*, 2012) are represented as targets (T) in the chromatogram.

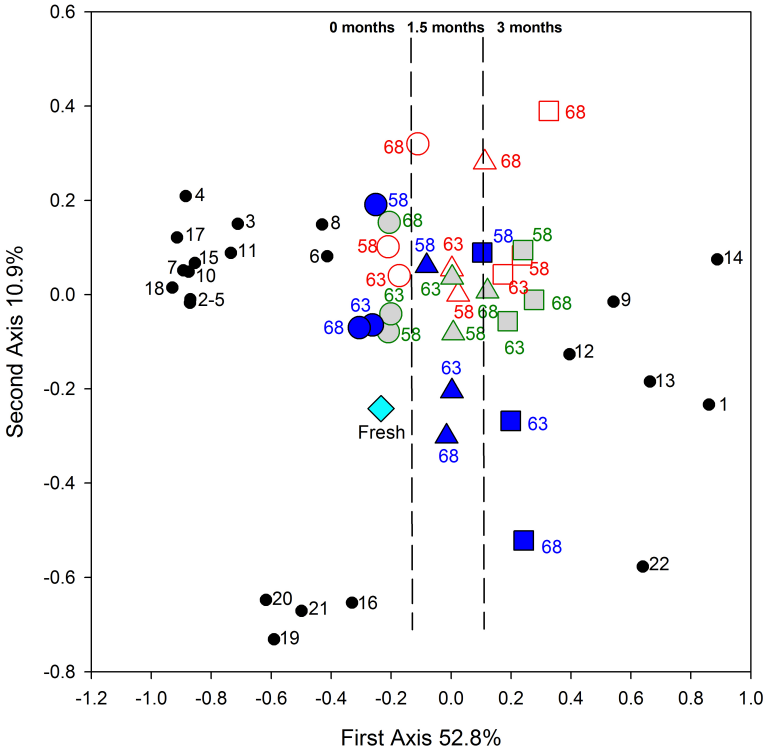

Figure 5 Principal component analysis (PCA) from the contents of trimethylsilyl (TMS) derivatives of sugars, organic acids and amino acids (numbered as listed in Table S2) determined in Lane Late orange juices: fresh (♦); high-pressure homogenised (HPH) juices with 100% of pulp content (solid filled); HPH juices with 50% of pulp content (grey filled); HPH juices with 25% of pulp content (white filled). Storage time at 3 °C is represented as: (●) 0 months, (▲) 1.5 months and (■) 3 months. Temperatures reached (58, 63 and 68 °C for 15 s) during homogenisation at 150 MPa appear beside each sample. Vertical dashed lines represent the group of assayed samples according to their storage times.

and oxidative pathways. Under acidic conditions of orange juice, loss of sucrose by nonenzymatic hydrolysis releasing fructose and glucose has been reported (del Castillo *et al.*, 1998). At the same time, reducing saccharides seemed to be involved in nonenzymatic browning of juices by the formation of carbonyl compounds from the degradation of ascorbic acid, thus theoretically counteracting the rise in monosaccharides induced by the sucrose hydrolysis. This phenomenon is also promoted by organic acids and amino acids (Roig *et al.*, 1999; Shinoda *et al.*, 2004), thus changing their concentration during storage. In any case, the sucrose/fructose/glucose ratio determined in all assayed samples was 2:1.2:0.8 and remained unchanged during storage, in agreement with the 2:1:1 ratio previously described for orange juice (Vervoort *et al.*, 2011).

Finally, putrescine (#14) deserves special attention because it is a resultant product from the breakdown of amino acids. Its content in natural sources is usually regulated by the ripening stage of plants, but it can also be influenced by treatments and storage (Kalac & Krausová, 2005). Just considering treatments, the initial putrescine content (Table S2, 0 months of storage) determined in all homogenised samples (WJs and LPJs) was practically the same as in fresh juice. On the contrary and as expected, putrescine levels increased in all stored samples independently of the processing condition tested.

Conclusions

The methodology used in this study allowed the exhaustive metabolite profiling of orange juice. The abundant and detailed information obtained facilitated the interpretation of the compositional changes observed. The volatile fraction (for both fresh and off-flavours) of pulp-reduced juices was poorer than those with no pulp reduction. Moreover, homogenisation at 150 MPa enhanced fresh flavour concentration in all processed samples, reaching even higher contents in whole juices than in the fresh juice as is. During storage, fresh aroma compounds were better preserved in the whole juice homogenised at 68 °C during storage, also showing the lowest off-flavour concentrations. In general, nonvolatile polar constituents of juices were not influenced by HPH and pulp reduction. In conclusion, the versatility, speed and high-throughput capacity of the methodology of analysis used in this study could contribute to develop innovative processes aimed to produce high-quality products, while facilitating the

detection of quality losses during processing and storage.

Declaration of interest

The authors report no conflicts of interest.

Acknowledgments

This study was supported by MICIN (Spanish Government) project AGL 2009-11805ALI. Authors acknowledge the financial support from Consolider Ingenio Fun-C-Food (CSD2007-00063) and the contract of M. Cerdán-Calero (JAE-PREdoc program, CSIC-FEDER funds). Corresponding author is also indebted with Laura García from Virgin Active (Valencia, Spain) for her motivation and encouragement that greatly helped to maintain eagerness needed to move forward this work.

References

Ahmed, E.M., Dennison, R.A. & Shaw, P.E. (1978). Effect of selected oil and essence volatile components on flavor quality of pumpout orange juice. *Journal of Agricultural and Food Chemistry*, **26**, 368–372.

Arena, E., Guarrera, N., Campisi, S. & Asmundo, C.N. (2006). Comparison of odour active compounds detected by gas-chromatography- olfactometry between hand-squeezed juices from different orange varieties. *Food Chemistry*, **98**, 59–63.

Belloch, C., Gurrea, M.C., Tárrega, A., Sampedro, F. & Carbonell, J.V. (2012). Inactivation of microorganisms in orange juice by high-pressure homogenization combined with its inherent heating effect. *European Food Research and Technology*, **234**, 753–760.

Carbonell, J.V., Navarro, J.L., Izquierdo, L. & Sentandreu, E. (2013). Influence of high pressure homogenization and pulp reduction on residual pectinmethylesterase activity, cloud stability and acceptability of Lane Late orange juice: a study to obtain high quality orange juice with extended shelf life. *Journal of Food Engineering*, **119**, 696–700.

del Castillo, M.D., Corzo, N., Polo, M.C., Pueyo, E. & Olano, A. (1998). Changes in the Amino Acid Composition of Dehydrated Orange Juice during Accelerated Nonenzymatic Browning. *Journal of Agricultural and Food Chemistry*, **46**, 277–280.

Cerdán-Calero, M., Sendra, J.M. & Sentandreu, E. (2012). Gas chromatography coupled to mass spectrometry analysis of volatiles, sugars, organic acids and aminoacids in Valencia Late orange juice and reliability of the Automated Mass Spectral Deconvolution and Identification System for their automatic identification and quantification. *Journal of Chromatography A*, **1241**, 84–95.

Cerdán-Calero, M., Izquierdo, L. & Sentandreu, E. (2013). Valencia Late orange juice preserved by pulp reduction and high pressure homogenization: sensory quality and gas chromatography–mass spectrometry analysis of volatiles. *LWT - Food Science and Technology*, **51**, 476–483.

Cheng, G. (2002). *Procedures for Analysis of Citrus Products*. Citrus Systems Pp. 52–53. Florida: FMC Technologies Inc.

Kalac, P. & Krausová, P.A. (2005). Review of dietary polyamines: formation, implications for growth and health and occurrence in foods. *Food Chemistry*, **90**, 219–230.

Lacroix, N., Fliss, I. & Makhlouf, J. (2005). Inactivation of pectin methylesterase and stabilization of opalescence in orange juice by dynamic high pressure. *Food Research International*, **38**, 569–576.

Pérez-Cacho, P. & Rouseff, R. (2008a). Fresh squeezed orange juice odor: a review. *Critical Reviews in Food Science and Nutrition*, **48**, 681–695.

Pérez-Cacho, P. & Rouseff, R. (2008b). Processing and storage effects on orange juice aroma: a review. *Journal of Agricultural and Food Chemistry*, **56**, 9785–9796.

Petersen, M.A., Tønder, D. & Poll, L. (1998). Comparison of normal and accelerated storage of commercial orange juice—Changes in flavour and content of volatile compounds. *Food Quality and Preference*, **9**, 43–51.

Roig, M., Bello, J., Rivera, Z. & Kennedy, J. (1999). Studies on the occurrence of non-enzymatic browning during storage of citrus juice. *Food Research International*, **32**, 609–619.

Seideneck, R. & Schieberle, P. (2011). Comparison of the key aroma compounds in hand-squeezed and unpasteurised, commercial NFC juices prepared from Brazilian Pera Rio oranges. *European Food Research and Technology*, **232**, 995–1005.

Shinoda, Y., Murata, M., Homma, S. & Komura, H. (2004). Browning and Decomposed Products of Model Orange Juice. *Bioscience, Biotechnology and Biochemistry*, **68**, 529–536.

Tonder, D., Petersen, A., Poll, L. & Olsen, C. (1998). Discrimination between freshly made and stored reconstituted orange juice using GC Odour Profiling and aroma values. *Food Chemistry*, **61**, 223–229.

Vervoort, L., Van der Plancken, I., Grauwet, T. *et al*. (2011). Comparing equivalent thermal, high pressure and pulsed electric field processes for mild pasteurization of orange juice: part II: impact on specific chemical and biochemical quality parameters. *Innovative Food Science and Emerging Technologies*, **12**, 466–477.

Vervoort, L., Grauwet, T., Kebede, B.T. *et al*. (2012). Headspace fingerprinting as an untargeted approach to compare novel and traditional processing technologies: a case-study on orange juice pasteurisation. *Food Chemistry*, **134**, 2303–2312.

Welti-Chanes, J., Ochoa-Velasco, C.E. & Guerrero-Beltrán, J.A. (2009). High-pressure homogenization of orange juice to inactivate pectynmethylesterase. *Innovative Food Science and Emerging Technologies*, **10**, 457–462.

Supporting Information

Additional Supporting Information may be found in the online version of this article:

Table S1. Volatile fraction of fresh, homogenised and stored (3 ºC) Lane Late orange juices determined[a] by GC–MS and AMDIS analysis according to their pulp content.

Table S2. Nonvolatile polar compounds in fresh, homogenised and stored (3 ºC) Lane Late orange juices determined[a] by GC–MS and AMDIS analysis according to their pulp content.

Table S1. Volatile fraction of fresh, homogenized and stored (3 ºC) Lane Late orange juices determined[a] by GC-MS and AMDIS analysis according to their pulp content.

Compound	Retention time (min)	Ion model (*m/z*)	Fresh Juice	100% pulp content									msd
				[b]58ºC			[b]63ºC			[b]68ºC			
				0 months	1.5 months	3 months	0 months	1.5 months	3 months	0 months	1.5 months	3 months	
1 Z-3-Hexanal	**3.96**	**43**	**1.989±0.218**	**2.142±0.064**	**1.520±0.033**	**0.504±0.052**	**2.572±0.319**	**2.484±0.025**	**0.679±0.012**	**2.428±0.164**	**2.212±0.140**	**1.553±0.095**	**0.084**
2 Ethyl butyrate	**4.07**	**88**	**4.471±0.513**	**3.964±0.663**	**7.342±0.716**	**8.653±0.286**	**3.974±0.422**	**7.442±0.652**	**8.385±0.640**	**3.573±0.304**	**3.533±0.091**	**3.416±0.040**	**0.342**
3 E-2-Hexenal	**5.56**	**41**	**0.146±0.014**	**0.282±0.036**	**0.128±0.017**	**0.084±0.003**	**0.142±0.013**	**0.024±0.000**	**0.019±0.002**	**0.325±0.014**	**0.011±0.001**	**0.010±0.001**	**0.009**
4 Heptanal	7.63	43	1.073 0.138	0.590 0.115	0.562 0.018	0.371 0.005	0.693 0.105	0.663 0.012	0.611 0.065	0.628 0.055	0.606 0.021	0.578 0.042	
5 -Thujene	8.83	91	0.336 0.040	0.647 0.038	0.204 0.006	0.136 0.003	0.674 0.081	0.196 0.026	0.142 0.008	0.603 0.016	0.253 0.019	0.124 0.012	
6 α-Pinene	**9.09**	**91**	**42.44±3.04**	**94.09±3.18**	**74.43±3.16**	**59.54±2.45**	**95.30±11.40**	**66.35±3.50**	**56.35±2.66**	**90.79±3.86**	**83.82±6.39**	**77.35±4.55**	**3.24**
7 Sabinene	9.89	93	0.249 0.010	0.501 0.039	0.401 0.047	0.396 0.021	0.510 0.071	0.452 0.025	0.332 0.029	0.509 0.012	0.500 0.055	0.497 0.025	
8 β-Pinene	**11.57**	**93**	**8.416±0.286**	**10.47±0.45**	**4.883±0.299**	**3.993±0.066**	**10.33±1.45**	**4.946±0.418**	**3.755±0.293**	**9.698±0.431**	**4.951±0.441**	**4.078±0.445**	**0.365**
9 β-Mircene	**12.95**	**93**	**153.9±6.7**	**290.2±15.7**	**348.7±21.36**	**366.8±38.6**	**256.4±3.2**	**359.1±19.7**	**387.0±31.4**	**284.1±4.3**	**324.1±37.4**	**329.6±2.5**	**16.3**
10 -Fellandrene	13.59	91	10.39 1.41	16.14 1.11	16.46 0.45	16.58 0.69	9.766 0.567	14.29 1.32	17.91 1.41	10.11 1.07	12.56 0.99	13.58 0.88	
11 Octanal	**13.79**	**67**	**28.29±3.83**	**37.82±3.02**	**22.68±0.68**	**9.310±0.550**	**34.50±2.48**	**31.05±1.31**	**24.02±2.94**	**36.78±1.70**	**30.88±2.77**	**30.13±3.12**	**1.88**
12 3-Carene	13.96	91	11.93 1.14	22.34 1.91	20.16 1.49	16.11 0.92	26.57 2.19	17.85 1.26	14.16 1.64	23.78 1.56	23.78 1.18	22.69 1.04	
13 -Terpinene	14.50	93	5.400 0.409	9.758 0.034	8.463 0.666	8.065 0.523	9.158 0.947	8.219 1.068	6.734 0.816	9.295 0.771	10.22 0.12	10.78 0.37	
14 trans- -Ocimene	17.33	91	4.263 0.109	8.564 0.871	5.718 0.335	5.226 0.334	8.916 0.745	5.283 0.871	4.366 0.028	8.494 0.418	7.642 0.688	7.239 0.492	
15 γ-Terpinene	**17.92**	**91**	**12.85±1.60**	**27.49±2.48**	**22.46±3.06**	**21.32±0.89**	**28.92±2.30**	**23.15±2.64**	**17.48±2.12**	**27.25±0.95**	**25.85±2.70**	**24.75±1.17**	**1.36**
16 1-Octanol	**19.21**	**55**	**103.8±11.6**	**77.23±10.34**	**90.29±7.09**	**103.2±0.8**	**69.30±4.65**	**97.03±6.69**	**105.6±7.7**	**69.26±1.48**	**69.70±0.83**	**74.55±3.55**	**4.93**
17 α-Terpinolene	**20.06**	**93**	**5.273±0.679**	**11.92±1.13**	**8.727±0.998**	**8.698±0.329**	**10.88±1.32**	**9.124±0.919**	**7.318±0.628**	**11.65±0.65**	**11.00±1.08**	**10.63±0.41**	**0.574**
18 6-Camphenone	20.53	93	1.327 0.163	1.463 0.211	2.088 0.138	2.261 0.071	1.291 0.087	2.275 0.133	2.820 0.343	1.305 0.048	1.863 0.084	2.338 0.272	
19 Linalool	**21.55**	**93**	**209.1±26.7**	**159.8±17.4**	**193.3±12.4**	**196.8±2.2**	**149.8±12.9**	**221.1±11.5**	**224.1±22.8**	**151.4±1.1**	**157.2±3.0**	**163.9±20.1**	**11.9**
20 Nonanal	**21.76**	**67**	**7.144±0.524**	**7.695±0.744**	**5.846±0.411**	**2.257±0.163**	**7.534±0.698**	**6.911±0.870**	**4.514±0.361**	**6.154±0.040**	**5.903±0.291**	**5.675±0.551**	**0.401**
21 p-Mentha-1,3,8-triene	21.89	119	0.928 0.102	1.781 0.060	1.811 0.236	1.910 0.054	1.924 0.167	1.940 0.236	1.980 0.166	2.147 0.190	3.087 0.406	3.292 0.274	
22 trans-p-Mentha-2,8-dienol	22.65	91	3.731 0.398	5.805 0.857	7.855 0.583	7.996 0.695	6.397 0.482	9.226 0.808	9.876 0.516	6.322 0.148	7.465 0.776	8.820 0.927	
23 4-Acetyl-1-methyl-1-cyclohexene	23.55	95	1.250 0.177	2.054 0.273	3.480 0.311	3.591 0.236	2.218 0.154	4.650 0.310	4.878 0.174	1.822 0.148	3.122 0.186	3.460 0.436	
24 cis-p-Mentha-2,8-dienol	23.85	91	3.576 0.149	4.224 0.240	5.144 0.306	5.631 0.626	4.484 0.480	5.861 0.512	6.036 0.478	4.569 0.236	4.590 0.033	5.268 0.384	
25 Ethyl 3-hydroxyhexanoate	**24.20**	**77**	**0.677±0.060**	**0.745±0.046**	**1.026±0.104**	**1.127±0.059**	**0.707±0.020**	**1.053±0.055**	**1.249±0.092**	**0.688±0.080**	**0.925±0.102**	**1.249±0.037**	**0.054**
26 Camphor	24.27	95	0.598 0.020	0.653 0.048	0.875 0.027	0.879 0.029	0.469 0.043	0.905 0.064	0.971 0.062	0.542 0.025	0.635 0.057	0.683 0.020	
27 Citronellal	**24.64**	**79**	**0.904±0.095**	**0.941±0.066**	**1.735±0.231**	**2.581±0.059**	**0.866±0.041**	**2.286±0.216**	**3.437±0.229**	**0.910±0.021**	**1.845±0.169**	**3.110±0.358**	**0.168**
28 Eucalyptol	24.88	93	0.918 0.112	1.125 0.166	1.647 0.065	1.898 0.172	0.900 0.122	1.596 0.198	1.842 0.183	0.946 0.064	1.086 0.094	2.001 0.099	
29 β-Terpineol	**25.06**	**91**	**2.343±0.150**	**3.200±0.383**	**3.164±0.307**	**2.682±0.060**	**3.606±0.181**	**3.502±0.033**	**3.117±0.262**	**3.764±0.255**	**4.047±0.266**	**4.230±0.380**	**0.195**
30 3,6-Nonadienal	25.52	67	0.349 0.012	0.618 0.037	0.873 0.065	0.987 0.047	0.725 0.066	1.062 0.110	1.176 0.147	0.879 0.017	1.019 0.111	1.124 0.126	
31 Z-Limonene oxide	26.03	123	1.867 0.063	2.902 0.154	3.226 0.186	3.361 0.098	3.258 0.175	3.701 0.159	3.913 0.264	3.630 0.183	4.620 0.453	4.718 0.261	
32 E-limonene oxide	26.46	91	0.803 0.009	1.161 0.114	1.279 0.118	1.651 0.162	1.229 0.044	1.368 0.070	1.433 0.094	1.119 0.147	1.559 0.111	2.200 0.159	
33 1-Terpinen-4-ol	**27.44**	**71**	**74.23±8.66**	**83.12±3.31**	**127.5±12.0**	**129.8±2.2**	**86.22±8.87**	**147.6±8.5**	**158.2±13.2**	**86.88±2.68**	**88.22±6.52**	**98.02±13.18**	**6.02**
34 Nonanol	**27.61**	**55**	**5.890±0.346**	**5.447±0.728**	**5.498±0.099**	**5.847±0.196**	**4.999±0.335**	**5.358±0.390**	**5.664±0.153**	**4.945±0.170**	**4.965±0.297**	**4.972±0.379**	**0.263**
35 (+)-p-Menth-1-ene	28.10	95	0.265 0.003	0.504 0.068	0.446 0.030	0.228 0.010	0.453 0.047	0.566 0.005	0.572 0.027	0.505 0.064	0.491 0.044	0.454 0.015	
36 Thymol	28.48	135	0.229 0.018	0.973 0.063	0.780 0.017	0.774 0.014	1.196 0.073	0.912 0.040	0.419 0.048	0.962 0.010	0.848 0.073	0.644 0.045	
37 α-Terpineol	**28.75**	**59**	**8.569±1.202**	**8.538±0.941**	**29.93±2.36**	**47.81±0.78**	**8.095±0.853**	**35.43±1.30**	**61.39±2.83**	**8.348±0.465**	**17.40±1.11**	**29.91±2.99**	**1.848**
38 cis-Carvyl acetate	29.73	91	0.347 0.033	5.276 0.594	5.964 0.169	6.168 0.373	4.797 0.310	7.300 0.586	7.594 0.101	5.564 0.248	6.349 0.377	8.099 0.669	
39 Dihydrocarvone	30.04	67	3.414 0.224	1.930 0.017	2.629 0.281	5.357 0.081	2.034 0.212	2.500 0.079	2.860 0.132	2.193 0.082	2.275 0.035	2.481 0.193	
40 Ethyl octanoate	30.53	55	0.868 0.009	1.267 0.118	0.672 0.048	0.495 0.012	1.183 0.101	0.756 0.092	0.504 0.037	1.220 0.085	1.123 0.066	0.939 0.059	
41 Piperitol	30.85	91	1.244 0.109	0.489 0.018	0.755 0.039	0.784 0.041	0.564 0.025	0.881 0.074	1.018 0.131	0.464 0.049	0.744 0.101	1.057 0.076	
42 Decanal	**31.04**	**41**	**5.115±0.626**	**11.19±0.45**	**6.049±0.709**	**4.817±0.343**	**9.505±1.088**	**8.314±0.605**	**6.332±0.819**	**10.44±0.35**	**5.352±0.372**	**3.819±0.197**	**0.442**
43 p-Menth-1-en-9-al	31.60	94	1.102 0.090	0.723 0.032	0.359 0.033	0.292 0.004	0.610 0.069	0.457 0.051	0.260 0.033	0.957 0.124	0.316 0.038	0.141 0.019	
44 cis-Carveol	**32.01**	**109**	**7.986±0.504**	**8.252±0.976**	**12.45±1.54**	**12.97±0.72**	**7.562±0.920**	**15.40±0.57**	**16.18±1.42**	**8.103±0.253**	**9.569±1.157**	**10.12±0.39**	**0.708**

45 L-Carveol	32.54	91	2.021 0.216	1.845 0.250	1.019 0.112	0.460 0.004	1.596 0.145	1.474 0.149	1.419 0.166	1.729 0.077	1.537 0.120	1.494 0.118	
46 Nerol	**33.46**	**91**	**6.115±0.194**	**0.922±0.110**	**0.996±0.115**	**2.840±0.122**	**4.746±0.480**	**4.791±0.065**	**4.810±0.196**	**1.626±0.130**	**5.487±0.469**	**7.068±0.382**	**0.281**
47 β-Citronellol	**34.04**	**67**	**10.53±1.33**	**10.15±1.00**	**10.74±0.20**	**10.97±0.92**	**8.948±0.661**	**11.08±0.09**	**11.25±0.37**	**9.495±0.422**	**9.916±0.410**	**11.16±0.87**	**0.611**
48 Carvone	**35.03**	**54**	**5.130±0.247**	**8.300±0.618**	**12.60±0.93**	**13.23±0.81**	**9.064±1.251**	**15.38±1.58**	**15.94±1.56**	**7.983±0.669**	**11.49±1.09**	**12.01±1.22**	**0.726**
49 Neral/cis-Citral	**35.34**	**119**	**10.19±1.20**	**8.128±1.221**	**0.401±0.017**	**0.069±0.007**	**7.521±0.790**	**0.500±0.046**	**0.109±0.011**	**7.366±0.169**	**0.333±0.019**	**0.032±0.002**	**0.400**
50 Piperitone	36.39	95	0.284 0.039	0.299 0.033	0.216 0.026	0.213 0.015	0.167 0.021	0.215 0.017	0.221 0.012	0.244 0.005	0.203 0.015	0.184 0.012	
51 Geraniol	**37.64**	**91**	**5.755±0.764**	**2.865±0.371**	**3.554±0.235**	**3.930±0.151**	**2.517±0.158**	**3.150±0.101**	**3.413±0.256**	**2.439±0.197**	**2.479±0.325**	**3.488±0.377**	**0.240**
52 Lynalyl acetate	37.96	93	1.503 0.048	2.253 0.225	0.795 0.009	0.124 0.014	1.955 0.186	0.749 0.061	0.299 0.035	2.010 0.248	0.721 0.071	0.464 0.024	
53 E-2-decenal	38.32	41	0.035 0.001	0.015 0.001	ND	ND	0.011 0.000	ND	ND	0.013 0.001	ND	ND	
54 Perillaldehyde	**38.86**	**79**	**6.529±0.660**	**7.122±0.922**	**5.549±0.344**	**4.072±0.042**	**6.541±0.740**	**7.598±0.668**	**7.844±0.136**	**7.027±0.205**	**6.627±0.504**	**6.474±0.717**	**0.468**
55 Geranial	**39.42**	**41**	**8.668±0.583**	**8.428±0.724**	**0.353±0.040**	**0.108±0.003**	**7.189±0.649**	**0.438±0.032**	**0.109±0.010**	**8.054±0.774**	**0.215±0.025**	**0.061±0.002**	**0.305**
56 1-Decanol	**40.06**	**41**	**3.416±0.299**	**4.675±0.243**	**5.129±0.341**	**6.216±0.536**	**4.347±0.106**	**5.383±0.415**	**5.968±0.135**	**4.496±0.367**	**3.323±0.425**	**3.180±0.241**	**0.318**
57 Perilla alcohol	43.65	67	1.107 0.149	1.795 0.104	0.743 0.049	0.429 0.015	1.734 0.157	1.145 0.065	0.521 0.028	1.826 0.122	1.028 0.034	0.710 0.020	
58 2,4-decadienal	**44.33**	**81**	**0.840±0.077**	**0.922±0.051**	**0.262±0.009**	**0.110±0.009**	**0.656±0.056**	**0.245±0.027**	**0.201±0.026**	**0.554±0.041**	**0.263±0.012**	**0.237±0.018**	**0.026**
59 Selinane	46.33	95	2.110 0.306	1.945 0.049	2.891 0.243	3.281 0.256	1.743 0.059	3.034 0.090	3.189 0.153	1.941 0.124	3.718 0.280	3.825 0.109	
60 -Terpenyl acetate	47.32	93	16.86 1.03	28.01 0.81	21.69 0.81	19.33 0.34	24.77 1.92	23.65 0.88	18.00 1.31	26.41 1.44	24.77 0.76	24.09 0.68	
61 Citronellyl acetate	48.22	67	1.531 0.192	2.699 0.057	1.001 0.091	0.438 0.017	2.476 0.233	0.788 0.052	0.561 0.030	2.536 0.108	1.361 0.082	0.849 0.033	
62 -Copaene	49.03	105	1.333 0.154	2.164 0.241	2.440 0.125	2.614 0.103	2.344 0.255	1.452 0.129	1.198 0.131	1.307 0.199	0.886 0.121	0.774 0.054	
63 Neryl acetate	49.22	93	2.107 0.226	4.414 0.191	1.425 0.179	0.488 0.028	3.565 0.227	1.197 0.068	0.737 0.071	3.708 0.122	2.075 0.135	1.209 0.056	
64 -Cubebene	50.40	105	0.873 0.047	1.527 0.112	0.450 0.043	0.436 0.023	1.546 0.210	0.344 0.014	0.141 0.008	1.028 0.121	0.397 0.048	0.233 0.007	
65 -Elemene	50.63	93	15.71 0.76	16.63 2.04	14.66 1.15	10.86 0.73	17.05 1.00	13.38 0.72	10.34 0.46	13.37 0.89	8.931 0.813	7.587 0.084	
66 Camphene	50.86	41	0.591 0.004	0.992 0.056	0.283 0.022	0.124 0.011	0.865 0.083	0.359 0.023	0.158 0.018	1.012 0.093	0.281 0.017	0.148 0.020	
67 -Caryophyllene	52.45	91	11.90 0.75	14.41 1.05	14.66 1.47	12.91 1.23	14.43 1.21	11.46 0.58	10.02 0.70	10.56 0.90	8.603 1.203	10.17 0.38	
68 Geranyl acetate	52.62	41	1.162 0.015	1.542 0.107	4.447 0.273	1.598 0.152	1.511 0.101	4.905 0.066	1.640 0.109	1.605 0.110	4.630 0.081	2.502 0.154	
69 Longifolene-(V4)	53.18	105	2.626 0.072	3.772 0.165	4.149 0.577	6.037 0.563	3.593 0.396	2.853 0.244	2.247 0.043	2.865 0.346	2.809 0.080	2.776 0.126	
70 -Ionone	53.68	121	3.258 0.437	4.802 0.299	4.707 0.549	4.486 0.123	4.342 0.206	4.057 0.101	3.847 0.282	4.427 0.148	5.446 0.078	5.642 0.544	
71 p-Menth-1-en-9-ol	54.39	91	1.265 0.126	1.636 0.084	0.506 0.026	0.302 0.006	1.493 0.117	0.581 0.016	0.297 0.029	1.466 0.188	0.623 0.049	0.455 0.032	
72 -Caryophyllene	54.88	93	8.261 0.560	9.454 0.902	10.32 0.98	11.93 1.57	9.505 0.973	8.506 0.292	7.532 0.421	6.995 0.565	6.335 0.252	6.073 0.607	
73 (Z)- -Guaiene	56.11	120	0.122 0.011	0.156 0.016	0.370 0.023	0.391 0.013	0.181 0.006	0.156 0.010	0.108 0.008	0.115 0.014	0.105 0.002	0.121 0.010	
74 -Selinane	56.48	107	6.508 0.315	7.591 0.754	7.876 0.473	10.94 0.68	7.537 0.996	7.323 0.453	6.932 0.351	5.442 0.472	5.996 0.432	6.160 0.339	
75 Viridiflorene	56.71	133	3.130 0.014	3.473 0.400	5.375 0.269	9.106 0.119	3.614 0.477	4.724 0.290	4.756 0.054	2.573 0.261	2.989 0.273	4.752 0.235	
76 Germacrene D	56.93	105	1.869 0.134	2.923 0.182	2.351 0.192	2.290 0.115	2.491 0.200	1.987 0.036	1.640 0.122	1.891 0.179	1.629 0.079	1.508 0.070	
77 -Gurjunene	57.27	189	19.87 0.99	17.48 12.61	41.82 3.60	46.34 2.97	26.15 3.09	32.21 3.94	37.89 1.43	19.20 1.84	27.78 2.25	35.47 2.38	
78 Valencene	**57.78**	**105**	**606.3±2.5**	**711.7±87.6**	**874.1±118.6**	**1040.0±59.8**	**701.2±70.8**	**777.8±46.9**	**781.8±17.9**	**536.3±51.0**	**586.4±12.3**	**683.6±44.0**	**43.3**
79 -Muurolene	58.54	105	11.20 0.83	13.50 0.87	15.02 2.08	21.04 2.34	12.41 1.05	13.54 0.99	13.56 0.29	9.956 0.494	10.80 0.05	11.87 0.86	
80 -Guaiene	58.79	107	0.227 0.020	0.268 0.022	0.274 0.007	0.365 0.031	0.258 0.030	0.178 0.012	0.163 0.005	0.169 0.018	0.104 0.005	0.094 0.012	
81 Selina-3,7(11)-diene	59.39	105	32.24 1.30	35.91 4.22	45.01 6.24	55.94 3.63	35.74 3.59	40.85 1.85	43.08 1.45	27.26 1.88	27.43 3.37	36.33 0.79	
82 -Farnesene	59.61	91	0.441 0.039	0.538 0.033	0.545 0.020	0.675 0.025	0.568 0.073	0.302 0.022	0.288 0.004	0.309 0.015	0.211 0.013	0.203 0.026	
83 Cadinene	60.08	119	5.042 0.453	7.010 0.879	8.872 0.230	12.16 1.25	7.750 0.468	8.084 0.491	8.463 0.474	5.031 0.498	5.402 0.117	7.231 0.491	
84 Germacrene B	60.24	41	0.123 0.014	0.218 0.009	0.232 0.013	0.298 0.016	0.180 0.002	0.238 0.016	0.255 0.013	0.164 0.017	0.152 0.009	0.112 0.008	
85 Caryophyllene oxidade	63.41	79	4.141 0.458	5.323 0.453	4.295 0.253	3.142 0.100	5.076 0.310	4.954 0.560	2.938 0.116	4.933 0.133	4.682 0.472	3.606 0.265	
86 -Guaiene	67.19	105	0.278 0.016	0.493 0.034	0.933 0.121	0.992 0.129	0.541 0.072	1.103 0.138	1.168 0.073	0.447 0.018	0.859 0.009	1.138 0.129	
87 y-Eudesmol	67.45	105	0.170 0.019	0.153 0.015	0.136 0.017	0.121 0.013	0.165 0.019	0.160 0.003	0.150 0.009	0.161 0.009	0.139 0.013	0.135 0.011	
88 y-Selinane	67.99	189	1.961 0.220	2.353 0.199	5.647 0.091	6.453 0.070	2.216 0.279	6.295 0.850	6.965 0.019	2.012 0.123	5.677 0.425	6.602 0.535	
89 y-Gurjunene	68.35	161	5.228 0.396	7.186 0.783	12.35 0.41	13.68 0.48	7.705 0.939	12.40 0.60	15.24 0.92	7.325 0.317	12.72 0.65	12.94 0.67	
90 β-Sinensal	**70.69**	**91**	**0.717±0.002**	**0.979±0.111**	**0.710±0.044**	**0.540±0.026**	**0.998±0.109**	**0.761±0.083**	**0.648±0.042**	**0.954±0.061**	**0.818±0.070**	**0.635±0.056**	**0.050**
91 α-Sinensal	**73.73**	**91**	**0.678±0.061**	**0.840±0.110**	**0.461±0.045**	**0.326±0.015**	**0.857±0.103**	**0.520±0.046**	**0.445±0.028**	**0.784±0.053**	**0.552±0.064**	**0.421±0.034**	**0.040**
92 Nootkatone	**75.81**	**146**	**19.89±2.68**	**15.43±2.22**	**22.36±0.68**	**23.56±1.69**	**14.57±1.60**	**30.12±3.36**	**30.39±0.88**	**14.64±0.25**	**21.64±0.23**	**24.74±3.01**	**1.64**

Table S1 (continued)

Compound	Retention time (min)	Ion model (*m/z*)	Fresh Juice	50% pulp content									Msd
				[b]58°C			[b]63°C			[b]68°C			
				0 months	1.5 months	3 months	0 months	1.5 months	3 months	0 months	1.5 months	3 months	
1 Z-3-Hexanal	**3.96**	**43**	**1.989±0.218**	**0.820±0.011**	**0.498±0.012**	**0.360±0.015**	**0.757±0.099**	**0.387±0.008**	**0.325±0.014**	**0.677±0.046**	**0.491±0.019**	**0.328±0.038**	**0.084**
2 Ethyl butyrate	**4.07**	**88**	**4.471±0.513**	**2.115±0.221**	**2.743±0.270**	**3.420±0.257**	**2.123±0.212**	**2.406±0.263**	**3.266±0.323**	**1.679±0.175**	**1.812±0.052**	**2.729±0.255**	**0.342**
3 E-2-Hexenal	**5.56**	**41**	**0.146±0.014**	**0.023±0.001**	**0.015±0.000**	**0.014±0.001**	**0.021±0.001**	**0.016±0.001**	**0.016±0.002**	**0.019±0.001**	**0.017±0.002**	**0.017±0.001**	**0.009**
4 Heptanal	7.63	43	1.073 0.138	0.391 0.047	0.372 0.051	0.490 0.002	0.414 0.012	0.595 0.027	0.621 0.072	0.411 0.011	0.456 0.007	0.470 0.008	
5 -Thujene	8.83	91	0.336 0.040	0.200 0.020	0.064 0.004	0.038 0.001	0.184 0.023	0.045 0.001	0.022 0.001	0.186 0.003	0.051 0.003	0.021 0.001	
6 α-Pinene	**9.09**	**91**	**42.44±3.04**	**32.05±2.13**	**25.89±0.12**	**21.23±0.99**	**29.06±1.62**	**23.74±1.04**	**22.40±1.57**	**29.58±1.73**	**28.03±1.20**	**24.29±1.67**	**3.24**
7 Sabinene	9.89	93	0.249 0.010	0.198 0.016	0.181 0.010	0.152 0.006	0.208 0.003	0.207 0.009	0.168 0.010	0.151 0.005	0.185 0.007	0.185 0.007	
8 β-Pinene	**11.57**	**93**	**8.416±0.286**	**3.660±0.126**	**1.815±0.213**	**1.748±0.186**	**3.103±0.179**	**1.712±0.135**	**1.617±0.209**	**3.152±0.048**	**1.849±0.119**	**1.779±0.093**	**0.365**
9 β-Mircene	**12.95**	**93**	**153.9±6.7**	**138.9±9.0**	**145.1±1.9**	**157.2±20.7**	**123.8±8.2**	**143.3±3.8**	**178.0±19.1**	**128.4±14.9**	**131.2±1.2**	**183.9±4.1**	**16.3**
10 -Fellandrene	13.59	91	10.39 1.41	8.435 0.151	8.962 1.318	11.13 0.33	8.529 0.219	8.543 1.010	11.73 1.19	5.792 0.547	5.938 0.122	10.076 1.356	
11 Octanal	**13.79**	**67**	**28.29±3.83**	**36.81±1.38**	**16.66±0.33**	**12.16±1.63**	**33.76±2.40**	**26.78±1.88**	**25.40±2.13**	**27.66±2.42**	**26.66±2.84**	**24.77±0.58**	**1.88**
12 3-Carene	13.96	91	11.93 1.14	9.724 0.465	7.427 0.247	6.391 0.133	8.949 0.668	7.703 0.263	7.495 0.808	8.761 0.192	8.791 0.238	8.011 0.660	
13 -Terpinene	14.50	93	5.400 0.409	5.672 0.544	3.258 0.252	3.027 0.173	4.970 0.340	3.184 0.102	3.022 0.022	5.300 0.439	4.255 0.104	3.611 0.233	
14 trans- -Ocimene	17.33	91	4.263 0.109	3.219 0.223	2.069 0.136	1.813 0.221	2.933 0.331	2.481 0.212	2.139 0.223	2.832 0.169	2.652 0.214	2.132 0.243	
15 γ-Terpinene	**17.92**	**91**	**12.85±1.60**	**12.65±1.06**	**7.706±0.430**	**6.639±0.563**	**11.11±0.92**	**7.677±0.238**	**7.057±0.297**	**11.26±0.75**	**10.29±0.63**	**8.904±1.201**	**1.36**
16 1-Octanol	**19.21**	**55**	**103.8±11.6**	**46.85±1.61**	**83.68±7.40**	**85.30±3.19**	**43.12±5.52**	**51.26±1.70**	**69.08±5.97**	**40.47±2.51**	**48.72±1.87**	**63.45±7.32**	**4.93**
17 α-Terpinolene	**20.06**	**93**	**5.273±0.679**	**5.366±0.441**	**3.498±0.344**	**3.229±0.263**	**4.769±0.402**	**3.572±0.016**	**3.514±0.112**	**4.781±0.299**	**4.669±0.305**	**4.255±0.743**	**0.574**
18 6-Camphenone	20.53	93	1.327 0.163	1.283 0.065	1.646 0.068	2.458 0.267	0.963 0.076	1.598 0.158	2.838 0.145	0.883 0.048	1.126 0.099	2.363 0.272	
19 Linalool	**21.55**	**93**	**209.1±26.7**	**151.2±1.5**	**195.3±15.56**	**201.0±10.3**	**129.3±12.4**	**151.9±8.1**	**207.5±21.1**	**122.9±2.21**	**138.5±2.3**	**168.0±10.84**	**11.9**
20 Nonanal	**21.76**	**67**	**7.144±0.524**	**6.529±0.575**	**5.205±0.506**	**5.142±0.309**	**5.061±0.494**	**4.915±0.180**	**4.598±0.276**	**3.634±0.257**	**3.418±0.204**	**2.691±0.095**	**0.401**
21 p-Mentha-1,3,8-triene	21.89	119	0.928 0.102	1.781 0.084	1.904 0.233	2.121 0.042	1.831 0.038	1.861 0.152	2.798 0.199	1.856 0.142	2.227 0.232	2.732 0.213	
22 trans-p-Mentha-2,8-dienol	22.65	91	3.731 0.398	3.249 0.156	5.324 0.706	6.792 0.311	3.442 0.344	4.166 0.251	7.574 0.157	3.251 0.319	3.269 0.229	5.435 0.751	
23 4-Acetyl-1-methyl-1-cyclohexene	23.55	95	1.250 0.177	0.815 0.024	1.203 0.134	1.258 0.161	0.842 0.069	0.988 0.084	1.343 0.137	0.843 0.100	0.861 0.043	1.205 0.127	
24 cis-p-Mentha-2,8-dienol	23.85	91	3.576 0.149	2.728 0.125	3.509 0.350	3.871 0.371	2.612 0.253	2.807 0.167	4.532 0.170	2.545 0.258	2.857 0.301	3.939 0.495	
25 Ethyl 3-hydroxyhexanoate	**24.20**	**77**	**0.677±0.060**	**0.405±0.041**	**0.777±0.091**	**1.097±0.069**	**0.382±0.009**	**0.673±0.043**	**1.179±0.062**	**0.367±0.020**	**0.405±0.051**	**0.941±0.036**	**0.054**
26 Camphor	24.27	95	0.598 0.020	0.532 0.043	0.714 0.063	0.872 0.058	0.508 0.020	0.629 0.031	0.966 0.047	0.439 0.031	0.594 0.007	0.806 0.024	
27 Citronellal	**24.64**	**79**	**0.904±0.095**	**0.583±0.009**	**1.981±0.225**	**3.361±0.094**	**0.513±0.022**	**1.658±0.144**	**3.433±0.271**	**0.495±0.004**	**1.058±0.135**	**2.783±0.175**	**0.168**
28 Eucalyptol	24.88	93	0.918 0.112	0.414 0.042	0.865 0.084	1.253 0.178	0.422 0.042	0.616 0.051	1.075 0.139	0.363 0.045	0.546 0.007	1.180 0.080	
29 β-Terpineol	**25.06**	**91**	**2.343±0.150**	**1.735±0.140**	**1.917±0.164**	**2.214±0.161**	**1.965±0.047**	**2.024±0.133**	**2.352±0.230**	**1.805±0.230**	**1.882±0.082**	**2.556±0.262**	**0.195**
30 3,6-Nonadienal	25.52	67	0.349 0.012	0.435 0.038	0.738 0.057	1.077 0.022	0.618 0.062	0.755 0.008	1.162 0.121	0.659 0.079	0.680 0.031	1.148 0.122	
31 Z-Limonene oxide	26.03	123	1.867 0.063	1.845 0.184	2.094 0.210	2.179 0.291	1.972 0.106	2.154 0.051	2.663 0.174	1.903 0.164	1.903 0.124	2.937 0.159	
32 E-limonene oxide	26.46	91	0.803 0.009	0.511 0.053	0.751 0.064	1.161 0.069	0.465 0.044	0.641 0.029	1.068 0.135	0.414 0.009	0.641 0.078	1.280 0.137	
33 1-Terpinen-4-ol	**27.44**	**71**	**74.23±8.66**	**32.67±3.29**	**52.45±7.39**	**60.75±2.93**	**31.22±2.65**	**42.03±2.31**	**59.59±6.62**	**28.93±2.72**	**30.17±2.90**	**50.19±5.10**	**6.02**
34 Nonanol	**27.61**	**55**	**5.890±0.346**	**3.571±0.305**	**5.538±0.270**	**5.776±0.242**	**3.493±0.098**	**5.077±0.037**	**5.313±0.140**	**3.287±0.116**	**3.432±0.131**	**4.895±0.330**	**0.263**
35 (+)-p-Menth-1-ene	28.10	95	0.265 0.003	0.201 0.013	0.244 0.018	0.206 0.011	0.197 0.001	0.194 0.021	0.210 0.025	0.183 0.007	0.184 0.016	0.216 0.020	
36 Thymol	28.48	135	0.229 0.018	0.459 0.025	0.473 0.024	0.481 0.014	0.510 0.047	0.557 0.058	0.560 0.032	0.614 0.035	0.892 0.026	0.946 0.010	
37 α-Terpineol	**28.75**	**59**	**8.569±1.202**	**6.992±0.226**	**17.01±1.79**	**22.91±2.48**	**6.600±0.747**	**12.03±0.24**	**23.43±2.56**	**6.100±0.800**	**9.525±0.333**	**19.11±2.55**	**1.848**
38 cis-Carvyl acetate	29.73	91	0.347 0.033	3.035 0.184	5.267 0.635	5.473 0.644	3.284 0.231	3.796 0.165	6.160 0.782	3.296 0.364	3.306 0.347	6.587 0.511	
39 Dihydrocarvone	30.04	67	3.414 0.224	1.211 0.082	2.049 0.111	2.232 0.061	1.497 0.089	1.542 0.023	2.175 0.170	1.284 0.288	1.717 0.022	1.919 0.117	
40 Ethyl octanoate	30.53	55	0.868 0.009	0.602 0.027	0.330 0.038	0.234 0.024	0.494 0.031	0.356 0.012	0.301 0.037	0.549 0.012	0.460 0.024	0.373 0.018	
41 Piperitol	30.85	91	1.244 0.109	0.254 0.016	0.586 0.040	0.911 0.068	0.234 0.023	0.397 0.017	0.811 0.111	0.207 0.016	0.290 0.032	0.664 0.018	
42 Decanal	**31.04**	**41**	**5.115±0.626**	**7.172±0.442**	**4.233±0.428**	**2.921±0.204**	**6.208±0.313**	**5.340±0.433**	**3.889±0.424**	**6.638±0.610**	**4.334±0.139**	**3.531±0.057**	**0.442**
43 p-Menth-1-en-9-al	31.60	94	1.102 0.090	0.419 0.032	0.225 0.024	0.216 0.007	0.397 0.029	0.300 0.029	0.196 0.022	0.269 0.035	0.153 0.007	0.126 0.005	
44 cis-Carveol	**32.01**	**109**	**7.986±0.504**	**5.329±0.397**	**8.422±0.837**	**8.513±0.202**	**4.444±0.254**	**7.838±0.599**	**9.959±1.058**	**4.867±0.426**	**5.479±0.248**	**8.199±0.369**	**0.708**
45 L-Carveol	32.54	91	2.021 0.216	1.944 0.216	1.385 0.079	1.230 0.171	1.650 0.190	1.742 0.007	1.982 0.139	1.463 0.153	1.510 0.010	1.751 0.008	

46 Nerol	**33.46**	**91**	**6.115±0.194**	**3.572±0.322**	**4.452±0.162**	**5.711±0.642**	**3.441±0.147**	**3.658±0.082**	**5.460±0.481**	**3.143±0.132**	**3.434±0.136**	**4.297±0.518**	**0.281**
47 β-Citronellol	**34.04**	**67**	**10.53±1.33**	**8.370±0.373**	**11.54±0.90**	**11.84±0.21**	**7.425±0.660**	**8.929±0.181**	**11.26±0.63**	**7.285±0.462**	**7.491±0.057**	**10.82±0.17**	**0.611**
48 Carvone	**35.03**	**54**	**5.130±0.247**	**3.323±0.069**	**6.107±0.203**	**6.753±0.206**	**3.596±0.468**	**5.590±0.407**	**6.393±0.826**	**2.864±0.284**	**3.660±0.443**	**6.395±0.527**	**0.726**
49 Neral/cis-Citral	**35.34**	**119**	**10.189±1.20**	**8.196±0.441**	**0.365±0.016**	**0.030±0.002**	**7.244±0.948**	**0.266±0.023**	**0.077±0.004**	**6.577±0.028**	**0.222±0.032**	**0.056±0.001**	**0.400**
50 Piperitone	36.39	95	0.284 0.039	0.184 0.011	0.186 0.022	0.268 0.029	0.129 0.001	0.193 0.018	0.261 0.035	0.160 0.001	0.177 0.007	0.239 0.022	
51 Geraniol	37.64	91	5.755 0.764	2.589 0.039	3.616 0.366	3.943 0.419	1.790 0.235	2.173 0.167	3.529 0.261	1.736 0.097	1.813 0.141	2.712 0.159	**0.240**
52 Lynalyl acetate	37.96	93	1.503 0.048	0.963 0.017	0.223 0.017	ND	0.764 0.012	0.162 0.009	ND	0.844 0.068	0.211 0.006	ND	
53 E-2-decenal	38.32	41	0.035 0.001	ND	ND	ND	ND	ND	ND	ND	ND	ND	
54 Perillaldehyde	**38.86**	**79**	**6.529±0.660**	**6.418±0.144**	**5.660±0.683**	**4.851±0.675**	**6.131±0.659**	**5.038±0.306**	**4.643±0.104**	**5.414±0.503**	**5.224±0.327**	**3.541±0.068**	**0.468**
55 Geranial	**39.42**	**41**	**8.668±0.583**	**8.140±0.644**	**0.479±0.010**	**0.103±0.006**	**7.714±0.165**	**0.610±0.012**	**0.120±0.011**	**7.675±0.350**	**0.400±0.053**	**0.185±0.023**	**0.305**
56 1-Decanol	**40.06**	**41**	**3.416±0.299**	**2.821±0.195**	**3.320±0.335**	**4.088±0.136**	**2.674±0.325**	**3.282±0.166**	**3.514±0.062**	**3.044±0.095**	**3.114±0.188**	**3.747±0.392**	**0.318**
57 Perilla alcohol	43.65	67	1.107 0.149	1.021 0.017	0.656 0.023	0.458 0.060	0.735 0.002	0.682 0.094	0.676 0.038	0.745 0.044	0.523 0.041	0.358 0.028	
58 2,4-decadienal	**44.33**	**81**	**0.840±0.077**	**0.548±0.030**	**0.359±0.017**	**0.245±0.020**	**0.431±0.012**	**0.367±0.012**	**0.245±0.016**	**0.428±0.024**	**0.220±0.028**	**0.185±0.011**	**0.026**
59 Selinane	46.33	95	2.110 0.306	5.657 0.551	7.234 0.670	7.481 0.025	4.965 0.313	5.673 0.372	7.477 0.892	4.664 0.341	4.954 0.064	6.588 0.393	
60 -Terpenyl acetate	47.32	93	16.86 1.03	15.64 1.09	11.44 1.65	8.522 0.152	13.57 0.50	12.18 0.54	9.513 0.301	14.51 0.81	12.31 0.43	11.31 0.57	
61 Citronellyl acetate	48.22	67	1.531 0.192	1.117 0.031	0.248 0.013	0.219 0.008	0.931 0.007	0.357 0.017	0.231 0.023	1.049 0.067	0.457 0.021	0.236 0.007	
62 -Copaene	49.03	105	1.333 0.154	0.235 0.009	0.555 0.047	0.658 0.023	0.438 0.034	0.472 0.035	0.406 0.015	0.222 0.010	0.280 0.005	0.512 0.005	
63 Neryl acetate	49.22	93	2.107 0.226	1.641 0.054	0.389 0.024	0.134 0.011	1.395 0.029	0.502 0.019	0.192 0.014	1.516 0.046	0.681 0.027	0.332 0.041	
64 -Cubebene	50.40	105	0.873 0.047	0.221 0.013	0.147 0.017	0.124 0.011	0.376 0.009	0.154 0.015	0.154 0.006	0.272 0.025	0.160 0.004	0.153 0.016	
65 -Elemene	50.63	93	15.71 0.76	6.822 0.387	4.596 0.609	3.773 0.445	8.684 0.747	4.379 0.062	2.213 0.163	7.100 0.251	2.637 0.062	2.185 0.058	
66 Camphene	50.86	41	0.591 0.004	0.533 0.056	0.079 0.001	0.036 0.002	0.429 0.037	0.131 0.009	0.048 0.003	0.558 0.034	0.195 0.002	0.077 0.002	
67 -Caryophyllene	52.45	91	11.90 0.75	3.701 0.418	5.050 0.066	5.551 0.084	5.208 0.546	4.749 0.598	4.472 0.110	4.352 0.535	4.700 0.348	4.743 0.053	
68 Geranyl acetate	52.62	41	1.162 0.015	7.157 0.148	1.645 0.088	1.044 0.066	6.831 0.097	2.061 0.050	1.207 0.167	6.928 0.246	1.776 0.060	1.161 0.117	
69 Longifolene-(V4)	53.18	105	2.626 0.072	1.027 0.100	1.122 0.107	1.206 0.097	1.178 0.109	0.998 0.018	0.764 0.035	1.010 0.012	0.857 0.004	0.852 0.024	
70 -Ionone	53.68	121	3.258 0.437	3.101 0.308	3.167 0.395	2.726 0.133	2.792 0.034	3.185 0.232	3.002 0.136	2.763 0.138	2.958 0.109	3.219 0.048	
71 p-Menth-1-en-9-ol	54.39	91	1.265 0.126	0.829 0.033	0.264 0.014	0.174 0.022	0.679 0.010	0.319 0.014	0.186 0.015	0.769 0.071	0.310 0.024	0.212 0.024	
72 -Caryophyllene	54.88	93	8.261 0.560	2.583 0.197	3.317 0.159	3.496 0.187	3.602 0.340	3.412 0.200	2.969 0.097	2.603 0.288	2.929 0.069	3.218 0.199	
73 (Z)- -Guaiene	56.11	120	0.122 0.011	0.032 0.002	0.048 0.002	0.057 0.004	0.037 0.003	0.049 0.002	0.052 0.001	0.036 0.001	0.038 0.003	0.053 0.003	
74 -Selinane	56.48	107	6.508 0.315	2.119 0.190	3.428 0.083	3.713 0.522	2.997 0.225	3.102 0.385	3.247 0.048	2.358 0.239	2.600 0.071	3.122 0.291	
75 Viridiflorene	56.71	133	3.130 0.014	1.240 0.099	2.532 0.099	3.038 0.090	1.880 0.244	2.508 0.081	2.450 0.006	1.386 0.178	2.265 0.166	2.435 0.223	
76 Germacrene D	56.93	105	1.869 0.134	0.519 0.043	0.588 0.059	0.741 0.042	0.868 0.046	0.588 0.041	0.492 0.028	0.641 0.079	0.392 0.037	0.264 0.014	
77 -Gurjunene	57.27	189	19.87 1.00	12.76 1.66	16.67 0.49	18.60 1.71	16.79 1.88	15.02 1.78	14.93 0.61	12.93 1.33	14.29 0.47	15.92 0.52	
78 Valencene	**57.78**	**105**	**606.3±2.5**	**255.9±25.6**	**390.6±33.0**	**466.0±45.3**	**339.4±39.4**	**348.3±17.2**	**359.8±3.6**	**269.7±26.9**	**280.3±11.7**	**366.9±28.1**	**43.3**
79 -Muurolene	58.54	105	11.20 0.83	13.33 1.12	7.314 0.454	6.197 0.674	6.290 0.259	5.982 0.082	5.362 0.196	4.815 0.117	5.831 0.540	6.154 0.267	
80 -Guaiene	58.79	107	0.227 0.020	0.287 0.027	0.152 0.016	0.129 0.008	0.139 0.002	0.125 0.010	0.116 0.010	0.129 0.013	0.187 0.022	0.194 0.007	
81 Selina-3,7(11)-diene	59.39	105	32.24 1.30	14.62 0.72	20.13 0.53	21.55 2.09	18.57 2.06	18.21 2.17	17.96 0.62	14.55 1.42	15.08 0.16	20.78 1.92	
82 -Farnesene	59.61	91	0.441 0.039	0.046 0.002	0.138 0.014	0.136 0.011	0.107 0.006	0.078 0.001	0.077 0.005	0.058 0.005	0.059 0.003	0.102 0.005	
83 Cadinene	60.08	119	5.042 0.453	1.522 0.093	3.076 0.390	3.359 0.348	2.380 0.281	2.592 0.311	2.680 0.203	1.776 0.228	2.218 0.153	2.843 0.239	
84 Germacrene B	60.24	41	0.123 0.014	0.070 0.002	0.102 0.008	0.120 0.007	0.059 0.004	0.090 0.002	0.091 0.003	0.080 0.007	0.086 0.008	0.105 0.006	
85 Caryophyllene oxidade	63.41	79	4.141 0.458	3.688 0.379	2.110 0.187	1.437 0.091	3.278 0.101	2.507 0.168	1.429 0.065	3.455 0.269	2.258 0.170	1.695 0.088	
86 -Guaiene	67.19	105	0.278 0.016	0.497 0.031	0.595 0.053	0.452 0.027	0.447 0.005	0.596 0.029	0.483 0.046	0.384 0.028	0.455 0.041	0.844 0.036	
87 y-Eudesmol	67.45	105	0.170 0.019	0.118 0.006	0.111 0.005	0.098 0.010	0.104 0.006	0.135 0.006	0.137 0.004	0.101 0.005	0.101 0.009	0.131 0.016	
88 y-Selinane	67.99	189	1.961 0.220	2.269 0.141	4.872 0.665	4.903 0.036	2.145 0.131	5.605 0.619	6.957 0.568	2.026 0.175	4.120 0.520	6.349 0.768	
89 y-Gurjunene	68.35	161	5.228 0.396	8.824 0.572	10.29 1.37	10.54 0.43	9.035 0.112	10.81 1.16	11.41 0.49	9.013 0.487	8.681 0.184	9.957 1.311	
90 β-Sinensal	**70.69**	**91**	**0.717±0.002**	**0.472±0.054**	**0.330±0.031**	**0.353±0.036**	**0.395±0.019**	**0.435±0.055**	**0.437±0.005**	**0.413±0.043**	**0.428±0.018**	**0.511±0.072**	**0.050**
91 α-Sinensal	**73.73**	**91**	**0.678±0.061**	**0.300±0.029**	**0.218±0.012**	**0.207±0.013**	**0.281±0.005**	**0.270±0.003**	**0.268±0.016**	**0.276±0.024**	**0.289±0.007**	**0.312±0.036**	**0.040**
92 Nootkatone	**75.81**	**146**	**19.89±2.68**	**16.22±1.22**	**17.77±2.12**	**19.74±2.44**	**15.40±1.19**	**21.63±1.79**	**22.39±0.43**	**15.31±0.91**	**16.91±0.66**	**21.37±2.87**	**1.64**

Compound	Retention time (min)	Ion model (*m/z*)	Fresh Juice	25% pulp content									msd
				[b]58ºC			[b]63ºC			[b]68ºC			
				0 months	1.5 months	3 months	0 months	1.5 months	3 months	0 months	1.5 months	3 months	
1 Z-3-Hexanal	**3.96**	**43**	**1.989±0.218**	**0.773±0.028**	**0.524±0.039**	**0.346±0.027**	**0.528±0.008**	**0.296±0.008**	**0.266±0.023**	**0.764±0.066**	**0.450±0.025**	**0.366±0.008**	**0.084**
2 Ethyl butyrate	**4.07**	**88**	**4.471±0.513**	**2.006±0.221**	**2.726±0.328**	**2.852±0.311**	**1.357±0.132**	**2.632±0.012**	**2.697±0.233**	**1.575±0.059**	**1.727±0.206**	**2.396±0.287**	**0.342**
3 E-2-Hexenal	**5.56**	**41**	**0.146±0.014**	**0.014±0.000**	**0.005±0.000**	**0.003±0.000**	**0.016±0.001**	**0.010±0.000**	**0.021±0.002**	**0.016±0.002**	**0.011±0.001**	**0.011±0.001**	**0.009**
4 Heptanal	7.63	43	1.073 0.138	0.369 0.001	0.382 0.044	0.806 0.021	0.329 0.011	0.377 0.029	0.553 0.055	0.326 0.015	0.346 0.018	0.445 0.017	
5 -Thujene	8.83	91	0.336 0.040	0.118 0.015	0.026 0.001	0.026 0.002	0.100 0.008	0.031 0.003	0.017 0.002	0.102 0.007	0.021 0.002	0.009 0.000	
6 α-Pinene	**9.09**	**91**	**42.44±3.04**	**19.90±1.41**	**16.01±0.42**	**14.45±0.35**	**18.56±0.38**	**15.27±0.38**	**15.11±0.22**	**19.23±0.83**	**16.56±1.64**	**14.78±1.70**	**3.24**
7 Sabinene	9.89	93	0.249 0.010	0.141 0.006	0.132 0.016	0.129 0.005	0.138 0.002	0.139 0.010	0.117 0.005	0.121 0.011	0.101 0.007	0.094 0.001	
8 β-Pinene	**11.57**	**93**	**8.416±0.286**	**2.299±0.143**	**1.454±0.029**	**1.277±0.089**	**2.258±0.149**	**1.142±0.098**	**1.072±0.068**	**2.096±0.114**	**1.349±0.063**	**0.968±0.084**	**0.365**
9 β-Mircene	**12.95**	**93**	**153.9±6.7**	**119.3±11.6**	**132.9±13.2**	**158.7±9.0**	**93.17±6.35**	**112.6±3.7**	**143.3±16.9**	**93.74±1.53**	**109.9±6.3**	**115.0±10.9**	**16.3**
10 -Fellandrene	13.59	91	10.39 1.41	7.039 0.666	8.943 1.084	9.229 0.815	4.703 0.405	7.729 0.454	9.722 0.017	5.023 0.640	7.611 0.263	7.917 0.049	
11 Octanal	**13.79**	**67**	**28.29±3.83**	**32.85±1.40**	**26.53±1.72**	**16.24±2.03**	**25.81±0.90**	**23.93±1.01**	**21.97±1.59**	**22.65±0.82**	**17.59±0.29**	**12.33±0.42**	**1.88**
12 3-Carene	13.96	91	11.93 1.14	6.524 0.513	5.175 0.171	4.882 0.077	5.936 0.148	5.673 0.326	5.514 0.088	6.261 0.222	5.398 0.636	5.121 0.581	
13 -Terpinene	14.50	93	5.400 0.409	3.723 0.233	3.298 0.358	2.921 0.321	3.285 0.044	3.153 0.092	2.937 0.121	3.541 0.240	2.541 0.294	2.518 0.442	
14 trans- -Ocimene	17.33	91	4.263 0.109	2.006 0.217	1.232 0.059	1.135 0.075	1.949 0.091	1.677 0.077	1.577 0.036	1.940 0.024	1.449 0.204	1.469 0.144	
15 γ-Terpinene	**17.92**	**91**	**12.85±1.60**	**8.640±0.644**	**4.636±0.156**	**3.564±0.142**	**7.945±0.390**	**6.387±0.173**	**5.931±0.213**	**7.973±0.027**	**5.769±0.704**	**5.722±0.507**	**1.36**
16 1-Octanol	**19.21**	**55**	**103.8±11.6**	**45.86±4.36**	**66.78±3.68**	**77.80±8.37**	**34.25±3.73**	**60.87±1.67**	**63.83±1.77**	**33.73±2.01**	**36.65±2.95**	**52.97±3.55**	**4.93**
17 α-Terpinolene	**20.06**	**93**	**5.273±0.679**	**3.709±0.361**	**2.341±0.092**	**2.176±0.087**	**3.411±0.073**	**3.107±0.119**	**3.084±0.143**	**3.399±0.013**	**2.861±0.336**	**2.968±0.256**	**0.574**
18 6-Camphenone	20.53	93	1.327 0.163	1.206 0.151	2.265 0.232	2.620 0.184	0.801 0.094	2.153 0.051	2.525 0.232	0.852 0.011	1.108 0.114	1.989 0.077	
19 Linalool	**21.55**	**93**	**209.1±26.7**	**145.8±10.4**	**188.6±9.8**	**195.4±17.6**	**125.4±4.6**	**183.5±4.3**	**193.5±14.5**	**121.6±7.1**	**146.5±10.3**	**151.4±5.1**	**11.9**
20 Nonanal	**21.76**	**67**	**7.144±0.524**	**6.415±0.157**	**4.867±0.296**	**3.746±0.069**	**6.139±0.174**	**4.345±0.280**	**3.463±0.197**	**5.481±0.476**	**4.610±0.211**	**3.630±0.301**	**0.401**
21 p-Mentha-1,3,8-triene	21.89	119	0.928 0.102	1.635 0.192	2.044 0.097	2.285 0.271	1.719 0.188	2.321 0.180	2.333 0.156	1.829 0.126	2.116 0.166	2.238 0.126	
22 trans-p-Mentha-2,8-dienol	22.65	91	3.731 0.398	3.289 0.340	5.472 0.635	5.761 0.572	2.307 0.249	5.290 0.171	6.004 0.544	2.916 0.254	3.010 0.367	5.195 0.371	
23 4-Acetyl-1-methyl-1-cyclohexene	23.55	95	1.250 0.177	0.512 0.026	1.082 0.096	1.101 0.023	0.349 0.025	1.035 0.045	1.072 0.019	0.662 0.011	0.676 0.025	0.683 0.047	
24 cis-p-Mentha-2,8-dienol	23.85	91	3.576 0.149	2.675 0.099	3.602 0.354	3.630 0.150	1.825 0.162	3.549 0.288	3.871 0.315	2.271 0.122	2.474 0.266	3.083 0.372	
25 Ethyl 3-hydroxyhexanoate	**24.20**	**77**	**0.677±0.060**	**0.398±0.017**	**0.803±0.010**	**0.926±0.040**	**0.256±0.019**	**0.689±0.004**	**0.955±0.023**	**0.300±0.021**	**0.415±0.016**	**0.930±0.059**	**0.054**
26 Camphor	24.27	95	0.598 0.020	0.517 0.019	0.830 0.016	0.847 0.056	0.366 0.026	0.772 0.016	0.813 0.058	0.337 0.045	0.408 0.026	0.675 0.033	
27 Citronellal	**24.64**	**79**	**0.904±0.095**	**0.582±0.031**	**1.826±0.206**	**2.947±0.335**	**0.395±0.048**	**1.628±0.047**	**2.969±0.173**	**0.464±0.032**	**0.991±0.018**	**2.332±0.201**	**0.168**
28 Eucalyptol	24.88	93	0.918 0.112	0.303 0.025	0.977 0.037	1.245 0.050	0.290 0.036	0.903 0.105	1.147 0.060	0.244 0.002	0.510 0.034	0.943 0.082	
29 β-Terpineol	**25.06**	**91**	**2.343±0.150**	**1.603±0.067**	**2.029±0.067**	**2.125±0.128**	**1.275±0.069**	**2.321±0.176**	**2.338±0.125**	**1.324±0.107**	**1.755±0.079**	**1.951±0.140**	**0.195**
30 3,6-Nonadienal	25.52	67	0.349 0.012	0.435 0.029	0.659 0.039	0.715 0.027	0.377 0.029	0.661 0.032	0.805 0.087	0.584 0.061	0.649 0.026	0.800 0.063	
31 Z-Limonene oxide	26.03	123	1.867 0.063	1.694 0.131	1.872 0.065	2.134 0.271	1.475 0.131	2.230 0.120	2.256 0.270	1.547 0.055	1.581 0.148	1.992 0.122	
32 E-limonene oxide	26.46	91	0.803 0.009	0.434 0.052	0.773 0.020	1.081 0.124	0.435 0.005	0.807 0.079	0.961 0.024	0.435 0.039	0.608 0.047	0.873 0.040	
33 1-Terpinen-4-ol	**27.44**	**71**	**74.23±8.66**	**32.13±3.14**	**47.08±3.48**	**49.57±0.99**	**22.97±2.59**	**44.18±0.92**	**45.96±3.32**	**25.22±1.00**	**29.24±3.71**	**39.66±5.25**	**6.02**
34 Nonanol	**27.61**	**55**	**5.890±0.346**	**3.403±0.331**	**4.519±0.099**	**4.528±0.107**	**2.422±0.220**	**4.176±0.127**	**4.189±0.046**	**2.916±0.185**	**3.091±0.235**	**4.004±0.166**	**0.263**
35 (+)-p-Menth-1-ene	28.10	95	0.265 0.003	0.166 0.016	0.235 0.024	0.244 0.008	0.175 0.011	0.195 0.002	0.208 0.002	0.184 0.020	0.100 0.005	0.140 0.011	
36 Thymol	28.48	135	0.229 0.018	0.437 0.041	0.439 0.024	0.534 0.011	0.394 0.051	0.521 0.037	0.766 0.043	0.600 0.078	0.559 0.040	0.559 0.046	
37 α-Terpineol	**28.75**	**59**	**8.569±1.202**	**6.934±0.397**	**17.16±1.38**	**21.20±1.99**	**5.234±0.622**	**15.67±0.51**	**22.54±1.78**	**5.915±0.277**	**9.221±0.979**	**19.06±1.45**	**1.848**
38 cis-Carvyl acetate	29.73	91	0.347 0.033	2.894 0.252	4.555 0.257	4.722 0.545	2.243 0.069	4.606 0.291	5.415 0.215	2.801 0.295	2.825 0.095	4.273 0.318	
39 Dihydrocarvone	30.04	67	3.414 0.224	1.209 0.067	1.707 0.116	2.279 0.148	0.870 0.066	1.753 0.041	1.818 0.117	1.225 0.081	1.376 0.161	1.467 0.109	
40 Ethyl octanoate	30.53	55	0.868 0.009	0.397 0.013	0.217 0.027	0.191 0.022	0.347 0.017	0.195 0.017	0.191 0.011	0.368 0.007	0.254 0.016	0.207 0.014	
41 Piperitol	30.85	91	1.244 0.109	0.219 0.005	0.663 0.077	0.747 0.085	0.206 0.013	0.564 0.040	0.729 0.045	0.145 0.002	0.294 0.024	0.606 0.068	
42 Decanal	**31.04**	**41**	**5.115±0.626**	**3.545±0.242**	**3.805±0.355**	**5.751±0.244**	**2.969±0.275**	**3.409±0.338**	**4.523±0.168**	**4.879±0.055**	**4.741±0.137**	**3.976±0.305**	**0.442**
43 p-Menth-1-en-9-al	31.60	94	1.102 0.090	0.436 0.035	0.224 0.023	0.204 0.019	0.229 0.013	0.133 0.018	0.135 0.009	0.362 0.045	0.232 0.019	0.154 0.013	
44 cis-Carveol	**32.01**	**109**	**7.986±0.504**	**5.261±0.335**	**8.890±0.680**	**8.981±0.041**	**3.543±0.088**	**8.414±0.205**	**8.737±0.409**	**4.560±0.547**	**4.705±0.321**	**6.371±0.864**	**0.708**
45 L-Carveol	32.54	91	2.021 0.216	1.836 0.214	1.869 0.110	1.943 0.030	1.262 0.129	2.107 0.026	2.143 0.112	1.591 0.199	1.880 0.145	2.336 0.134	
46 Nerol	**33.46**	**91**	**6.115±0.194**	**3.554±0.196**	**5.798±0.203**	**5.953±0.165**	**3.475±0.024**	**1.102±0.050**	**5.602±0.363**	**3.033±0.133**	**3.047±0.043**	**4.477±0.211**	**0.281**

47 β-Citronellol	**34.04**	**67**	**10.53±1.33**	**7.869±0.591**	**11.42±0.39**	**11.69±0.21**	**6.350±0.625**	**11.26±0.50**	**12.31±1.16**	**6.808±0.203**	**6.950±0.117**	**9.333±1.301**	**0.611**
48 Carvone	**35.03**	**54**	**5.130±0.247**	**2.912±0.215**	**6.079±0.486**	**6.279±0.325**	**2.137±0.026**	**5.995±0.126**	**6.196±0.335**	**2.604±0.254**	**3.094±0.375**	**4.366±0.273**	**0.726**
49 Neral/cis-Citral	**35.34**	**119**	**10.19±1.20**	**8.162±0.848**	**0.539±0.052**	**0.079±0.004**	**5.165±0.388**	**0.378±0.026**	**0.072±0.007**	**6.537±0.381**	**0.214±0.008**	**0.101±0.013**	**0.400**
50 Piperitone	36.39	95	0.284 0.039	0.178 0.002	0.233 0.014	0.305 0.023	0.116 0.008	0.284 0.012	0.289 0.007	0.154 0.015	0.173 0.017	0.229 0.021	
51 Geraniol	37.64	91	**5.755±0.764**	**2.832±0.070**	**3.437±0.297**	**3.510±0.362**	**1.648±0.152**	**3.184±0.082**	**3.408±0.198**	**1.893±0.187**	**1.961±0.055**	**2.984±0.291**	**0.240**
52 Lynalyl acetate	37.96	93	1.503 0.048	0.606 0.020	ND	ND	0.603 0.056	ND	ND	0.565 0.049	ND	ND	
53 E-2-decenal	38.32	41	0.035 0.001	ND	ND	ND	ND	ND	ND	ND	ND	ND	
54 Perillaldehyde	**38.86**	**79**	**6.529±0.660**	**6.092±0.584**	**5.583±0.476**	**4.701±0.257**	**6.034±0.188**	**6.526±0.175**	**6.046±0.420**	**5.448±0.322**	**3.686±0.333**	**4.959±0.334**	**0.468**
55 Geranial	**39.42**	**41**	**8.668±0.583**	**5.740±0.448**	**0.775±0.021**	**0.167±0.012**	**3.411±0.223**	**0.692±0.046**	**0.124±0.007**	**3.586±0.318**	**0.756±0.030**	**0.128±0.010**	**0.305**
56 1-Decanol	**40.06**	**41**	**3.416±0.299**	**1.570±0.119**	**2.914±0.321**	**4.841±0.542**	**1.418±0.164**	**3.022±0.207**	**5.128±0.636**	**2.666±0.166**	**4.323±0.201**	**4.843±0.437**	**0.318**
57 Perilla alcohol	43.65	67	1.107 0.149	0.679 0.021	0.544 0.009	0.512 0.036	0.592 0.019	0.521 0.015	0.371 0.005	0.632 0.037	0.441 0.042	0.256 0.018	
58 2,4-decadienal	**44.33**	**81**	**0.840±0.077**	**0.502±0.016**	**0.379±0.012**	**0.270±0.009**	**0.388±0.022**	**0.376±0.018**	**0.242±0.004**	**0.417±0.052**	**0.285±0.014**	**0.212±0.022**	**0.026**
59 Selinane	46.33	95	2.110 0.306	5.626 0.430	6.427 0.291	6.760 0.278	5.044 0.592	6.412 0.156	6.618 0.077	4.660 0.466	5.505 0.768	6.105 0.427	
60 -Terpenyl acetate	47.32	93	16.86 1.03	12.15 0.76	8.133 0.405	7.526 0.024	11.73 0.59	8.491 0.412	7.094 0.089	11.58 0.17	8.744 0.230	7.276 0.454	
61 Citronellyl acetate	48.22	67	1.531 0.192	0.743 0.033	0.203 0.009	0.120 0.006	0.757 0.031	0.194 0.007	0.159 0.004	0.782 0.008	0.227 0.021	0.157 0.005	
62 -Copaene	49.03	105	1.333 0.154	0.151 0.004	0.350 0.031	0.427 0.031	0.235 0.019	0.289 0.037	0.438 0.039	0.153 0.013	0.176 0.011	0.303 0.038	
63 Neryl acetate	49.22	93	2.107 0.226	1.294 0.109	0.239 0.009	0.105 0.005	1.098 0.138	0.321 0.013	0.145 0.007	1.209 0.015	0.406 0.022	0.162 0.007	
64 -Cubebene	50.40	105	0.873 0.047	0.181 0.011	0.099 0.004	0.134 0.001	0.203 0.010	0.096 0.003	0.129 0.005	0.189 0.016	0.077 0.005	0.083 0.003	
65 -Elemene	50.63	93	15.71 0.76	5.538 0.375	2.427 0.045	2.362 0.210	5.822 0.530	1.899 0.230	1.853 0.124	5.961 0.501	1.704 0.143	0.999 0.030	
66 Camphene	50.86	41	0.591 0.004	0.245 0.013	0.060 0.001	0.027 0.001	0.228 0.017	0.082 0.005	0.053 0.004	0.400 0.025	0.173 0.014	0.064 0.002	
67 -Caryophyllene	52.45	91	11.90 0.75	3.341 0.278	3.865 0.226	4.193 0.591	3.112 0.186	3.341 0.401	4.999 0.215	3.307 0.287	3.552 0.356	3.634 0.195	
68 Geranyl acetate	52.62	41	1.162 0.015	5.896 0.074	1.076 0.026	0.878 0.043	5.602 0.248	1.267 0.089	0.909 0.024	2.182 0.059	1.254 0.057	0.701 0.025	
69 Longifolene-(V4)	53.18	105	2.626 0.072	0.758 0.047	0.716 0.009	0.697 0.055	0.755 0.005	0.535 0.038	0.409 0.013	0.781 0.024	0.590 0.022	0.415 0.048	
70 -Ionone	53.68	121	3.258 0.437	2.339 0.079	2.244 0.060	2.157 0.028	2.170 0.116	2.165 0.104	1.856 0.026	2.380 0.083	2.040 0.074	2.006 0.181	
71 p-Menth-1-en-9-ol	54.39	91	1.265 0.126	0.614 0.027	0.186 0.003	0.144 0.004	0.631 0.050	0.227 0.004	0.147 0.010	0.637 0.010	0.209 0.004	0.147 0.011	
72 -Caryophyllene	54.88	93	8.261 0.560	2.018 0.040	2.202 0.267	2.800 0.234	2.054 0.091	2.258 0.269	3.015 0.402	2.099 0.185	2.156 0.141	2.280 0.075	
73 (Z)- -Guaiene	56.11	120	0.122 0.011	0.033 0.004	0.029 0.003	0.041 0.002	0.061 0.003	0.089 0.004	0.084 0.002	0.032 0.004	0.026 0.002	0.039 0.004	
74 -Selinane	56.48	107	6.508 0.315	1.813 0.165	2.244 0.242	2.762 0.228	1.920 0.128	2.318 0.243	3.293 0.068	1.909 0.247	2.090 0.070	2.230 0.062	
75 Viridiflorene	56.71	133	3.130 0.014	1.130 0.067	1.869 0.019	2.413 0.120	1.123 0.028	1.347 0.124	2.505 0.215	1.202 0.018	1.722 0.114	1.953 0.023	
76 Germacrene D	56.93	105	1.869 0.134	0.440 0.035	0.433 0.011	0.381 0.031	0.465 0.034	0.263 0.028	0.212 0.022	0.477 0.031	0.388 0.026	0.357 0.010	
77 -Gurjunene	57.27	189	19.87 1.00	10.78 0.51	11.88 1.39	12.99 1.84	10.53 0.83	11.22 0.54	14.67 1.89	11.38 1.12	11.51 0.76	11.65 0.61	
78 Valencene	**57.78**	**105**	**606.3±2.5**	**212.0±14.5**	**279.7±25.2**	**295.0±39.3**	**211.2±5.7**	**282.9±1.5**	**328.7±43.5**	**227.6±23.9**	**256.9±3.2**	**264.8±7.1**	**43.3**
79 -Muurolene	58.54	105	11.20 0.83	3.832 0.085	4.442 0.490	5.081 0.103	3.731 0.210	4.171 0.122	5.260 0.404	3.930 0.116	3.948 0.015	4.048 0.140	
80 -Guaiene	58.79	107	0.227 0.020	0.106 0.012	0.128 0.004	0.187 0.006	0.091 0.008	0.150 0.001	0.203 0.008	0.100 0.002	0.110 0.007	0.140 0.011	
81 Selina-3,7(11)-diene	59.39	105	32.24 1.23	12.23 0.63	14.50 1.61	16.55 1.79	11.49 0.52	14.57 0.87	18.14 1.78	12.27 0.31	12.71 0.23	13.97 0.09	
82 -Farnesene	59.61	91	0.441 0.039	0.048 0.001	0.075 0.002	0.084 0.004	0.043 0.002	0.063 0.003	0.083 0.002	0.051 0.003	0.018 0.002	0.064 0.004	
83 Cadinene	60.08	119	5.042 0.453	1.564 0.174	2.157 0.178	2.250 0.161	1.427 0.074	1.609 0.107	2.754 0.397	1.428 0.128	1.921 0.060	2.048 0.135	
84 Germacrene B	60.24	41	0.123 0.014	0.058 0.006	0.104 0.002	0.142 0.003	0.046 0.005	0.088 0.003	0.163 0.015	0.067 0.001	0.149 0.014	0.137 0.006	
85 Caryophyllene oxidade	63.41	79	4.141 0.458	2.812 0.144	1.321 0.055	0.920 0.130	2.708 0.275	1.498 0.166	0.887 0.022	2.656 0.057	1.354 0.045	0.817 0.063	
86 -Guaiene	67.19	105	0.278 0.016	0.209 0.016	0.584 0.036	0.616 0.029	0.201 0.018	0.358 0.020	0.665 0.039	0.358 0.027	0.334 0.017	0.592 0.018	
87 y-Eudesmol	67.45	105	0.170 0.019	0.112 0.008	0.114 0.006	0.120 0.006	0.101 0.003	0.112 0.009	0.129 0.009	0.108 0.006	0.112 0.010	0.131 0.006	
88 y-Selinane	67.99	189	1.961 0.220	2.240 0.216	4.923 0.352	5.223 0.225	2.033 0.122	4.748 0.141	5.141 0.317	2.250 0.079	3.924 0.322	5.635 0.419	
89 y-Gurjunene	68.35	161	5.228 0.396	9.274 0.467	9.224 0.176	9.200 0.438	9.761 0.087	9.701 0.078	9.492 0.596	9.293 1.073	9.275 0.093	9.250 0.361	
90 β-Sinensal	**70.69**	**91**	**0.717±0.002**	**0.395±0.042**	**0.285±0.013**	**0.285±0.006**	**0.382±0.028**	**0.311±0.018**	**0.291±0.014**	**0.360±0.007**	**0.323±0.016**	**0.315±0.020**	**0.050**
91 α-Sinensal	**73.73**	**91**	**0.678±0.061**	**0.279±0.020**	**0.194±0.017**	**0.192±0.004**	**0.265±0.033**	**0.219±0.009**	**0.212±0.003**	**0.265±0.007**	**0.191±0.022**	**0.190±0.020**	**0.040**
92 Nootkatone	**75.81**	**146**	**19.89±2.68**	**17.08±0.58**	**19.59±1.17**	**20.33±1.22**	**16.33±1.60**	**17.90±1.18**	**17.96±0.62**	**15.92±1.78**	**16.24±0.58**	**16.51±1.58**	**1.64**

[a]Values are the average of three replicates (relative contents, mean std. dev.) using ethyl nonanoate (ion model at *m/z* 73) as internal standard as described by Cerdán-Calero *et al*. (2012).
[b]Homogenization temperature assayed.
In bold, targeted volatile descriptors used for statistical analysis (see Table 1 and Fig. 2).
N.D.: not detected.
msd: minimum significant difference (P 0.005).

Table S2. Non-volatile polar compounds in fresh, homogenized and stored (3 ºC) Lane Late orange juices determined[a] by GC-MS and AMDIS analysis according to their pulp content.

				100% pulp content									
Compound	Retention time (min)	Ion model (*m/z*)	Fresh Juice	[b]58ºC			[b]63ºC			[b]68ºC			msd
				0 months	1.5 months	3 months	0 months	1.5 months	3 months	0 months	1.5 months	3 months	
1 D-Alanine $(TMS)_2$	9.52	116	51.38 5.48	59.20 1.89	64.72 1.06	71.92 6.57	48.08 4.73	55.60 1.61	83.97 2.07	58.70 6.42	77.08 9.87	98.86 5.44	4.78
2 L-Valine $(TMS)_2$	13.62	144	7.43 0.64	7.25 0.14	7.56 0.23	4.10 0.18	5.93 0.68	4.79 0.15	3.84 0.49	7.12 0.56	5.98 0.11	2.79 0.11	0.33
3 L-Leucine $(TMS)_2$	15.62	158	3.03 0.24	3.87 0.15	4.98 0.20	3.72 0.18	2.22 0.34	2.22 0.14	2.01 0.18	3.34 0.30	2.35 0.25	1.51 0.13	0.20
4 L-Proline $(TMS)_2$	16.31	142	946.5 93.1	951.2 41.9	912.4 16.8	819.5 22.3	910.5 63.7	445.4 39.4	172.1 21.9	995.7 94.9	485.5 51.1	142.5 14.2	43.8
5 L-Isoleucine $(TMS)_2$	16.36	158	4.70 0.19	4.58 0.44	2.74 0.28	1.80 0.24	4.43 0.20	2.04 0.28	1.81 0.19	4.70 0.30	2.54 0.20	1.55 0.21	0.21
6 Glycine $(TMS)_3$	16.7	174	7.75 0.87	8.15 0.02	8.46 0.16	8.64 0.05	7.61 0.06	7.19 0.10	7.54 0.13	7.32 0.12	7.50 0.81	7.22 0.58	0.35
7 L-Serine $(TMS)_3$	18.79	204	81.88 6.86	71.32 2.13	66.11 6.70	63.31 3.47	67.63 3.25	35.02 4.53	11.98 1.40	86.13 3.09	77.88 3.04	11.01 0.37	2.97
8 L-Threonine $(TMS)_3$	19.67	101	4.56 0.35	4.23 0.16	2.76 0.24	2.05 0.09	4.14 0.11	2.56 0.01	2.27 0.20	4.70 0.19	1.95 0.19	1.71 0.18	0.29
9 Malic Acid $(TMS)_3$	22.89	245	1527.7 99.9	1501.7 63.8	1652.6 72.7	1750.4 71.3	1697.2 133.2	1724.2 70.7	1818.9 148.4	1686.8 183.6	1677.3 38.1	1741.6 198.5	106.2
10 L-Aspartic acid $(TMS)_3$	23.8	232	219.2 22.6	199.6 17.8	173.6 9.9	62.78 6.94	222.1 4.6	193.7 19.8	69.93 7.78	232.6 16.2	168.6 15.3	85.19 3.23	11.61
11 L-Phenylalanine $(TMS)_2$	26.51	218	13.11 0.25	10.84 0.28	8.43 0.33	8.15 0.01	11.91 1.19	9.73 0.57	8.30 1.13	11.89 0.54	9.49 0.29	6.99 0.48	0.70
12 D-Glutamic Acid $(TMS)_3$	26.64	246	107.5 14.2	35.58 4.07	97.21 5.15	100.1 4.8	46.70 0.37	49.75 1.61	54.24 3.18	38.50 3.73	76.36 5.72	83.76 0.33	4.71
13 L-Asparagine $(TMS)_3$	28.06	188	337.7 20.9	176.3 19.9	272.4 3.2	291.2 7.6	158.9 3.4	306.9 5.2	324.6 40.5	174.7 19.2	266.7 10.4	271.6 32.4	17.4
14 Putrescine $(TMS)_4$	29.6	174	88.79 10.62	75.25 0.40	91.68 1.77	101.5 1.9	76.68 1.85	91.97 1.28	101.5 1.0	78.00 5.27	91.07 7.63	101.3 7.0	4.40
15 Citric Acid $(TMS)_4$	32.26	273	6861.4 410.5	6709.4 419.5	6648.3 294.2	6017.2 545.9	6957.7 234.9	6784.5 149.3	6474.3 57.7	6117.8 173.2	5729.8 57.7	5163.6 509.1	303.9
16 Quinic Acid $(TMS)_5$	33.46	345	66.15 5.81	50.30 1.99	57.78 0.08	65.58 1.41	67.99 4.31	68.59 4.82	76.05 0.42	66.14 4.40	6117.8 3.0	6040.7 4.2	4.51
17 [c]Fructose $(TMS)_5$	33.92 / 34.18	307	18066 483	17437 1080	16860 472	14511 1356	17455 390	15778 439	14083 1017	17699 954	14185 957	11570 114	945
18 [c]Glucose $(TMS)_5$	34.52 / 34.93	319	14012 1749	14196 515	13637 4	11655 552	15786 219	13214 689	11924 459	15811 471	13882 1181	10811 504	744.5
19 Scyllo-Inositol $(TMS)_6$	35.54	318	411.6 48.3	376.1 34.2	374.9 2.6	370.7 26.4	402.1 12.8	408.1 6.6	403.6 4.7	411.5 15.3	403.5 16.6	402.3 22.7	26.4
20 Myo-Inositol $(TMS)_6$	38.88	305	1060.9 78.3	1009.7 136.7	1007.9 14.8	936.8 63.7	1045.6 46.1	1047.8 51.9	1019.8 26.9	1038.4 96.9	1048.2 7.6	986.5 91.4	80.9
21 Sucrose $(TMS)_8$	50.47	361	37830 3025	30931 2752	30071 844	29749 2554	34178 2012	33644 543	31100 424	35306 4517	34929 387	34156 1511	2351
22 Raffinose $(TMS)_{11}$	62.91	361	327.4 26.7	176.2 20.8	334.1 21.2	348.7 26.4	224.9 6.1	381.8 9.3	553.5 18.6	225.1 25.6	376.8 23.2	472.3 3.6	20.4

Table S2 (continued)

Compound	Retention time (min)	Ion model (*m/z*)	Fresh Juice	50% pulp content									msd
				[b]58°C			[b]63°C			[b]68°C			
				0 months	1.5 months	3 months	0 months	1.5 months	3 months	0 months	1.5 months	3 months	
1 D-Alanine $(TMS)_2$	9.52	116	51.38 5.48	48.66 2.06	69.51 3.65	80.02 1.98	42.66 1.83	68.36 3.82	83.52 2.90	51.32 2.74	71.76 1.28	90.32 1.28	4.78
2 L-Valine $(TMS)_2$	13.62	144	7.43 0.64	7.08 0.16	7.32 0.17	3.28 0.33	5.50 0.29	5.32 0.44	2.89 0.20	7.00 0.22	4.17 0.40	3.30 0.20	0.33
3 L-Leucine $(TMS)_2$	15.62	158	3.03 0.24	3.60 0.11	2.09 0.03	1.32 0.11	2.21 0.14	2.23 0.04	1.71 0.11	3.45 0.28	1.53 0.22	1.42 0.19	0.20
4 L-Proline $(TMS)_2$	16.31	142	946.5 93.1	853.0 10.3	519.0 28.7	517.8 10.4	889.3 31.8	710.0 94.4	217.3 18.5	1028.7 44.0	413.8 39.9	182.8 22.0	43.8
5 L-Isoleucine $(TMS)_2$	16.36	158	4.70 0.19	3.72 0.05	1.78 0.19	1.27 0.11	3.46 0.16	2.59 0.24	1.64 0.02	3.36 0.23	2.53 0.35	1.51 0.09	0.21
6 Glycine $(TMS)_3$	16.7	174	7.75 0.87	8.11 0.12	7.63 0.20	7.12 0.22	8.08 0.49	7.61 0.14	7.24 0.16	7.67 0.41	7.31 0.28	7.26 0.31	0.35
7 L-Serine $(TMS)_3$	18.79	204	81.88 6.86	71.01 0.12	23.90 2.70	9.40 0.08	73.32 5.38	61.62 0.70	25.53 0.69	68.18 3.55	44.18 2.31	13.26 0.64	2.97
8 L-Threonine $(TMS)_3$	19.67	101	4.56 0.35	4.31 0.64	3.45 0.52	2.21 0.21	4.03 0.21	3.83 0.61	3.53 0.22	4.02 0.17	2.60 0.15	2.41 0.14	0.29
9 Malic Acid $(TMS)_3$	22.89	245	1527.7 99.9	1467.9 15.5	1522.4 6.0	1693.6 65.3	1604.2 36.1	1684.1 45.6	1743.9 15.9	1645.3 16.0	1716.2 17.7	1756.6 164.7	106.2
10 L-Aspartic acid $(TMS)_3$	23.8	232	219.2 22.6	170.9 9.2	110.7 11.0	106.1 9.9	189.3 6.4	154.5 14.5	129.8 4.2	213.5 9.6	162.0 9.4	72.78 2.11	11.61
11 L-Phenylalanine $(TMS)_2$	26.51	218	13.11 0.25	10.66 0.17	7.74 0.34	7.12 0.48	10.73 0.20	8.29 0.08	8.02 0.77	11.70 1.04	9.26 0.54	7.55 0.15	0.70
12 D-Glutamic Acid $(TMS)_3$	26.64	246	107.5 14.2	41.11 7.13	75.92 0.62	105.4 4.2	49.08 1.74	54.12 2.62	63.03 1.67	39.12 1.39	74.30 5.82	81.92 1.87	4.71
13 L-Asparagine $(TMS)_3$	28.06	188	337.7 20.9	239.6 5.0	269.4 8.0	317.3 16.5	211.8 14.2	279.7 9.2	321.7 22.5	212.3 13.9	274.6 13.2	295.2 13.4	17.4
14 Putrescine $(TMS)_4$	29.6	174	88.79 10.62	81.18 1.01	92.14 1.94	102.0 1.5	81.38 0.86	94.06 0.46	102.5 0.4	82.14 1.02	96.43 2.27	102.7 0.3	4.40
15 Citric Acid $(TMS)_4$	32.26	273	6861.4 410.5	6543.0 306.2	5987.1 347.9	5625.4 122.1	6722.7 393.8	6350.8 291.6	5941.2 330.4	6511.9 298.5	5551.4 370.3	5461.6 237.5	303.9
16 Quinic Acid $(TMS)_5$	33.46	345	66.15 5.81	58.63 1.01	55.05 2.89	55.95 7.23	68.36 0.97	66.33 0.89	66.54 2.44	65.08 7.85	60.88 4.25	61.89 1.37	4.51
17 [c]Fructose $(TMS)_5$	33.92 / 34.18	307	18066 483	16221 490	15892 524	14513 1265	17055 338	15028 61	14154 404	17548 175	14024 1011	11646 181	945
18 [c]Glucose $(TMS)_5$	34.52 / 34.93	319	14012 1749	13825 556	13622 1357	10935 335	14752 491	13158 305	11994 84	15057 81	12919 459	10803 485	744.5
19 Scyllo-Inositol $(TMS)_6$	35.54	318	411.6 48.3	412.1 38.3	385.7 12.1	346.9 46.1	398.5 22.3	369.1 22.1	369.1 26.3	379.2 38.9	363.0 17.7	359.3 9.6	26.4
20 Myo-Inositol $(TMS)_6$	38.88	305	1060.9 78.3	1052.1 131.2	1041.4 50.3	871.0 99.5	1035.5 73.6	979.4 13.6	972.3 16.3	923.4 110.0	913.9 89.1	905.7 6.2	80.9
21 Sucrose $(TMS)_8$	50.47	361	37830 3025	37116 1773	36022 1833	31913 1787	32687 303	30497 2549	30174 4486	31978 672	31659 3904	30028 3118	2351
22 Raffinose $(TMS)_{11}$	62.91	361	327.4 26.7	161.9 2.3	244.8 29.2	321.9 1.0	219.4 5.0	261.7 10.0	404.7 29.4	221.8 14.8	260.1 19.8	335.1 15.6	20.4

Table S2 (continued)

Compound	Retention time (min)	Ion model (*m/z*)	Fresh Juice	25% pulp content									msd
				[b]58ºC			[b]63ºC			[b]68ºC			
				0 months	1.5 months	3 months	0 months	1.5 months	3 months	0 months	1.5 months	3 months	
1 D-Alanine $(TMS)_2$	9.52	116	51.38 5.48	43.35 3.45	79.00 8.55	83.11 10.91	34.08 4.21	54.81 4.61	81.64 1.21	46.89 3.33	67.07 5.34	82.63 4.50	4.78
2 L-Valine $(TMS)_2$	13.62	144	7.43 0.64	7.06 0.09	6.98 0.12	2.89 0.04	5.33 0.47	4.90 0.15	2.78 0.01	5.41 0.80	3.85 0.26	3.08 0.06	0.33
3 L-Leucine $(TMS)_2$	15.62	158	3.03 0.24	3.47 0.40	2.60 0.06	1.60 0.08	2.16 0.15	2.14 0.10	189.6 0.0	2.44 0.34	2.24 0.28	1.68 0.04	0.20
4 L-Proline $(TMS)_2$	16.31	142	946.5 93.1	832.5 56.8	510.8 8.3	471.0 51.8	842.8 3.4	386.1 8.1	236.3 12.4	793.4 93.2	591.4 21.5	125.7 2.8	43.8
5 L-Isoleucine $(TMS)_2$	16.36	158	4.70 0.19	3.71 0.33	3.61 0.05	1.72 0.06	2.27 0.14	2.52 0.09	1.72 0.04	2.42 0.06	2.69 0.25	1.70 0.08	0.21
6 Glycine $(TMS)_3$	16.7	174	7.75 0.87	8.17 0.44	7.88 0.25	7.15 0.06	8.11 0.19	7.76 0.19	7.43 0.47	7.70 0.67	7.52 0.52	7.27 0.37	0.35
7 L-Serine $(TMS)_3$	18.79	204	81.88 6.86	69.00 1.25	40.10 0.96	10.95 0.16	60.90 4.73	47.70 0.90	11.06 0.76	67.75 6.18	41.10 0.06	13.24 1.41	2.97
8 L-Threonine $(TMS)_3$	19.67	101	4.56 0.35	3.99 0.21	3.30 0.19	1.41 0.00	4.12 0.07	2.49 0.24	1.56 0.58	4.15 0.45	2.53 0.06	2.62 0.08	0.29
9 Malic Acid $(TMS)_3$	22.89	245	1527.7 100.0	1342.7 98.2	1526.1 104.9	1555.5 60.5	1381.6 161.2	1473.6 52.3	1537.8 155.3	1665.2 227.8	1833.3 40.6	1865.2 10.3	106.2
10 L-Aspartic acid $(TMS)_3$	23.8	232	219.2 22.6	209.8 7.4	175.0 14.6	124.3 2.2	173.3 19.2	131.4 10.6	114.8 9.4	211.9 21.4	151.6 9.1	63.03 2.23	11.61
11 L-Phenylalanine $(TMS)_2$	26.51	218	13.11 0.25	12.33 1.19	7.91 0.23	8.04 0.07	10.23 1.33	8.31 0.23	8.04 0.21	12.39 1.72	9.63 0.12	8.16 0.78	0.70
12 D-Glutamic Acid $(TMS)_3$	26.64	246	107.5 14.2	46.35 4.17	96.12 6.29	114.0 13.6	55.83 2.59	58.25 2.18	72.68 8.24	56.24 3.03	70.76 2.52	72.86 2.72	4.71
13 L-Asparagine $(TMS)_3$	28.06	188	337.7 20.9	294.0 15.0	312.9 17.9	350.6 13.2	220.9 14.4	265.2 10.6	275.9 10.4	217.2 15.6	275.1 36.3	278.3 4.1	17.4
14 Putrescine $(TMS)_4$	29.6	174	88.79 10.62	82.67 7.73	109.1 10.4	110.9 3.6	86.07 0.23	108.4 4.1	109.3 1.8	90.27 6.34	100.8 10.6	109.9 1.5	4.40
15 Citric Acid $(TMS)_4$	32.26	273	6861.4 410.5	6370.3 289.6	5736.2 288.6	5586.6 182.1	6586.4 468.9	6549.4 252.1	6278.3 257.7	6035.3 250.8	5742.4 45.5	5601.9 218.3	303.9
16 Quinic Acid $(TMS)_5$	33.46	345	66.15 5.81	60.92 6.02	57.30 8.17	43.97 3.19	62.17 7.36	61.95 5.01	66.57 6.15	57.48 7.83	55.53 1.42	50.29 1.95	4.51
17 [c]Fructose $(TMS)_5$	33.92 / 34.18	307	18066 483	16286 2234	15720 36	14301 1277	17617 2090	15885 792	13926 591	17323 392	14446 592	11632 1168	945
18 [c]Glucose $(TMS)_5$	34.52 / 34.93	319	14012 1749	13901 1195	12873 1586	10989 1347	14202 583	13923 488	10637 664	15004 571	12497 1102	10528 454	744.5
19 Scyllo-Inositol $(TMS)_6$	35.54	318	411.6 48.3	379.9 35.6	378.7 15.0	352.5 41.3	378.5 37.9	364.1 8.3	353.2 22.3	357.7 30.6	350.9 5.6	346.6 43.9	26.4
20 Myo-Inositol $(TMS)_6$	38.88	305	1060.9 78.3	1006.8 128.6	983.6 23.5	975.8 120.1	1027.3 133.9	991.6 73.9	921.5 11.4	956.5 105.8	933.8 40.2	755.3 66.6	80.9
21 Sucrose $(TMS)_8$	50.47	361	37830 3025	33564 2413	33015 307	32475 1304	36462 4501	32236 1372	32032 1150	27370 2983	23969 1173	22116 1362	2351
22 Raffinose $(TMS)_{11}$	62.91	361	327.4 26.7	158.2 10.6	231.4 13.7	315.3 24.9	173.6 16.1	236.5 5.3	376.3 46.7	167.2 19.1	242.1 30.9	290.0 19.5	20.4

[a] Values are the average of three replicates (absolute concentrations in mg/L, mean Std. dev.) using ribitol (ion model at *m/z* 319) as internal standard and the respective relative response factors as described by Cerdán-Calero *et al*. (2012).

[b] Homogenization temperature assayed.

[c] Fructose and glucose appear as α- and β-isomers.

TMS: trimethylsilyl.

msd: minimum significant difference (P 0.05).

CAPÍTULO 3

Caracterización del perfil de fenoles de zumos de granada (*Punica granatum*) de la variedad "Wonderful".

1. **Phenolic profile characterization of pomegranate (*Punica granatum*) juice by high-performance liquid chromatography with diode array detection coupled to an electrospray ion trap mass analyzer**. (2013). *Journal of Food Composition and Analysis,* 30(1), 32–40. Impact Factor: 2.259.

2. **Determination of the antiradical activity and kinetics of pomegranate juice using 2,2-diphenylpicyrl-1-hydrazyl as the antiradical probe**. (2014). *Food Science and Technology International.* (En prensa). Impact Factor: 0.981.

Journal of Food Composition and Analysis 30 (2013) 32–40

Contents lists available at SciVerse ScienceDirect

Journal of Food Composition and Analysis

journal homepage: www.elsevier.com/locate/jfca

Original Research Article

Phenolic profile characterization of pomegranate (*Punica granatum*) juice by high-performance liquid chromatography with diode array detection coupled to an electrospray ion trap mass analyzer

Enrique Sentandreu *, Manuela Cerdán-Calero, José M. Sendra

Instituto de Agroquímica y Tecnología de Alimentos (IATA-CSIC), Avda. Agustín Escardino 7, 46980 Paterna, Valencia, Spain

ARTICLE INFO

Article history:
Received 16 July 2012
Received in revised form 14 January 2013
Accepted 14 January 2013

Keywords:
Pomegranate juice
LC–MS^n analysis
Ion trap
Food analysis
Molecule structure elucidation
Phenolic profile
Anthocyanin trihexosides
Food composition

ABSTRACT

"Wonderful" pomegranate (*Punica granatum*) juice, obtained by pressure extraction of the whole fruit, was analyzed for its content in anthocyanin and non-anthocyanin phenolic components using high-performance liquid chromatography with diode array detection and tandem mass spectrometry analysis with positive and negative electrospray ionization (HPLC-DAD-ESI$^{+/-}$/MS^n) powered by an ion trap. High-throughput identification capacity from the ion trap featuring different MS^n experiments (reaching up to MS^4 level) led to detection of a total of 151 phenolics, 65 anthocyanin, anthocyanin–flavanol and flavanol–anthocyanin adducts, 25 of them reported for the first time in pomegranate juice, including some unusual cyanidin and pelargonidin trihexosides not previously described in natural extracts. Similarly, a total of 86 non-anthocyanin phenolic components were also identified, 39 of them reported for the first time in this juice.

1. Introduction

In recent years, consumers have witnessed the apparition and growth of a series of foodstuffs that make claims about their antioxidant properties and goodness for human health. Such products (popularly known as "ANTIOX") are intended for preventing disorders caused by aging, pollutants, carcinogenic agents and stress, among others, and are normally based on a high content in antioxidants (Kaur and Kapoor, 2001). They are usually commercialized either as concentrated tablets from extracts of natural products or as beverages from different fruit juices, provided that such beverages exhibit an attractive color. Hence, most of these commercial "ANTIOX" beverages are based on juices that are rich in anthocyanins, such as red grapes, berries and pomegranate, among others, which in addition to their strong antiradical activity also exhibit a nice color. It is noteworthy that pomegranate juice has become so popular in some developed countries that many consumers believe it to be a preferred food to be included in everyday nutrition. As a consequence, pomegranate fruit and juice have been catapulted into a prominent position in international commerce (Zhang et al., 2009).

Pomegranate juice is very rich in phenolic components, including anthocyanins which are the responsible of its nice red color. Majority of the bibliographic information reports only the presence of six major anthocyanins in pomegranate juice, namely the 3-mono- and 3,5-diglucoside derivatives of the anthocyanidins delphinidin, cyanidin and pelargonidin (Du et al., 1975; Gil et al., 2000; Alighourchi et al., 2008; Elfalleh et al., 2011). However, there have recently been reported a quite large number of colored anthocyanins-flavanol (Sentandreu et al., 2010) and flavanol–anthocyanin (Sentandreu et al., 2012) adducts, but at very low concentration. With respect to the presence of phenolic components others than anthocyanins (Gil et al., 2000; Madrigal-Carballo et al., 2009; Borges et al., 2010), almost all the consulted bibliography reports a number between 5 and 15, mainly ellagitannins and gallotannins, excepting a more recent study (Fischer et al., 2011) which reported the presence of about 55 of these metabolites. It must be noted that natural extracts use to be complex matrices with intricate metabolite composition, thus the use of ion traps (normally reaching a mass fragmentation analysis up to MS^3 level) has been claimed for molecular structure elucidation (Fountain, 2002; Kantharaj et al., 2003).

The aim of this work was to thoroughly study the phenolic composition of pomegranate juice, including both anthocyanin and non-anthocyanin compounds, by using the high-performance liquid chromatography with diode array detection and tandem

* Corresponding author. Tel.: +34 963 90 00 22; fax: +34 963 63 63 01.
E-mail address: elcapi@iata.csic.es (E. Sentandreu).

0889-1575/$ – see front matter © 2013 Elsevier Inc. All rights reserved.
http://dx.doi.org/10.1016/j.jfca.2013.01.003

mass spectrometry analysis with positive and negative electrospray ionization (HPLC-DAD-ESI$^{+/-}$/MS^n) methodology with an ion trap mass analyzer.

2. Materials and methods

2.1. Reagents and standards

Water, acetonitrile, tetrahydrofuran (THF) and formic acid of analytical grade were from Scharlab (Scharlab S.L., Barcelona, Spain). Nylon filters (0.45 μm) were from Teknokroma (Teknokroma Ltd., Barcelona, Spain).

2.2. Pomegranate juice

Pomegranate fruits, cultivar "Wonderful", were grown and imported from CA, USA. Pomegranate juice was obtained by pressure extraction of the whole fruit (50 units of fruit which weighted 25 kg), previously cut into halves, using a pressure extractor Europ (Vapfluid, Sant Boi de Llobregat, Barcelona, Spain) working at an air pressure of 6 kg/cm^2. Juice was sieved in a paddle finisher (Ø 0.4 mm, Luzzysa, El Puig, Spain) and yield of juice was 42% (w/w), having the following characteristics: °Brix, 17.2 (determined using a digital refractometer Pal-1; Atago Co. Ltd., Tokyo, Japan); pH 3.3 (determined using a Crison GLP 21 pH-meter; Crison Inst. S.A., Barcelona, Spain); acidity index, 1.07 (assessed by titration with 0.1 N NaOH and expressed as percentage of citric acid); dry matter, 12.7% (determined by oven dying at 70 °C until constant weight); and maturity index, 16.1. Immediately after extraction, separate aliquots (20 mL) of the juice were poured into vials, which were hermetically sealed and stored at −30 °C until analysis (two months as a maximum).

2.3. Sample preparation

An aliquot of the juice was defrosted at room temperature and darkness in a water bath and then centrifuged at 5000 rpm during 5 min. The supernatant was filtered through a 0.45 μm nylon filter and then injected into the platform of analysis.

2.4. HPLC-DAD-ESI/MS^n analysis

Chromatographic separation was performed using a Thermo Surveyor Plus HPLC (Thermo Scientific, San Jose, CA, USA), equipped with a quaternary pump, vacuum degasser and temperature-controlled autosampler. The column used was a 250 mm × 2.1 mm i.d., 3 μm, YMC C-18 pack-*pro* (YMC Europe GmbH, Dinslaken, Germany). The chromatographic conditions were: injection volume, 10 or 5 μL for the analysis of anthocyanins or non-anthocyanin phenols, respectively; flow rate, 0.2 mL/min; oven temperature, 24 °C; autosampler temperature, 10 °C; solvent A, water/THF/formic acid (97.5:2.0:0.5, v/v/v); solvent B, acetonitrile/THF/formic acid (97.5:2.0:0.5, v/v/v); gradient, initial 0% B, linear 0–6% B in 5 min, linear 6–18% B in 25 min, linear 18–80% B in 20 min, purging with 100% B during 10 min and re-equilibration of the column during 30 min; detection wavelengths, λ = 280, 320 and 520 nm.

MS analysis and fragmentation experiments were performed on a ThermoFinningan LCQ Advantage (Thermo Scientific, San Jose, CA, USA) ion trap mass spectrometer, equipped with an ESI source. The HPLC-DAD/MS^n platform was controlled and the resulting data were analyzed by using the software Xcalibur v. 2.06, loaded into a PC computer. Separate injections were run for analysis of the sample in both positive and negative electrospray ionization (ESI) modes.

2.4.1. Identification of anthocyanins, flavanol–anthocyanin and anthocyanin–flavanol adducts

The mass spectrometer was operated in the ESI positive ion mode under the common following conditions: source voltage, 3.5 kV; capillary voltage, 9 V; capillary temperature, 300 °C; sheath gas flow, 50 (arbitrary units); sweep gas flow, 20 (arbitrary units); full max ion time, 300 ms; and full micro scans, 3.

The ion trap mass analyzer used in this work is quite aged and so it hardly allows more than four scan events per injected sample. Therefore, it was necessary to run many separate injections to maximize its sensitivity and selectivity, so avoiding an excessive number of scan events per injected sample, and each run was subjected to a specific set of a few MS^n experiments. Moreover, the MS^n experiments were of two types, namely, general data dependent scan analyses and specific non-data dependent scan analyses. The first general type gives information about the major components of the juice but normally neglects the minor ones. The second type was planned to gain information about these minor components as well as to clarify dubious ion fragmentation sequences from the first general type.

2.4.1.1. Data dependent scan analyses. Data dependent scan analyses were carried out with the following general conditions: collision energy, 35% (arbitrary units); reject mass-to-charge ratio (*m*/*z*) width, 1.00; repeat count, 2; repeat duration, 0.5 min; exclusion size list, 25; exclusion duration, 1.00 min; exclusion mass width, 3.00.

General MS^3 analysis. This analysis included three scan events: *scan event 1*, full MS; *scan event 2*, MS^2 of the most intense ions from *scan event 1*; and *scan event 3*, MS^3 of the most intense ions from *scan event 2*. The scanned *m*/*z* range was 260–2000.

General MS^2 analysis for the detection of anthocyanin monoglycosides. This analysis included two scan events: *scan event 1*, full MS; and *scan event 2*, MS^2 of the ions populated in the target list: *m*/*z* 403, 417, 419, 433, 435, 449 and 465. The scanned mass range was *m*/*z* 260–500.

General MS^3 analysis for the detection of anthocyanin diglycosides. This analysis included three scan events: *scan event 1*, full MS; *scan event 2*, MS^2 of the ions populated in the target list: *m*/*z* 565, 579, 581, 595, 597, 611 and 627; and *scan event 3*, MS^3 of the most intense ion from *scan event 2*. The scanned mass range was *m*/*z* 260–700.

Neutral loss triple play analysis. This analysis was carried out to determine the presence of major anthocyanin glycosides and included three scan events: *scan event 1*, full MS; *scan event 2*, MS^2 of the four most intense ions from *scan event 1* which undergo any of the following neutral losses: *m*/*z* 132, 146, 162, 294, 308, 324 or 486; and *scan event 3*, MS^3 of the most intense ion generated in *scan event 2*. The scanned mass range was *m*/*z* 260–2000.

2.4.1.2. Non-data dependent scan analyses. Specific MS^3 analysis for the detection of rutinoside derivatives of anthocyanidins. Three separate injections (I–III) were run for the detection of rutinoside derivatives of anthocyanins, each one including three specific scan events: *scan event 1*, common full MS; *scan event 2*, specific MS^2 of the ion at *m*/*z* 579 (I), 595 (II) and 611 (III); and *scan event 3*, specific MS^3 of the ion at *m*/*z* 433 (I), 449 (II) and 465 (III). The scanned mass range was *m*/*z* 260–650.

Specific MS^4 analysis for the detection of dihexoside derivatives of anthocyanin–*flavanol and flavanol–anthocyanin adducts.* Five separate injections (I–V) were run, each one including four specific scan events: scan event 1, common full MS; scan event 2, specific MS^2 of the ion at *m*/*z* 867 (I), 883 (II), 899 (III), 915 (IV) and 931 (V); scan event 3, specific MS^3 of the ion at *m*/*z* 705 (I), 721 (II), 737 (III), 753 (IV) and 769 (V); and scan event 4, specific MS^4 of the ion at *m*/*z*

543 (I), 559 (II), 575 (III), 591 (IV) and 607 (V). The scanned mass range was *m*/*z* 260–1000.

Specific MS³ analysis for the detection of monohexoside derivatives of anthocyanin–*flavanol and flavanol–anthocyanin adducts.* Five separate injections (I–V) were run, each one including three specific scan events: scan event 1, common full MS; scan event 2, specific MS² of the ion at *m*/*z* 705 (I), 721 (II), 737 (III), 753 (IV) and 769 (V); and scan event 3, specific MS³ of the ion at *m*/*z* 543 (I), 559 (II), 575 (III), 591 (IV) and 607 (V). The scanned mass range was *m*/*z* 260–800.

2.4.2. Identification of the non-anthocyanin phenolic components

The mass spectrometer was operated in the ESI negative ion mode under the following conditions: source voltage, 4.0 kV; capillary voltage, −18 V; capillary temperature, 300 °C; sheath gas flow, 50 (arbitrary units); sweep gas flow, 20 (arbitrary units); full max ion time, 300 ms, and full micro scans, 3. Again and to maximize the sensitivity and selectivity of the ion trap mass analyzer, several separate injections of the sample were run. However, in this case only data dependent scan experiments were carried out by using the same collision energy and dynamic exclusion settings previously described for the detection of anthocyanins.

General MS³ analysis. This general MS³ analysis was all in all similar to that described for anthocyanins, excepting that the scanned mass range was *m*/*z* 100–2000.

Neutral loss triple play analysis for detecting the loss of carboxylic groups. This analysis included three scan events: *scan event 1*, full MS; scan event 2, MS² of the four most intense ions from *scan event 1* which undergo a neutral loss of 44 amu; and *scan event 3*, MS³ of the most intense ion generated from *scan event 2*. The scanned mass range was *m*/*z* 100–2000.

Neutral loss triple play analysis for detecting the loss of functional groups. In a similar way to the above section, five separate injections (I–V) were run for detecting the loss of different functional groups. In this case, however, the specified losses of neutral fragments were: (I) *m*/*z* 132, 146, 162, 294, 308, 324 and 486 for sugars; (II) *m*/*z* 152 and 170 for gallic or galloyl derivates; (III) *m*/*z* 180 and 302 for hexoside derivatives of hexahydroxydiphenic acid (HHDP), quercetin and ellagic acid; (IV) *m*/*z* 276 and 602 for 3,4,8,9,10-pentahydroxy-dibenzo[b,d]pyran-6-one and gallagyl derivatives; and (V) *m*/*z* 46 for formic acid adducts. In all cases, the scanned mass range was *m*/*z* 100–2000.

3. Results and discussion

3.1. Anthocyanins profiling

Fig. 1A shows the HPLC chromatogram of pomegranate juice acquired at λ = 520 nm, wavelength at which practically only the anthocyanins and anthocyanins adducts are detected. In this chromatogram, the six major peaks (numbered as in Table 1) correspond to the well-known 3-glucoside and 3,5-diglucoside derivatives of the anthocyanidins delphinidin, cyanidin and pelargonidin. A zooming of this chromatogram, as shown in Fig. 1B, reveals the presence of a rather large number of other components that also absorb at this wavelength, thus suggesting that presence of additional anthocyanidin derivatives in pomegranate juice, but at much lower concentrations. Table 1 lists the 65 anthocyanins, flavanol-anthocyanin and anthocyanin–flavanol adducts detected in this work, as well as their chromatographic retention times and MS^n fragmentation patterns.

3.1.1. Colored flavanol-anthocyanin and anthocyanin–flavanol adducts

A total of thirty 3-hexoside and 3,5-dihexoside derivatives of flavanol-anthocyanin and anthocyanin–flavanol adducts were

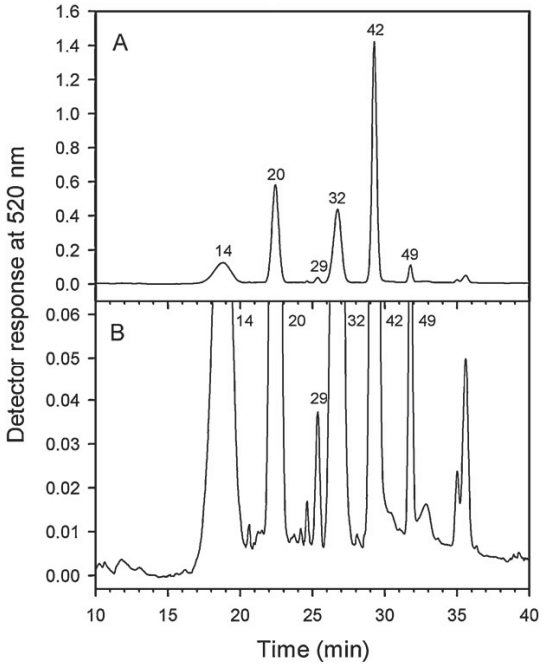

Fig. 1. HPLC chromatogram of pomegranate juice acquired at λ = 520 nm. (A) Normalized standard chromatogram showing the major anthocyanin components: delphinidin-3,5-diglucoside (peak 14), cyanidin-3,5-diglucoside (peak 20), pelargonidin-3,5-diglucoside (peak 29), delphinidin-3-glucoside (peak 32), cyanidin-3-glucoside (peak 42), and pelargonidin-3-glucoside (peak 49). (B) Zoomed chromatogram showing additional minor anthocyanin components.

detected in this work. This number is smaller than the reported one in bibliography for the same variety ("Wonderful") of pomegranate (Sentandreu et al., 2010, 2012), but this discrepancy could be due to the different ripening state of the analyzed fruits and/or to their different origin, California (this work) and Peru. In any case, these components were present at very low concentration.

3.1.2. Tri-substituted anthocyanidin derivatives

As shown in Table 1, peaks 3 and 8 exhibit a molecular ion $[M]^+$ at *m*/*z* 789. Its MS² yields fragments at *m*/*z* 627 ($[M]^+$-162), 465 ($[M]^+$-324) and 303 ($[M]^+$-486), thus indicating a tri-hexoside derivative of delphinidin. This fragmentation sequence, without additional information, is compatible with the structure of delphinidin-3-diglucoside-5-glucoside (Olsen et al., 2010), but in this case the MS³ of the daughter ion at *m*/*z* 627 would yield a lonely ion at *m*/*z* 303 ($[M]^+$-162-324). In our case, however, the MS³ of the daughter ion at *m*/*z* 627 yielded ions at *m*/*z* 465 ($[M]^+$-162-162) and 303 ($[M]^+$-162-162-162), thus indicating a tri-hexoside derivative of delphinidin, but with each hexoside located at a different position within the aglycone structure. To our best knowledge, no one free tri-substituted hexoside derivative of delphinidin has been reported in bibliography from a natural source. Nevertheless, Yoshitama et al. (1975) identified delphinidin-3,7,3′-trihexoside from the deacylation of cineranin, a pigment from the blue flowers of Cineraria (*Senecio cruentus* DC.), whereas Fukuchi-Mizutani et al. (2003) demonstrated that the activity of the specific anthocyanin-3′-O-glucosyltransferases, from Gentian (*Gentiana triflora*) petals, on delphinidin-3,5-diglucoside yields delphinidin-3,5,3′-triglucoside.

Similarly to peaks 3 and 8, peaks 6 and 11 exhibit a molecular ion $[M]^+$ at *m*/*z* 773 and its MS² yields fragments at *m*/*z* 611

Table 1
Anthocyanins detected in pomegranate juice.

Rt (min)	Peak no.	$[M]^+$ (*m*/*z*)	MS^2	MS^3	MS^4	Identification[a]
5.58	1	**931**	**769**, 607	**607**	589, 481, 439, 345, 303	*(epi)gcat-dpd-3,5-dihexoside*
6.88	2	**931**	**769**, 607	**607**	589, 481, 439, 345, 303	*(epi)gcat-dpd-3,5-dihexoside*
7.67	3	**789**	**627**, 465, 303	465, 303		Dpd-trihexoside
7.99	4	**815**	**753**, 591	**591**	573, 465, 423, 329, 287	*(epi)gcat-cyd-3,5-dihexoside*
8.23	5	**627**	**465**, 303	303		Dpd-3,5-dihexoside
8.82	6	**773**	**611**, 449, 287	449, 287		Cyd-trihexoside
10.65	7	**769**	**607**	589, 481, 439, 345, 303		*(epi)gcat-dpd-3-hexoside*
12.17	8	**789**	**627**, 465, 303	465, 303		Dpd-trihexoside
13.82	9	**627**	**465**, 303	303		Dpd-3,5-dihexoside
14.07	10	**915**	**753**, 591	**591**	573, 465, 439, 345, 303	*(epi)cat-dpd-3,5-dihexose*
15.76	11	**773**	**611**, 449, 287	449, 287		Cyd-trihexoside
16.56	12	**753**	**591**	573, 465, 423, 329, 287		*(epi)gcat-cyd-3-hexoside*
17.97	13	**931**	**769**, 607	**607**	589, 481, 439, 345, 303	*(epi)gcat-dpd-3,5-dihexoside*
18.45	14	**627**	**465**, 303	303		*Dpd-3,5-diglucoside*
19.42	15	**899**	**737**, 575	**575**	557, 449, 423, 329, 287	*(epi)cat-cyd-3,5-dihexoside*
19.96	16	**737**	**575**	557, 449, 407, 313, 271		*(epi)gcat-pgd-3-hexoside*
20.69	17	**915**	**753**, 591	**591**	573, 465, 423, 329, 287	*(epi)gcat-cyd-3,5-dihexose*
21.13	18	**769**	**607**	589, 481, 439, 345, 303		*(epi)gcat-dpd-3-hexoside*
21.48	19	**753**	**591**	573, 465, 423, 329, 287		*(epi)gcat-cyd-3-hexoside*
22.17	20	**611**	**449**, 287	287		*Cyd-3,5-diglucoside*
22.23	21	**753**	**591**	573, 465, 439, 345, 303		*(epi)cat-dpd-3-hexoside*
22.48	22	**627**	**465**, 303	303		Dpd-3,5-dihexoside
22.58	23	**737**	**575**	557, 449, 407, 313, 271		*(epi)gcat-pgd-3-hexoside*
23.16	24	**753**	**591**	573, 465, 439, 345, 303		*(epi)cat-dpd-3-hexoside*
23.33	25	**597**	**465**, 435, 303	303		Dpd-3,5-pentoside-hexoside
24.01	26	**915**	**753**, 591	**591**	573, 465, 439, 345, 303	*(epi)cat-dpd-3,5-dihexose*
24.19	27	**883**	**721**, 559	**559**	541, 433, 423, 329, 287	*(epi)afz-cyd-3,5-dihexoside*
24.56	28	**737**	**575**	557, 449, 423, 329, 287		*(epi)cat-cyd-3-hexoside*
25.08	29	**595**	**433**, 271	271		*Pgd-3,5-diglucoside*
25.17	30	**753**	**591**	573, 465, 439, 345, 303		*(epi)cat-dpd-3-hexoside*
26.05	31	**899**	**737**, 575	**575**	557, 449, 423, 329, 287	*(epi)cat-cyd-3,5-dihexoside*
26.51	32	**465**	303			*Dpd-3-glucoside*
26.61	33	**581**	**449**, 419, 287	287		*Cyd-3,5-pentoside-hexoside*
26.78	34	**721**	**559**	541, 433, 407, 313, 271		*(epi)cat-pgd-3-hexoside*
26.87	35	**737**	**575**	557, 449, 423, 329, 287		*(epi)cat-cyd-3-hexoside*
27.33	36	**611**	**465**, **449**, 303, 287	465→303		Dpd-3-rutinoside
	37			449→287		Cyd-3,5-caffeoyl-hexoside
27.72	38	**627**	**465**, 303	303		Dpd-3,5-caffeoyl-hexoside
28.49	39	**753**	**591**	573, 423		Cyd-3-hexoside-(epi)gcat
28.83	40	**721**	**559**	541, 433, 423, 329, 287		*(epi)afz-cyd-3-hexoside*
28.91	41	**737**	**575**	557, 449, 439, 345, 303		*(epi)afz-dpd-3-hexoside*
29.12	42	**449**	287			*Cyd-3-glucoside*
29.82	43	**565**	**433**, 403, 271	271		Pgd-3,5-pentoside-hexoside
29.95	44	**595**	**449**, 287	287		*Cyd-3-rutinoside*
30.65	45	**595**	**433**, 271	271		Pgd-3,5-caffeoyl-hexoside
30.83	46	**449**	287		Cyd-3-hexoside	
30.99	47	**705**	**543**	525, 417, 407, 313, 271		*(epi)afz-pgd-3-hexoside*
31.54	48	**721**	**559**	541, 433, 423, 329, 287		*(epi)afz-cyd-3-hexoside*
31.76	49	**433**	271			*Pgd-3-glucoside*
32.83	50	**435**	303		Dpd-3-pentoside	
32.98	51	**611**	**449**, 287	287		Cyd-3,5-caffeoyl-hexoside
33.62	52	**705**	**543**	525, 417, 407, 313, 271		*(epi)afz-pgd-3-hexoside*
34.02	53	**611**	**449**, 287	287		Cyd-3,5-caffeoyl-hexoside
35.23	54	**419**	287			*Cyd-3-pentoside*
35.78	55	**419**	287			*Cyd-3-pentoside*
35.81	56	**737**	**575**	557, 423		*Cyd-3-hexoside-(epi)cat*
37.18	57	**403**	271		Pgd-3-pentoside	
39.10	58	**465**	303		Dpd-caffeoyl	
39.54	59	**721**	**559**	541, 423		*Cyd-3-hexoside-(epi)afz*
44.90	60	**449**	287		Cyd-caffeoyl	
46.15	61	**627**	**465**, 303	303		Dpd-3,5-caffeoyl-hexoside
46.83	62	**611**	303		Dpd-3-(p-coumaroyl)hexoside	
47.33	63	**611**	**449**, 287	287		Cyd-3,5-caffeoyl-hexoside
47.61	64	**595**	287		Cyd-3-(p-coumaroyl)hexoside	
48.37	65	**465**	303		Dpd-caffeoyl	

Only those ions with relative abundance greater than 10% are shown. *Abbreviations used*: dpd, delphinidin; cyd, cyanidin; pgd, pelargonidin; (epi)gcat, (epi)gallocatechin; (epi)cat, (epi)catechin; (epi)afz, (epi)afzelechin; Rt, retention time; $[M]^+$, molecular mass under positive ionization conditions; *m*/*z*, mass-to-charge ratio; MS^n, tandem mass spectrometry level reached. Each successive MS^n analysis applies on the ion shown in bold in the preceding column, and the result is given in its own column.

[a] Components in italic have been previously reported in pomegranate juice (Seeram et al., 2006; Sentandreu et al., 2010, 2012; Fischer et al., 2011).

($[M]^+$-162), 449 ($[M]^+$-324) and 287 ($[M]^+$-486), thus indicating a tri-hexoside derivative of cyanidin. As in the above case, this MS^2 fragmentation is compatible with the structure of cyanidin-3-diglucoside-5-glucoside (Wu and Prior, 2005), but the MS^3 of the daughter ion at *m*/*z* 611 yielded ions at *m*/*z* 449 ($[M]^+$-162-162) and at *m*/*z* 287 ($[M]^+$-162-162-162), thus indicating a tri-substituted hexoside derivative of cyanidin. Again, no one free tri-substituted hexoside derivative of cyanidin has been reported

in bibliography from natural sources, although Yoshitama and Abe (1977) detected cyanidin-3,7,3′-trihexoside after deacetylation of an extract from the red petals of Cirenaria, as well as Tatsuzawa et al. (1994) when studying the red flowers of Cattleya and Laelia (*xLaeliocattleya* cv mini purple).

3.1.3. Di-substituted anthocyanidin derivatives

In addition to the major and well-known 3,5-diglucoside derivatives of delphinidin (peak 14), cyanidin (peak 20) and pelargonidin (peak 29), some additional di-substituted "hexoside" derivatives of delphinidin (peaks 5, 9, 22, 38 and 61), cyanidin (peaks 37, 51, 53 and 63) and pelargonidin (peak 45) were also detected. These components exhibited the same characteristic fragmentation pattern than the known di-substituted hexoside derivatives of anthocyanidins, that is, the loss of two consecutive 162 amu and the releasing of the characteristic ion of the aglycone. Therefore, they would correspond to different substitutions of the anthocyanidins with galactose/glucose/caffeoyl moieties, located at different positions within the aglycone structure (normally at positions 3 and 5).

Moreover, several di-substituted glycoside derivatives of anthocyanidins were also detected, namely delphinidin-3,5-pentoside-hexoside (peak 25), the previously reported (Fischer et al., 2011) cyanidin-3,5-pentoside-hexoside (peak 33), cyanidin-3,5-caffeoyl-hexoside (peak 37), and pelargonidin-3,5-pentoside-hexoside (peak 43).

3.1.4. Mono-substituted anthocyanidin derivatives

In addition to the major and well-known 3-glucoside derivatives of delphinidin (peak 32), cyanidin (peak 42) and pelargonidin (peak 49), some other minor "hexoside" derivatives of delphinidin (peaks 58 and 65) and cyanidin (peaks 46 and 60) were also detected. With respect to other mono-glycoside derivatives, the following components were also detected: delphinidin-3-pentoside (peak 50), the previously reported (Fischer et al., 2011) cyanidin-3-pentoside (peaks 54 and 55), and pelargonidin-3-pentoside (peak 57).

Moreover, the following mono-substituted "diglycoside" derivatives of anthocyanidins were detected: delphinidin-3-rutinoside (peak 36), the previously reported (Seeram et al., 2006; Fischer et al., 2011) cyanidin-3-rutinoside (peak 44), delphinidin-3-(*p*-coumaroyl)hexoside (peak 62) and cyanidin-3-(*p*-coumaroyl)-hexoside (peak 64).

The molecular ion corresponding to peaks 62 and 64 was *m*/*z* 611 and 595, respectively. Although these *m*/*z* values are typical for cyanidin and pelargonidin "dihexoside" derivatives, their MS^2 analysis revealed a loss of 308 amu and the releasing of the delphinidin and cyanidin aglycones at *m*/*z* 303 and 287, respectively. These data, in conjunction with the lacking of the typical ion for anthocyanidin rutinosides at *m*/*z* ($[M]^+$-146) and the noticeable delay of their retention times, suggested the presence of an acylated hexoside. Since similar results were reported by Wu et al. (2004) when determining the anthocyanins in black currant, peaks 62 and 64 were identified as delphinidin-3-(*p*-coumaroyl)-hexoside and cyanidin-3-(*p*-coumaroyl)hexoside, respectively.

The mass spectrum of the chromatographic peak eluting at 27.33 min showed a single molecular ion at *m*/*z* 611. However, its MS^2 fragmentation yielded daughter ions at *m*/*z* 465, 449, 303 and 287, being the ion at *m*/*z* 449 by far more intense than that at *m*/*z* 465. The main ion fragmentation sequence, *m*/*z* 611 → 449 → 287, was widely documented from the programmed general data dependent MS^n experiments. Therefore, taking into account its delayed retention time, this component was tentatively identified as cyanidin-3,5-caffeoyl-hexoside (peak 37). On the contrary, the other minor sequence, most probably *m*/*z* 611 → 465 → 303, was not documented at all from the same general MS^n experiments. Finally, this sequence was confirmed from the run (III) of the MS^3 specific analysis for the detection of rutinoside derivatives of anthocyanidins, thus allowing the detection of delphinidin-3-rutinoside (peak 36).

3.2. Non-anthocyanins phenolic profiling

Fig. 2A shows the HPLC chromatogram of pomegranate juice acquired at λ = 320 nm, wavelength at which the anthocyanins exhibit a weak absorbance. In this chromatogram, the six major peaks (numbered as in Table 2) correspond to a punicalin derivative (*m*/*z* 1101, peak 19), punicalagin (peaks 49 and 57), ellagic acid-hexoside dimmer (peak 62), granatin B (peak 79) and ellagic acid (peak 83). As in the case of anthocyanins, a zooming of this chromatogram, as shown in Fig. 2B, reveals the presence of a rather large number of other components that also absorbs at this wavelength, thus indicating that additional non-anthocyanins phenolic components are also present in pomegranate juice, but at lower concentrations. Table 2 lists the 86 non-anthocyanin phenols determined in this work, as well as their chromatographic retention times and MS^n fragmentation patterns.

As pointed out by Fischer et al. (2011), the major non-anthocyanin phenolic component of pomegranate juice is punicalagin (peaks 49 and 57), whose mass spectrum exhibit a molecular ion at *m*/*z* 1083, but also a minor one at *m*/*z* 541, which corresponds to the double charged molecular ion. Some other minor components, namely peaks 29, 33 and 34, also exhibited a deprotonated molecular ion at *m*/*z* 1083, but the ion corresponding to the double charged deprotonated molecular ion at *m*/*z* 541 was lacking in their corresponding mass spectrum. Moreover, the MS^n fragmentation pattern of these components was clearly different

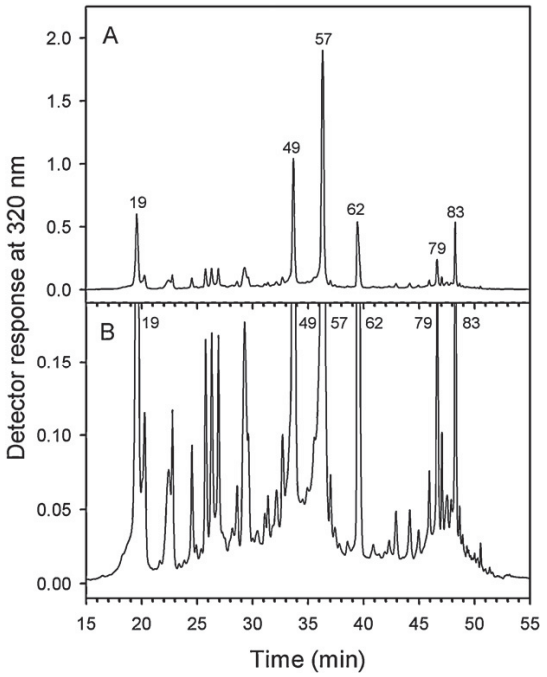

Fig. 2. HPLC chromatogram of pomegranate juice acquired at λ = 320 nm. (A) Normalized standard chromatogram showing the major non-anthocyanin phenolic components: a punicalin derivative (peak 19), punicalagin (peaks 49 and 57), ellagic acid-hexoside dimmer (peak 62), granatin B (peak 79) and ellagic acid (peak 83). (B) Zoomed chromatogram showing additional minor non-anthocyanin phenolic components.

Table 2
Non-anthocyanin phenols detected in pomegranate juice.

Rt (min)	Peak no.	[M−H] (*m*/*z*)	MS^2	MS^3	Identification[a]
5.20	1	**191**	173, **111**	67	Citric acid
5.27	2	**481**	**301**, 275	301, 257, 229	*HHDP-hexoside*
5.86	3	**649**	497, **301**	301, 257, 229	*Lagerstannin C*
6.38	4	**801**	**757**, 481, 301, 275	481, 301, 275	Ellagitannin
6.54	5	**481**	**301**, 275	301, 257, 229	*HHDP-hexoside*
7.03	6	**537** (FA)	491, **329**, 167	209, 167	Vanillic acid-dihexoside
7.52	7	**331**	271, 211, 193, **169**, 151, 125	125	*Monogalloyl-hexoside*
8.47	8	**331**	**271**, 169	169	*Monogalloyl-hexoside*
8.83	9	**801**	**757**, 481, 301, 275	481, 301, 275	Ellagitannin
9.76	10	**969**	**925**, 881, 623, 481, 399	881, 579, 481, 399, 301	Ellagitannin
11.17	11	**331**	**271**	211, 169, 125	*Monogalloyl-hexoside*
13.48	12	**633**	**301**, 275, 249	301, 257, 229	*Galloyl-HHDP-hexoside*[b]
13.78	13	**805**	**643**, 625, 481, 463	517, 481, 463, 355, 301, 283	Ellagitannin
13.86	14	**649**	497, **301**	301, 257, 229	*Lagerstannin C*
16.45	15	**649**	**605**, 301	481, 421, 301	Ellagitannin
17.52	16	**483**	**331**, 313, 169	271, 211, 193, 169	*Digalloyl-hexoside*
18.70	17	**643**	481, **463**, 355, 301, 283	301, 300, 283	Ellagitannin
19.12	18	**625**	**463**, 301	301, 257, 191	*Ellagic acid-dihexoside*
19.95	19	**1101**	1057, **781**, 721, 601	721, 601	Punicalin derivative
20.15	20	**633**	**301**, 275, 249	301, 257, 229	*HHDP-galloylhexoside*[b]
20.34	21	**803**	**759**, 483, 275	483, 331, 275	Gallotannin
20.55	22	**1101**	1057, **781**, 721, 601	721, 601	Punicalin derivative
20.97	23	**329**	269, 209, 181, **167**	152, 123, 108	*Vanillic acid-4-O-hexoside*
21.18	24	**649**	497, **301**	301, 257, 229	*Lagerstannin C*
22.84	25	**643**	**481**	355, 319, 301, 257, 193, 175	Ellagitanin
23.23	26	**483**	**331**, 313, 169	271, 211, 193, 169	*Digalloyl-hexoside*
23.47	27	**341**	**179**, 135	135	*Caffeic acid-hexoside*
24.54	28	**783**	481, **301**, 275	301, 257, 229	*Pedunculagin I*
24.64	29	**1083**	1065, 1021, 959, 807, **601**, 575	301, 299	Gallagyl ester
25.55	30	**783**	481, **301**, 275	301, 257, 229,	*Pedunculagin I*
25.85	31	**341**	**179**, 161, 135	135	*Caffeic acid-hexoside*
25.93	32	**633**	421, **301**, 275	301, 275, 229	*Galloyl-HHDP-hexose*[b]
25.97	33	**1083**	1021, 1003, 959, 807, 721, **601**, 575	583, 301, 299, 271	Gallagyl ester
26.41	34	**1083**	1065, 1021, **807**, 721, 601, 575	763, 601, 575, 549, 425, 301, 299	Gallagyl ester
26.58	35	**463**	**301**, 300	300, 283, 257, 229	*Ellagic acid-hexoside*
27.54	36	**803**	**759**, 483, 275	483, 331, 275	Gallotannin
27.62	37	**933**	915, 781, **721**, 601, 451	601	Galloyl-gallgyl-hexoside (Pedunculagin III)
27.99	38	**1415**	1397, 933, **783**, 763, 633, 613	721, 645, 481, 341, 301	Pedunculagin I derivative
28.67	39	**933**	781, **721**, 601	601	Galloyl-gallagyl-hexoside (Pedunculagin III)
29.67	40	**469**	**425**	425, 407, 300	*Valoneic acid bilactone*
30.05	41	**951**	**907**	783, 481, 301	Pedunculagin I derivative
30.34	42	**341**	281, 251, 221, **179**, 135	135	*Caffeic acid-hexoside*
30.67	43	**461** (FA)	**415**	269, 161	Apigenin-rhamnoside
31.11	44	**325**	187, **163**, 145, 119	119	Coumaric acid-hexoside
31.53	45	**633**	481, 421, **301**, 275	301, 257, 229	*Galloyl-HHDP-hexoside*[b]
31.88	46	**783**	481, **301**, 275	301, 257, 229	*Bis-HHDP-hexoside (pedunculagin I)*
32.44	47	**951**	**907**	889, 783, 605, 481, 301, 271	Ellagitannin
32.66	48	**1265**	1247, 933, **783**, 781, 763, 745, 481	481, 421, 301, 275, 257, 229	Pedunculagin I derivative
33.71	49	**1083**/541	**781**, 721, **601**, 575	781→721, 601, 299 601→299, 271	*Punicalagin*
34.39	50	**951**	**907**	889, 783, 605, 481, 301, 271	Ellagitannin
34.51	51	**291**	**247**	203	*Brevifolin carboxylic acid*
34.66	52	**1265**	1247, 933, **783**, 763, 745	301, 275, 245, 229	Pedunculagin I derivative
35.38	53	**633**	**301**, 275	301, 275, 229	*Galloyl-HHDP-hexoside*[b]
35.55	54	**1415**	1397, 933, **783**, 763, 633, 613	481, 359, 301, 275, 257	Pedunculagin I derivative
35.83	55	**799**	781, **479**, 301	461, 451, 435, 299, 287, 273	*Granatin A/Lagerstannin A*
35.96	56	**785**	633, 615, 483, **301**	301, 257, 229	*Digalloyl-HHDP-hexoside*
36.21	57	**1083**/541	**781**, 721, **601**, 575	781→721, 601, 299 601→299, 271	*Punicalagin*
36.82	58	**1417**	**785**, 765, 633, 613, 451	483, 419, 401, 301, 275, 231	Ellagitannin
37.32	59	**1083**	781, 721, **601**, 575	299, 271	*Punicalagin*
37.67	60	**801**	649, 499, 347, **301**	301, 257	*Punigluconin*
38.86	61	**801**	649, 499, 347, **301**	301→301, 257 649→497, 301	*Punigluconin*
39.12	62	**463/927**	463→**301** 927→463, 301	301→301, 257, 229	Ellagic acid-hexoside dimmer
39.16	63	**633**	463, **301**, 275	301, 257, 229	*Galloyl-HHDP-hexoside*[b]
39.24	64	**463**	**301**	301, 257, 229	*Ellagic acid hexoside*
39.28	65	**935**	659, **633**, 571, 301	571, 301	*Galloyl-bis-HHDP-hexoside (casuarinin)*
40.61	66	**1085**	**933**, 915, 719, 601, 575, 549	781,721, 601, 549, 299	Digalloyl-gallagyl-hexoside
41.30	67	**783**	**765**, 301, 275	597, 301, 275	*Pedunculagin I*

Table 2 (*Continued*)

Rt (min)	Peak no.	[M−H] (*m*/*z*)	MS^2	MS^3	Identification[a]
41.39	68	**507**	**345**, **327**, 315	327→312, 296, 283, 268 345→327, 315	Syringetin-hexoside
41.98	69	**785**	767, 633, 483, 419, **301**	301, 257, 229	*Digalloyl-HHDP-hexoside*
42.77	70	**1085**	783, **765**	597, 301, 275	Tri-HHDP-hexoside
43.01	71	**783**	**765**, 481, **301**	765→746, 301, 299 301→275, 229	*Pedunculagin I*
43.97	72	**1085**	783, **765**	597, 301	Tri-HHDP-hexoside
44.79	73	**468**	**425**	301, 299	*Valoneic acid bilactone*
45.34	74	**953**	**935**, 463, 301	891, 463, 343, 301	Ellagitannin
45.54	75	**785**	633, 615, 483, 419, **301**, 275, 249	301, 257, 229	*Digalloyl-HHDP-hexoside*
45.65	76	**615**	**463**, 301	301, 257	Ellagic acid-galloyl-hexoside
45.68	77	**433**	**301**	301, 300, 257, 229	*Ellagic acid-pentoside*
45.80	78	**507**	489, **345**, **327**, 315	327→312, 296, 283, 268 345→327, 315	Syringetin-hexoside
46.01	79	**951**	**933**, 631, **613**, 301	933→631, 613, 301 613→301, 299	*Granatin B*
46.39	80	**447**	**301**, 300	301, 300, 257, 229	*Ellagic acid-rhamnoside*
46.50	81	**433**	300, **301**	300, 301	*Ellagic acid-pentoside*
47.45	82	**601**	**299**, 271	271	Gallagic acid
48.08	83	**301**	**301**, 257, 229	301, 257, 229	*Ellagic acid*
49.98	84	**609**	**463**, 445, **301**	301→257 463→301	Ellagic acid-(*p*-coumaroyl)hexoside
52.32	85	**449**	**431**, 287	287	*Dihydrokaempferol-hexoside*
52.82	86	**593**	445, **301**	301, 300, 257	Ellagitannin

Only those ions with a relative abundance greater than 10% are shown. (FA), detected as formic acid adduct. Each successive MS^n analysis applies on the ions shown in bold in the preceding column, and the result is given in its own column. *Abbreviations used*: Rt, retention time; [M−H] , molecular mass under negative ionization conditions; *m*/*z*, mass-to-charge ratio; MS^n, tandem mass spectrometry level reached; HHDP, hexahydroxydiphenic acid.

[a] Components in italic have been previously reported by Fischer et al. (2011).

[b] The ion at *m*/*z* 633 could correspond to corilagin, strictinin or punicacortein A/B.

from that of punicalagin (see Table 2), and the presence as main fragments of the specific daughter ions at *m*/*z* 601 and *m*/*z* 301/299 clearly suggested for them a structure of gallagyl derivative, most probably ester.

When the ion at *m*/*z* 1101 was searched across the total ion current (TIC) chromatogram (Fig. 3A), two significant peaks were found (Fig. 3B), one of them corresponding to the aforementioned

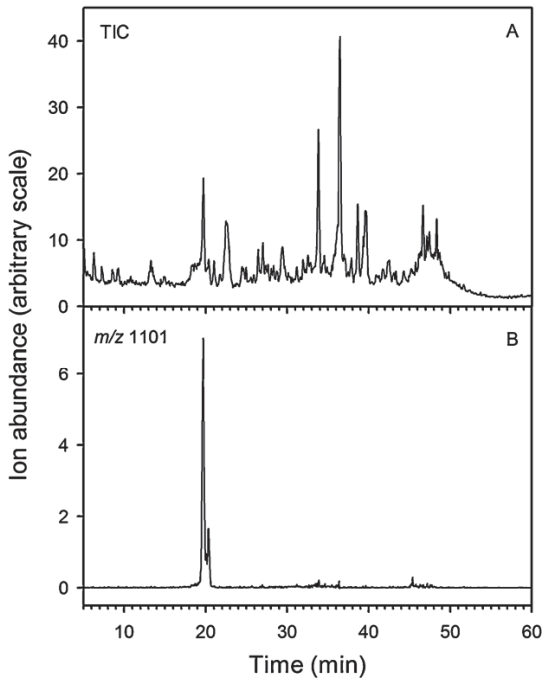

Fig. 3. (A) Total ion current (TIC) chromatogram of pomegranate juice under negative ESI ionization mode. (B) Single ion monitoring (SIM) chromatogram corresponding to the extraction of the ion with *m*/*z* 1101 from the TIC chromatogram.

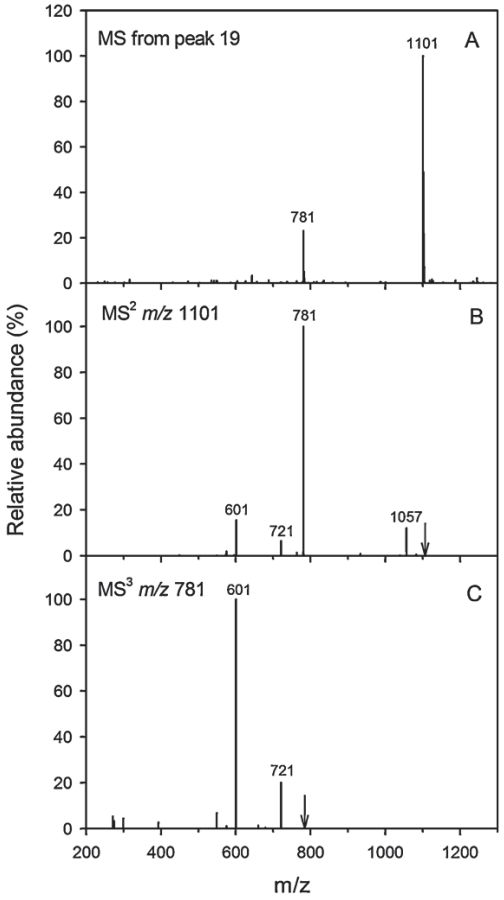

Fig. 4. MS^n analysis of the parent ion at *m*/*z* 1101 (peaks 19 and 22, punicalin derivatives). (A) Full MS of the ion at *m*/*z* 1101; (B) MS^2 of the ion at *m*/*z* 1101; (C) MS^3 of the major daughter ion at *m*/*z* 781 (arrows show targeted *m*/*z*'s for the MS^2 and MS^3 analyses).

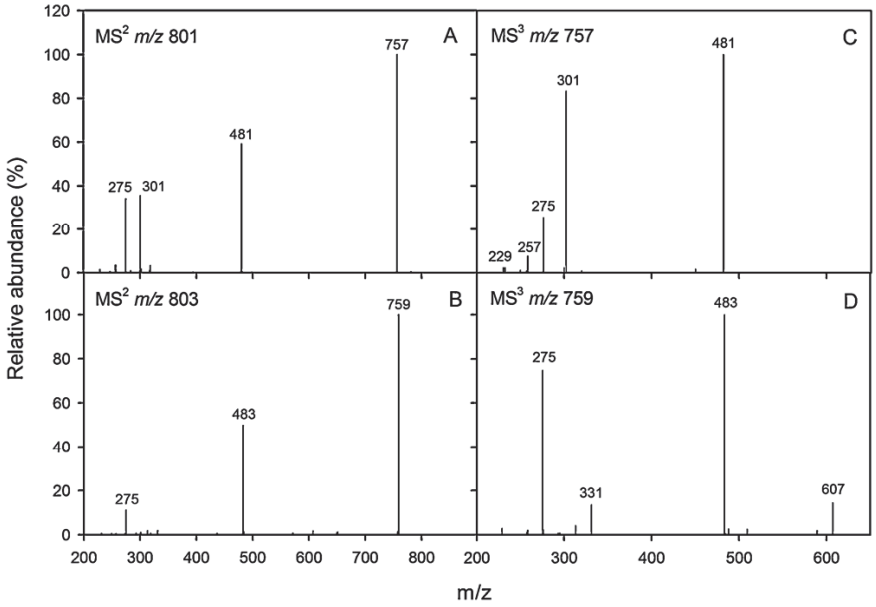

Fig. 5. MS^n analysis of the parent ions at *m/z* 801 (peaks 4 and 9) and 803 (peaks 21 and 36). (A) MS^2 of the parent ion at *m/z* 801; (B) MS^2 of the parent ion at *m/z* 803; (C) MS^3 of the major daughter ion at *m/z* 757 from the MS^2 of the parent ion at *m/z* 801; (D) MS^3 of the major daughter ion at *m/z* 759 from the MS^2 of the parent ion at *m/z* 803.

peak 19 and the other to the minor peak 22. The MS spectrum of both compounds were very similar, Fig. 4A, showing a deprotonated molecular ion at *m/z* 1101 and a minor one at *m/z* 781, thus suggesting their close relationship with punicalin. Hence, the MS^2 of *m/z* 1101 (Fig. 4B) yielded ions at *m/z* 1057, 781, 721 and 601, whilst the MS^3 of the main fragment at *m/z* 781 (Fig. 4C) yielded ions at *m/z* 721 and 601. Borges et al. (2010) cited the presence of a component with a rather similar MS^n fragmentation pattern, excepting that the ion at *m/z* 1057 ([M−H] -44) (loss of a carboxyl group) was lacking, and suggested for it a structure of punicalagin derivative. In our case, however, taking into account the presence of the ions at *m/z* 1057, 721 and 601, as well as that the main fragment ion from the MS^2 of the deprotonated molecular ion was *m/z* 781 ([M−H] -44-276) for both components, it seems more appropriate to tentatively identify them as punicalin derivatives. On the other hand, the observed difference of 276 amu between the ions at *m/z* 1057 and *m/z* 781 (the punicalin ion) deserves special attention. This mass most probably correspond to 3,4,8,9,10-pentahydroxy-dibenzo[b,d]pyran-6-one which, similarly to breviofolin and chebullic acid, is a biosynthetic transformation product from hexahydroxydiphenic acid (Nawwar and Souleman, 1984). Moreover, when Ito (2011) identified the metabolites formed during the metabolism of geraniin in rats, proposed 3,4,8,9,10-pentahydroxy-dibenzo[b,d]pyran-6-one to be a direct metabolism product of ellagic acid which, in its turn, comes from gallic acid in the shikimic acid biosynthetic pathway (Ishikura et al., 1984). Finally, Nawwar et al. (1994) cited the presence of this compound in the leaves of Egyptian pomegranates. In spite of this, 3,4,8,9,10-pentahydroxy-dibenzo[b,d]pyran-6-one could not be detected as a free component in pomegranate juice.

Although the gallagyl group is a part of the chemical structure of many of the phenols that are commonly found in pomegranate juice, such as punicalin and punicalagin derivatives, its presence as free gallagic acid has only been referenced in peel extracts (Zahin et al., 2010). Hence, its detection in pomegranate juice (peak 82) could be due to the pressure applied to the whole fruit during the extraction step. In addition, some gallagic acid derivatives, such as pedunculagin III (peaks 37 and 39) and digalloyl-gallagyl-hexoside (peak 66), were detected for the first time in pomegranate juice.

Similarly to peaks 19 and 22, the main transition from the MS^2 of peaks 4 and 9 (*m/z* 801) and 21 and 36 (*m/z* 803) was the release of a neutral fragment of 44 amu (carboxylic group), yielding major fragments at *m/z* 757 (Fig. 5A) and at *m/z* 759 (Fig. 5B), respectively. Moreover, the main transition from the MS^3 of ions at *m/z* 757 and *m/z* 759 was again the releases of a neutral fragment of 276 amu, yielding major fragments at *m/z* 481 (Fig. 5C) and at *m/z* 483 (Fig. 5D). Although both groups of components shared the fragment at *m/z* 275, the MS^3 of peaks 4 and 9 (Fig. 5C) showed also the presence of ions at *m/z* 301, 257 and 229, clearly suggesting that they were ellagic acid derivatives. In contrast, in the MS^3 of peaks 21 and 36 (Fig. 5D) the ion at *m/z* 301 was lacking, but there were ions at *m/z* 607 (loss of a galloyl group) and at *m/z* 331 (galloyl-hexoside), thus indicating the gallotannin nature of both components. It is remarkable the different behavior of the neutral fragment of 276 amu from peaks 19/22 and peaks 4/9/21/36. Although in all cases a neutral fragment of 44 amu followed by an additional fragment of 276 u were released, the ion at *m/z* 275 could be observed in the MS^n spectra from peaks 4/9/21/36, but not in those from peaks 19/22. A plausible explanation could be that whilst 3,4,8,9,10-pentahydroxy-dibenzo[b,d]pyran-6-one (probably carrying a carboxylic acid) is part of the basic structure of components 4, 9, 21 and 36, and hence it is finally generated during their MS^n fragmentation, it is a mere substituent in components 19 and 22.

Several ellagic acid derivatives were detected as new components in pomegranate juice, such as pedunculagin I derivatives (peaks 38, 41, 48, 52 and 54), a dimmer of ellagic acid-hexoside (peak 62), tri-HHDP-hexoside (peaks 70 and 72), ellagic acid-galloyl-hexoside (peak 76), and ellagic acid-(*p*-coumaroyl)glucoside (peak 84). Moreover, additional components with ellagitannin structure were peaks 10, 13, 17, 25, 47, 50, 58, 74 and 86, all them sharing the ion at *m/z* 301 in their respective MS^n fragmentation patterns. The structures of these later components were determined from the generation of typical ion fragments in their MS^n spectrum, such as *m/z* 783 (pedunculagin I), 633 (HHDP-galloylhexoside), 481

(HHDP-hexoside) and 463 (ellagic acid-hexoside), which came from the loss of different functional groups (mainly hexosides).

It is of major importance to take into account, as stated by Fischer et al. (2011) that the ion at *m*/*z* 301 can correspond to both ellagic acid and quercetin. Therefore, it must be checked before the final assignment of a chemical structure to a component. The MS^n of *m*/*z* 301 yields fragments at *m*/*z* 257, 229 and 185 when it corresponds to ellagic acid and at *m*/*z* 179 and 151 when it corresponds to quercetin. Another consideration that must be taken into account is the capacity of HHDP to lactonize to ellagic acid. Hence, the HHDP derivatives, normally glycosides, exhibit a molecular mass 18 u higher than their respective ellagic acid counterparts, such as peaks 5 (*m*/*z* 481, HHDP-hexoside) and 37 (*m*/*z* 463, ellagic acid-hexoside).

Additionally, some other families of chemicals were also detected, such as phenolic acid derivatives, organic acids and flavonoids. Among them, vanillic acid-dihexoside (peak 6), apigenin-rhamnoside (peak 43), coumaric acid-hexoside (peak 44) and syringetin-hexoside (peaks 68 and 78) were detected for the first time in pomegranate juice.

4. Conclusions

Pomegranate juice has been characterized as a function of its profiles in anthocyanin and non-anthocyanin phenols. An exhaustive methodology of analysis, using different scan modes for mass analysis featured by a conventional three-dimensional ion trap analyzer, has been developed, thus making possible the detection of a total of 151 phenols, 64 not previously reported in pomegranate juice including several cyanidin and pelargonidin tri-hexoside derivatives, which have been detected as free forms from a natural source for the first time.

Acknowledgements

This research was supported by the Ministerio de Ciencia e Innovación (MICINN, Spain), project AGL2009-11805. Authors acknowledge the financial support for the contracts of E. Sentandreu (JAEdoc Program, CSIC-FEDER funds) and M. Cerdán-Calero (JAE-predoc program, CSIC-FEDER funds). Authors also thank Dr. José L. Navarro for his assessment during the planning of the present work.

References

Alighourchi, H., Barzegar, M., Abbasi, S., 2008. Anthocyanins characterization of 15 Iranian pomegranate (*Punica granatum* L.) varieties and their variation after cold storage and pasteurization. European Food Research and Technology 227 (3), 881–887.

Borges, G., Mullen, W., Crozier, A., 2010. Comparison of the polyphenolic composition and antioxidant activity of European commercial fruit juices. Food & Function 1 (1), 73.

Du, C.T., Wang, P.L., Francis, F.J., 1975. Anthocyanins of pomegranate, *Punica granatum*. Journal of Food Science 40 (2), 417–418.

Elfalleh, W., Tlili, N., Nasri, N., Yahia, Y., Hannachi, H., Chaira, N., Ying, M., 2011. Antioxidant capacities of phenolic compounds and tocopherols from Tunisian pomegranate (*Punica granatum*) fruits. Journal of Food Science 76 (5), 707–713.

Fischer, U.A., Carle, R., Kammerer, D.R., 2011. Identification and quantification of phenolic compounds from pomegranate (*Punica granatum* L.) peel, mesocarp, aril and differently produced juices by HPLC-DAD–ESI/MS^n. Food Chemistry 127 (2), 807–821.

Fountain, S.T., 2002. A mass spectrometry primer. In: Rossi, D.T., Sinz, M.W. (Eds.), Mass Spectrometry in Drug Discovery. Marcel Dekker Inc., New York, USA, pp. 25–84.

Fukuchi-Mizutani, M., Okuhara, H., Fukui, Y., Nakao, M., Katsumoto, Y., Yonekura-Sakakibara, K., Kusumi, T., 2003. Biochemical and molecular characterization of a novel UDP-glucose:anthocyanin 3′-O-glucosyltransferase, a key enzyme for blue anthocyanin biosynthesis, from Gentian. Plant Physiology 132 (3), 1652–1663.

Gil, M.I., Tomas-Barberan, F.A., Hess-Pierce, B., Holcroft, D.M., Kader, A.A., 2000. Antioxidant activity of pomegranate juice and its relationship with phenolic composition and processing. Journal of Agricultural and Food Chemistry 48 (10), 4581–4589.

Ishikura, N., Hayashida, S., Tazaki, K., 1984. Biosynthesis of gallic and ellagic acids with 14C-labeled compounds in Acer and Rhus leaves. The Botanical Magazine Tokyo 97 (3), 355–367.

Ito, H., 2011. Metabolites of the ellagitannin geraniin and their antioxidant activities. Planta Medica 77 (11), 1110–1115.

Kantharaj, E., Tuytelaars, A., Proost, P.E.A., Ongel, Z., Van Assouw, H.P., Gilissen, R.A.H.J., 2003. Simultaneous measurement of drug metabolic stability and identification of metabolites using ion-trap mass spectrometry. Rapid Communications in Mass Spectrometry 17, 2661–2668.

Kaur, C., Kapoor, H.C., 2001. Antioxidants in fruits and vegetables – the millennium's health. International Journal of Food Science & Technology 36, 703–725.

Madrigal-Carballo, S., Rodriguez, G., Krueger, C., Dreher, M., Reed, J., 2009. Pomegranate (*Punica granatum*) supplements: authenticity, antioxidant and polyphenol composition. Journal of Functional Foods 1 (3), 324–329.

Nawwar, M., Souleman, A., 1984. 3,4,8,9,10-Pentahydroxy-dibenzo[b,d]pyran-6-one from *Tamarix nilotica*. Phytochemistry 23 (12), 2966–2967.

Nawwar, M.A., Hussein, S.A., Merfort, I., 1994. NMR spectral analysis of polyphenols from *Punica granatum*. Phytochemistry 36 (3), 793–798.

Olsen, H., Aaby, K., Borge, G.I.A., 2010. Characterization, quantification, and yearly variation of the naturally occurring polyphenols in a common red variety of curly kale (*Brassica oleracea* L. convar. acephala var. sabellica cv. 'Redbor'). Journal of Agricultural and Food Chemistry 58 (21), 11346–11354.

Seeram, N.P., Zhang, Y., Reed, J.D., Krueger, C.G., Vaya, J., 2006. Pomegranate phytochemicals. In: Seeram, N.P., Schulman, R.N., Heber, D. (Eds.), Pomegranates: Ancient Roots to Modern Medicine. CRC Press, Taylor & Francis Group, Boca Raton, FL, USA, pp. 4–27.

Sentandreu, E., Navarro, J.L., Sendra, J.M., 2010. LC-DAD-ESI/MS^n determination of direct condensation flavanol–anthocyanin adducts in pressure extracted pomegranate (*Punica granatum* L.) juice. Journal of Agricultural and Food Chemistry 58 (19), 10560–10567.

Sentandreu, E., Navarro, J.L., Sendra, J.M., 2012. Identification of new coloured anthocyanin–flavanol adducts in pressure-extracted pomegranate (*Punica granatum* L.) juice by high-performance liquid chromatography/electrospray ionization mass spectrometry. Food Analytical Methods 5 (4), 702–709.

Tatsuzawa, F., Saito, N., Yokoi, M., Shigihara, A., Honda, T., 1994. An acylated cyanidin glycoside in the red–purple flowers of x Laeliocattleya cv mini purple. Phytochemistry 37 (4), 1179–1183.

Wu, X., Gu, L., Prior, R.L., McKay, S., 2004. Characterization of anthocyanins and proanthocyanidins in some cultivars of ribes, aronia, and sambucus and their antioxidant capacity. Journal of Agricultural and Food Chemistry 52 (26), 7846–7856.

Wu, X., Prior, R.L., 2005. Identification and characterization of anthocyanins by high-performance liquid chromatography–electrospray ionization–tandem mass spectrometry in common foods in the united states: vegetables, nuts, and grains. Journal of Agricultural and Food Chemistry 53 (8), 3101–3113.

Yoshitama, K., Abe, K., 1977. Chromatographic and spectral characterization of 3′-glycosylation in anthocyanidins. Phytochemistry 16 (5), 591–593.

Yoshitama, K., Hayashi, K., Abe, K., Kakisawa, H., 1975. Further evidence for the glycoside structure of cinerarin. The Botanical Magazine Tokyo 88 (3), 213–217.

Zahin, M., Aqil, F., Ahmad, I., 2010. Broad spectrum antimutagenic activity of antioxidant active fraction of *Punica granatum* L. peel extracts. Mutation Research – Genetic Toxicology and Environmental Mutagenesis 703 (2), 99–107.

Zhang, Y., Krueger, D., Durst, R., Lee, R., Wang, D., Seeram, N., Heber, D., 2009. International multidimensional authenticity specification (IMAS) algorithm for detection of commercial pomegranate juice adulteration. Journal of Agricultural and Food Chemistry 57 (6), 2550–2557.

Article

FOOD SCIENCE AND TECHNOLOGY INTERNATIONAL

Determination of the antiradical activity and kinetics of pomegranate juice using 2,2-diphenylpicyrl-1-hydrazyl as the antiradical probe

Manuela Cerdán-Calero, José M Sendra and Enrique Sentandreu

Abstract

Whole fruit pomegranate (*Punica granatum* L.) juice of the 'Wonderful' cultivar was characterized through the elucidation of its antiradical kinetics and activity using 2,2-diphenyl-1-picrylhydrazyl as the antiradical probe. Time-dependent concentration of 2,2-diphenyl-1-picrylhydrazyl during its reduction by the juice has been adjusted through a non-linear parametric fitting. Determined total antiradical activity was high, able to reduce 84.58 μmol/l of 2,2-diphenyl-1-picrylhydrazyl per concentration unit of juice (μl/ml), equivalent to a concentration of 42.29 mmol/l of ascorbic acid (or Trolox). Partial antiradical activities due to the fast-, medium- and slow-kinetics were 49.09, 18.16 and 17.33 μmol/l of reduced 2,2-diphenyl-1-picrylhydrazyl per concentration unit of juice (μl/ml), respectively. The corresponding rate constant for the fast-, medium- and slow-kinetics were $\kappa_1 = 6.03$, $\kappa_2 = 0.169$ and $\kappa_3 = 0.0094$ (μl l)/(ml μmol min), respectively. This methodology allows characterization of samples through the accurate determination of the kinetics of their antiradical features, avoiding the use of empirical approximations that hinder the realistic comparison between extracts independently of their origin.

Keywords

Natural antioxidants, fruit juices, antiradical kinetics

Date received: 3 September 2013; accepted: 2 April 2014

INTRODUCTION

Intake of pomegranate (*Punica granatum* L.) arils or juice has been linked to important pharmacodynamic activities such as prevention and treatment of cancer, inflammation and lipid oxidation processes (Aviram et al., 2000; Lansky and Newman, 2007). These functions are mainly attributed to the antioxidant and antiradical activity of their phenolic components (Seeram et al., 2006; Sentandreu et al., 2013). The in vitro antiradical capacity of pomegranate juice and derived extracts from different parts of the fruit have been determined though different methodologies (Elfalleh et al., 2011; El Kar et al., 2011; Gil et al., 2000; Ricci et al., 2006). Total antiradical activity of pomegranate juice, or natural extracts in general, determined by the classical 2,2-diphenyl-1-picrylhydrazyl ($DPPH^{\bullet}$) methodology (Blois, 1958; Brand-Williams et al., 1995) has indirectly been quantified either through the ad hoc EC_{50} empirical parameter or as the ascorbic acid equivalent antioxidant capacity (AEAC) and/or Trolox equivalent antioxidant capacity (TEAC). There is a lack of information about the kinetics of the antiradical activity of natural extracts (or model solutions) against $DPPH^{\bullet}$. Since only the starting and end points (after a fixed reaction time) of the empirical reduction reaction of $DPPH^{\bullet}$ by the antiradical activity of a considered extract are taken

Food Science and Technology International 0(0) 1–7

DOI: 10.1177/1082013214533687
fst.sagepub.com
SAGE

Instituto de Agroquímica y Tecnología de Alimentos (IATA-CSIC), Paterna, Spain

Corresponding author:
Enrique Sentandreu, Instituto de Agroquímica y Tecnología de Alimentos (IATA-CSIC), Avda. Agustín Escardino 7, 46980 Paterna, Valencia, Spain.
Email: elcapi@iata.csic.es

Food Science and Technology International 0(0)

into account, thus determining only its total antiradical capacity, the reduction kinetics is completely ignored. There is a dearth in literature on kinetic data from antiradical extracts and to the best of our knowledge none has been reported in pomegranate juice.

The aim of this work is therefore to characterize pomegranate juice through the accurate determination of its total and partial antiradical activities as well as the related specific kinetic parameters, the average rate and stoichiometric constants of the antiradical reaction, using DPPH$^{\bullet}$ as the antiradical probe.

MATERIALS AND METHODS

Reagents and standards

Spectrophotometric grade methanol was from Sigma (Sigma-Aldrich Co., St. Louis, MO, USA). DPPH$^{\bullet}$ (94.6% purity) was from Fluka (Fluka AG Chemische, Buchs, Switzerland). Nylon filters (0.45 μm) were from Teknokroma (Teknokroma Ltd, Barcelona, Spain) while anhydrous sodium sulphate was from Panreac (Panreac Química S.A., Barcelona, Spain).

Pomegranate juice and sample preparation

Pomegranate fruits, cultivar 'Wonderful', were imported from California, USA. Pomegranate juice was obtained by pressure extraction of the whole fruit (50 units of fruit which weighed 25 kg), previously cut into halves, using a pressure extractor Europ (Vapfluid, Sant Boi de Llobregat, Barcelona, Spain) working at an air pressure of 6 kg/cm^2. Juice was sieved in a paddle finisher (Ø 0.4 mm, Luzzysa, El Puig, Spain) and yield of juice was 42% (w/w), having the following characteristics: °Brix, 17.2 (determined using a digital refractometer Pal-1; Atago Co. Ltd, Tokyo, Japan); pH, 3.3 (determined using a Crison GLP 21 pH-meter; Crison Inst. S.A., Barcelona, Spain); acidity index, 1.07 (assessed by titration with 0.1 N NaOH and expressed as percentage of citric acid); dry matter, 12.7% (determined by oven dying at 70 °C until constant weight); and maturity index, 16.1. Immediately after extraction, separate aliquots (20 ml) of the juice were poured into sterile vials, which were hermetically sealed and stored at −30 °C until analysis (one month as a maximum).

The spectrophotometric grade methanol was dried overnight over anhydrous sodium sulphate, and working solutions of pomegranate juice and DPPH$^{\bullet}$ were freshly prepared before analysis. One milliliter of pomegranate juice was filtered through a 0.45 μm nylon filter and then 0.4 ml of the filtrate was completely dried under a nitrogen stream and re-suspended in 7 ml (dilution factor = 17.5) of anhydrous methanol pH 4.5 (acidified with formic acid) for a final pH value of 4.0. A volume of the diluted working solution (10, 20 and 30 μl) was added in situ, using a chromatographic syringe, into a thermostated (24 °C) and stirred (600 r/min) quartz spectrophotometric cuvette (3.5 ml of capacity and 1 cm path length). The cuvette contained 1.9 ml of the DPPH$^{\bullet}$ solution, prepared in anhydrous methanol pH 4.5 also used to yield a final volume of 2 ml (the final concentration of DPPH$^{\bullet}$ was 100.714 μmol/l), and was immediately end-capped after the addition of the working solution. Reaction time commenced with the addition of pomegranate juice.

UV–Vis analysis

Changes in absorbance were measured using an Agilent UV–Vis spectrophotometer model 8453 (Agilent Technologies GmbH, Karlsruhe, Germany), equipped with a diode array detector and a thermostated cell holder with magnetic stirring. The operating conditions were vis lamp, on; UV lamp, off; detection wavelength, $\lambda = 515$ nm (maximum of absorbance for DPPH$^{\bullet}$ probe in methanolic solution); slit width, 1 nm; data acquisition rate, 2.1 s/data point; reaction temperature, 24 °C; and monitored reaction time, 60 min. Samples were analyzed in triplicate.

Before the analysis of samples, the standard calibration curve absorbance versus DPPH$^{\bullet}$ concentration was determined ($R^2 > 0.999$). From the resulting data, the molar extinction coefficient of DPPH$^{\bullet}$ in methanol was found to be $\varepsilon = 1.12 \times 10^4$ l/(mol cm).

Taking into consideration the detection wavelength ($\lambda = 515$ nm) used, the strong red colour of pomegranate juice interfered with the determination of its antiradical activity against DPPH$^{\bullet}$, even when using diluted working solutions in methanol. However, the well-known capacity of anthocyanins in solution to undergo reversible structural transformations as a function of the pH of the medium could be used to overcome the problem. Hence, at pH < 3 the predominant structure is that of flavylium cation (oxonium form) and the colour of the anthocyanins varies from orange to purple; at pH = 4–5 main structure is that of carbinol pseudo-base (hemiketal form) in equilibrium with the corresponding chalcone, and the anthocyanins are colourless; and at pH > 7 the predominant structure is that of quinonoidal base and the colour of the anthocyanins is blue (Giusti and Wrolstad, 2001). From the above, reactions were carried out at pH around 4.4 after mixing the DPPH$^{\bullet}$ solution (pH 4.5) with the re-suspended juice (pH 4.0), just having the reaction solutions the colour provided by the dissolved antiradical probe. It must be emphasized that use of a diluted solution of anthocyanins at pH 4–5, where they are in colourless hemiketal and chalcone forms, does not affect at all their antiradical capacity. This is so

because both structures preserve the vicinal free hydroxyls on B-ring, which are mainly responsible for their antiradical activity. The other important antiradical group, that is the conjugated vinyl-hydroxyl at C3 position in B-ring is always glycosylated in the anthocyanins present in pomegranate juice (Sentandreu et al., 2013), and so it does not exhibit antiradical activity.

RESULTS AND DISCUSSION

Considering that pomegranate juice assayed was diluted 17.5-fold before the addition of 30, 20 and 10 µl to the cuvette containing DPPH•, for a total reaction volume of 2 ml, the precise added volumes of pomegranate juice were $v_1 = 1.714$, $v_2 = 1.143$ and $v_3 = 0.571$ µl, which corresponded to concentrations of $c_1 = 0.857$, $c_2 = 0.571$ and $c_3 = 0.286$ µl/ml, respectively. Figure 1 shows the time evolution of the reduction reaction of DPPH• (initial concentration, $y_o = 100.714$ µmol/l) due to the antiradical activity of pomegranate juice for its three assayed concentrations. For visibility reasons, only a limited number of experimental data points were plotted, although subsequent fittings were carried out using all of them. The curves excellently reflected the expected overall antiradical activity of the juice, typical for matrices with complex compositions. Thus, Sentandreu et al. (2008) proposed that the antiradicals composition of a bioactive sample (either for a natural extract or model solution) could be schematized regarding the three partial antiradical kinetics that make up its total scavenging capacity (fast- for vinyl alcohol and tri-vicinal hydroxyl groups, i.e. ascorbic acid; medium- for the *p*-catechol group, i.e. chlorogenic acid and slow- for free hydroxyls, i.e. ferulic acid). In addition, authors also mentioned how

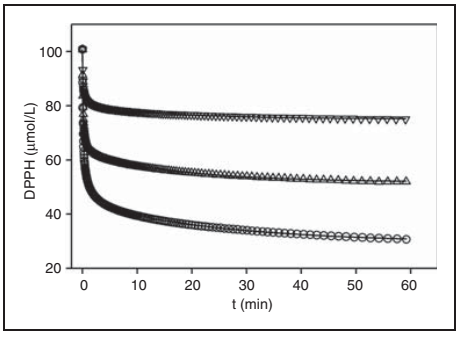

Figure 1. Time evolution of the concentration of DPPH• in methanol ($y_o = 100.714$ µmol/l) during its reduction by three different initial concentrations of pomegranate juice: (O) 0.857, (Δ) 0.571 and (▽) 0.286 µl/ml, and their fitting to the three rate/three stoichiometric constants kinetic equation. $R^2 > 0.999$ in all cases.

in a hydrophilic media (i.e. methanol) the *p*-catechol group shows different antiradical kinetics (medium by direct reduction of the antiradical probe and as a consequence of its first regeneration step by the media and slow by the second and further regenerations). Hence, total antiradical activity of a considered extract can be contributed by one, two or three partial antiradical kinetics as a function of its compositional complexity.

In order to simplify understanding of experimental results (Figure 1), let us consider just anthocyanins present in pomegranate juice which exhibit all three partial antiradical kinetics described earlier, also contributed by non-anthocyanin phenols present in the juice (Sentandreu et al., 2013). The short but very fast DPPH• reduction step would be due to the *tri*-vicinal hydroxyls on the aromatic rings (pomegranate juice almost does not contain ascorbic acid and free vinyl-hydroxyls), such as in delphinidin-based anthocyanins, whilst the quite long but medium and the very long but slow DPPH• reduction steps would be mainly due to phenolics with *p*-catechol (i.e. cyanidin-based anthocyanins) and free hydroxyl groups (i.e. pelargonidin-based anthocyanins). To determine antiradical kinetics and activities (total and partial) of the studied juice, each experimental curve was fitted through a non-linear parametric fitting (using SigmaPlot 10.0) to the 'general' three rate/three stoichiometric constants kinetic equation described by Sentandreu et al. (2008), theoretically developed from model solutions and proposed to positively characterize natural antiradical extracts, that is

$$y - ys = \frac{y_1(y_o - y_1)}{y_1 - y_o\left(1 - e^{r_1 y_1 t}\right)} + \frac{y_2(y_o - y_2)}{y_2 - y_o\left(1 - e^{r_2 y_2 t}\right)} + \frac{y_3(y_o - y_3)}{y_3 - y_o\left(1 - e^{r_3 y_3 t}\right)}$$

with the constraint

$$y_3 = 2y_o + y_s - y_1 - y_2$$

and the identities (i = 1, 2, 3)

$$r_i = k_i/\sigma_i$$

$$y_o - y_i = \sigma_i a_o$$

$$y_o - y_s = (\Sigma\sigma_i)a_o = \sigma_t a_o$$

where y (µmol/l) is the time-dependent concentration of DPPH•; y_o (µmol/l) is the initial concentration of DPPH•; a_o (µmol/l) is the initial concentration of the antiradical; t (min) is the reaction time; y_1, y_2 and y_3 (µmol/l) are the asymptotes that would be reached due

solely to the fast-, medium- and slow-kinetic steps of the reaction, respectively; y_s (μmol/l) is the experimental asymptote of the reaction; k_1, k_2 and k_3 (l/(μmol min)) are the rate constants of the fast-, medium- and slow-kinetic steps of the reaction, respectively; σ_1, σ_2 and σ_3 are the stoichiometric constants of the fast-, medium- and slow-kinetic steps of the reaction, respectively; and σ_t ($=\sigma_1+\sigma_2+\sigma_3$) is the total stoichiometric constant of the reaction. The values of the adjustable parameters, y_1, y_2, y_3, y_s, r_1, r_2 and r_3, obtained from the corresponding fittings, are given in Table 1.

If the assayed antiradical was a pure compound with an initial concentration a_o (μmol/l), the stoichiometric constants would be $\sigma_1=(y_o-y_1)/a_o$, $\sigma_2=(y_o-y_2)/a_o$, $\sigma_3=(y_o-y_3)/a_o$ and $\sigma_t=\sigma_1+\sigma_2+\sigma_3=(y_o-y_s)/a_o$, and their corresponding rate constants $k_1=r_1\sigma_1$, $k_2=r_2\sigma_2$ and $k_3=r_3\sigma_3$, respectively. In the case that many different initial concentrations of the antiradical were assayed, the stoichiometric constants, σ_i (i = 1, 2, 3, s), should be determined as the slopes from the corresponding linear fittings (y_o-y_i) (i = 1, 2, 3, s) versus the assayed a_o's, and the corresponding rate constants as $k_i=\check{r}_i/\sigma_i$, where $\check{r}_i$ is the average of the determined r_i from each assayed concentration. Pomegranate juice, however, is not a pure antiradical compound but contains a mixture of many different antiradical compounds and so an initial molar concentration cannot be defined. In any case, it seems evident that partial and total antiradical activities must directly be proportional to the added volume of the assayed sample (v_i, μl) and so to its concentration (c_i, μl/ml). Figure 2 shows the plotting of (y_o-y_1), (y_o-y_2), (y_o-y_3) and (y_o-y_s) versus the assayed initial concentrations (c_o) of pomegranate juice. As can be seen, all the plots were straight lines whose slopes, $m_1=(y_o-y_1)/c_o=49.09\pm0.11$, $m_2=(y_o-y_2)/c_o=18.16\pm0.05$, $m_3=(y_o-y_3)/c_o=17.33\pm0.06$ and $m_s=(y_o-y_s)/c_o=84.58\pm0.15$ ((μmol/l)/(μl/ml)) were equivalents to the stoichiometric constants for a pure compound, giving the amount of DPPH• (μmol/l) that was reduced due to the fast (m_1), medium (m_2), slow (m_3) and total (m_s) antiradical activity per concentration unit (μl/ml) of juice. Similarly, equivalents to the rate constants (k_i) were $\kappa_1=\check{r}_1m_1=6.03\pm0.06$, $\kappa_2=\check{r}_2m_2=0.167\pm0.005$ and $\kappa_3=\check{r}_3m_3=0.0094\pm0.0002$ (μl l)/(ml μmol min). Therefore, the values of m_1, m_2, m_3, m_s, κ_1, κ_2 and κ_3 completely determined the reaction of reduction of DPPH• by the antiradical activity of pomegranate juice.

In many bibliographic references, value of total antiradical activity against DPPH•, either from a pure antiradical or from a mixture of antiradicals, was quantified by means of the parameter EC_{50}, which is defined as the amount of antiradical necessary to

Table 1. Reduction kinetics[f] of the free radical DPPH• reduced by pomegranate juice[a,b]

	c_o (μl/ml)[c]	y_1 (μmol/l)[d]	y_2 (μmol/l)[d]	y_3 (μmol/l)[d]	y_s (μmol/l)[d]	r_1 [l/(μmol min)][e]	r_2 [l/(μmol min)][e]	r_3 [l/(μmol min)][e]
O	0.857	59.370 ± 0.040	85.810 ± 0.072	85.464 ± 0.120	29.215 ± 0.011	0.1053 ± 0.0008	0.0064 ± 0.0001	$4.172\bullet10^{-4}\pm0.015\bullet10^{-4}$
△	0.571	72.658 ± 0.052	90.582 ± 0.080	89.864 ± 0.111	51.675 ± 0.042	0.1266 ± 0.0009	0.0111 ± 0.0002	$5.883\bullet10^{-4}\pm0.010\bullet10^{-4}$
▽	0.286	84.520 ± 0.101	96.377 ± 0.110	95.519 ± 0.105	74.987 ± 0.033	0.1364 ± 0.0006	0.0101 ± 0.0001	$6.174\bullet10^{-4}\pm0.011\bullet10^{-4}$

[a]Initial concentration of DPPH•, $y_o=100.714$ μmol/l.
[b]Regression coefficient for all experimental curves, $R^2>0.999$.
[c,d,e]See Appendix.
[f]Results are the average of three replicates (mean ± SD).

decrease the initial DPPH• concentration by 50% (Sendra et al., 2006). To determine this parameter, a constant initial concentration (y_o, μmol/l) of DPPH• is partially reduced by using different amounts of antiradical, and the remaining concentration of DPPH• is measured after a fixed reaction time (normally between 10 and 40 min) and is considered as the real asymptotic value of the empirical reaction. From these data, the amount of antiradical (α_{st}) that is stoichiometric with the assayed concentration of DPPH• is calculated, and consequently $EC_{50} = \alpha_{st}/2$. However, to avoid this value to be dependent on the initial concentration of DPPH•, it is normally expressed as ml(sample)/g(DPPH•). In terms of the kinetic parameters, if m_s is the total stoichiometric constant of a mixture of antiradicals (or σ_t in the case of a pure antiradical), its stoichiometric concentration (c_{st}) is given by $c_{st} = y_o/m_s$ (or $a_{st} = y_o/\sigma_t$) since $y_s = 0$, making that in our case $EC_{50} = c_{st}/2 = (y_o/2)/m_s = 50.36/84.58 = 0.595$ μl/ml (or $EC_{50} = y_o/2\sigma_t$). This value expressed as ml/g is $EC_{50} = 50.36 \bullet 394.32 \bullet 10^{-3}/0.595 = 33.37$ ml/g, which is in accordance to published values (Calín-Sánchez et al., 2011) of EC_{50} ($= 30.1 - 40.7$ ml/g) for juices from Spanish pomegranates.

Another way to quantify total antiradical activity of a sample is by means of the equivalent molar concentration (mmol/l) of a standard antiradical (usually ascorbic acid and Trolox). Hence, a solution containing the equivalent molar concentration of the standard must exhibit exactly the same total antiradical activity that the assayed antiradical of mixture of antiradicals. Thus, a constant initial concentration (y_o, μmol/l) of DPPH• is partially reduced by using different amounts of both the assayed and standard antiradicals, and the remaining concentration of DPPH• after a fixed reaction time (normally between 10 and 40 min) is measured and assumed to be its true asymptotic value. This assumption is normally true for the standard antiradical, since its kinetics is very rapid, but also normally false for the assayed antiradical, since its kinetics is usually much slower (and prolonged in time). From the obtained data, the equivalent molar concentration of the standard antiradical is determined. From the kinetic parameters, the calculus of the equivalent concentration of a given standard antiradical is immediate due to the fact that its total stoichiometric constant against DPPH• is known. This is the case for both ascorbic acid (Molyneux, 2004; Sendra et al., 2006) and Trolox (Friaa and Brault, 2006), both exhibiting a total stoichiometric constant =2. In our study, the equivalent molar concentration of ascorbic acid (AEAC) or Trolox (TEAC), is given by $AEAC = TEAC = m_s/2 = 42.29$ mmol/l (or $= \sigma_t/2$ for a pure antiradical). In contrast with the determined value for EC_{50}, the determined value for TEAC (42.29) is almost twice regarding previous results (TEAC ≈ 20) described for a commercial pomegranate juice from the variety 'Wonderful', also grown in California, USA (Gil et al., 2000). Although this later value for TEAC (which evidently was very close to the value obtained by the same authors for AEAC) was obtained from a rather short reaction time (15 min), which according to Figure 1 leads to determine only 88% of total antiradical activity, this great difference could be attributed to the extraction process of the juice. In the present study, the assayed juice was obtained by pressure extraction of the whole fruit under gentle conditions; however, additional amounts of some strong antiradicals present in the peel at high concentration can be incorporated into the juice by strong extracting pressures, thus explaining this discrepancy.

Obviously, if antiradical activities of a set of similar samples are to be determined, it seems unrealistic to carry out a complete antiradical analysis of all samples, even if only one concentration per sample is assayed. However, authors believe that, at least for a convincing comparison of the antiradical activity between samples from different origin, it would be a good practice to fully characterize the antiradical activity of at least one sample, whilst the other samples could be quantified by determining only the DPPH• concentrations at the beginning of the reaction and after a selected reaction time. As an additional advantage, from the fully characterized sample it would be immediate to determine the percentage of total antiradical activity that is measured at the selected reaction time and

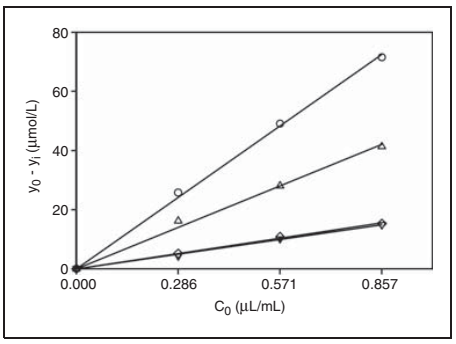

Figure 2. Graphical representation of DPPH• concentration (μmol/l) reduced versus the initial concentration (c_o) of pomegranate juice. Total concentration reduced by the juice, $y_i = y_s$ (O); concentration reduced during the fast-kinetics step, $y_i = y_1$ (Δ); concentration reduced during the medium-kinetics step, $y_i = y_2$ (▽) and concentration reduced during the slow-kinetics step, $y_i = y_3$ (◇). $R^2 > 0.995$ in all cases. See Appendix.

then perform the opportune corrections for the other samples.

Finally, bibliographic data reporting values of the kinetic and rate constants for the assayed antiradical samples would allow a convincing comparison within them. By this way, the antiradical activity of samples from different origin could be compared not only with respect to their total antiradical activity (m_s) but also with respect to their partial antiradical activities (m_1, m_2 and m_3) and partial DPPH$^\bullet$ reduction rates (κ_1, κ_2 and κ_3). This is of major importance, since time evolution of the DPPH$^\bullet$ concentration reflects the type and concentration of antiradicals present in the assayed sample: vinyl-OH and vicinal phenolic tri-OH exhibit at least a fast kinetics step; *p*-catechol groups exhibit both medium and slow kinetics steps and isolated phenolic hydroxyls exhibit only a slow kinetics step. Although it is true that an aqueous solution containing 42.29 mmol/l of ascorbic acid exhibits the same total antiradical activity against DPPH$^\bullet$ than the assayed pomegranate juice, perhaps their antiradical 'goodness and properties' for human health are somewhat different. Therefore, it is possible that in many cases the simple and mere comparison of two samples by comparing only their total antiradical activities (and not their characteristic antiradical kinetics) could be useless or, even worse, could be deceptive.

CONCLUSIONS

For the first time, pomegranate juice has been rigorously characterized through its specific in vitro antiradical properties strictly determined by non-linear parametric fitting using DPPH$^\bullet$ as the antiradical probe. Determined total and partial antiradical capacities as well as the related reduction kinetics (including stoichiometric and antiradical rate constants) act as a specific 'fingerprint' of the juice. This methodology if applied to bioactive samples from different origins (either for natural extracts or model solutions) would allow the realistic comparison of their antiradical features, in contrast to the current situation where only total antiradical activities are approximately approached.

FUNDING

This research was supported by the Ministerio de Ciencia e Innovación (MICINN, Spain), project AGL2009-11805.

CONFLICT OF INTEREST

None declared.

ACKNOWLEDGEMENTS

Authors acknowledge the financial support from Consolider Ingenio Fun-C-Food (CSD2007-00063) and for the contract of M. Cerdán-Calero (JAEpredoc program, CSIC-FEDER funds). Activity of Dr E Sentandreu during this research was self-funded.

REFERENCES

Aviram M, Dornfeld L, Rosenblat M, Volkova N, Kaplan M, Coleman R, et al. (2000). Pomegranate juice consumption reduces oxidative stress, atherogenic modifications to LDL, and platelet aggregation: studies in humans and in atherosclerotic apolipoprotein E-deficient mice. *The American Journal of Clinical Nutrition* 71: 1062–1076.

Blois MS. (1958). Antioxidant determination by the use of a stable free radical. *Nature* 181: 1199–1200.

Brand-Williams W, Cuvelier ME and Berset C. (1995). Use of a free radical method to evaluate antioxidant activity. *Lebensmittel Wissenschaft und Technologie* 28: 25–30.

Calín-SánchezÁ, Martínez JJ, Vázquez-Araújo L, Burló F, Melgarejo P and Carbonell-Barrachina ÁA. (2011). Volatile composition and sensory quality of Spanish pomegranates (Punica granatum L.). *Journal of the Science of Food and Agriculture* 91: 586–592.

Elfalleh W, Tlili N, Nasri N, Yahia Y, Hannachi H, Chaira N, et al. (2011). Antioxidant capacities of phenolic compounds and tocopherols from Tunisian pomegranate (Punica granatum) fruits. *Journal of Food Science* 76: 707–713.

El Kar C, Ferchichi A, Attia F and Bouajila J. (2011). Pomegranate (Punica granatum) juices: Chemical composition, micronutrient cations, and antioxidant capacity. *Journal of Food Science* 76: 795–800.

Friaa O and Brault D. (2006). Kinetics of the reaction between the antioxidant Trolox® and the free radical DPPH$^\bullet$ in semi-aqueous solution. *Organic and Biomolecular Chemistry* 4: 2417.

Gil MI, Tomas-Barberan FA, Hess-Pierce B, Holcroft DM and Kader AA. (2000). Antioxidant activity of pomegranate juice and its relationship with phenolic composition and processing. *Journal of Agricultural and Food Chemistry* 48: 4581–4589.

Giusti M and Wrolstad RE. (2001). Characterization and measurement of anthocyanins by UV-Visible spectroscopy. In: Wrolstad RE, Acree TE, Decker EA, Penner MH, Reid DS, Schwartz SJ, et al (eds) *Current Protocols in Food Analytical Chemistry*. Hoboken, NJ: John Wiley & Sons Inc, pp. F1.2.1–F1.2.13.

Lansky EP and Newman RA. (2007). Punica granatum (pomegranate) and its potential for prevention and treatment of inflammation and cancer. *Journal of Ethnopharmacology* 109: 177–206.

Molyneux P. (2004). The use of the stable free radical diphenylpicrylhydrazyl (DPPH$^\bullet$) for estimating antioxidant activity. *Songklanakarin Journal of Science and Technology* 26: 211–219.

Ricci D, Giamperi L, Bucchini A and Fraternale D. (2006). Antioxidant activity of Punica granatum fruits. *Fitoterapia* 77: 310–312.

Seeram NP, Zhang Y, Reed JD, Krueger CG and Vaya J. (2006). Pomegranate phytochemicals. In: Seeram NP, Schulman RN and Heber D (eds) *Pomegranates: Ancient Roots to Modern Medicine*. Boca Raton, FL: CRC Press, Taylor & Francis group, pp. 3–30.

Sendra JM, Sentandreu E and Navarro JL. (2006). Reduction kinetics of the free stable radical 2,2-diphenyl-1-picrylhydrazyl (DPPH•) for determination of the antiradical activity of citrus juices. *European Food Research and Technology* 223: 615–624.

Sentandreu E, Cerdán-Calero M and Sendra JM. (2013). Phenolic profile characterization of pomegranate (*Punica granatum*) juice by high-performance liquid chromatography with diode array detection coupled to an electrospray ion trap mass analyzer. *Journal of Food Composition and Analysis* 30: 32–40.

Sentandreu E, Navarro JL and Sendra JM. (2008). Reduction kinetics of the antiradical probe 2,2-diphenyl-1-picrylhydrazyl in methanol and acetonitrile by the antiradical activity of protocatechuic acid and protocatechuic acid methyl ester. *Journal of Agricultural and Food Chemistry* 56: 4928–4936.

APPENDIX

Notation

- c_o initial concentration of the antiradical (μl/ml)
- c_{st} total stoichiometric concentration of pomegranate juice (μmol/l)
- EC_{50} amount of antiradical that decreases the initial DPPH• concentration by 50% (ml/g)
- t reaction time (min)
- k_1 rate constant of the fast kinetic steps of the reaction (l/(μmol min))
- k_2 rate constant of the medium kinetic steps of the reaction (l/(μmol min))
- k_3 rate constant of the slow kinetic steps of the reaction (l/(μmol min))
- m_1 (= $(y_o - y_1)/c_o$) slope from the representation $(y_o - y_1)$ versus c_o ((μmol/l)/(μl/ml))
- m_2 (= $(y_o - y_2)/c_o$) slope from the representation $(y_o - y_2)$ versus c_o ((μmol/l)/(μl/ml))
- m_3 (= $(y_o - y_3)/c_o$) slope from the representation $(y_o - y_3)$ versus c_o ((μmol/l)/(μl/ml))
- m_s (= $(y_o - y_s)/c_o$) slope from the representation $(y_o - y_s)$ versus c_o ((μmol/l)/(μl/ml))
- r_1 (= k_1/σ_1) kinetic constant for the fast antiradical step (l/(μmol min))
- r_2 (= k_2/σ_2) kinetic constant for the medium antiradical step (l/(μmol min))
- r_3 (= k_3/σ_3) kinetic constant for the slow antiradical step (l/(μmol min))
- $\check{r}_i$ average of the determined r_i from each assayed concentration (l/(μmol min))
- y time-dependent concentration of DPPH• (μmol/l)
- y_o initial concentration of DPPH• (μmol/l)
- y_1 asymptote that would be reached due solely to the fast step of the reaction (μmol/l)
- y_2 asymptote that would be reached due solely to the medium step of the reaction (μmol/l)
- y_3 asymptote that would be reached due solely to the slow step of the reaction (μmol/l)
- y_s experimental asymptote of the reaction (μmol/l)
- α_{st} amount of pomegranate juice that is stoichiometric with the assayed concentration of DPPH• (ml/g)
- κ_1 (=$\check{r}_1 m_1$) equivalents to the fast rate constant (μl l)/(ml μmol min)
- κ_2 (=$\check{r}_2 m_2$) equivalents to the medium rate constant (μl l)/(ml μmol min)
- κ_3 (=$\check{r}_3 m_3$) equivalents to the slow rate constant (μl l)/(ml μmol min)
- v_i volume of pomegranate juice (μl)
- σ_1 stoichiometric constant of the fast kinetic steps of the reaction
- σ_2 stoichiometric constant of the medium kinetic steps of the reaction
- σ_3 stoichiometric constant of the slow kinetic steps of the reaction
- σ_t (= $\sigma_1 + \sigma_2 + \sigma_3$) total stoichiometric constant of the reaction

CAPÍTULO 4

Caracterización del perfil de fenoles de la pulpa de caqui (*Diospyros kaki*) de la variedad "Rojo Brillante".

1. **Metabolite profiling of pigments from acid-hydrolyzed persimmon (*Diospyros kaki*) extracts by HPLC-DAD/ESI-MS^n analysis**. (2014). *Journal of Food Composition and Analysis*. (Aceptado para su publicación). Impact Factor: 2.259.

2. **Rapid screening of low molecular weight phenols from persimmon (*Diospyros kaki*) pulp using liquid chromatography-UV/Vis-electrospray mass spectrometry analysis**. (2014). *Journal of the Science of Food and Agriculture*. (En prensa). Impact Factor: 1.879.

Contents lists available at SciVerse ScienceDirect

Journal of Food Composition and Analysis

journal homepage: www.elsevier.com/locate/jfca

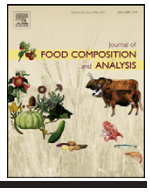

Metabolite profiling of pigments from acid-hydrolyzed persimmon (*Diospyros kaki*) extracts by HPLC-DAD/ESI-MS^n analysis

Enrique Sentandreu*, Manuela Cerdán-Calero, José L. Navarro

Instituto de Agroquímica y Tecnología de Alimentos (IATA-CSIC), Avda. Agustín Escardino 7, 46980 Paterna, Valencia, Spain

The profile of pigments from acid-hydrolysed Rojo Brillante' persimmon (*Diospyros kaki*) extracts was elucidated by high-performance liquid chromatography with diode array detection coupled to tandem mass spectrometry analysis with positive electrospray ionization (HPLC-DAD-ESI$^+$/MS^n). In total, seventeen anthocyanidin-based aglycones were tentatively identified: four free anthocyanidins (delphinidin, petunidin, cyanidin and peonidin) and, for the first time in a naturally derived extract, thirteen 3-O-galloyl flavanol-anthocyanidin adducts (dimers formed by a galloylated (epi)catechin or (epi)gallocatechin with an anthocyanidin). Furthermore, evidence of non-galloylated flavanol-anthocyanidin adducts was also found in the samples studied. The anthocyanidin derivatives reported could promote the use of persimmon by the food industry to obtain innovative coloured products, opening up new possibilities to satisfy consumer demands. The methodology of analysis developed, which included the use of a routine three-dimensional ion trap, represents an affordable solution to achieve detailed metabolite profiles of foodstuffs.

Keywords: *Diospyros kaki*; food analysis; persimmon fruits; acid-hydrolyzed extracts; LC-DAD/ESI-MS^n analysis; molecular structure elucidation; anthocyanidin adducts; food composition; innovative foodstuffs: metabolite profiling.

Chemical compounds studied in this article

Delphinidin (PubChem CID: 68245); Petunidin (PubChem CID: 73386); Cyanidin (PubChem CID: 68247); Peonidin (PubChem CID: 441773).

1. Introduction

Tannins are phenols widely distributed throughout the plant kingdom whose nature varies from simple structures (known as low molecular weight tannins, LMWT), normally consisting of glycosides of one or several units of gallic acid (hydrolysable tannins) and flavan aglycones (condensed tannins), to quite complex polymers with a high molecular weight. The study of the molecular structure of persimmon (*Diospyros kaki* L.) tannins goes back in time when Komatsu and Matsunami (1924 and 1925) first reported that they consisted mainly of gallic acid and phloroglucin, although they also emphasized the presence of many unknown "impurities" of a potentially tannic nature in their extracts. Matsuo and Ito (1978) pointed out that the structure of persimmon tannins is complex and they reporte that after thiolysis degradation these compounds consisted mainly of polymers of catechin, catechin-3-gallate, gallochatechin and gallocatechin-3-gallate. Moreover, the same authors also detected the presence of various proanthocyanindin B-type dimmers (through C-4 and C-6 or C-8 carbon-carbon interflavan linkages). Currently, all these complex polymers are popularly known as high molecular weight tannins (HMWT), condensed tannins or simply proanthocyanidins and their presence in persimmon extracts has been widely described in recent years (Gu *et al.*, 2008; Nakatsubo *et al.*, 2002). It has also been reported (Li *et al.*, 2010; Xu *et al.*, 2012) that crude persimmon extracts generally have a high proanthocyanidin content (over 50% of total phenols) highly galloylated (over 70% of total proanthocyanidins), normally finding B-type polymers (most commonly C4-C8 linkage), although some unusual A-type derivatives (with C4-C8 and C2-C7 linkages) have also been identified. Furthermore, very interestingly, Matsuo and Ito (1978) also reported that colourless methanolic persimmon extracts turned to solutions with a deep red colour (a feature much appreciated by food industry to produce coloured products such as smoothies and soft drinks) after heating under strong acidic conditions, and they detected delphinidin, cyanindin and some unknown condensed phenols. Moreover, the same authors highlighted that the study of persimmon pigments was difficult becuase polyphenols condense easily under acidic conditions. The formation of phenolic polymers by acid-catalyzed modulation was confirmed by Haslam (1980) when he studied wine proanthocyanidins and, more recently, by Salas *et al.* (2003) when they proposed the mechanisms of condensation between anthocyanins and tannins in model solutions.

Regarding the strategies followed by researchers to determine the complex composition of persimmon tannins, thiolysis degradation is, by far, the method most commonly selected (*Gu et al.*, 2008; Matsuo and Ito, 1978) to identify their basic structural units (as mentioned earlier, catechin, gallocatechin and their 3-*O*-galloyl derivatives). However, the literature about persimmon pigments released by acid hydrolysis is negligible apart from the work of Matsuo and Ito (1978) with the sole further exception of the research carried out by Gu *et al.* (2008), which mentions the presence not only of delphinidin and cyanidin but also of petunidin in methanolic extracts from Chinese persimmons. However, more complex pigments beyond free anthocyanidins in acid-hydrolyzed persimmon extracts have not yet been described.

The aim of this work an exhaustive metabolite profiling of pigments that appear in methanolic extracts from persimmon fruits belonging to the ´Rojo Brillante´ variety after acid hydrolysis. Accordingly, samples were analyzed by high-performance liquid chromatography coupled to diode array detection and positive electrospray tandem mass spectrometry analysis (HPLC-DAD/ESI^+-MS^n) to elucidate structure of the anthocyanidin-based compounds released.

2. Material and Methods

2.1. Chemicals

LC-MS grade water, LC-MS grade acetonitrile, analytical grade tetrahydrofuran (THF), analytical grade hydrochloric acid, methanol (MeOH) and analytical grade formic acid were from Scharlab (Scharlab S.L., Barcelona, Spain).

2.2. Sample preparation

Thirty persimmon (*Diospyros kaki*, cv. 125 Rojo Brillante) fruits, belonging to the Denomination of Origin "Kaki Ribera del Xúquer", were harvested in December 2012 from a local orchard in Carlet (Valencia, Spain) and analysed in less than fifteen days (stored at 4 °C). Various freshly prepared samples were used to perform the planned MS experiments. Briefly, each individual sample was from one persimmon fruit previously washed in tap water and heated in a water bath at 100 °C for 10 minutes to inactivate polyphenol oxidases (PPOs). Calyx and peel were removed and then 150 mg of pulp was mixed with 600 mL of a weakly acidified (1% HCl) MeOH solution. The sample was homogenized with an analytical mill (IKA A11 basic Yellow Line model, IKA Werke GmbH & Co. KG, Staufen, Germany) and 25 g of the

resulting puree was centrifuged at 4500 g (rotor radius, 16.1 cm) for 5 minutes. The yellowish supernatant was kept and the pellet was re-extracted with acidified MeOH until it became colourless. The supernatants were collected and the resulting solution was evaporated until complete dryness in a speed-vac system (ThermoScientific SPD 121P model, Thermo Fisher Scientific S.L.U., Madrid, Spain). The sample was re-suspended in 20 mL of acidified (1% HCl) water and passed through a Waters Sep-Pak C-18 cartridge (Sep-Pak C-18 classic model, Waters Co., Milford, MA, USA). Non-phenolic polar compounds were removed with acidized water and phenols were finally eluted with 5 mL of acidified MeOH. The eluate was concentrated to complete dryness in the same evaporator device as previously described and then re-suspended in 5 mL of a strongly acidified (2M HCl) MeOH solution. The sample was incubated at 80 °C for 4 hours in a thermo-block device (Selecta Agimatic-N model, Teknokroma S.A., Barcelona, Spain), then cooled with ice and centrifuged at 4500 g for 5 minutes. One mL from the top of the test tube was poured into a glass HPLC vial and injected in the HPLC-DAD/ESI-MS^n system.

2.3. HPLC-DAD-ESI/MS^n Analysis

Chromatographic separation was carried out using a Thermo Surveyor Plus HPLC (ThermoScientific, San Jose, CA, USA), equipped with a quaternary pump, vacuum degasser, temperature-controlled autosampler and diode array detector. Column loaded was a 250 mm × 2.1 mm i.d., 3 μm, YMC C-18 pack-*pro* (YMC Europe GmbH, Dinslaken, Germany). Separation conditions were: injection volume, 5 μL; flow rate, 0.2 mL/min; oven temperature, 24 ºC; autosampler temperature, 10 ºC; solvent A, water/THF/formic acid (97.5:2.0:0.5, v/v/v); solvent B, acetonitrile/THF/formic acid (97.5:2.0:0.5, v/v/v); separation gradient, initially 0% B, linear 0–6% B in 5 min, linear 6–18% B in 25 min, linear 18–80% B in 20 min, purging with 100% B during 10 min and column equilibration with 0% B for 30 min; DAD detection wavelength, λ = 520 nm.

MS analysis and fragmentation experiments were performed on a ThermoFinningan LCQ Advantage (ThermoScientific, San Jose, CA, USA) ion trap mass analyzer equipped with an electrospray ionization source operating in positive mode (ESI^+) under the following conditions: source voltage, 3.5 kV; capillary voltage, 9 V; capillary temperature, 300 ºC; sheath gas flow, 50 (arbitrary units); sweep gas flow, 20 (arbitrary units); full max ion time, 300 ms; full micro scans, 3; SIM max ion time, 300 ms; SIM micro scans, 3; MS^n max ion time, 600 ms; and MS^n

micro scans, 3. Control of the HPLC-DAD/ESI-MS^n device and data analysis were managed by the software Xcalibur v. 2.06, loaded into a PC computer.

To ensure an exhaustive metabolite profiling of samples and taking into consideration intrinsic technological limitations of aged ion traps as in our case (regarding poor sensitivity and MS scan speed as pointed out by Sentandreu *et al.* (2013) when studied pomegranate phenols), separate injections were run to perform different MS analyses:

2.3.1. Untargeted general data dependent MS^3 scan analysis

The aim of this MS experiment was to obtain a global picture of main pigments that appeared in the samples studied. Data-dependent conditions were: collision energy, 35% (arbitrary units); reject mass-to-charge ratio (*m/z*) width, 1.00; repeat count, 2; repeat duration, 0.5 min; exclusion size list, 25; exclusion duration, 1.00 min; exclusion mass width, 3.00. Moreover, the analysis included three scan events: *scan event 1*, full MS; *scan event 2*, MS^2 of the most intense ions from *scan event 1*; and *scan event 3*, MS^3 of the most intense ions from *scan event 2*. The scanned *m/z* range was 260-2000.

2.3.2. Targeted non-data dependent MS^n scan analyses

The aim of these MS experiments was to maximize sensitivity and selectivity of analyses that were initially orientated by previous studies and results from the data-dependent analysis described above. Consequently, this targeted search was governed by the following considerations: firstly and as mentioned above (see the Introduction section), condensed persimmon tannins consist mainly of highly galloylated (epi)catechin and (epi)gallocatechin units, and secondly, the preliminary data-dependent analysis demonstrated the presence of delphinidin, petunidin, cyanidin and peonidin in the studied extracts (see Results and discussion section). Accordingly, 14 specific injections were run separately (one per selected *m/z* parent mass) corresponding to free anthocyanidins (delphinidin, petunidin, cyanidin, peonidin, malvidin and pelargonidin) and their derived adducts originated by their condensation with 3-*O*-galloyl-flavanols ((epi)afzelechin, (epi)catechin and (epi)gallocatechin). The first six injections were devoted solely to detecting anthocyanidins and they included two MS scan events: *scan event 1*, full MS; *scan event 2*, MS^2 of each populated ion in the target mass list: *mz* 271, 287, 301, 303, 317 and 331. The last eight injections were devoted solely to detecting galloylated flavanol-anthocyanidin (or vice versa) adducts and included three scan events: *scan event 1*, full

MS; *scan event 2*, MS^2 of each populated ion in the target mass list with *m/z´s*: 711, 725, 727, 741, 743, 757, 759 and 773; and *scan event 3*, MS^3 of the most intense ions from *scan event 2*. In all cases, the collision energy was 35% (arbitrary units) and the scanned *m/z* range was 260-800.

3. Results and discussion

Table 1 lists all the pigments detected in the samples studied. The main components of the acid-hydrolysed persimmon extracts were initially approached through the untargeted data-dependent MS^3 analysis (described above). To illustrate the results from this preliminary study, **Fig. 1A** represents the DAD chromatogram recorded at 520 nm. As we can see, four main peaks were found (numbered as in **Table 1**), corresponding to delphinidin, petunidin and cyanidin (previously described in acid-hydrolysed persimmon extracts by Gu *et al.* (2008)), but in this case peonidin was also detected. Furthermore, the zoomed chromatogram (**Fig. 1B**) reveals many other minor peaks, thus confirming the idea originally proposed by Komatsu and Matsunami (1924 and 1925) and later by Matsuo and Ito (1978) about the existence of more complex pigments in acid-hydrolysed persimmon extracts.

Very interestingly, MS results from this preliminary analysis also indicated the presence of some intriguing analytes with parent masses ($[M]^+$) at *m/z* 727, 743 and 759. The MS^2 fragmentation patterns shown by these compounds revealed that they were delphinidin- and cyanidin-based derivatives. Moreover, their MS^3 analysis (from the most intense ions generated at MS^2 level, which corresponded to $[M]^+$ -170, loss of 231 gallic acid) also confirmed their anthocyanidin nature. Detection of only some galloylated derivatives from the main free anthocyanidins detected (but not from those based on petunidin and peonidin) led us to perform more specific MS analyses. Accordingly, targeted non-data-dependent MS^3 experiments (described above) were carried out separately for each "feasible" galloylated flavanol-anthocyanidin (or vice versa) combination that might be present in the extracts analysed. The aim of this type of experiment is to maximize the sensitivity of detection powered by the MS device, a very challenging task for veteran three-dimensional ion traps when carrying out simultaneous MS^n analyses to study minor compounds, as in our case.

Taking into consideration the literature about proanthocyanidins in persimmon extracts (polymers consisting mainly of galloylated (epi)catechin and (epi)gallocatechin units, see the

Introduction section) and the four free anthocyanidins detected by the untargeted MS analysis in this research, it seemed logical to assume that a more sensitive MS study could lead to the detection of aglycone adducts formed between the galloylated catechins and the anthocyanidins. Moreover, the presence of galloyl derivatives of flavanol-anthocyanidin (or vice versa) adducts in the samples made sense because acidic media promote the formation of tannin-anthocyanin adducts (Salas *et al.*, 1980) and because of the resistance of procyanidin dimers and trimers to acid hydrolysis (Heim *et al*., 2002; Salas *et al*., 1980).

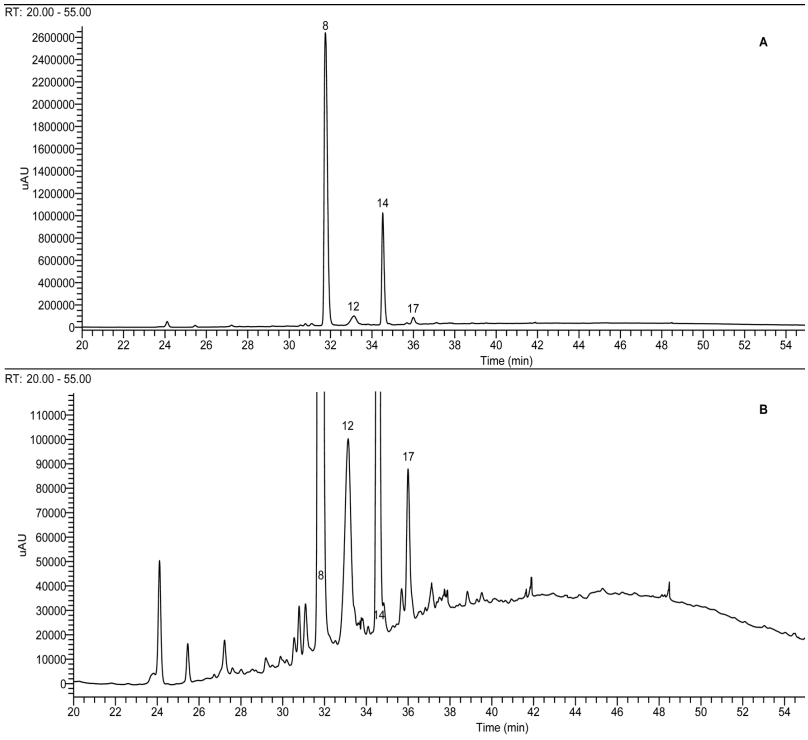

Fig. 1. HPLC chromatogram of the acid-hydrolyzed extracts from persimmon fruits studied, recorded at λ = 520nm. (A) Standard chromatogram showing major pigments: delphinidin (peak 8), petunidin (peak 12), cyanidin (peak 14) and peonidin (peak 17). (B) Zoomed chromatogram showing additional minor anthocyanidin-based components.

Table 1 reveals that the targeted MS analysis led to the detection of thirteen galloylated flavanol-anthocyanidin adducts (including the structural isomers derived from the molecular chirality of flavanols) corresponding to all the expected combinations. As a first conclusion, the results obtained corroborated previous studies on persimmon extracts regarding the absence of (epi)afzelechin derivatives, the high degree of galloylation of persimmon tannins (only galloylated catechin and gallocatechin adducts were found) and the presence of complex pigments as a consequence of the acid hydrolysis. It must be noted that the coloured adducts identified were detected as minor compounds. Furthermore, evidence of some other different pigments (adducts of non-galloylated (epi)catechin and (epi)gallocatechin with anthocyanidins)

also seemed to be present in the samples, but the MS^n data generated were too incomplete (owing to instrumental limitations regarding sensitivity) to obtain positive assignments. Accordingly, further studies involving faster and more sensitive MS devices combined with Nuclear Magnetic Resonance (NMR) analysis are needed to refine our knowledge.

Table 1. Pigments detected in acid-hydrolysed methanolic extracts from 'Rojo Brillante' persimmon pulp.

Rt (min)	Peak No.	$[M]^+$ (*m/z*)	Characteristic MS^2 fragments	Characteristic MS^3 fragments	Tentative identification
23.93	1	759	741, 633, 607, **589**, 571, 497, 481, 463, 439, 345, 327, 303	571, **463**, 439, 327, 303	Galloyl-3-*O*-(epi)gcat-delphinidin
27.30	2	759	741, 633, 607, **589**, 571, 497, 481, 463, 439, 345, 327, 303	571, **463**, 439, 327, 303	Galloyl-3-*O*-(epi)gcat-delphinidin
27.88	3	743	725, 617, 591, **573**, 555, 481, 465, 447, 423, 329, 311, 287	555, **447**, 423, 311, 287	Galloyl-3-*O*-(epi)gcat-cyanidin
28.06	4	743	725, 617, 591, **573**, 555, 497, 465, 447, 439, 345, 327, 303	555, **447**, 439, 327, 303	Galloyl-3-*O*-(epi)cat-delphinidin
29.74	5	773	755, 647, 621, **603**, 585, 511, 495, 477, 453, 359, 341, 317	585, **477**, 453, 341. 317	Galloyl-3-*O*-(epi)gcat-petunidin
30.64	6	743	725, 617, 591, **573**, 555, 481, 465, 447, 423, 329, 311, 287	555, **447**, 423, 311, 287	Galloyl-3-*O*-(epi)gcat-cyanidin
30.92	7	743	725, 617, 591, **573**, 555, *497, 465, 447, 439, 345, 327, 303	555, **447**, 439, 327, 303	Galloyl-3-*O*-(epi)cat-delphinidin
31.90	8	303	303	-	Delphinidin
31.99	9	759	741, 633, 607, **589**, 571, 497, 481, 463, 439, 345, 327, 303	571, **463**, 439, 327, 303	Galloyl-3-*O*-(epi)gcat-delphinidin
32.86	10	757	739, 631, 605, **587**, 569, 495, 479, 461, 437, 343, 325, 301	569, **461**, 437, 325, 301	Galloyl-3-*O*-(epi)gcat-peonidin
33.20	11	757	739, 631, 605, **587**, 569, 511, 479, 461, 453, 359, 341 317	569, **461**, 453, 341, 317	Galloyl-3-*O*-(epi)cat-petunidin
33.29	12	317	**317**, 302	-	Petunidin
33.62	13	727	709, 601, 575, **557**, 539, 481, 449, 431, 423, 329, 311, 287	539, **431**, 423, 311, 287	Galloyl-3-*O*-(epi)cat-cyanidin
34.69	14	287	287	-	Cyanidin
35.74	15	743	725, 617, 591, **573**, 555, 497, 465, 447, 439, 345, 327, 303	555, **447**, 439, 327, 303	Galloyl-3-*O*-(epi)cat-delphinidin
35.78	16	741	723, 615, 589, **571**, 553, *495, 463, 445, 437, 343, 325, 301	553, **445**, 437, 325, 301	Galloyl-3-*O*-(epi)cat-peonidin
36.15	17	301	**301**, 286	-	Peonidin

In bold, main ion generated at MS^2 and MS^3 stages.
MS^3 analysis from main ion generated at MS^2 stage.
*Corresponds to ion (c) from MS^2 of $[M]^+$, the MS^3 of which gave underlined ions (h) and (i), subsequently confirmed by the Ion Tree Breadth MS analysis (see Figure 2 for nomenclature and discussion section for description of the MS experiment).
Abbreviations used: Rt, retention time; $[M]^+$, molecular mass under positive ionization conditions; *m/z*, mass-to-charge ratio; (epi)gcat, (epi)gallocatechin; (epi)cat, (epi)catechin.

To understand the nature of the identified adducts, let us consider as an example the compound eluted at 30.64 minutes with molecular mass at *m/z* 743 (3-O-galloyl-(epi)gallocatechin-cyanidin, compound 6 in **Table 1**). Because of its galloylation, the MS^n analysis of compound 6 should reveal fragments from the intact molecule ($[M]^+$) as well as from the structures without the galloyl and gallic acid substituents ($[M]^+$ -152) and [M]+-170 amu, respectively). Therefore, proposed fragmentation pathways and a series of characteristic ions belonging to compound 6 were schematized in **Fig. 2**, supported by the experimental data from the sensitive (targeted) MS^2 and MS^3 analyses (both illustrated in **Figs. 3A** and **3B**, respectively). To enhance the clarity of the results obtained, all the proposed fragmentation pathways will be discussed separately.

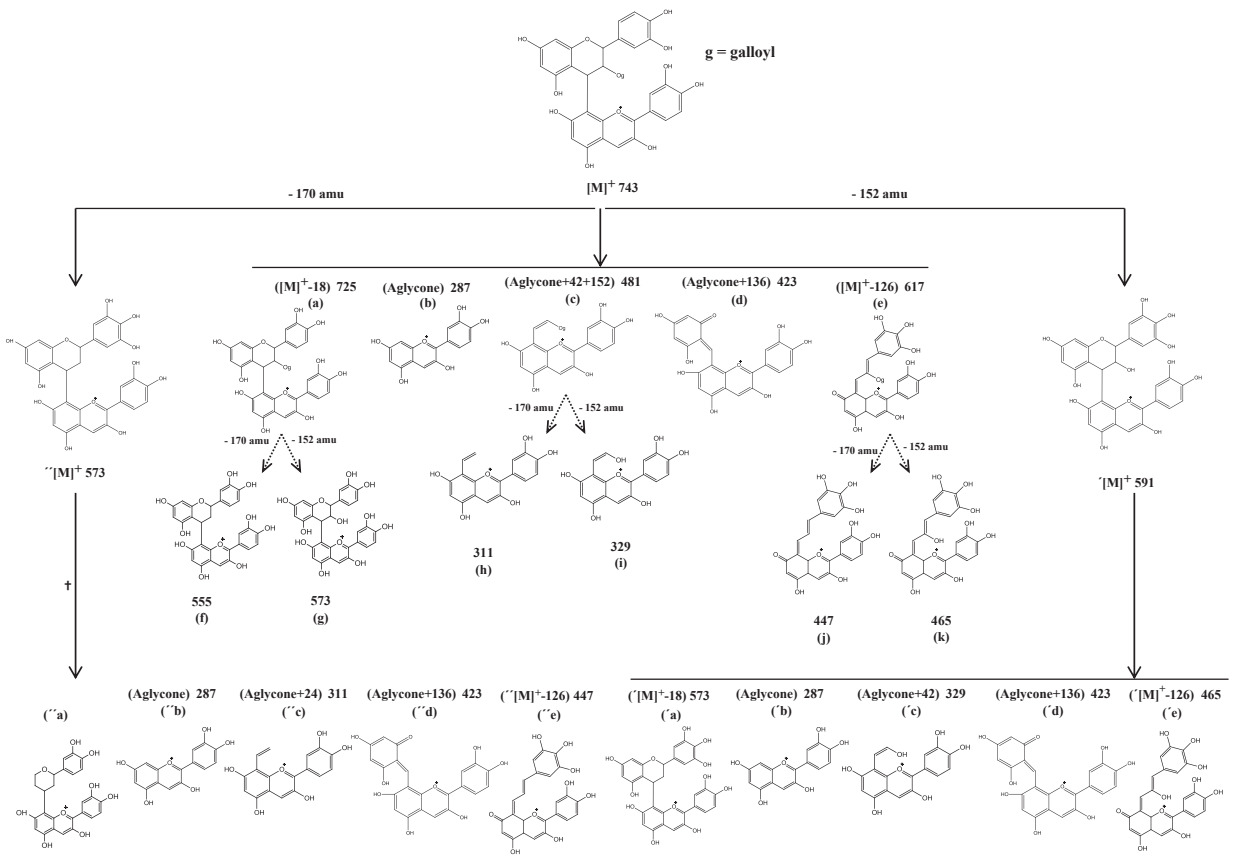

Fig. 2. Breakdown pathways proposed to 3-*O*-galloyl-(epi)gallocatechin-cyanidin (compound 6 in **Table 1**) elucidated by MS^2 analysis. †Indicates that fragmentation pattern corresponding to $[M]^+$-170 (´´$[M]^+$ in figure) was lately confirmed by MS^3 analysis.

Just considering the intact ion corresponding to compound 6 ($[M]^+$ with *m/z* 743), **Fig. 3A** shows a fragment at *m/z* 617 (named (e) in **Fig. 2**) which corresponded to $[M]^+$ -126, clearly indicating the presence of a flavanol group in the upper position of a potential flavanol-anthocyanidin ($F\text{-}A^+$) adduct, as pointed out by Sentandreu *et al.* (2010), thus ruling out the possibility of there being an anthocyanidin-flavanol (A^+ -F) derivative (Sentandreu *et al*., 2012). To corroborate that we were in the presence of a $F\text{-}A^+$adduct (and assuming that the two units were linked through the most common C4-C8 union mentioned above for procyanidins), its breakdown pattern should follow the fragmentation guidelines previously described by Sentandreu *et al*. (2010) when they studied glycosides of pomegranate juice adducts (that is, obtaining five characteristic ions from the aglycone, three of them depending exclusively on the

anthocyanidin and the other two on both the flavanol and the anthocyanidin units). The fragmentation pathway of $[M]^+$ systematized in **Fig. 2** was confirmed by the MS^2 results illustrated in **Fig. 3A** through the appearance of the following ions: *m/z* at 725(a), corresponding to a loss of water, $[M]^+$ -18 (most probably from the B-ring); *m/z* at 287(b), corresponding to the anthocyanidin (cyanidin); *m/z* at 481(c), corresponding to the anthocyanidin+42+galloyl; *m/z* at 423(d), corresponding to the retro Diels-Alder reaction suffered by the upper flavanol unit (anthocyanidin+136 or $[M]^+$-320, $[M]^+$ -304 in the case of having (epi)catechin); and the previously mentioned fragment at *m/z* 617(e). It should be taken into account that, unlike what happened in the study of Sentandreu *et al.* (2010), ions still having the galloyl group could also suffer subsequent breakdowns and release fragments that do not have the gallic acid and galloyl moieties. For this reason, ions (a), (c) and (e) represented in **Fig. 2** should promote the appearance of their respective fragments from the neutral losses of 170 and 152 amu respectively, finally having pairs of ions at *m/z* 555(f)-573(g), 311(h)-329(i) and 447(j)-465(k) respectively. As we can see, all these fragments were confirmed by the MS^2 spectra represented by **Fig. 3A**.

The fragmentation pathway corresponding to the intact parent mass but without the galloyl group, $[M]^+$ -152 represented as ´$[M]^+$ in **Fig. 2** with a molecular mass at *m/z* 591, was also present in the MS^2 spectra (**Fig. 3A**). The particularity of ´$[M]^+$ lies in the fact that its molecular structure is the same as that described by Sentandreu *et al.* (2010) for condensed F-A^+ adducts detected in pomegranate juice (having a hydroxyl group in the C3 position of the C-ring instead of the galloyl substituent). Thus, MS^2 ions from´$[M]^+$ should be: *m/z* 573(´a), corresponding to a loss of water (`$[M]^+$ -18) from C3 in the C-ring; *m/z* 287(´b), from the anthocyanidin (cyanidin); *m/z* 329(´c), from the anthocyanidin+42; *m/z* 423(´d), from the retro Diels-Alder reaction of the upper flavanol unit (anthocyanidin+136 or ´$[M]^+$-168, ´$[M]^+$ -152 for (epi)catechin); and *m/z* 465(´e), from ´[M]-126 (explained above). Again, all the expected characteristic MS^2 ions from ´$[M]^+$ are present in **Fig. 3A**. Obviously, no subsequent fragments were derived from ions (´a), (´c) and (´e) because ´$[M]^+$ had a de-galloylated structure.

Finally, the third fragmentation pathway that appeared in Fig. 3A seemed to correspond to the ion generated by the loss of gallic acid from the original parent mass, having its molecular mass at m/z 573 ($[M]^+$ -170 represented as ´´$[M]^+$ in **Fig. 2**). It should be pointed out that the simultaneous occurrence of all these three fragmentation pathways from $[M]^+$, ´$[M]^+$ and ´´$[M]^+$ (illustrated by **Fig. 2** and corroborated by the experimental analysis shown by **Fig. 3A**) led to

the obtaining, at different levels, of isotopic ions with the same (i.e. ions (´a) and ´´$[M]^+$) or different (i.e. ions (g) and ´´$[M]^+$) molecular structures. In any case, characteristic MS^2 fragments from ´´$[M]^+$ that appeared in **Fig. 3A** were: *m/z* 555(´´a), corresponding to a loss of water (´´$[M]^+$ -18), ion (g) originated by $[M]^+$ and ion (´a) from ´$[M]^+$ as well as a consequence of ion (f) from $[M]^+$; *m/z* 287(´´b), from the anthocyanidin; *m/z* 311(´´c), from the anthocyanidin+24 (not 42 as usual, owing to the loss of the hydroxyl group in the C3 position of the C-ring of ´´$[M]^+$); *m/z* 423(´´d), corresponding to the retro Diels-Alder reaction of the upper flavanol unit (anthocyanidin+136 or ´´$[M]^+$-150, ´´$[M]^+$ -136 if having (epi)catechin); and *m/z* 447(´´e), from ´´$[M]^+$ -126. Again, no late fragments from ions (´´a), (´´c) and (´´e) were generated as a consequence of the absence of gallic acid in the structure of ´´$[M]^+$.

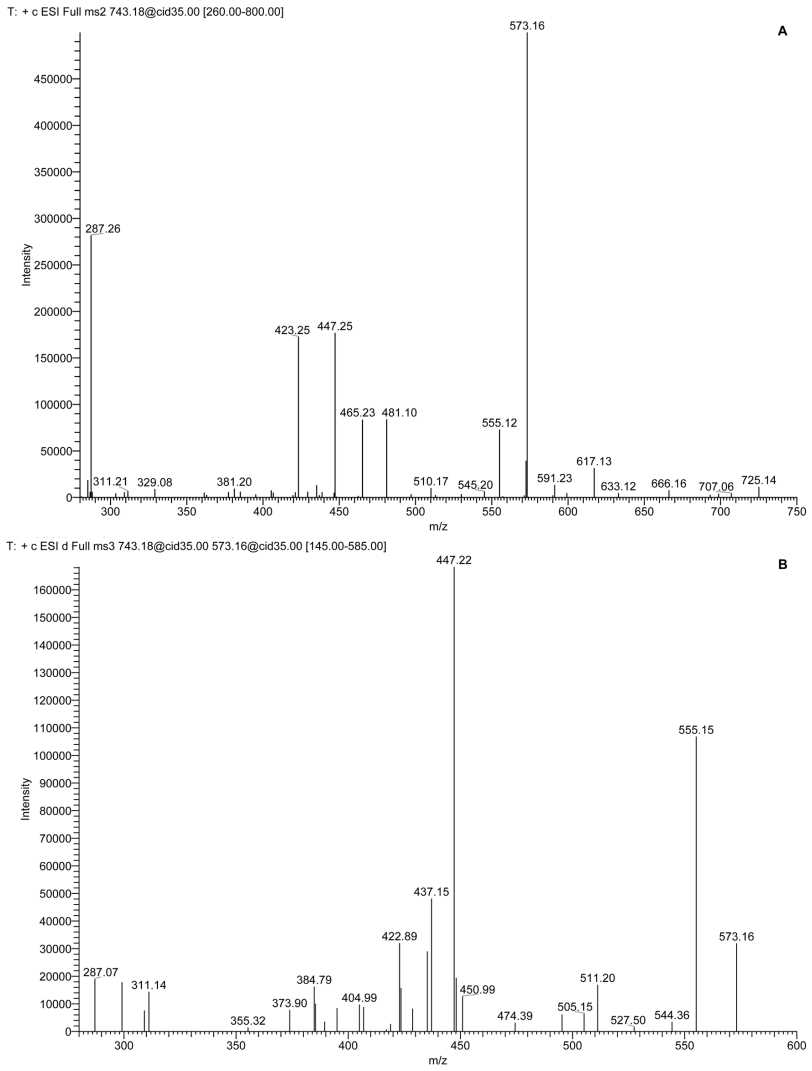

Fig. 3. Experimental MS^n analysis of the parent ion ($[M]^+$) at *m/z* 743 corresponding to galloyl-3-*O*-(epi)gallocatechin-cyanidin (compound 6 in **Table 1**). (A) Fragmentation pattern from MS^2 analysis. (B) MS^3 of the major daughter ion at *m/z* 573 (corresponding to the loss of gallic acid of $[M]^+$) generated at MS^2 step of analysis). *Abbreviations used*: *m/z*, mass-to-charge ratio.

Considering the above, the targeted MS^3 analysis (see the experimental section) could greatly help in the attempt to validate the veracity of the fragmentation pathways proposed. **Fig. 3B** shows the MS^3 fragmentation pattern of the main ion (with *m/z* 573) generated in the MS^2 analysis (**Fig. 3A**) of compound 6 (**Table 1**). The results seemed to indicate that the preferred breakdown of the intact molecule ($[M]^+$) was that given by the loss of gallic acid ($[M]^+$-170 or ´´$[M]^+$ in **Fig. 2**). This finding was repeated in all the adducts detected in the samples (see bolded ions listed in **Table 1** at MS^2 level). Therefore, the MS^3 of the fragment at *m/z* 573 (**Fig. 3B**) revealed the presence of the previously mentioned characteristic five fragments at *m/z* 555(´´a); *m/z* 287(´´b); *m/z* 311(´´c); *m/z* 423(´´d); and *m/z* 447(´´e). Very noticeable was the absence in the MS^3 spectra of a fragment at *m/z* 329 that should correspond to the breakdown of ion (g) (anthocyanidin+42, from $[M]^+$), shown in **Fig. 2**. This seemed to suggest that the ion at *m/z* 573 that appeared in **Fig. 3A** was contributed solely by the loss of gallic acid from the original intact molecule (´´$[M]^+$) and not from ion (g). In all cases, MS^3 results from each detected adduct followed the same trend, finding as the main ion generated the one corresponding to ´´$[M]^+$-126 (see bolded ions in **Table 1** at MS^3 level, fragment (´´e) in **Fig. 2**).

Unfortunately, as previously mentioned, the identified adducts were detected as minor components, thus hampering complementary MS analyses. Consequently, specific Chain Reaction Monitoring (CRM) experiments were carried out to confirm the breakdown pattern of the ions generated. The characteristic neutral losses from $[M]^+$ were considered as those corresponding to the galloyl moiety ($[M]^+$ -152 or ´$[M]^+$ in **Fig. 2**) or the specific moiety for F-A^+ adducts ($[M]^+$ -126). At best, the lack of sensitivity led to the obtaining of partial but not conclusive MS information. Datadependent Neutral Loss experiments (MS^3 analysis of ions presenting losses of 170 and 152 amu at MS^2 level) were also performed without obtaining any additional data other than those generated by the specific MS^n analyses described in the experimental section. The only complementary MS analysis that provided some supplementary information of value was from the Ion Tree Breadth analysis (consisting of three scan events: scan event 1, full MS; scan event 2, MS^2 of the three most intense ions populated in the target mass list corresponding to all the possible galloylated flavanol-anthocyanidin adducts; scan event 3, MS^3 of the three most intense ions from scan event 2). This last analysis provided confirmation of the generation of ions (h) and (i) from fragment (c) described in **Fig. 2** (related with the breakdown pathway of $[M]^+$), corresponding to compounds 7 and 16 (see **Table 1**).

4. Conclusions

To date, this research represents the most complete metabolite profiling of pigments that appear in acid-hydrolyzed persimmon extracts. Four free anthocyanidins were identified (delphinidin, petunidin, cyanidin and peonidin), and, what is more important, for the first time thirteen 3-*O*-galloylated flavanol-anthocyanidin adducts (structures made of galloyled (epi)catechin and (epi)gallocatechin with anthocyanidins) were detected in naturally derived extract. The proposed methodology of analysis led to the overcoming of problems caused by the existence of these novel minor components with an intricate molecular structure. It was also demonstrated that a detailed metabolite analysis of a complex extract can be achieved maximizing the scan features of a conventional three-dimensional ion trap despite its intrinsic technological limitations. Furthermore, some evidences was found for the existence of some other different non-galloyled anthocyanidin-based adducts after the acidic treatment of persimmon extracts. Finally, use of persimmon derivatives as a source of pigments could promote this cultivar for the design of innovative foodstuffs.

Acknowledgements

This study was supported by MICIN (Spanish Government) project AGL 2009-11805ALI. Authors acknowledge the financial support for the contract of M. Cerdán-Calero (JAE-PREdoc program, CSIC-FEDER funds) and from Consolider Ingenio Fun-C-Food (CSD2007-00063). Activity of Dr. E. Sentandreu during this research was self-funded. Corresponding author is also indebted with Miguelín Llibrer for his companionship that greatly helped to maintain his motivation during this work.

References

Edwin, H., 1980. In vino veritas: Oligomeric procyanidins and the ageing of red wines. Phytochemistry 19(12), 2577-2582.

Gu, H. F., Li, C. M., Xu, Y., Hu, W., Chen, M., Wan, Q., 2008. Structural features and antioxidant activity of tannin from persimmon pulp. Food Research International 41(2), 208-217.

Heim, K. E., Tagliaferro, A. R., Bobilya, D. J., 2002. Flavonoid antioxidants: chemistry, metabolism and structure-activity relationships. The Journal of Nutritional Biochemistry 13(10), 572-584.

Komatsu, S., Matsunami, N., 1924. Constitution of Shibuol. Memoirs of College of Science Kyoto Imperial University A 7, 15-23.

Komatsu, S., Matsunami, N., 1925. Constitution of Shibuol II. Memoirs of College of Science Kyoto Imperial University A 11, 231-240.

Li, C., Leverence, R., Trombley, J. D., Xu, S., Yang, J., Tian, Y., Reed, J. D., Hagerman, A. E., 2010. High Molecular Weight Persimmon (Diospyros kaki L.) Proanthocyanidin: A Highly Galloylated, A-Linked Tannin with an Unusual Flavonol Terminal Unit, Myricetin. Journal of Agricultural and Food Chemistry 58(16), 9033-9042.

Matsuo, T., Ito, S., 1978. The Chemical Structure of Kaki-tannin from Immature Fruit of the Persimmon (*Diospyros kaki* L.). Agricultural and Biological Chemistry 42(9), 1637-1643.

Nakatsubo, F., Enokita, K., Murakami, K., Yonemori, K., Sugiura, A., Utsunomiya, N., Subhadrabandhu, S., 2002. Chemical structures of the condensed tannins in the fruits ofDiospyros species. Journal of Wood Science 48(5), 414-418.

Salas, E., Fulcrand, H., Meudec, E., Cheynier, V., 2003. Reactions of Anthocyanins and Tannins in Model Solutions. Journal of Agricultural and Food Chemistry 51(27), 7951-7961.

Sentandreu, E., Cerdán-Calero, M., Sendra, J. M., 2013. Phenolic profile characterization of pomegranate (punica granatum) juice by high-performance liquid chromatography with diode array detection coupled to an electrospray ion trap mass analyzer. Journal of Food Composition and Analysis 30(1), 32-40.

Sentandreu, E., Navarro, J. L., Sendra, J. M., 2010. LC-DAD-ESI/MS^n Determination of Direct Condensation Flavanol−Anthocyanin Adducts in Pressure Extracted Pomegranate (Punica granatum L.) Juice. Journal of Agricultural and Food Chemistry 58(19), 10560-10567.

Sentandreu, E., Navarro, J. L., Sendra, J. M., 2012. Identification of New Coloured Anthocyanin–Flavanol Adducts in Pressure-Extracted Pomegranate (Punica granatum L.) Juice by High-Performance Liquid Chromatography/Electrospray Ionization Mass Spectrometry. Food Analytical Methods 5(4), 702-709.

Xu, S., Zou, B., Yang, J., Yao, P., Li, C., 2012. Characterization of a highly polymeric proanthocyanidin fraction from persimmon pulp with strong Chinese cobra PLA2 inhibition effects. Fitoterapia 83(1), 153-160.

Research Article

Received: 1 April 2014 Revised: 4 July 2014 Accepted article published: 8 August 2014 Published online in Wiley Online Library:

(wileyonlinelibrary.com) DOI 10.1002/jsfa.6867

Rapid screening of low-molecular-weight phenols from persimmon (*Diospyros kaki*) pulp using liquid chromatography/UV–visible/electrospray mass spectrometry analysis

Enrique Sentandreu,[a*] Manuela Cerdán-Calero,[a] John M Halket[b,c] and José L Navarro[a]

Abstract

BACKGROUND: Persimmon fruits have been widely used in traditional medicine owing to their phenolic composition. This research aims to perform a rapid, detailed and affordable study of the profile of low-molecular-weight phenols from persimmon pulp.

RESULTS: Two different HPLC-DAD/ESI-MS^n analyses were performed using a routine three-dimensional ion trap mass spectrometer to analyze the ethanolic extract of persimmon pulp: (1) an untargeted data-dependent analysis to identify the majority of small phenols that included full MS and MS^2 scan events; (2) a targeted data-dependent analysis to identify polymerized phenols (dimers and formic acid adducts) through a source-induced dissociation analysis that included full MS and MS^2 scan events. Thirty-two low-molecular-weight phenols were detected, comprising gallic acid and its glycoside and acyl derivatives, glycosides of *p*-coumaric, vanillic and cinnamic acids and different flavone di-*C*-hexosides, most of them reported for the first time in persimmon.

CONCLUSION: The use of a straightforward and affordable methodology of analysis led to obtain an up-to-date profiling of low-molecular-weight phenols in persimmon. The results can help future actions aimed to expand the understanding of the phenolic metabolome of persimmon cultivars.

Keywords: *Diospyros kaki*; persimmon pulp; low-molecular-weight phenols; HPLC-DAD/ESI-MS^n analysis; routine three-dimensional ion trap

INTRODUCTION

Persimmon (*Diospyros kaki* L.) fruits have commonly been used in Chinese traditional medicine for their positive effects on human health, mainly against hypertension, bleeding, elevated body temperature and general oxidative processes.[1,2] Moreover, in recent years the popularity of persimmons has grown outside of the traditional production areas (China, Japan and Korea), becoming a promising crop in Brazil and some Mediterranean countries such as Spain and Italy.[3]

Sugars, vitamin C, carotenoids and polyphenols are the constituents most commonly cited in the pulp (the edible part) of persimmon,[1,4–7] with phenolic compounds having special relevance in its claimed health effects. Persimmon phenols can be grouped as a function of their molecular complexity.[1,4,7] Thus low-molecular-weight phenols are represented by free phenolic acids and catechins as well as hydrolyzable tannins (mainly glycosides of gallic acid and flavanols). Another group is composed of high-molecular-weight phenols, also known as condensed tannins or proanthocyanins, which are large polymers of catechins with or without galloylation.

As pointed out by Li *et al.*,[8] the high molecular weight of persimmon proanthocyanins (normally above 2000 amu) represents a significant drawback for their rapid study, since their detection implies the combination of different methods of analysis (normally coupling matrix-assisted laser desorption/ionization with time-of-flight detection mass spectrometry (MALDI-TOF-MS) and thiolysis degradation with high-performance liquid chromatography with tandem mass spectrometry detection (HPLC/MS^n)). In contrast, the analysis of low-molecular-weight phenols in natural extracts can be relatively easy owing to the simplicity of

* *Correspondence to: Enrique Sentandreu, Instituto de Agroquímica y Tecnología de Alimentos (IATA-CSIC), Avda Agustín Escardino 7, E-46980, Paterna, Valencia, Spain. E-mail: elcapi@iata.csic.es*

a *Instituto de Agroquímica y Tecnología de Alimentos (IATA-CSIC), Avda Agustín Escardino 7, E-46980, Paterna, Valencia, Spain*

b *Mass Spectrometry Facility/Drug Control Centre, Franklin-Wilkins Building, King's College London, 150 Stamford Street, London, SE1 9NH, UK*

c *Specialist Bioanalytical Services Ltd, Egham, Surrey, TW20 9LZ, UK*

the sample preparation procedure and the platform of analysis requested (usually based on liquid chromatography with diode array detection coupled with electrospray ionization tandem mass spectrometry (HPLC-DAD/ESI-MS^n)). However, the diversity of small phenols reported to date in persimmon pulp extracts is surprisingly scarce, being normally restricted to three to ten components (mainly cinnamic acid derivatives) depending on the variety assayed.[4] From this, we can conclude that the metabolite profile of low-molecular-weight phenols in persimmon pulp still remains unclear.

This research aims to perform a rapid and detailed metabolite profiling of low-molecular-weight phenols of extracts from the most widely cultivated persimmon variety in Spain (cv. Rojo Brillante). To achieve this goal, a straightforward and affordable HPLC-DAD/ESI-MS^n methodology of analysis is proposed. Conditions and settings of analysis featured by a routine three-dimensional ion trap were optimized to maximize the obtaining of relevant information from samples.

EXPERIMENTAL

Reagents and standards

Water and acetonitrile (ACN) of LC/MS grade and ethanol (EtOH) and formic acid (FA) of analytical grade were from Scharlab SL (Barcelona, Spain). Gallic acid of HPLC grade was from Sigma Aldrich (St Louis, MO, USA).

Sample preparation

Persimmon (*D. kaki*, cv. Rojo Brillante) fruits of Denomination of Origin 'Kaki Ribera del Xúquer' supplied by the cooperative 'San Bernardo' (Carlet, Valencia, Spain) in December 2012 were stored at 4 °C and analyzed within 15 days.

Glassware was used throughout the sample preparation procedure. Two different batches (with three freshly prepared samples each) were used to run the planned MS experiments. Each sample was from one persimmon fruit previously washed in tap water and heated in a water bath at 100 °C for 10 min to inactivate polyphenol oxidases (PPOs). The chalice and peel were removed and 150 g of the pulp was mixed with 600 mL of aqueous EtOH (800 mL L^{-1}). The sample was homogenized in an analytical mill (IKA A11 Yellow Line, IKA Werke GmbH & Co. KG, Staufen, Germany) and 25 g of the resultant puree was centrifuged at 4500 × *g* for 5 min. The yellowish supernatant was retained and the pellet was re-extracted with EtOH (800 mL L^{-1}) until colorless. The supernatants were combined and the resultant solution was evaporated to complete dryness in a speed-vac system (ThermoScientific SPD 121P, Thermo Fisher Scientific SLU, Madrid, Spain). The sample was re-suspended in 5 mL of water, centrifuged at 4500 × *g* for 5 min, filtered through a 0.25 μm nylon filter, poured into a glass vial and injected into the HPLC-DAD/ESI-MS^n system.

HPLC-DAD/ESI-MS^n analysis

Chromatographic separation was carried out using a Thermo Surveyor Plus HPLC system (ThermoScientific, San Jose, CA, USA) equipped with a quaternary pump, vacuum degasser, temperature-controlled autosampler and diode array detector. A 250 mm × 2.1 mm i.d., 3 μm, YMC C-18 Pack-Pro column (YMC Europe GmbH, Dinslaken, Germany) was used. Chromatographic conditions were as follows: injection volume, 5 μL; flow rate, 0.2 mL min^{-1}; oven temperature, 24 °C; autosampler temperature, 10 °C; solvent A, water containing 1 mL L^{-1} FA; solvent B, ACN containing 1 mL L^{-1} FA; separation gradient, initially 0% B, linear 0–5% B at 10 min, linear 5–30% B at 60 min, linear 30–100% B at 70 min, purging with 100% B for 15 min and column equilibration with 0% B for 30 min; detection wavelengths, $\lambda = 280$ and 320 nm.

MS analysis and fragmentation experiments were performed using a ThermoFinningan LCQ Advantage conventional three-dimensional ion trap mass analyzer (ThermoScientific, San Jose, CA, USA) equipped with an electrospray ionization source operating in negative mode (ESI$^-$) under the following general conditions: source voltage, 4 kV; capillary voltage, −29 V; capillary temperature, 300 °C; sheath gas flow, 50 (arbitrary units); sweep gas flow, 20 (arbitrary units); full max ion time, 300 ms; full micro scans, 3; selected ion monitoring (SIM) max ion time, 300 ms; SIM micro scans, 3; MS^n max ion time, 300 ms; MS^n micro scans, 3. Control of the HPLC-DAD/ESI-MS^n device and data analysis were managed by the software Xcalibur v. 2.06 loaded into a PC.

Considering the natural tendency of low-molecular-weight phenols to polymerize (dimerizing or forming adducts with the mobile phase modifiers) during sample ionization at the ESI source of the mass analyzer, two separate MS analyses were carried out in this study.

Conventional untargeted data-dependent MS analysis

This analysis aimed to obtain a global picture of the main phenolic compounds in the samples. Data-dependent conditions were as follows: normalized collision-induced dissociation (CID) energy, 35% (arbitrary units); reject mass-to-charge ratio (*m/z*) width, 1; repeat count, 3; repeat duration, 0.5 min; exclusion size list, 25; exclusion duration, 1 min; exclusion mass width, 3. Moreover, this analysis included two scan events: scan event 1, full MS; scan event 2, MS^2 of the most intense ions from scan event 1. The scanned *m/z* range was 100–2000.

Samples were analyzed in triplicate (first batch of samples).

Targeted data-dependent MS analysis with activated source fragmentation (SID analysis)

This analysis was performed to overcome the interferences induced by the polymerization of small phenols during sample ionization (masking their real molecular masses and making it difficult to obtain relevant information from their fragmentation study). Thus this analysis was run under the same conditions as described above for the conventional MS analysis but with the option 'source fragmentation' enabled at −30 V. This feature induces the fragmentation of ionized molecules before mass selection (in our case it occurs at the tube lens section, before the first octupole). This process is known as 'source-induced dissociation (SID)' or most popularly as 'poor man's MS/MS' from those cases where tandem mass spectrometry is not possible (i.e. using a single-quadrupole spectrometer). Later, SID ions (actually fragments) will be conventionally fragmented by CID dissociation to obtain MS^2 fragments (although we can consider that the whole SID process is a pseudo-MS^3 analysis).

It should be emphasized that SID analysis is not selective and affects all ionized molecules of the sample and also decreases the sensitivity of their detection in general. For this reason, this is a complementary analysis that must be applied to specific (target) ions selected from scan event 1 (full MS) of the conventional untargeted data-dependent MS analysis that were prone to polymerization.

Samples were analyzed in triplicate (second batch of samples).

Table 1. Low-molecular-weight phenols detected in pulp of 'Rojo Brillante' persimmon fruits

Peak no.	Rt (min)	UV–visible (nm)[a]	$[M-H]^-$ *m/z*	MS^2 [b]	Tentative identification
1	17.21	261	737	719, **705**, 547, 397	UK 1
2	18.43	274	331	313, 271, **211**, 193, 169, 125	Monogalloyl-hexoside
3	20.38	257	541	**406**, 405, 271, 270	UK 2
4	22.23	278	**331**/663	271, 211, 193, **169**, 125	Monogalloyl-hexoside
5	22.61	–	493	**331**, 169	Monogalloyl-dihexoside
6	22.97	271	169	125	Gallic acid
7	24.23	253, 275	777	745, **717**, 699, 645, 585	UK 3
8	24.68	272	**331**/663	**271**, 169	Monogalloyl-hexoside
9	26.11	–	493	**331**, 169	Monogalloyl-dihexoside
10	27.46	273	**331**/663	313, **271**, 241, 169, 125	Monogalloyl-hexoside
11	31.17	273, 279, 287	479 (FA) → **433**	**293**, 149, 131	UK 4
12	32.23	274	405	405, **313**, 271, 253, 169, 151, 125	Galloyl derivative
13	34.92	–	447	331	Maloyl-monogalloyl-hexoside
14	34.97	–	609	**493**, 331	Diacyl-monogalloyl-hexoside
15	35.03	–	535	373, **331**, 169	Acetylhexoside-monogalloyl-hexoside
16	36.85	265	373	**169**, 125	Monogalloyl-acetylhexoside
17	39.11	280	499	**337**, 319, 293	UK 5 (hexoside)
18	41.79	–	611	593, 521, **491**, 473, 431, 413, 401, 371	Flavone di-*C*-hexoside
19	42.81	265	373	**169**, 125	Monogalloyl-acetylhexoside
20	42.92	294	495	341	UK 6
21	44.66	282	457	325, 205, **163**	Coumaric acid-pentoside-hexoside
22	45.16	289	595	577, 505, 487, **475**, 457, 415, 385, 355	Flavone di-*C*-hexoside
23	45.50	268	639 (FA) → **593**	593, 575, 509, 466, **395**, 197	UK 7 (syringic acid trimer)
24	45.84	268	485	305, 221, **189**	UK 8
25	47.05	265	427 (FA) → **381**	**249**, 161	UK 9 (pentoside)
26	47.27	–	521	359	UK 10 (lariciresinol-hexoside)
27	47.96	288	545 (FA) → **499**	191	Quinnic acid derivative (rutinoside)
28	48.87	280	461	233, 191, **167**	Vanillic acid derivative (diglycoside)
29	49.56	281	775	757, 685, 667, **655**, 637, 619, 607, 595, 565, 535	Flavone di-*C*-hexoside
30	50.29	288	759	741, 669, 651, **639**, 621, 579, 549, 519	Flavone di-*C*-hexoside
31	51.73	281	775	757, 685, 667, **655**, 637, 619, 607, 595, 565, 535	Flavone di-*C*-hexoside
32	54.24	288	613	595, 523, 505, **493**, 475, 433, 403, 373	Flavone di-*C*-hexoside

Rt, chromatographic retention time; UK, unknown compound. In **bold**: $[M-H]^-$ stage, parent mass considered to perform MS^2 analysis in the case of dimers (compounds 4, 8 and 10) or formic acid (FA) adducts (compounds 11, 23, 25 and 27); MS^2 stage, main fragment generated.
[a] Only clear maximum absorption of UV–visible spectrum is shown (weak signals were discarded).
[b] Only those fragments with relative abundance greater than 10% are shown. Fragmentation pathways are from the conventional untargeted MS^2 analysis, except for FA adducts that are from the targeted SID analysis (see 'Experimental' for description of MS analyses).

RESULTS AND DISCUSSION

The 32 phenolic compounds detected in the assayed extracts are listed in Table 1 (showing their chromatographic retention times, UV–visible and MS^n characteristics and tentative identifications). The phenolic composition of samples was first approached through their HPLC-DAD chromatogram recorded at 280 nm (Fig. 1A), since at 320 nm their response was negligible. As we can see, eight major compounds were found (numbered as listed in Table 1). However, the zoomed chromatogram (Fig. 2B) revealed that many other minor components were also present.

In this study the results will be discussed according to the different families of phenols detected and not as a function of the assayed conditions of analysis. In general, identifications were assigned considering the data from the conventional untargeted MS analysis, with the exception of adducts/clusters (compounds 11, 23, 25 and 27) that are discussed along with the results from the targeted SID analysis.

Considering Table 1, gallic acid derivatives formed the main group of phenols detected in the persimmon variety studied (13 out of 32). All these analytes had the ion at *m/z* 169 (gallic acid), and in most cases its corresponding decarboxylated ion at *m/z* 125, in their MS^2 fragmentation patterns. These galloyl-based compounds evidenced different molecular structures. The simplest was gallic acid (compound 6, also confirmed through a commercial standard), by far the most largely cited phenol in pulp extracts from different persimmon varieties.[1,4,9] The complexity increased with the first detected mono- and di-hexosides (compounds 2, 4, 5, 8, 9 and 10, with neutral losses of 162 and 324 amu respectively) as well as with the acylated hexosides (compounds 12, 13, 14, 15, 16 and 19). Obviously, instrumental limitations did not allow us to differentiate glycoside stereoisomers (i.e. glucose/galactose and xylose/arabinose). Furthermore, a very noticeable finding was the longer elution time of compounds 5 and 9 (tentatively identified as monogalloyl-dihexosides) compared with some monogalloyl-hexosides. This delay can be easily understood in the case of caffeoylated species (showing a neutral loss of 162 amu to yield caffeic acid). However, the fragment at *m/z* 179 (caffeic acid) did not appear in the MS^2 spectra of components 5

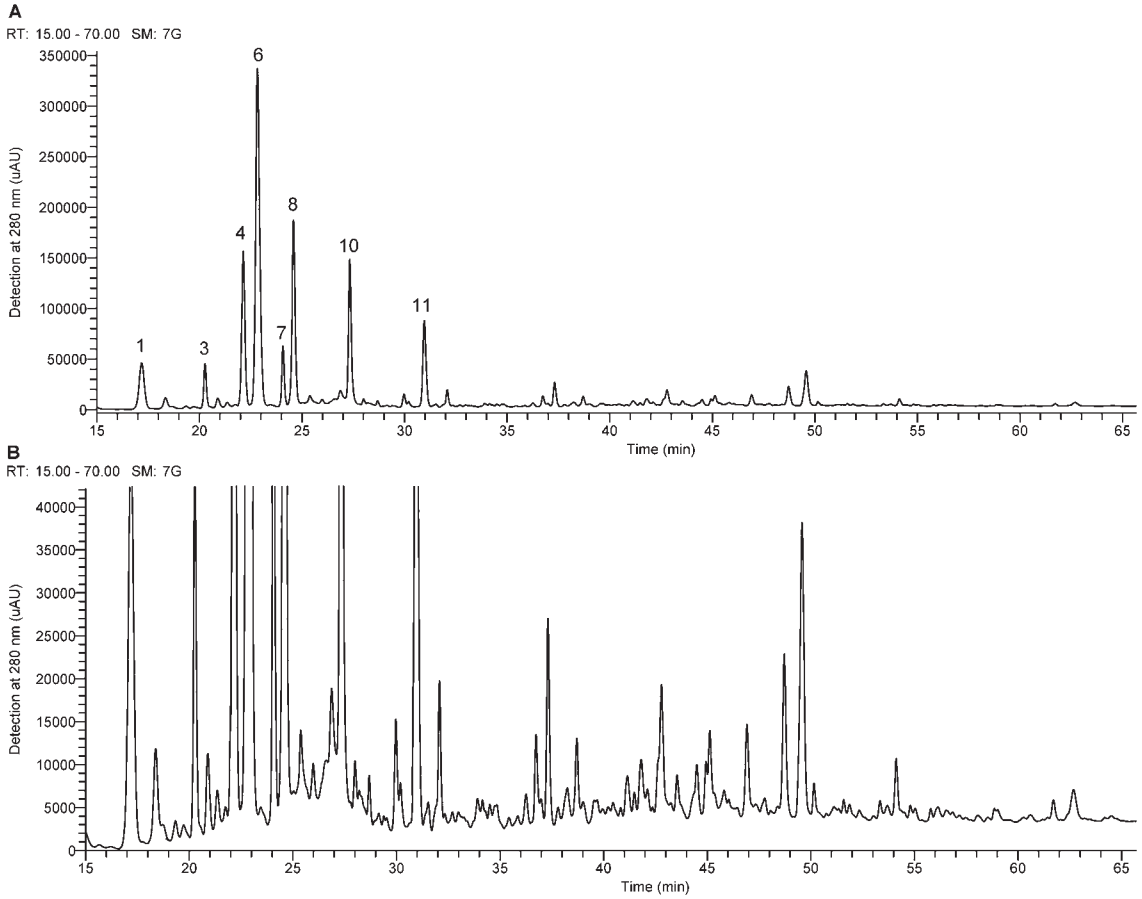

Figure 1. HPLC chromatograms of studied ethanolic persimmon extracts recorded at $\lambda = 280$ nm. (A) Standard chromatogram showing major low-molecular-weight phenols detected (numbered as listed in Table 1). (B) Zoomed chromatogram showing additional minor phenolic components.

and 9. Most probably, the glycoside stereoisometry could explain the obtained results. A further analysis based on nuclear magnetic resonance (NMR) is needed to refine our knowledge.

Regarding acyl derivatives of gallic acid hexosides, we have compounds 13 (with a neutral loss of 116 amu, corresponding to a maloyl group), 14 (with losses of 116 and 162 amu, most probably a diacylated compound according to its long retention time) and 15, 16 and 19 (all with a main MS^2 transition propitiated by the loss of 204 amu, acetylhexoside). Among this group, only the positive assignment of compound 12 remained partially unclear since, although its fragmentation pattern clearly revealed the presence of gallic acid (with fragments at *m/z* 169 and 125), it did not present any conventional MS^2 transition (although the neutral loss between the main fragment generated and gallic acid, *m/z* 313 → *m/z* 169, was 144 amu and could correspond to an anhydro-hexoside substituent).

Moreover, this study revealed the presence of several unreported phenolic acid derivatives in persimmon outside of those based on gallic acid. These components (peaks 21, 27 and 28) were tentatively identified as *p*-coumaric, quinnic and vanillic acid disaccharides respectively. These phenols were previously cited in persimmon, but only as free aglycons,[4] in addition to others such as chlorogenic, protocatechuic, caffeic and ferulic acids (not detected in this research, most probably as consequence of the variety studied, ripening stage and growth factors among others). Thus the fragmentation pathway of peak 21 (*m/z* 457) yielded the ion at *m/z* 163 (*p*-coumaric acid) as the main fragment generated, corresponding to a neutral loss of 294 amu (pentoside + hexoside). Noteworthy is the apparition of the fragment at *m/z* 325 ($[M-H]^-$ − 132 amu, loss of pentoside) and the lack of the ion at *m/z* 295 (loss of hexoside). This seems to suggest that both saccharides were not linked to the coumaroyl molecule through different positions. The presence of apiose instead of xylose/arabinose as a branched-chain sugar (to make an apiosylglucoside substituent) could explain this finding in addition to the apparition of the fragment at *m/z* 205 in the MS^2 spectrum of compound 21. Again, NMR analysis will be needed to clarify the obtained results.

Compound 27 revealed a unique MS^2 transition from the neutral loss of 308 amu (rutinoside), yielding the ion at *m/z* 191(quinnic acid) as the main fragment generated. Finally, the main MS^2 transition of compound 28 corresponded to a neutral loss of 294 amu (pentoside + hexoside) to yield the ion at *m/z* 167 (vanillic acid) as the most abundant fragment. No fragments from the isolated loss of a pentoside or hexoside group were found, inducing one to

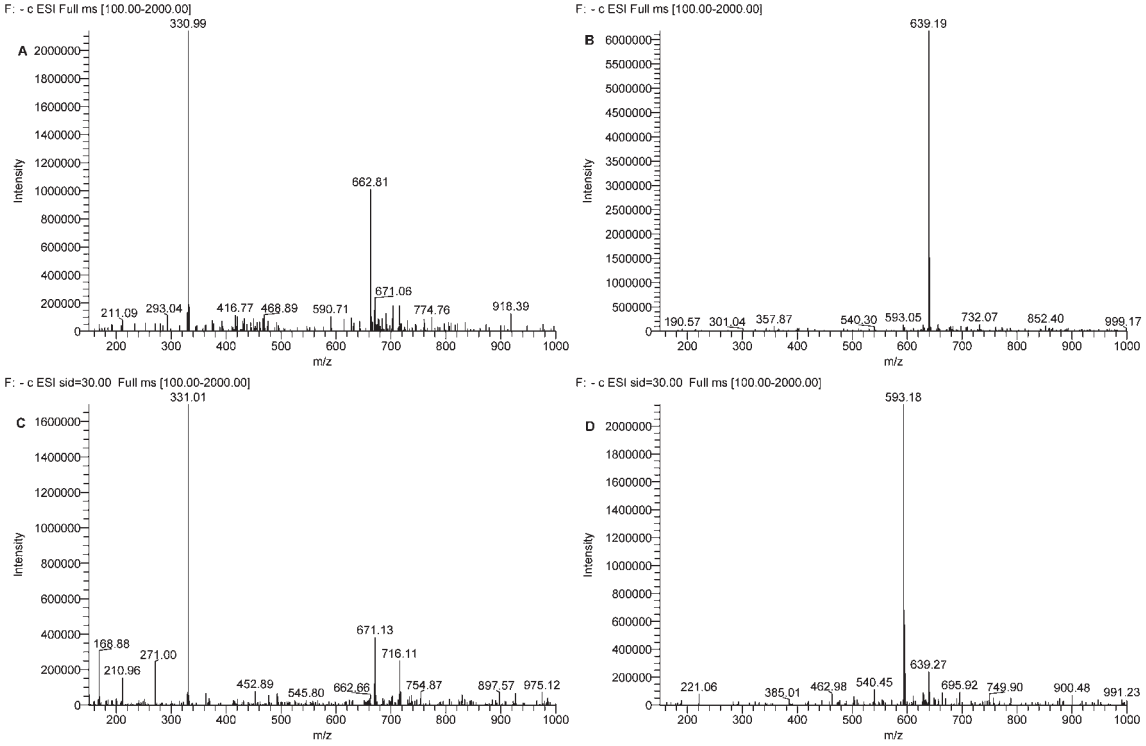

Figure 2. (A) TIC chromatogram of compound 4 from conventional untargeted data-dependent analysis. (B) TIC chromatogram of compound 23 from conventional untargeted data-dependent analysis. (C) TIC chromatogram of compound 4 from targeted data-dependent SID analysis. (D) TIC chromatogram of compound 23 from targeted data-dependent SID analysis. See Table 1 for nomenclature of compounds 4 and 23 and 'Experimental' for description of MS analyses.

think that compound 28 could be a vanillic acid derivative monosubstituted with a sambubiose or lathyrose group.

Although monomeric (epi)catechin and (epi)gallocatechin aglycons have been reported (even at very low levels) together with free phenolic acids in extracts from different Japanese persimmon varieties,[9,10] we found no evidence of their presence in the assayed samples.

As mentioned, small phenols can easily polymerize during sample ionization. As an example of dimerization, we have Fig. 2A that represents the total ion current (TIC) chromatogram from the conventional untargeted full MS analysis of compound 4 (also extended to compounds 8 and 10). As we can see, in addition to the 'real' molecular mass at *m/z* 331 of compound 4, also noticeable was the dimer at *m/z* 663. In this case, since the main ion generated corresponded to the real parent mass, the automated (data-dependent) MS^2 analysis (scan event 2 of the untargeted analysis) led to obtain valuable structural information on compound 4. In contrast, we have compounds 11, 23, 25 and 27 whose parent masses were masked by the formation of their respective formic acid adducts ($[M-H]^-$ + 46 amu) as shown by Fig. 2B, which represents the TIC chromatogram of compound 23. In this case the most abundant ion by far was at *m/z* 639, while the real parent mass at *m/z* 593 was practically negligible. Consequently, the untargeted (conventional) MS^2 data-dependent analysis of the ion at *m/z* 639 led to obtain a single fragment that corresponded to the de-adducted (real) parent ion, not giving relevant information about the molecule structure of compound 23 (as in the case of compounds 11, 25 and 27).

To overcome these drawbacks, samples were reanalyzed with the SID feature enabled (see 'Experimental'). As expected, the TIC representation of compound 4 (Fig. 2C) did not show the corresponding dimer in the SID analysis. However, as mentioned, the SID analysis promoted the fragmentation of the parent mass (making noticeable the ions at *m/z* 271, 211 and 169; the same fragments appeared in the MS^2 spectrum of compound 4 under the conventional untargeted data-dependent analysis).

In this research the main interest of the SID analysis is illustrated by Fig. 2D, which shows how the main ion appearing in the TIC chromatogram of compound 23 corresponded to its real parent mass (*m/z* 593, although with a lower intensity when compared with its formic adduct counterpart at *m/z* 639 appearing in Fig. 2B). In contrast to what happened with dimers, the SID analysis of adducts did not induce the fragmentation of their parent masses and led to obtain relevant MS^2 results (see fragments of compounds 11, 23, 25 and 27 in Table 1).

Very interestingly, and for the first time in persimmon fruits, the fragmentation patterns of compounds 18, 22, 29, 30, 31 and 32 revealed the presence of flavone *C*-glycosides in the samples studied. This finding can be understood according to Fig. 3, which illustrates the fragmentation pathway of peak 30 (with a molecular $[M-H]^-$ mass at *m/z* 759). Considering the literature,[11,12] the fragmentation of flavone *O*-glycosides generates abundant aglycon

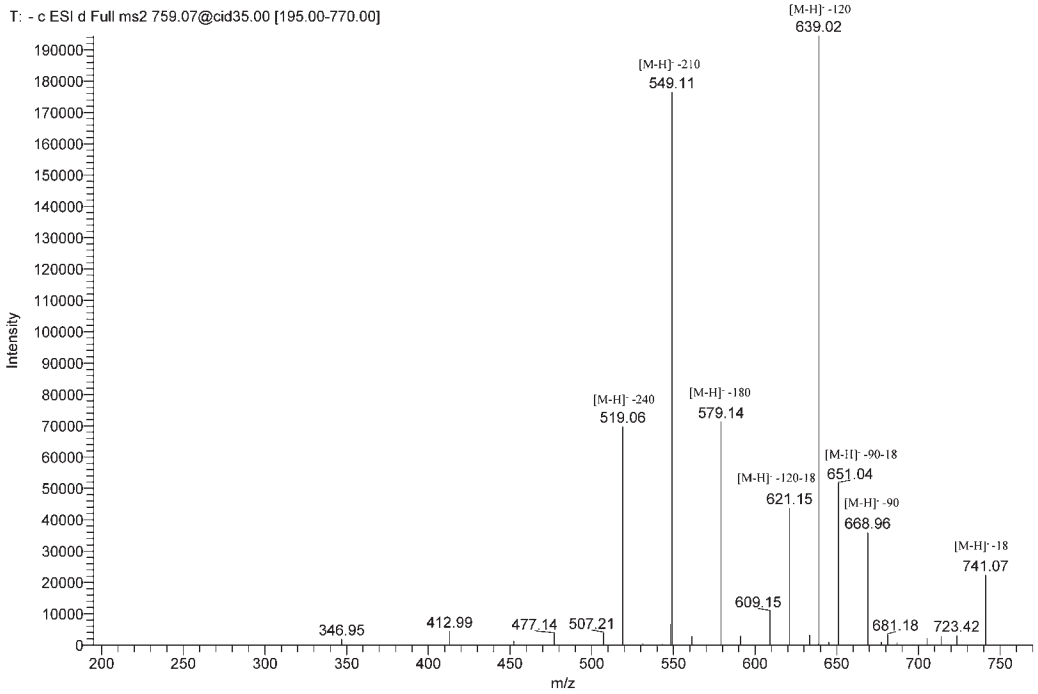

Figure 3. MS^2 spectrum of compound 30 (see Table 1) illustrating general fragmentation pathway of flavone di-*C*-hexosides detected in samples assayed.

ions by loss of the neutral mass of the sugar attachment, while *C*-glycosides do not generate aglycon ions; instead, specific ions from the fragmentation of the *C*-glycoside unit are very noticeable. Thereby, characteristic fragments from flavone di-*C*-hexosides are originated by neutral losses of 18, 90, 120, 180, 210 and 240 amu.[12] In this regard, no evidence was found about the aglycon identity of compound 30 according to its MS^2 breakdown (Fig. 3), although its UV–visible spectrum (Table 1) clearly suggested its flavone nature. Nevertheless, all six aforementioned characteristic neutral losses for flavone di-*C*-hexosides were present in the fragmentation pattern of compound 30 to yield ions at *m/z* 741 (−18 amu), 669 (−90 amu, and its corresponding dehydrated ion at *m/z* 651), 639 (−120 amu, and its corresponding dehydrated ion at *m/z* 621), 579 (−180 amu), 549 (−210 amu) and 519 (−240 amu). The same results were found for the rest of the flavone di-*C*-hexosides detected in samples, having in all cases that the main fragment generated corresponded to $[M - H]^- - 120$ amu in agreement with previous results regarding the fragmentation pathway of flavone *C*-glycosides.[13–15]

In this study, other phenols first detected in persimmon were those whose obtained MS^n data did not allow their complete identification (unknown compounds UK 1–10 in Table 1). Nonetheless, the results led to propose partial assignments for some of them. This was the case of peaks 17 (without caffeoylation evidence and with a main MS^2 transition propitiated by a neutral loss of 162 amu, hexoside), 23 (with two consecutive losses of 198 amu to finally yield the fragment at *m/z* 197, most probably a trimer of syringic acid), 25 (with a main MS^2 transition originated by a neutral loss of 132 amu, pentoside) and 26 (suggested as lariciresinol-hexoside). It is worth mentioning that the presence of lignans (from the dimerization of substituted cinnamic alcohols) has rarely been reported in persimmons outside of the research of Matsuura and Iinuma,[16] who identified divanillyltetrahydrofuran ferulate in calyces of 'Hachiya' variety. Thus, although the MS^n data of compound 26 (Table 1) could well explain the presence of lariciresinol-hexoside in samples, since its only MS^2 transition was from the loss of 162 amu (yielding the fragment at *m/z* 359, lariciresinol), the lack of literature on lignans in the pulp of persimmon fruits did not allow us to obtain a conclusive assignment.

CONCLUSION

This research demonstrates that a detailed metabolite profiling of natural extracts can be achieved through a straightforward and affordable methodology of analysis using a routine three-dimensional ion trap. Moreover, this methodology can easily be exported to other platforms of analysis. At present, this is the most complete study on low-molecular-weight phenols from persimmon pulp, reporting the majority of the detected compounds for the first time. Although in some cases the inherent instrumental limitations prevented conclusive identifications, the results from this metabolite approach can help forthcoming actions aimed to enhance the understanding of the persimmon metabolome.

ACKNOWLEDGEMENTS

This study was supported by MICIN (Spanish Government) project AGL 2009-11805ALI. The authors acknowledge the financial support for the contract of M Cerdán-Calero (JAE-PREdoc program, CSIC-FEDER funds) and from Consolider Ingenio Fun-C-Food (CSD2007-00063). Dr E Sentandreu greatly appreciates the support of Alicia Ferreres, Fran García and Pilar Ruíz for their positive

and optimistic influence during the difficult times in which this work was carried out – thank you chaps!

REFERENCES

1 Gu HF, Li CM, Xu Y, Hu W, Chen M and Wan Q, Structural features and antioxidant activity of tannin from persimmon pulp. *Food Res Int* **41**:208–217 (2008).
2 Hibino G, Nadamoto T, Fujisawa F and Fushiki T, Regulation of the peripheral body temperature by foods: a temperature decrease induced by the Japanese persimmon (kaki, *Diospyros kaki*). *Biosci Biotechnol Biochem* **67**:23–28 (2003).
3 FAO, *FAOSTAT* [Online]. (2011). Available: http://faostat.fao.org [12 January 2014].
4 Giordani E, Doumett S, Nin S and Del Bubba M, Selected primary and secondary metabolites in fresh persimmon (*Diospyros kaki* Thunb.): a review of analytical methods and current knowledge of fruit composition and health benefits. *Food Res Int* **44**:1752–1767 (2011).
5 Komatsu S and Matsunami N, Constitution of shibuol. *Mem Coll Sci Kyoto Imp Univ A* **7**:15–23(1924).
6 Komatsu S and Matsunami N, Constitution of shibuol. *II. Mem Coll Sci Kyoto Imp Univ A* **11**:231–240 (1925).
7 Matsuo T and Ito S, The chemical structure of kaki-tannin from immature fruit of the persimmon (*Diospyros kaki* L.). *Agric Biol Chem* **42**:1637–1643 (1978).
8 Li C, Leverence R, Trombley JD, Xu S, Yang J, Tian Y, *et al.*, High molecular weight persimmon (*Diospyros kaki* L.) proanthocyanidin: a highly galloylated, A-linked tannin with an unusual flavonol terminal unit, myricetin. *J Agric Food Chem* **58**:9033–9042 (2010).
9 Suzuki T, Someya S, Hu F and Tanokura M, Comparative study of catechin compositions in five Japanese persimmons (*Diospyros kaki*). *Food Chem* **93**:149–152 (2005).
10 Chen XN, Fan JF, Yue X, Wu XR and Li LT, Radical scavenging activity and phenolic compounds in persimmon (*Diospyros kaki* L. cv. Mopan). *J Food Sci* **73**:C24–C28 (2008).
11 Chen LJ, Games DE and Jones J, Isolation and identification of four flavonoid constituents from the seeds of *Oroxylum indicum* by high-speed counter-current chromatography. *J Chromatogr A* **988**:95–105 (2003).
12 Greenham JR, Grayer RJ, Harborne JB and Reynolds V, Intra- and interspecific variations in vacuolar flavonoids among *Ficus* species from the Budongo Forest, Uganda. *Biochem Syst Ecol* **35**:81–90 (2007).
13 Ferreres F, Gil-Izquierdo A, Andrade PB, Valentão P and Tomás-Barberán FA, Characterization of *C*-glycosyl flavones *O*-glycosylated by liquid chromatography–tandem mass spectrometry. *J Chromatogr A* **1161**:214–223 (2007).
14 Prasain JK, Jones K, Kirk M, Wilson L, Smith-Johnson M, Weaver C, *et al.*, Profiling and quantification of isoflavonoids in kudzu dietary supplements by high-performance liquid chromatography and electrospray ionization tandem mass spectrometry. *J Agric Food Chem* **51**:4213–4218 (2003).
15 Sánchez-Rabaneda F, Jáuregui O, Casals I, Andrés-Lacueva C, Izquierdo-Pulido M and Lamuela-Raventós RM, Liquid chromatographic/electrospray ionization tandem mass spectrometric study of the phenolic composition of cocoa (*Theobroma cacao*). *J Mass Spectrom* **38**:35–42 (2003).
16 Matsuura S and Iinuma M, Lignan from calyces of *Diospyros kaki*. *Phytochemistry* **24**:626–628 (1985).

RESUMEN DE LOS RESULTADOS

6. RESUMEN DE LOS RESULTADOS

6.1. Optimización de los parámetros de muestreo y análisis de la metodología GC-MS/AMDIS.

Para probar la fiabilidad del AMDIS a la hora de determinar de manera automática y precisa la composición de las muestras estudiadas, en nuestro caso volátiles (extraídos mediante HS/SPME) y compuestos polares no volátiles a partir de sus correspondientes TMS-derivados, fue necesario optimizar los parámetros de muestreo y análisis tanto del sistema GC-MS como del propio programa AMDIS de entre los que destacamos:

- La frecuencia de muestreo (sampling rate en su aceptación en inglés): es un parámetro que hay que ajustar específicamente para cada tipo de analito considerado y que depende enteramente del detector de masas. Es necesario que un pico cromatográfico contenga entre 15-25 puntos (medidas) para ser reconstituido matemáticamente y por lo tanto, pueda ser integrado con precisión. Así pues, se probaron diferentes velocidades de muestreo tanto para los volátiles como para los TMS-derivados. Velocidades rápidas de muestreo producen altas frecuencias de medida que en picos anchos, como es el caso de los volátiles, dan lugar a un excesivo número de puntos por pico, pudiendo considerar erróneamente que el pico cromatográfico esté conformado por dos o más compuestos coeluídos (apareciendo un pico con dientes de sierra). La solución a este problema es utilizar una velocidad de muestreo más lenta para obtener picos mejor definidos (0.58 scan/s) actuando a modo de "suavizado" (smoothing en su acepción original en inglés) al eliminar puntos de medida. En cambio, en los TMS-derivados ocurre lo contrario, ya que son picos más estrechos. Si se emplean velocidades de muestreo lentas se obtiene un número insuficiente de puntos para definir el pico cromatográfico, lo que da lugar a integraciones falsas. Así pues, en este tipo de analitos la velocidad de muestreo debe ser rápida (0.93 scan/s).

- Optimización de los parámetros de análisis del AMDIS para el procesamiento automático y fiable de los datos experimentales GC-MS. Para ello se realizaron 45 combinaciones diferentes de los parámetros más importantes del programa (sensitivity, shape requirement y resolution) y que influyen de manera decisiva en la capacidad de deconvolución del AMDIS. La mejor combinación obtenida fue sensitivity médium, shape requirement low y resolution low tanto para volátiles como para los compuestos polares no volátiles.
- Prueba de la eficiencia de deconvolución del AMDIS para picos cromatográficos superpuestos. Para ello se evaluó la configuración óptima mencionada anteriormente, obteniendo resultados muy satisfactorios para compuestos que presentaron coeluciones extremas.

Una vez optimizados todos los parámetros de análisis y construidas las respectivas librerías, el sistema AMDIS fue capaz de identificar y cuantificar automáticamente, en unos pocos segundos, un total de 85 compuestos volátiles y 22 compuestos polares en el zumo fresco de naranja Valencia Late. Estos resultados fueron comparados con los obtenidos manualmente mediante el uso de Xcalibur^{R}, software de procesamiento de datos proporcionado por el fabricante del sistema GC-MS empleado (Thermo Scientific). Ambos, AMDIS y Xcalibur^{R}, dieron lugar a los mismos resultados.

En conclusión, los resultados indican que la fiabilidad del AMDIS depende en gran medida de ciertos ajustes de funcionamiento tanto en el sistema MS empleado como en el programa AMDIS. Dichos parámetros deben ser optimizados en función del tipo de muestra y analitos ensayados, resultando un proceso un tanto tedioso. Obviamente, no es recomendable el uso del AMDIS cuando se pretenda analizar muestras aisladas o en reducido número. Por el contrario, para el análisis de un gran número de muestras o si se pretende realizar ensayos de rutina el uso del AMDIS supone una gran ventaja ya que la obtención de los resultados es rápida y fiable,

mereciendo la pena la inversión inicial de tiempo en el proceso de optimización de los parámetros de análisis.

Por último, es conveniente remarcar que una vez las condiciones de análisis (incluyendo la generación de librerías) han sido apropiadamente establecidas, estas pueden ser fácilmente exportadas a otras plataformas GC-MS de análisis con independencia del fabricante y del operador que las maneje.

6.2. Caracterización del perfil de volátiles y compuestos polares no volátiles de los zumos de naranja (*Citrus sinensis*).

Se ha estudiado la evaluación de la calidad de los zumos de naranja procedentes de dos variedades distintas (Valencia Late y Lane Late) los cuales fueron sometidos a diversos tratamientos industriales, entre los que se incluyen las HPH y la reducción de pulpa. Para ello se han analizado los zumos mediante la metodología GC-MS/AMDIS descrita en el apartado anterior para el estudio de sus perfiles de volátiles y compuestos polares no volátiles. Los resultados más relevantes fueron:

- Elucidación del perfil de volátiles de los zumos de naranja procedentes de la variedad Valencia Late reducidos en pulpa y sometidos a tres tipos de tratamiento: pasteurización clásica a 85 ºC durante 15 s, homogenización a alta presión (150 MPa) y doble homogenización (prehomogeneización suave a 20 MPa aplicada al zumo entero antes de la reducción de pulpa y posterior homogenización a 150 MPa de los zumos despulpados). Los zumos procesados fueron analizados al cabo de 0, 0,5, 1,5 y 3,5 meses de almacenamiento a 4 ºC. Como resultado, se determinaron un total de 88 compuestos volátiles, de los cuales se seleccionaron 32 como descriptores aromáticos para analizar estadísticamente los efectos del procesado y del almacenamiento en los zumos. De este análisis se obtuvo que inicialmente el zumo doblemente homogenizado mostró unos contenidos en volátiles y características sensoriales muy similares

al zumo fresco, presentando una menor concentración de volátiles no deseables (off-flavours) durante el almacenamiento.

- Perfil de volátiles y compuestos polares no volátiles de zumos de naranja procedentes de la variedad Lane Late mínimamente procesados. Los zumos estudiados contenían diferentes porcentajes de pulpa (0 %, 50 % y 100 %) y fueron sometidos a un proceso de homogenización a alta presión (150 MPa) a diferentes temperaturas (58, 63 y 68 ºC), siendo finalmente almacenados a 3 ºC durante un periodo de 3 meses. En este ensayo se determinaron un total de 92 compuestos volátiles, de los cuales se seleccionaron 33 como descriptores aromáticos, y 22 compuestos polares (trimetilsilil derivados de azucares, ácidos orgánicos y aminoácidos). Tras el análisis estadístico, se observó que los zumos homogenizados con el 100 % de pulpa presentaron un perfil aromático aún mejor que el zumo fresco y de entre ellos, el tratado a 68 ºC presentó la menor pérdida de compuestos deseables (fresh-flavours) con el menor aumento de off-flavours durante el almacenamiento. Por otra parte, la homogeneización a 150 MPa aumenta ligeramente la concentración de azúcares en las muestras procesadas en comparación con el zumo fresco. Sin embargo, los compuestos polares no volátiles no se ven afectados, en general, por el procesado ni por el almacenamiento.

Gracias a la alta capacidad de procesado y a la precisión de los resultados obtenidos mediante el empleo del programa AMDIS, se pueden establecer las pautas necesarias para el diseño de procesos industriales destinados a la obtención de zumos cítricos de alta calidad y con una vida útil extendida.

6.3. Caracterización del perfil de fenoles de los zumos de granada (*Punica granatum*) de la variedad "Wonderful".

Se ha realizado la caracterización del zumo de granada procedente de frutas de la variedad "Wonderful" obtenido de manera industrial en base a su perfil en compuestos fenólicos y capacidad antirradical *in vitro*.

Mediante el empleo de diversas metodologías HPLC-DAD/ESI$^{+/-}$-MS^{n} fueron identificados alrededor de 150 compuestos fenólicos (antociano y no antociano), muchos de los cuales descritos por primera vez en un extracto natural, constituyendo el estudio más completo hasta la fecha. Para la obtención de dichos resultados, fue necesario el empleo de diversos tipos de muestreo característicos de un detector de tipo trampa iónica alcanzando niveles de fragmentación hasta MS^{4}. Del total de los compuestos identificados, 65 corresponden a antocianinas, incluyendo aductos antocianina-flavonol y flavonol-antocianina. El resto de compuestos fenólicos identificados fueron de naturaleza no antociano de los cuales 39 fueron descriptos por primera vez en el zumo de granada.

El perfil de fenoles obtenido anteriormente se correlacionó con su propiedad antirradical *in vitro*, empleando el DPPH$^{\bullet}$ como sonda antirradical. Los datos experimentales fueron ajustados mediante el modelo matemático desarrollado por el Grupo de Zumos del IATA-CSIC, el cual es aplicable a todo tipo de mezclas complejas de compuestos con capacidad antirradical, obteniéndose los valores correspondientes tanto a la capacidad antirradical total como a las parciales (acumulada rápida y acumulada lenta), así como sus correspondientes cinéticas de actividad. De este modo, se puede conocer con exactitud y no de un modo aproximado los verdaderos parámetros que caracterizan la actividad antirradical de un extracto natural.

Para los zumos de granada estudiados se obtuvo una actividad antirradical total elevada, capaz de reducir 84,58 µmol/L de DPPH$^{\bullet}$ por unidad de zumo concentrado (µL/mL), equivalente a la concentración de 42,29 mmol/L de ácido ascórbico (o Trolox)

Además, las actividades antirradicales parciales, de las cinéticas de reacción rápidas, medias y lentas, fueron capaces de reducir 49.09, 18.16, y 17.33 μmol/L de $DPPH^{\bullet}$ por unidad zumo concentrado de (μL/mL), respectivamente. La constante de velocidad correspondiente a dichas cinéticas, rápida, media y lenta fueron $\kappa 1 = 6{,}03$, $\kappa 2 = 0{,}169$ y $\kappa 3 = 0{,}0094$ (μL·L)/(mL·μmol·min), respectivamente.

6.4. Caracterización del perfil de fenoles de la pulpa de caqui (*Diospyros kaki*) de la variedad "Rojo Brillante".

Al igual que en el caso de los zumos de granada, mediante el empleo de diferentes metodologías HPLC-DAD/$ESI^{+/-}$-MS^n, se ha podido realizar el estudio más completo hasta la fecha del perfil de fenoles procedente de la pulpa del caqui (variedad Rojo Brillante, denominación de origen Ribera del Xúquer) a partir de su extracto metanólico. En este caso, se ha llevado a cabo la identificación de pigmentos de tipo antociano en el extracto etanólico de la pulpa del caqui sometido a un proceso a un proceso de hidrólisis ácida, encontrando diversas antocianinas, antocianidinas y lo que es más interesante, diferentes aductos de tipo flavanol-antociano galoilados. Se identificaron un total de 17 agliconas, 4 antocianidinas libres (delfinidina, petunidina, cianidina y peonidina) y por primera vez en un extracto natural, 13 aductos de tipo galoil-3-O-flavanol-antociadinina (dímeros donde la unidad de flavanol es una (epi)catequina o (epi)galocatequina ocupa la posición superior y se encuentra unida con una de las antonicanidinas libres antes mencionadas).

Por otra parte, se ha estudiado el perfil de fenoles de bajo peso molecular (no antociano) presentes en el extracto etanólico procedente de la pulpa de caqui. Se han identificado un total de 32 compuestos fenólicos, siendo los más abundantes aquellos derivados del ácido gálico (glicósidos y acil derivados). Además, se han caracterizado otros compuestos entre los que encontramos: diversos glicósidos de los ácidos *p*-cumárico, vanílico y cinámico además de diferentes flavona C-hexósidos, siendo la mayoría de ellos descritos por primera vez en los frutos de caqui.

CONCLUSIONES

7. CONCLUSIONES

De este trabajo realizado se pueden concretar las siguientes conclusiones:

1. El sistema AMDIS es capaz de proporcionar resultados rápidos y precisos, obteniendo una correcta identificación y cuantificación de los compuestos presentes en la muestra analizada. Para ello, resulta esencial la optimización de los parámetros de muestreo del analizador de masas así como de los propios del AMDIS en función del tipo de muestra y analitos considerados.

2. No es conveniente dicha optimización para el análisis GC-MS de un escaso número de muestras ya que es un trabajo tedioso, complicado y lento. Sin embargo, la inversión de tiempo que precisa la puesta a punto del conjunto GC-MS/AMDIS se ve recompensada en aquellos casos que precisen el procesado de una gran cantidad de información (controles de rutina y/o en el desarrollo de nuevas pautas del procesamiento industrial de los alimentos). Como valor añadido, esta metodología una vez optimizada resulta fácilmente exportable a otras plataformas de análisis con independencia del operador y del fabricante.

3. La metodología GC-MS/AMDIS desarrollada permite el estudio detallado de los componentes volátiles y de los compuestos polares no volátiles de los zumos cítricos. De este modo, se facilita la detección de alteraciones no deseadas durante el procesamiento y el almacenamiento de los zumos, contribuyendo al desarrollo de procesos innovadores encaminados a la obtención de productos de alta calidad. En este sentido, los zumos de naranja (con su contenido en pulpa original) sometidos a un proceso de homogenización dinámica a 150 MPa y 68 ºC presentan la misma aceptación que los zumos en fresco y con una vida útil extendida que puede llegar hasta los 3 meses en refrigeración.

4. La formación del personal investigador en el ámbito de las técnicas instrumentales resulta esencial para el desarrollo de metodologías analíticas que permitan llevar a cabo actividades científicas de primer nivel aún empleando sistemas convencionales de análisis. De esta manera, el empleo de un detector de masas de tipo trampa iónica tridimensional ha permitido llevar a cabo el estudio más completo hasta la fecha del perfil de compuestos fenólicos del zumo de granada y de la pulpa de caqui. De manera muy relevante, muchos de los compuestos caracterizados han sido descritos por primera vez en un extracto natural, evidenciando la calidad de las metodologías HPLC-DAD/ESI$^{+/-}$-MS^{n} desarrolladas en este trabajo frente aquellas fundamentadas en el empleo de otros equipos de detección mucho más modernos y costosos.

5. La capacidad antirradical total y parcial de una muestra bioactiva así como sus cinéticas de actividad actúan a modo de "huella dactilar", por lo que su determinación *in vitro* permite la comparación realista (con valor biológico) de las características de capacidad antirradical de los extractos naturales.